frontiers | Research Topics

Nutrients, stress response, and human health

Edited by
Jagannath Misra and Julius Liobikas

Coordinated by
Vishakha Dey

Published in
Frontiers in Nutrition

ISSN 1664-8714
ISBN 978-2-8325-6760-9
DOI 10.3389/978-2-8325-6760-9

Generative AI statement
Any alternative text (Alt text) provided alongside figures in the articles in this ebook has been generated by Frontiers with the support of artificial intelligence and reasonable efforts have been made to ensure accuracy, including review by the authors wherever possible. If you identify any issues, please contact us.

About Frontiers

Frontiers is more than just an open access publisher of scholarly articles: it is a pioneering approach to the world of academia, radically improving the way scholarly research is managed. The grand vision of Frontiers is a world where all people have an equal opportunity to seek, share and generate knowledge. Frontiers provides immediate and permanent online open access to all its publications, but this alone is not enough to realize our grand goals.

Frontiers journal series

The Frontiers journal series is a multi-tier and interdisciplinary set of open-access, online journals, promising a paradigm shift from the current review, selection and dissemination processes in academic publishing. All Frontiers journals are driven by researchers for researchers; therefore, they constitute a service to the scholarly community. At the same time, the *Frontiers journal series* operates on a revolutionary invention, the tiered publishing system, initially addressing specific communities of scholars, and gradually climbing up to broader public understanding, thus serving the interests of the lay society, too.

Dedication to quality

Each Frontiers article is a landmark of the highest quality, thanks to genuinely collaborative interactions between authors and review editors, who include some of the world's best academicians. Research must be certified by peers before entering a stream of knowledge that may eventually reach the public - and shape society; therefore, Frontiers only applies the most rigorous and unbiased reviews. Frontiers revolutionizes research publishing by freely delivering the most outstanding research, evaluated with no bias from both the academic and social point of view. By applying the most advanced information technologies, Frontiers is catapulting scholarly publishing into a new generation.

What are Frontiers Research Topics?

Frontiers Research Topics are very popular trademarks of the *Frontiers journals series*: they are collections of at least ten articles, all centered on a particular subject. With their unique mix of varied contributions from Original Research to Review Articles, Frontiers Research Topics unify the most influential researchers, the latest key findings and historical advances in a hot research area.

Find out more on how to host your own Frontiers Research Topic or contribute to one as an author by contacting the Frontiers editorial office: frontiersin.org/about/contact

Nutrients, stress response, and human health

Topic editors

Jagannath Misra — Indiana University, Purdue University Indianapolis, United States

Julius Liobikas — Lithuanian University of Health Sciences, Lithuania

Topic coordinator

Vishakha Dey — Indiana University Bloomington, United States

Citation

Misra, J., Liobikas, J., Dey, V., eds. (2025). *Nutrients, stress response, and human health*. Lausanne: Frontiers Media SA. doi: 10.3389/978-2-8325-6760-9

Table of contents

frontiers | Frontiers in Nutrition

TYPE Editorial
PUBLISHED 27 February 2025
DOI 10.3389/fnut.2025.1558682

OPEN ACCESS

EDITED AND REVIEWED BY
Abraham Wall-Medrano,
Universidad Autónoma de Ciudad Juárez, Mexico

*CORRESPONDENCE
Jagannath Misra
jmisra@iu.edu

RECEIVED 10 January 2025
ACCEPTED 31 January 2025
PUBLISHED 27 February 2025

CITATION
Misra J and Liobikas J (2025) Editorial: Nutrients, stress response, and human health. *Front. Nutr.* 12:1558682. doi: 10.3389/fnut.2025.1558682

Editorial: Nutrients, stress response, and human health

Jagannath Misra[1]* and Julius Liobikas[2]

[1]Department of Biochemistry and Molecular Biology, Indiana University School of Medicine, Indianapolis, IN, United States, [2]Laboratory of Biochemistry, Neuroscience Institute, Medical Academy, Lithuanian University of Health Sciences, Kaunas, Lithuania

KEYWORDS

nutritional metabolites, oxidative stress, cardiometabolic health, aging and longevity, metabolic dysfunction, gene-diet interactions, stress response pathways

Editorial on the Research Topic
Nutrients, stress response, and human health

Although significant progress has been made in understanding nutrient signaling pathways and their role in cellular health, the complexity of these mechanisms has revealed that their impact extends far beyond basic metabolic functions. Nutrient availability and sensing are now recognized as critical determinants of cellular adaptation to stress, with far-reaching implications for human health. The interplay between nutrient sensing, stress response pathways, and metabolic regulation holds the key to addressing conditions ranging from cancer progression to metabolic disorders. This Research Topic, titled "*Nutrients, Stress Response, and Human Health*" brings together contributions that explore the intricate dynamics of nutrient signaling in cellular physiology. Each study sheds light on distinct yet interconnected aspects of how nutrient homeostasis influences health and disease, providing a comprehensive view of this essential biological theme.

Wang et al. explore the causal relationship between circulating serum metabolites (CSMs) and hemorrhagic stroke (HS) through rigorous Mendelian randomization analysis. Their findings identify specific metabolites, such as biliverdin and linoleate, as protective factors for intracerebral hemorrhage (ICH), while others like 1-eicosadienoylglycerophosphocholine increase the risk of subarachnoid hemorrhage (SAH). These results emphasize the role of metabolites in influencing inflammation, oxidative stress, and lipid homeostasis, thus uncovering actionable biomarkers and pathways relevant to stroke prevention. This study lays a foundational understanding of how metabolic health can be influenced by circulating biomarkers.

Expanding on the theme of metabolic influences, Yu et al. investigate the relationship between the triglyceride-glucose (TyG) index and the risk of aortic aneurysm and dissection (AAD). They highlight the predictive power of TyG-related indices, particularly TyG-waist circumference (TyG-WC), in identifying high-risk individuals. This study underscores the role of metabolic health markers in cardiovascular disease risk stratification, complementing Wang et al.'s focus on metabolic pathways by emphasizing the translational value of early detection metrics in clinical practice.

The role of dietary interventions in modulating metabolic pathways is explored by Liu et al., who studies the nutritional regulation of aging, examining the relationship between folate intake and serum Klotho levels in adults. This cross-sectional study identifies folate as a modulator of Klotho, a protein implicated in aging-related diseases and longevity. The findings highlight the role of specific nutrients in regulating aging pathways, suggesting that folate may help mitigate age-related diseases. This research emphasizes the importance

of nutrient-stress response interactions in promoting healthy aging, resonating with the findings of Wang et al. and Yu et al. by highlighting the significance of dietary components in systemic health regulation.

Adding to the dietary narrative, Roumi et al. investigate the interplay between polyphenol intake, genetic predispositions, and cardiometabolic risk factors in overweight and obese women. Their study demonstrates significant gene-diet interactions, with specific polyphenol types influencing markers like HDL cholesterol and triglycerides. These findings suggest the potential for personalized nutrition strategies, aligning with Liu et al.'s emphasis on tailored dietary interventions to mitigate metabolic risks.

Odetayo et al. address nutrient-driven modulation of oxidative stress and inflammation in their investigation of omega-3 fatty acids (O3FA) as protective agents against tamoxifen-induced gonadotoxicity. Their results highlight O3FA's ability to restore redox balance, suppress inflammatory pathways, and mitigate apoptosis, offering mechanistic insights into how dietary supplements can counteract drug-induced side effects. This study builds on the oxidative stress narratives introduced by Wang et al. and Roumi et al., emphasizing the therapeutic potential of nutrients in stress response pathways.

Continuing with oxidative balance, Yuan et al. explore the association between oxidative balance score (OBS) and serum cobalt levels in individuals with metal implants. Their findings reveal an inverse relationship, particularly in older males, and propose antioxidant-rich diets as strategies to mitigate implant-related oxidative stress. This study's emphasis on dietary antioxidants complements Odetayo et al.'s findings, reinforcing the role of oxidative stress modulation in health maintenance.

Finally, Amer et al. investigate the metabolic effects of glucose supplementation in high-fat diet mouse models, shedding light on the dual role of glucose in accelerating liver injury and promoting lipid oxidation. Their findings provide a critical perspective on how excessive dietary components can exacerbate metabolic dysfunction. While certain nutrient components exhibit clear protective effects on human health, as highlighted by Liu et al.'s findings on dietary folate and its positive role in enhancing serum Klotho levels, and Roumi et al.'s demonstration of polyphenols mitigating cardiometabolic risks, it is equally critical to recognize the potential harms associated with excessive nutrient intake. Amer et al.'s work underscores this cautionary principle by illustrating how excessive glucose supplementation, particularly with L-glucose, exacerbates liver injury in mice. These findings collectively offer a balanced view of nutrient impacts on metabolic health.

Conclusion

In conclusion, these articles collectively illuminate the intricate connections between nutrients, stress responses, and human health. They underscore the importance of metabolic markers, dietary components, and oxidative stress modulation in understanding disease mechanisms and developing preventive strategies. This Research Topic is both timely and crucial, given the rising global burden of metabolic and age-related disorders. Together, these studies provide a robust foundation for advancing our understanding of how targeted dietary and metabolic interventions can improve health outcomes, offering actionable insights for both clinical and public health applications.

Author contributions

JM: Writing – original draft, Writing – review & editing. JL: Writing – review & editing.

Funding

The author(s) declare financial support was received for the research, authorship, and/or publication of this article. This work was supported by Ralph W. and Grace M. Showalter Research Trust, Department of Biochemistry and Molecular Biology, Indiana University School of Medicine (080659-00002B to JM).

Conflict of interest

The authors declare that the research was conducted in the absence of any commercial or financial relationships that could be construed as a potential conflict of interest.

Publisher's note

frontiers | Frontiers in Nutrition

TYPE Original Research
PUBLISHED 15 May 2024
DOI 10.3389/fnut.2024.1376889

OPEN ACCESS

EDITED BY
Jagannath Misra,
Indiana University – Purdue University Indianapolis, United States

REVIEWED BY
Georgia Damoraki,
National and Kapodistrian University of Athens, Greece
Deng-Feng Zhang,
Kunming Institute of Zoology, Chinese Academy of Sciences (CAS), China
Marcus Scotti,
Federal University of Paraíba, Brazil

*CORRESPONDENCE
Hongsheng Liang
✉ lianghongsheng@hrbmu.edu.cn
Xiangtong Zhang
✉ zgxgtg@sina.com

†These authors have contributed equally to this work and share first authorship

‡These authors have contributed equally to this work and share last authorship

RECEIVED 26 January 2024
ACCEPTED 30 April 2024
PUBLISHED 15 May 2024

CITATION
Wang Y, Shen Y, Li Q, Xu H, Gao A, Li K, Rong Y, Gao S, Liang H and Zhang X (2024) Exploring the causal association between genetically determined circulating metabolome and hemorrhagic stroke. *Front. Nutr.* 11:1376889. doi: 10.3389/fnut.2024.1376889

Exploring the causal association between genetically determined circulating metabolome and hemorrhagic stroke

Yaolou Wang[1†], Yingjie Shen[1†], Qi Li[1], Hangjia Xu[1], Aili Gao[2], Kuo Li[2], Yiwei Rong[1], Shang Gao[1], Hongsheng Liang[1,3*‡] and Xiangtong Zhang[1,3*‡]

[1]Department of Neurosurgery, The First Affiliated Hospital of Harbin Medical University, Harbin, Heilongjiang, China, [2]School of Life Science, Northeast Agricultural University, Harbin, Heilongjiang, China, [3]NHC Key Laboratory of Cell Transplantation, Harbin, Heilongjiang, China

Background: Hemorrhagic stroke (HS), a leading cause of death and disability worldwide, has not been clarified in terms of the underlying biomolecular mechanisms of its development. Circulating metabolites have been closely associated with HS in recent years. Therefore, we explored the causal association between circulating metabolomes and HS using Mendelian randomization (MR) analysis and identified the molecular mechanisms of effects.

Methods: We assessed the causal relationship between circulating serum metabolites (CSMs) and HS using a bidirectional two-sample MR method supplemented with five ways: weighted median, MR Egger, simple mode, weighted mode, and MR-PRESSO. The Cochran Q-test, MR-Egger intercept test, and MR-PRESSO served for the sensitivity analyses. The Steiger test and reverse MR were used to estimate reverse causality. Metabolic pathway analyses were performed using MetaboAnalyst 5.0, and genetic effects were assessed by linkage disequilibrium score regression. Significant metabolites were further synthesized using meta-analysis, and we used multivariate MR to correct for common confounders.

Results: We finally recognized four metabolites, biliverdin (OR 0.62, 95% CI 0.40–0.96, $P_{MVMR} = 0.030$), linoleate (18. 2n6) (OR 0.20, 95% CI 0.08–0.54, $P_{MVMR} = 0.001$),1-eicosadienoylglycerophosphocholine* (OR 2.21, 95% CI 1.02–4.76, $P_{MVMR} = 0.044$),7-alpha-hydroxy-3 -oxo-4-cholestenoate (7-Hoca) (OR 0.27, 95% CI 0.09–0.77, $P_{MVMR} = 0.015$) with significant causal relation to HS.

Conclusion: We demonstrated significant causal associations between circulating serum metabolites and hemorrhagic stroke. Monitoring, diagnosis, and treatment of hemorrhagic stroke by serum metabolites might be a valuable approach.

KEYWORDS

causal association, circulating metabolome, hemorrhagic stroke, linkage disequilibrium score regression, Mendelian randomization

1 Introduction

In recent studies, stroke has been considered the second leading cause of death (6.6 million persons) and disability [143 million Disability Life Years (DALYs) loss] worldwide. In the last three decades, the global incidence of stroke has increased by 70%, the prevalence of stroke has increased by 85%, the mortality rate has risen by 43%, and DALYs attributable to stroke have risen by 32%, amongst which hemorrhagic stroke (HS) is a major contributor (1, 2), there is an urgent need to explore the underlying molecular mechanisms of hemorrhagic stroke. HS is the deadliest form of stroke and includes subtypes of intracerebral hemorrhage (ICH) and subarachnoid hemorrhage (SAH) (3). Currently, neuroinflammation, oxidative stress, chronic damage to the vascular wall, cell death, and hemodynamic alterations have been discovered to be tightly related to the development of hemorrhagic stroke (4, 5). Thus, searching for the molecules that drive these microscopic mechanisms is particularly significant.

Circulating serum metabolites are a series of metabolic substrates and products closely associated with human health (6). Circulating serum metabolites (CSMs) drive various cellular functions, such as energy production and storage, signal transduction, and apoptosis (7). They can act in the development of a variety of diseases, such as chronic kidney disease, oncological diseases, and myocardial infarction (8–10). As for the nervous system, lipid metabolites with a function of triggering nerve repair were discovered (11), and a group of circulating serum metabolites consisting of serine, isoleucine, betaine, PC (5:0/5:0), and LysoPE (18:2) were judged to be excellent biomarkers for the diagnostic and progression process of acute ischemic stroke (AIS) (12). Also, a meta-analysis from seven prospective cohorts investigating the connections between serum or circulating metabolites and stroke risk found that the amino acid histidine, the glycolysis-related metabolite pyruvate, the acute-phase response marker glycoprotein acetyls, and several lipoprotein subfractions were linked to stroke risk. All stroke events, as well as ischemic and hemorrhagic events, were included in the analysis (13); likewise, after stroke onset can reduce human blood plasma metabolites such as branched-chain amino acids (valine, leucine, and isoleucine) that correlate with poor neurological outcomes (14). These studies reveal an inextricable link between CSMs and stroke.

Mendelian randomization (MR) is an application of instrumental variable analysis. It utilizes genetic variation to ascertain whether an observed association between risk factors and outcome corresponds to the causal effect. The principle refers to Mendel's second law about the independent segregation of genetic alleles when DNA is passed from parents to offspring at gamete formation (15). Since MR analysis generates a random distribution of genetic variants through natural arbitrary classification, which is immutable, this method not only lowers the risk of confounding but also decreases the danger of reverse causality bias and is not influenced by disease state (16). Meanwhile, randomized controlled trials (RCTs) as the gold standard of causality have unavoidable problems such as substantial financial investment, weak patient compliance, and the ethics of randomized treatment allocation. Further, in situations where RCTs are unavailable, MR is extensively employed to infer a causal connection between exposure and outcome, with equally compelling results.

Based on the background mentioned above, we utilized MR analysis to detect the causal relationship between the circulating metabolome and hemorrhagic stroke to search for the metabolic pathways and mechanisms of effect behind the causality.

2 Materials and methods

2.1 Ethics statement and study design

This study did not require additional ethical approval since we used publicly available data, which had already received approval from the appropriate ethical and institutional review boards.

In this study, we evaluated the causal relationship between human blood metabolites and the risk of hemorrhagic stroke using a two-sample bidirectional MR design. A scientific MR study should comply with three hypotheses: (1) Instrumental variables (IVs) are strongly associated with the exposure of interest; (2) IVs must be independent of confounders; and (3) IVs are not related to the outcome, but only affect the outcome through exposure. And follow the Strengthening the Reporting of Observational Studies in Epidemiology Using Mendelian Randomization guidelines (STROBE-MR) (Supplementary Table S1) (17).

Notably, we each used four different GWAS summary data to perform a comprehensive MR analysis with hemorrhagic stroke as the outcome. False discovery rate correction for *p*-value, meta-analysis, and multivariate Mendelian randomization were performed to increase the reliability and stability of the results, linkage disequilibrium score regression (LDSC) was used by us to assess the genetic correlation between the screened exposures and the outcome, and similarly, we also explored the potential mechanisms of circulating serum metabolites for hemorrhagic stroke by metabolite pathway analyses, as outlined in the present study in Figure 1.

2.2 Data source for circulating serum metabolites

We downloaded summary-type GWAS data for human serum metabolites from the Metabolomics GWAS Server.[1] Notably, this is the most comprehensive report on the genetic loci of blood metabolites, which successfully screened out 486 metabolites with genetic influences on human serum metabolites by Shin et al. (18). Specifically, the study included 7,824 Europeans, including 1768 from the KORA F4 study in Germany and 6,056 from the United Kingdom Twin Study. This study analyzed 529 metabolites in plasma or serum from 7,824 adult individuals from two European population studies via liquid chromatography and gas chromatography separation-coupled tandem mass spectrometry. Four hundred and eighty-six serum metabolites were obtained after rigorous quality control. Among the 486 metabolites, 177 were defined as unknown due to poorly defined chemical properties. Another 309 metabolites were chemically authenticated and allocated to eight broad metabolic groups, including amino acid, carbohydrate, cofactors and vitamin, energy, lipid, nucleotide, peptide, and xenobiotic metabolism, as documented in the Kyoto Encyclopedia of Genes and Genomes (KEGG) database. We record additional information in Supplementary Table S2.

1 http://metabolomics.helmholtz-muenchen.de/gwas/

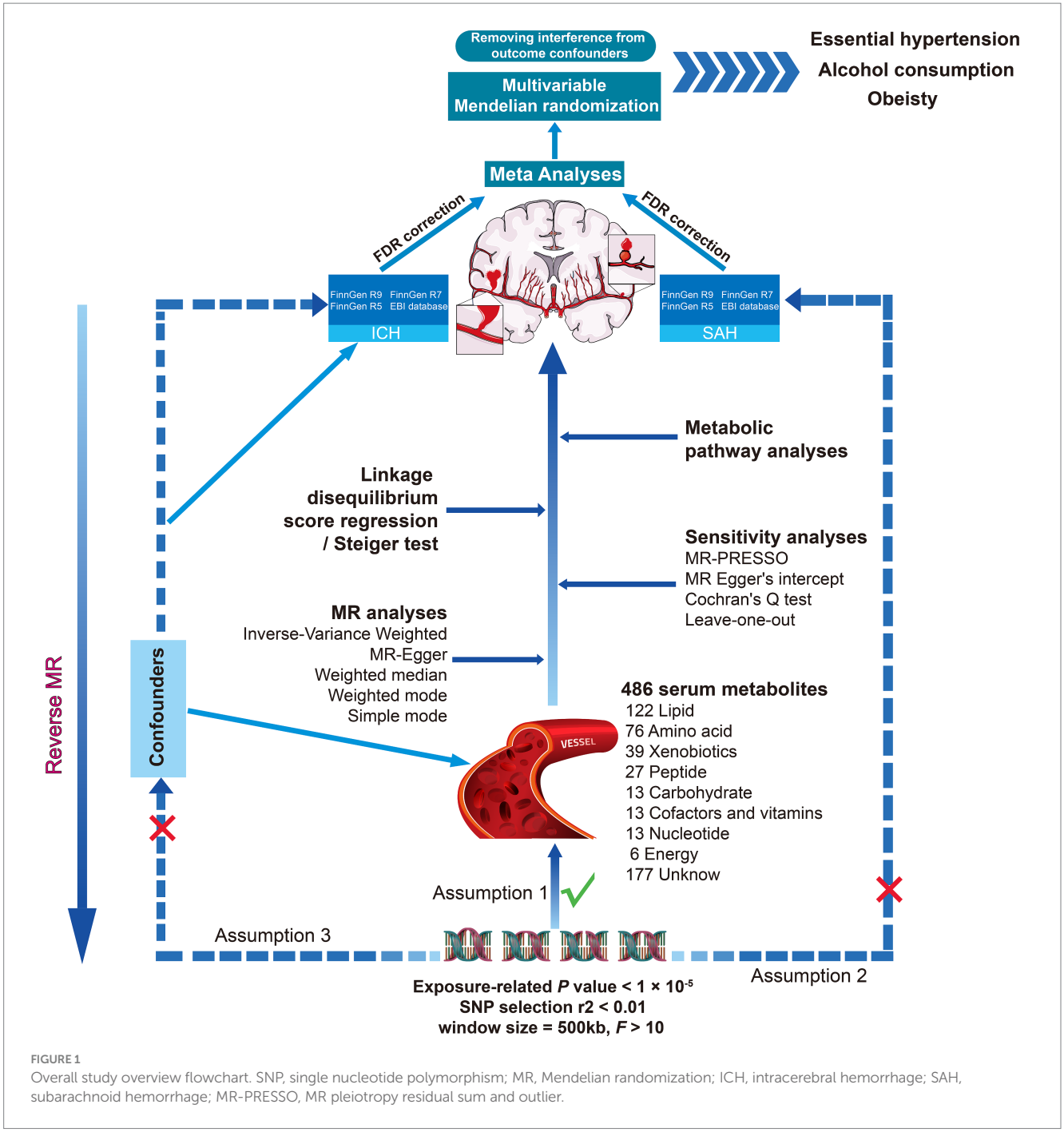

FIGURE 1
Overall study overview flowchart. SNP, single nucleotide polymorphism; MR, Mendelian randomization; ICH, intracerebral hemorrhage; SAH, subarachnoid hemorrhage; MR-PRESSO, MR pleiotropy residual sum and outlier.

2.3 Data source for hemorrhagic stroke

Hemorrhagic stroke includes two subtypes, intracerebral hemorrhage (ICH) and subarachnoid hemorrhage (SAH). GWAS summary data for hemorrhagic stroke were obtained from the FinnGen and European Bioinformatics Institute (EBI) databases. For more detail, for ICH and SAH summary data, we chose the R9, R7, and R5 versions of the FinnGen database as well as the registry numbers downloaded from the GWAS Catalog for the data sets GCST90018870 and GCST90018923 datasets, the latter being the result of the meta-analysis of FinnGen R3 and UK Biobank by Saori Sakaue et al. (19). We show the specific features of the above datasets in Supplementary Table S2. More information can be acquired by accessing (https://www.finngen.fi/fi) and (https://www.ebi.ac.uk/gwas/).

2.4 Selection of instrumental variables

We selected instrumental variables to satisfy the three main assumptions mentioned above, and the first step was to screen SNPs for subsequent MR analyses by an association threshold of $p < 1 \times 10^{-5}$ to maximize the amount of genetic variance explained by genetic predictors (20). Second, SNPs were clustered in the European 1,000 Genomes Project Phase III reference panel using the R software with

a linkage disequilibrium threshold $r^2 < 0.01$ within 500 kilobases (kb), a condition that has been widely used in previous studies (21, 22). Finally, at the same time, the *F*-statistic was used as a reliable measure to assess the tool's robustness. Ultimately, the F-statistic serves as a robust and reliable metric for evaluating the tool. We used the following formula to calculate:

$$F = \frac{R^2(n-1-k)}{(1-R^2)k}$$

Where R^2 denotes explained variance, n denotes sample size, and k denotes the number of selected IVs.

2.5 Bidirectional MR analysis and sensitivity analysis

For univariable MR analysis, given that the random-effects inverse variance weighted (IVW) estimates were derived from a pooled analysis of Wald ratios across all genetic variants and the premise that IVW could provide the most accurate assessment of causal effects based on the assumption that there was no horizontal pleiotropy across all the included SNPs (23). We chose a $p < 0.05$ for the results of IVW as a preliminary assessment of a causal relationship between circulating serum metabolites (CSMs) and hemorrhagic stroke (HS). We also used five methods, Weighted median, MR Egger, Simple mode, Weighted mode, and MR-PRESSO, as complementary analyses to the IVW method, although the Weighted median method produces unbiased estimates even when as much as 50% of the data come from invalid instruments (24). The Weighted mode method is reliable when most individual instrument causal effect estimates come from valid instruments, even if some are considered invalid (25). Simple mode represents an unweighted empirical density function for causal estimation (26). In addition, the MR-Egger method is a valuable tool for estimating causal effects through the slope coefficients of Egger regressions, which helps to identify and address potential slight study bias (27). When the condition of IVW method $p < 0.05$, even though the p value of the five methods of supplementary analysis does not satisfy all <0.05, but the β value of all methods show the same direction effect, the result is recognized as positive circulating serum metabolites (28), which are included in the next stage of analysis. Meanwhile, the MR-PRESSO method results in a $p < 0.05$, which can further increase the accuracy and stability of positive results. As for the reverse MR analysis, we chose HS for exposure, significant and potentially causal CSM as the outcome, and applied the identical SNP selection conditions of the forward MR analysis by which to test the directionality of causality.

For the MR results of positive primary screening in the above steps, we corrected the p value of false discovery rate (FDR) according to the different types of HS and the different classifications of CSM to derive the corresponding P_{FDR}. When the $p < 0.05$ and $P_{FDR} < 0.1$, we considered that there was a significant causative relationship between the exposure and outcome (29). Moreover, we thought of a potential causal relationship between exposure and outcome when $p < 0.05$ but $P_{FDR} \geq 0.1$.

For sensitivity analyses of significant and potential causality, we employed three methods, Cochran's Q test, MR-Egger intercept test, and MR-PRESSO, to identify horizontal pleiotropy and heterogeneity and to mitigate their effects by removing outliers. Cochran's *Q*-test was used to detect heterogeneity, while the MR-Egger intercept test and MR-PRESSO (Global test) were used to detect horizontal pleiotropy of selected SNP, and the MR analysis was repeated after excluding these pleiotropic SNP. $p > 0.05$ indicates the absence of heterogeneity or pleiotropy (27, 30, 31). Additionally, to ensure unbiased causal estimation, we performed a leave-one-out analysis, which assesses whether the results are affected by the severity of a single SNP by discarding each SNP in turn and then performing MR analysis (32).

2.6 Linkage disequilibrium score and directionality tests

Although SNPs associated with HS were excluded during screening for IV, SNPs that can mediate the inheritance of HS still exist. And MR analyses may violate the causal effect in the presence of a genetic correlation between exposure and outcome (33). LDSC regression observes the genetic contribution of complex traits and characteristics by estimating the strength of association between SNPs and traits. Therefore, we utilized the LDSC to examine the genetic correlation between positive circulating serum metabolites and HS to ascertain that the genetic concordance of exposure and outcome did not confound the inter-causal effects. We also performed a Steiger test to eliminate bias due to reverse causality and validate causality's directionality (34), providing a more informative interpretation of the reverse MR results.

2.7 Metabolic pathway analysis

We explored the possible pathways and mechanisms of action behind circulating serum metabolites with significant and potentially causal effects on hemorrhagic stroke using MetaboAnalyst 5.0[2] (35).

2.8 Meta-analysis and multivariate MR analysis

Aiming to make the final screening of circulating serum metabolites causally associated with hemorrhagic stroke comprehensive, precise, and constant, ICH and SAH in hemorrhagic stroke, we used four different GWAS data each. Then, a meta-analysis of the results of the IVW model was carried out using the R software package, followed by the screening of the corresponding P_{Meta}, with $P_{Meta} > 0.05$ removed. Meanwhile, we applied I^2 to perform the heterogeneity test of meta-results (36).

To adequately adjust for confounders, circulating serum metabolites after meta-analysis selection were further included as confounders (hypertension, obesity, alcohol consumption) in our MR analysis for multivariate MR analysis (MVMR). IVW, weighted median, and MR-Egger regression were also analyzed in the MVMR analysis. Besides, Egger-intercept and Cochran's *Q* tests were evaluated to assess the multiplicity and heterogeneity of the results (37).

2 https://www.metaboanalyst.ca/

2.9 Analysis software and packages

All the statistical analyses and data visualizations were performed using R software version 4.3.1. Bidirectional and multivariate MR analyses were implemented with the packages "TwoSampleMR" (26), "MR-PRESSO" (31), and "MendelianRandomization" (38); meta-analysis was done using the "meta" (39) package.

3 Results

3.1 Instrumental variables selection in causal analyses

Following rigorous instrumental variable selection rules and procedures, we performed MR analyses on 309 known circulating serum metabolites, acquiring IVs ranging from 3 to 485 SNPs. All selected SNPs had *F* values exceeding 10, showing instrumental solid efficacy.

3.2 Causal assessment of circulating metabolome leading to hemorrhagic stroke

Detailed results of the IVs and each method selected for positive MR analysis of 309 CSMs of known structure and function with HS are shown in their entirety in Supplementary Tables S3, S4, and the visualization of the results is available in Figures 2, 3. We judged that CSMs with IVW model $p < 0.05$ were positive for the presence of a causal effect, provided that the β values of the five analytical methods were in the same direction, and $P_{FDR} < 0.1$ were considered to have a significant causal effect.

As for the ICH results, following the above selection criteria, we identified a total of 39 positive CSMs in seven significant categories for the four ICH GWAS data, classified according to circulating serum metabolites, of which 18 were in Lipid, 9 in Amino acid, 3 in Peptide, 3 in Cofactors and vitamins, 3 in Xenobiotics, 1 in Carbohydrate, and 2 in Nucleotide. Corresponding β, OR, and *p* values can be searched in Supplementary Table S4 and Figure 2.

For the SAH results, with the same screening standard, we recognized 34 positive CSMs in six major categories for the four SAH GWAS data, according to the circulating serum metabolite classification, of which 18 belong to Lipid, 8 to Amino acid, 4 to Peptide, 2 to Carbohydrate, 1 to Cofactors and vitamins and 1 to Nucleotide. Matching β, OR, and *p* values are shown in Supplementary Table S2 and Figure 3.

Of the above 73 positive circulating serum metabolites after rectification (Figure 4), 7 of these ($P_{FDR} < 0.1$) were determined to be significant causative CSMs, ICH was the outcome for 4, namely pyroglutamylglycine in Peptide (OR 2.13, 95% CI 1.28–3.53, $p = 0.00348$, $P_{FDR} = 0.0939$), biliverdin in Cofactors and vitamins (OR 0.59, 95% CI 0.40–0.86, $p = 0.00679$, $P_{FDR} = 0.0883$), linoleate (18:2n6) in Lipid (OR 0.11, 95% CI 0.04–0.33, $p = 0.0000966$, $P_{FDR} = 0.0118$) and eicosenoate (20:1n9 or 11) (OR 0.26, 95% CI 0.13–0.52, $p = 0.000141$, $P_{FDR} = 0.00862$) in Lipid, and 3 for SAH as an ending, for gamma-glutamylmethionine* in Peptide(OR 3.25, 95% CI 1.51–7.00, $p = 0.00258$, $P_{FDR} = 0.0697$), 1-eicosadienoylglycerophosphocholine* in Lipid (OR 3.22, 95% CI 1.72–6.04, $p = 0.000255$, $P_{FDR} = 0.0311$) and 7-alpha-hydroxy-3-oxo-4-cholestenoate (7-Hoca) in Lipid (OR 0.13, 95% CI 0.04–0.42, $p = 0.000605$, $P_{FDR} = 0.0738$). The above results are presented in Table 1 and Figures 2–4, 5A.

3.3 Sensitivity tests in positive causal analysis

We did multiplicity and heterogeneity tests and leave-one-out analyses in the sensitivity analyses. MR-Egger regression intercepts were not significantly different from zero (all $P_{egger\text{-}intercept} > 0.05$) except for gamma-glutamylmethionine ($P_{egger\text{-}intercept} = 0.046$) for Peptide in FinnGen R7 SAH, in which the resulting causality was not plausible since there was horizontal multiplicity in this serum substance. The Cochran's Q test for heterogeneity *p*-values were all more than 0.05; after removing all outliers of X-14208-phenylalanylserine from Peptide in EBI SAH MR-PRESSO Global test P- values were more than 0.05, without significant heterogeneity and pleiotropy (Supplementary Tables S5, S6). Moreover, leave-one-out analysis demonstrated that no particular SNPs driving the correlation between CSMs and HS existed (Supplementary Table S7).

3.4 Genetic association assessment and directionality test for positive causality

Genetic correlation through linkage disequilibrium (LDSC), when assessing causality using circulating serum metabolites as exposures, indicated that 3-methylhistidine ($Rg = 1.199$, $SE_{Rg} = 0.543$, $P_{Rg} = 0.027$) as the outcome of FinnGen R7 ICH, ursodeoxycholate ($Rg = 1.026$, $SE_{Rg} = 0.475$, $P_{Rg} = 0.031$) as the outcome of FinnGen R5 ICH, gamma-glutamylvaline ($Rg = 0.580$, $SE_{Rg} = 0.285$, $P_{Rg} = 0.042$) as the outcome of FinnGen R9 SAH, guanosine ($Rg = 1.441$, $SE_{Rg} = 0.725$, $P_{Rg} = 0.047$) as the outcome of FinnGen R5 ICH, These four metabolites were genetically correlated with the outcome meaning that the results of the MR analysis mixed and coexisted with the genetic component, so the initially gained causality between them was not sufficiently robust, as well as some of the metabolites for which the genetic correlation was calculated to be negative, which we denoted as NA (Supplementary Table S8). Also, the directionality check Steiger test results implied that none of the reverse causality effects influenced the forward causality (Supplementary Table S5).

3.5 Alterations in the circulating metabolome after hemorrhagic stroke

Reverse MR analyses involving circulating serum metabolites as outcome to estimate causality included FinnGen R7 ICH as exposure to mannose (β 0.026, 95% CI 0.008–0.044, $p = 0.004$, $P_{FDR} = 0.065$), EBI ICH as exposure to taurochenodeoxycholate (β 0.063, 95% CI 0.016–0.109, $p = 0.008$, $P_{FDR} = 0.067$) and tetradecanedioate with EBI ICH as the exposure (β 0.047, 95% CI 0.013–0.080, $p = 0.007$, $P_{FDR} = 0.110$) were considered to have a causal effect, whereby the levels of the mentioned three metabolites increased after the occurrence of ICH (Supplementary Tables S9, S10). Also, we did not find heterogeneity and pleiotropy, nor were SNPs significantly correlated with the results in leave-one-out analysis (Supplementary Tables S11, S12).

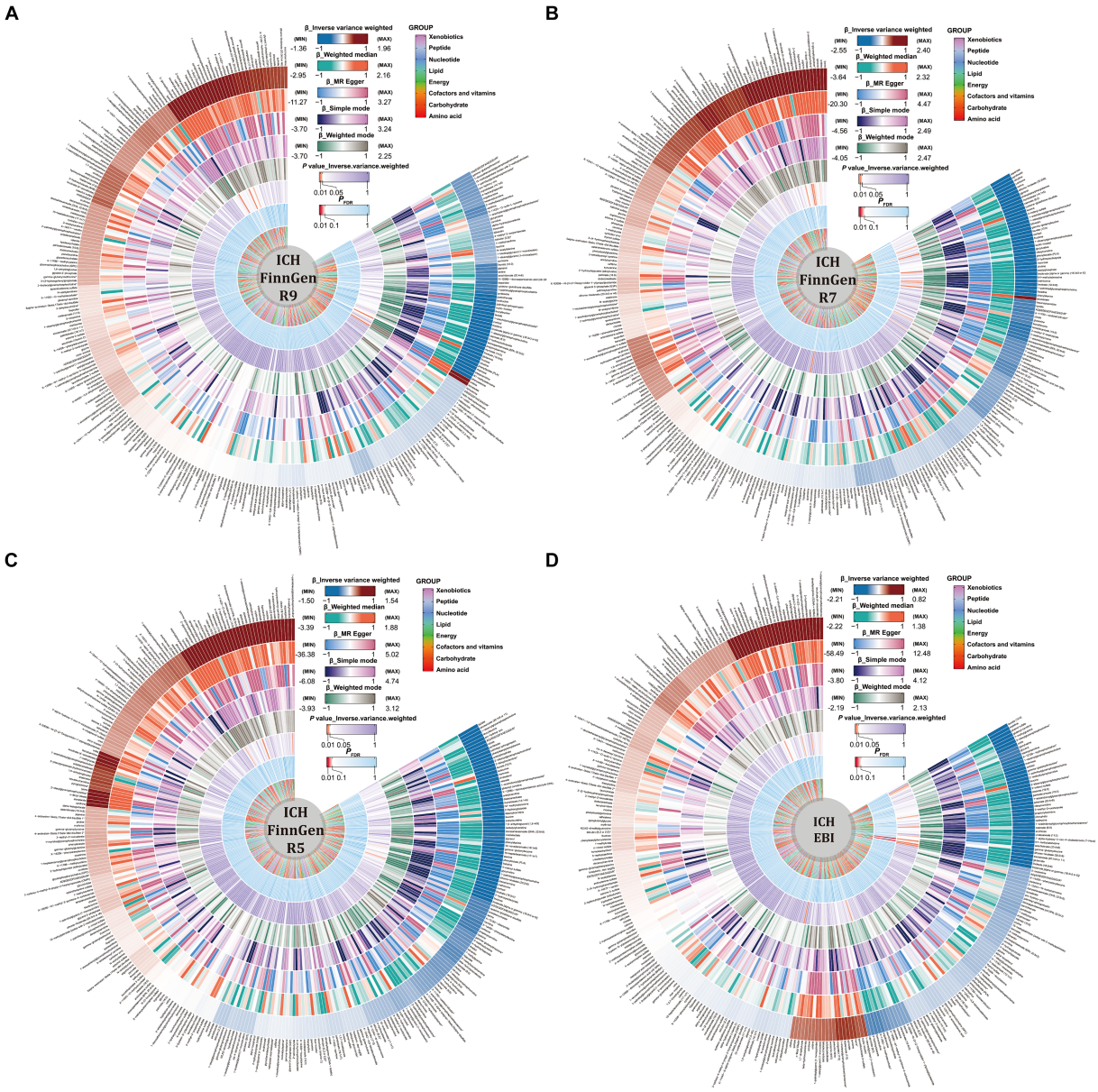

FIGURE 2
Causal relationships between circulating serum metabolites and intracerebral hemorrhage based on different data versions; respectively **(A)** FinnGen R9 **(B)** FinnGen R7 **(C)** FinnGen R5 **(D)** EBI database. From outside to inside, the β values of the five methods of inverse variance weighted (IVW), weighted median, MR egger, simple mode, weighted mode, the *p* values of IVW model, the P_{FDR}, and the metabolite species grouping are shown sequentially.

3.6 Effect pathway analysis of the circulating metabolome

By performing metabolic pathway analyses on GWAS data from 8 ICH and SAH as outcomes probing for causality, we characterized altogether 10 possible pathways of effect ($p < 0.05$), "Biosynthesis of unsaturated fatty acids" ($p = 0.00088$), "Linoleic acid metabolism" ($p = 0.02873$), "Ascorbate and aldarate metabolism" ($p = 0.04562$), "Porphyrin and chlorophyll metabolism" ($p = 0.00212$), and "Histidine metabolism" ($p = 0.04069$) might be the pathway mechanisms by which circulating serum metabolites contribute to the progression of ICH, while "Arginine biosynthesis" ($p = 0.02687$), "Glycine, serine and threonine metabolism" ($p = 0.00625$), "Aminoacyl-tRNA biosynthesis" ($p = 0.01301$), "Pantothenate and CoA biosynthesis "($p = 0.04818$) may be related to the SAH disease process, "Glycerophospholipid metabolism" ($p = 0.01705$ for EBI ICH, $p = 0.00742$ for FinnGen R7 SAH, $p = 0.00306$ for FinnGen R9 SAH) is a probable metabolite action pathway common to the development of ICH and SAH (Supplementary Table S13 and Figure 5B).

3.7 Meta-analyses based on multiple versions of hemorrhagic stroke

Aiming to further refine the exploration and evaluation of causal effects, we conducted a meta-analysis of the IVW model for each of

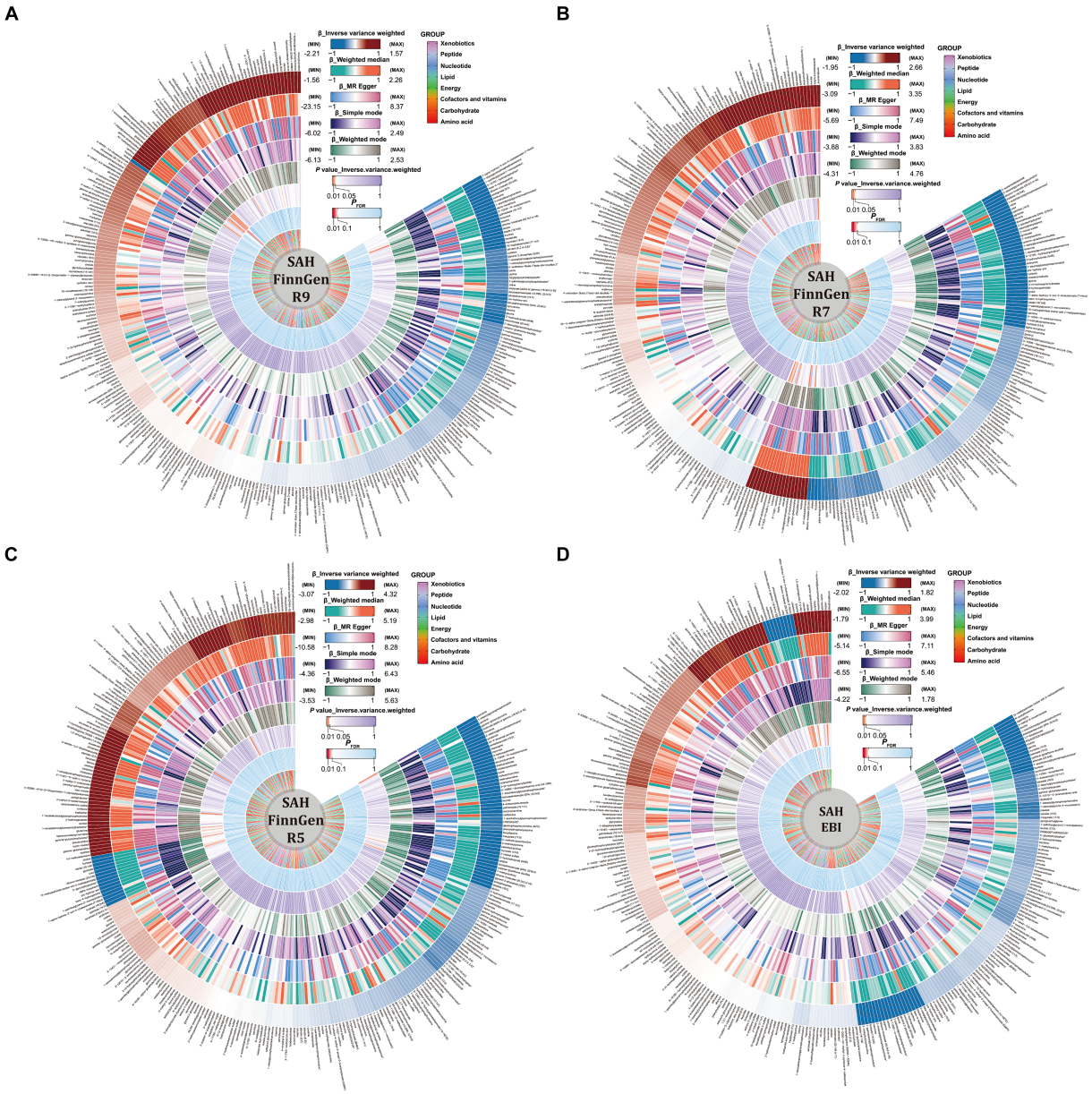

FIGURE 3
Causal relationships between circulating serum metabolites and subarachnoid hemorrhage based on different data versions; respectively **(A)** FinnGen R9 **(B)** FinnGen R7 **(C)** FinnGen R5 **(D)** EBI database. From outside to inside, the β values of the five methods of inverse variance weighted (IVW), weighted median, MR egger, simple mode, weighted mode, the *p* values of IVW model, the P_{FDR}, and the metabolite species grouping are shown sequentially.

the seven CSMs with significant causal associations with HS based on the results of the MR analyses of the four outcome data we selected, revealing that the results of biliverdin (OR 0.72, 95% CI 0.60–0.86, $P_{\text{random effects}} < 0.01$, $I^2 = 0\%$), pyroglutamylglycine (OR 1.83, 95% CI 1.24–2.72, $P_{\text{random effects}} < 0.01$, $I^2 = 40\%$), linoleate (18:2n6) (OR 0.23, 95% CI 0.12–0.46, $P_{\text{random effects}} < 0.01$, $I^2 = 4\%$) with a constant causal relationship between ICH, 1-eicosadienoylglycerophosphocholine* (OR 2.13, 95% CI 1.07–4.25, $P_{\text{random effects}} = 0.03$, $I^2 = 77\%$) (I^2 suggests that there is heterogeneity in this result, which needs to be interpreted with caution), gamma- glutamylmethionine* (OR 3.10, 95% CI 1.86–5.17, $P_{\text{random effects}} < 0.01$, $I^2 = 0\%$), 7-alpha-hydroxy-3-oxo-4-cholestenoate (7-Hoca) (OR 0.28, 95% CI 0.14–0.55, $P_{\text{random effects}} < 0.01$, $I^2 = 0\%$) stablely influenced the progression of SAH, while eicosenoate (20:1n9 or 11) (OR 0.59, 95% CI 0.30–1.17, $P_{\text{random effects}} = 0.13$, $I^2 = 67\%$) with ICH causality was not plausible, thus it will be excluded from the subsequent analysis (Figures 6A,B).

3.8 Removing confounding effects with multivariate MR analysis

To ensure that the eventually obtained CSMs directly influenced HS rather than through confounders, we incorporated alcohol consumption, hypertension, and obesity as confounders, using the respective types of HS data as the outcome and performing multivariate MR analyses considering them separately and collectively. The results

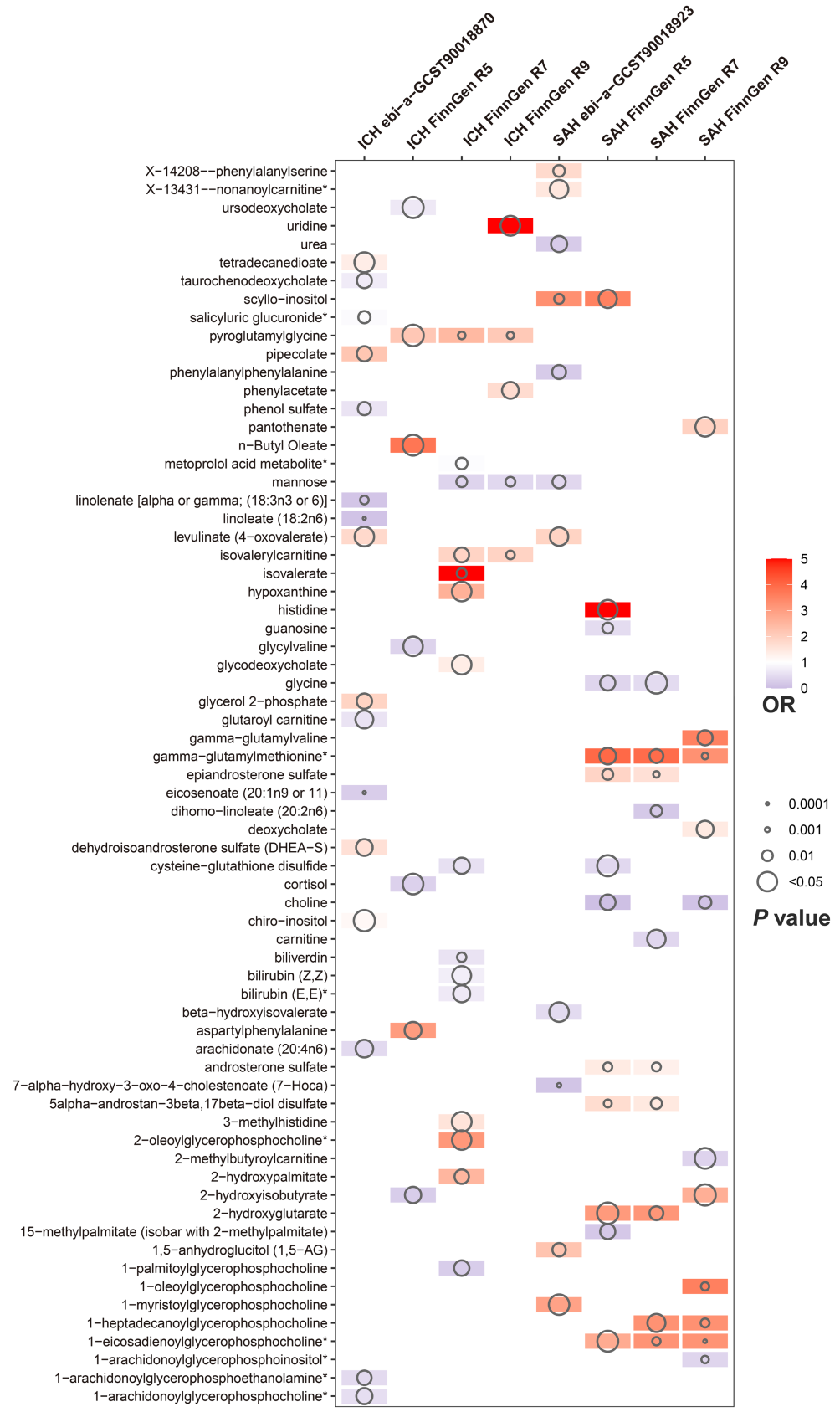

FIGURE 4
Circulating serum metabolites with causal effects on outcome in different versions of hemorrhagic stroke. Demonstrate the magnitude of ORs and *p*-values based on the IVW model. OR, odds ratio; IVW, inverse-variance weighted.

TABLE 1 Results of MR estimation of circulating serum metabolites significantly and causally associated with hemorrhagic stroke.

Hemorrhagic stroke/ outcome	Classification	Serum metabolites/ exposure	Resulting source dataset	nSNP	Method of MR	β	SE	*p*-value	OR (95%CI)	P_{FDR}
Intracerebral hemorrhage	Peptide	Pyroglutamylglycine	FinnGen R9	4	Inverse variance weighted	0.756	0.259	3.48E-03	2.129 (1.282–3.534)	9.39E-02
					Weighted median	0.592	0.337	7.95E-02	1.807 (0.933–3.502)	
					MR Egger	1.649	0.793	1.73E-01	5.204 (1.101–24.610)	
					Simple mode	0.534	0.410	2.83E-01	1.706 (0.764–3.808)	
					Weighted mode	0.565	0.354	2.09E-01	1.759 (0.879–3.522)	
	Cofactors and vitamins	Biliverdin	FinnGen R7	17	Inverse variance weighted	−0.528	0.195	6.79E-03	0.590 (0.403–0.865)	8.83E-02
					Weighted median	−0.517	0.232	2.62E-02	0.596 (0.378–0.941)	
					MR Egger	−0.353	0.328	2.99E-01	0.703 (0.369–1.337)	
					Simple mode	−1.461	0.558	1.87E-02	0.232 (0.078–0.693)	
					Weighted mode	−0.487	0.244	6.31E-02	0.614 (0.381–0.991)	
	Lipid	Linoleate (18:2n6)	ebi-a-GCST90018870	17	Inverse variance weighted	−2.206	0.566	9.66E-05	0.590 (0.403–0.865)	1.18E-02
					Weighted median	−2.220	0.811	6.21E-03	0.596 (0.378–0.941)	
					MR Egger	−2.988	2.166	1.88E-01	0.703 (0.369–1.337)	
					Simple mode	−2.108	1.388	1.48E-01	0.232 (0.078–0.693)	
					Weighted mode	−2.191	1.276	1.05E-01	0.614 (0.381–0.991)	
		Eicosenoate (20:1n9 or 11)		13	Inverse variance weighted	−1.360	0.357	1.41E-04	0.257 (0.127–0.517)	8.62E-03
					Weighted median	−1.481	0.507	3.49E-03	0.228 (0.084–0.614)	
					MR Egger	−0.938	0.950	3.44E-01	0.391 (0.061–2.517)	
					Simple mode	−1.822	0.898	6.52E-02	0.162 (0.028–0.940)	
					Weighted mode	−1.746	0.749	3.81E-02	0.175 (0.040–0.758)	
Subarachnoid hemorrhage	Peptide	Gamma-glutamylmethionine*	FinnGen R9	8	Inverse variance weighted	1.179	0.391	2.58E-03	3.251 (1.510–7.000)	6.97E-02
					Weighted median	1.110	0.538	3.90E-02	3.033 (1.058–8.698)	
					MR Egger	2.303	0.830	3.23E-02	10.007 (1.965–50.958)	
					Simple mode	0.969	0.769	2.48E-01	2.636 (0.584–11.904)	
					Weighted mode	1.096	0.711	1.67E-01	2.991 (0.743–12.045)	
	Lipid	1-Eicosadienoylglycerophosphocholine*		13	Inverse variance weighted	1.171	0.320	2.55E-04	3.224 (1.722–6.039)	3.11E-02
					Weighted median	1.300	0.456	4.41E-03	3.668 (1.499–8.972)	
					MR Egger	1.149	0.653	1.06E-01	3.156 (0.877–11.358)	
					Simple mode	1.644	0.681	3.26E-02	5.175 (1.363–19.653)	
					Weighted mode	1.524	0.545	1.62E-02	4.591 (1.577–13.369)	
		7-Alpha-hydroxy-3-oxo-4-cholestenoate (7-Hoca)	ebi-a-GCST90018923	16	Inverse variance weighted	−2.021	0.589	6.05E-04	0.132 (0.042–0.421)	7.38E-02
					Weighted median	−1.789	0.811	2.74E-02	0.167 (0.034–0.820)	
					MR Egger	−2.226	1.639	1.96E-01	0.108 (0.004–2.680)	
					Simple mode	−1.575	1.239	2.23E-01	0.207 (0.018–2.348)	
					Weighted mode	−1.710	1.114	1.46E-01	0.181 (0.020–1.607)	

SE, standard error; OR, odds ratio; SNP, single nucleotide polymorphism; FDR, false discovery rate.

10.3389/fnut.2024.1376889

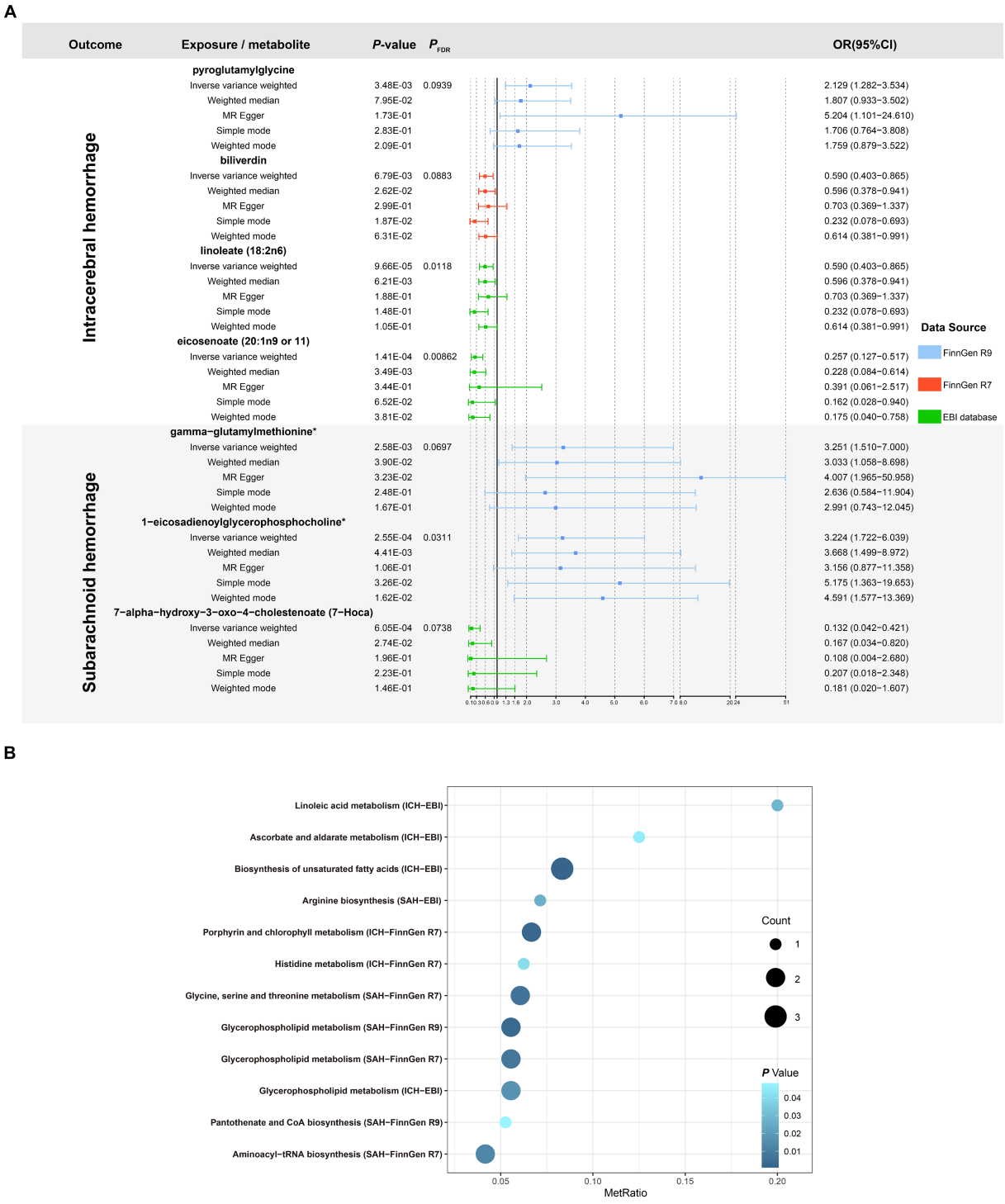

FIGURE 5
(A) Forest plot of five MR analysis methods for circulating serum metabolites significantly and causally associated with hemorrhagic stroke.
(B) Significant metabolic pathways enriched based on different versions of hemorrhagic stroke outcome. MetRatio = Metabolites enriched/Total number of metabolites in the metabolic pathway.

of the separate analyses are presented in Supplementary Table S14, and the results of the collective studies are shown in Table 2 and Figure 6C. In summary, four CSMs were identified that directly contributed to HS, of which biliverdin belonging to Cofactors and vitamins and linoleate (18:2n6) belonging to lipid were potential protective factors for ICH, while 1-eicosadienoylglycerophosphocholine* belonging to lipid and 7- alpha-hydroxy-3-oxo-4-cholestenoate (7-Hoca) belonging to lipid, the former being a possible risk factor for SAH and the latter a potential protective factor for SAH (Figure 7). We similarly conducted the Cochran's Q test for MVMR analysis (Multivariable IVW and Multivariable MR-Egger) and MR-Egger's intercept without potential heterogeneity and multiplicity (Supplementary Table S15).

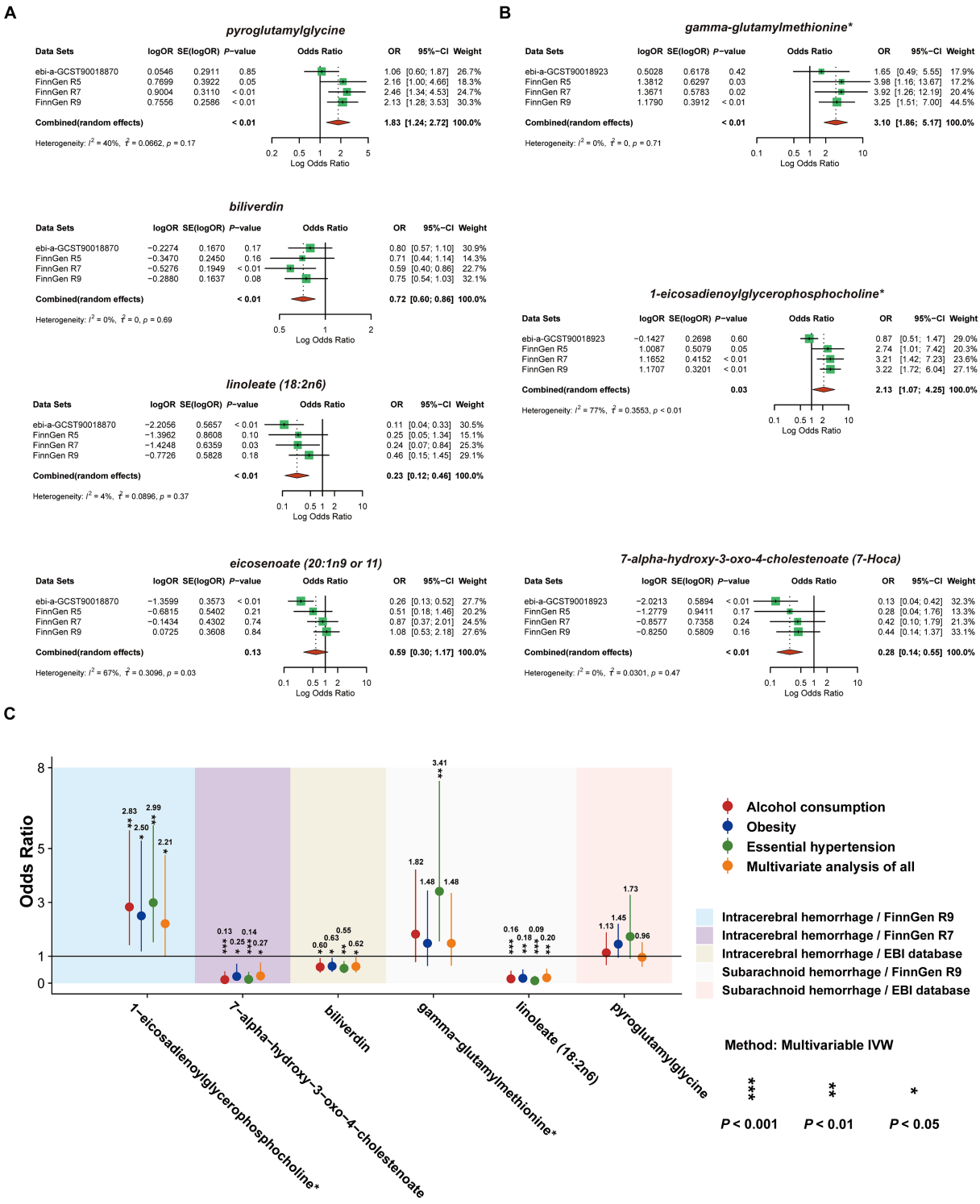

FIGURE 6
Meta-analysis of circulating serum metabolites with significant causality based on four versions of the outcome IVW model. Of these, **(A)** with ICH as the outcome **(B)** with SAH as the outcome. **(C)** De-confounded multivariate MR analysis incorporating alcohol consumption, obesity, and essential hypertension.

4 Discussion

For this study, we selected to explore the causal associations between 309 known CSMs and HS by using eight different large GWAS datasets on hemorrhagic stroke. We performed several bidirectional two-sample MR analyses, combined with robustness checks of the results, after correction for *p*-values, Pyroglutamylglycine (Peptide), biliverdin (Cofactors and vitamins), linoleate (18:2n6) (Lipid), eicosenoate (20:1n9 or 11) (Lipid), gamma-glutamylmethionine*(Peptide),

TABLE 2 Results of multivariable MR estimation of circulating serum metabolites and hemorrhagic stroke.

Type of outcome	Classification	Type/metabolism	nSNP	Methods of multivariable MR	β	SE	*p*-value	OR (95%CI)
Intracerebral hemorrhage/ FinnGen R9	Peptide	Pyroglutamylglycine	101	Multivariable IVW	−0.037	0.232	8.73E-01	0.96 (0.61–1.52)
				Multivariable median	0.164	0.303	5.89E-01	1.18 (0.65–2.13)
				Multivariable egger	0.002	0.234	9.93E-01	1.00 (0.63–1.59)
Intracerebral hemorrhage/ FinnGen R7	Cofactors and vitamins	Biliverdin	114	Multivariable IVW	−0.476	0.219	3.01E-02	0.62 (0.40–0.96)
				Multivariable median	−0.510	0.255	4.55E-02	0.60 (0.36–0.99)
				Multivariable egger	−0.448	0.220	4.19E-02	0.64 (0.42–0.98)
Intracerebral hemorrhage/ EBI database	Lipid	Linoleate (18:2n6)	105	Multivariable IVW	−1.599	0.503	1.48E-03	0.20 (0.08–0.54)
				Multivariable median	−1.641	0.699	1.88E-02	0.19 (0.05–0.76)
				Multivariable egger	−1.540	0.507	2.38E-03	0.21 (0.08–0.58)
Subarachnoid hemorrhage/ FinnGen R9	Peptide	Gamma-glutamylmethionine*	105	Multivariable IVW	0.391	0.417	3.47E-01	1.48 (0.65–3.35)
				Multivariable median	0.066	0.513	8.98E-01	1.07 (0.39–2.92)
				Multivariable egger	0.413	0.416	3.21E-01	1.51 (0.67–3.42)
Subarachnoid hemorrhage/ FinnGen R9	Lipid	1-Eicosadienoylglycerophosphocholine*	108	Multivariable IVW	0.792	0.392	4.35E-02	2.21 (1.02–4.76)
				Multivariable median	1.389	0.506	6.07E-03	4.01 (1.49–10.81)
				Multivariable egger	0.840	0.391	3.17E-02	2.32 (1.08–4.99)
Subarachnoid hemorrhage/ EBI database		7-Alpha-hydroxy-3-oxo-4-cholestenoate (7-Hoca)	119	Multivariable IVW	−1.322	0.543	1.48E-02	0.27 (0.09–0.77)
				Multivariable median	−1.461	0.740	4.83E-02	0.23 (0.05–0.99)
				Multivariable egger	−1.322	0.543	1.48E-02	0.27 (0.09–0.77)

SE, standard error; OR, odds ratio; SNP, single nucleotide polymorphism.

1-eicosadienoylglycerophosphocholine* (Lipid), 7-alpha-hydroxy-3-oxo-4-cholestenoate (7-Hoca) (Lipid), these 7 CSMs were recognized as having a significant causal link with HS. Subsequently, we made use of meta-analysis to thoroughly investigate the causal relationships of these CSMs with distinct versions of hemorrhagic stroke. We found that the relevance of eicosenoate (20:1n9 or 11) (Lipid) to the outcome became insignificant. Moreover, we conducted multivariate MR analysis to remove potential confounders. Ultimately, we identified four CSMs that had significant causality with HS. Specifically, biliverdin (Cofactors and vitamins) and linoleate (18:2n6) (lipid) can serve as protective factors for ICH, and increased levels of 1-eicosadienoylglycerophosphocholine* (lipid) raise the risk of SAH. In contrast, high levels of 7-alpha-hydroxy-3-oxo-4-cholestenoate (7-Hoca) (lipid) lower the risk of SAH. Besides, we also appraised the genetic correlation through LDSC from CSMs and HS to clarify the coexistence of inherited effects, strengthening the reliability of our findings. Finally, metabolic pathway analysis was applied to find ten potential action pathways binding the two, including a shared path (glycerophospholipid metabolism) that CSMs act on both ICH and SAH. In recent similar studies, Wang et al. (40) focused on the effect of selected serum metabolites produced by gut flora on stroke, and our attention is centered on the role of the more comprehensive circulating metabolome on the mechanisms of hemorrhagic stroke. Zhang et al. conducted a broad and general

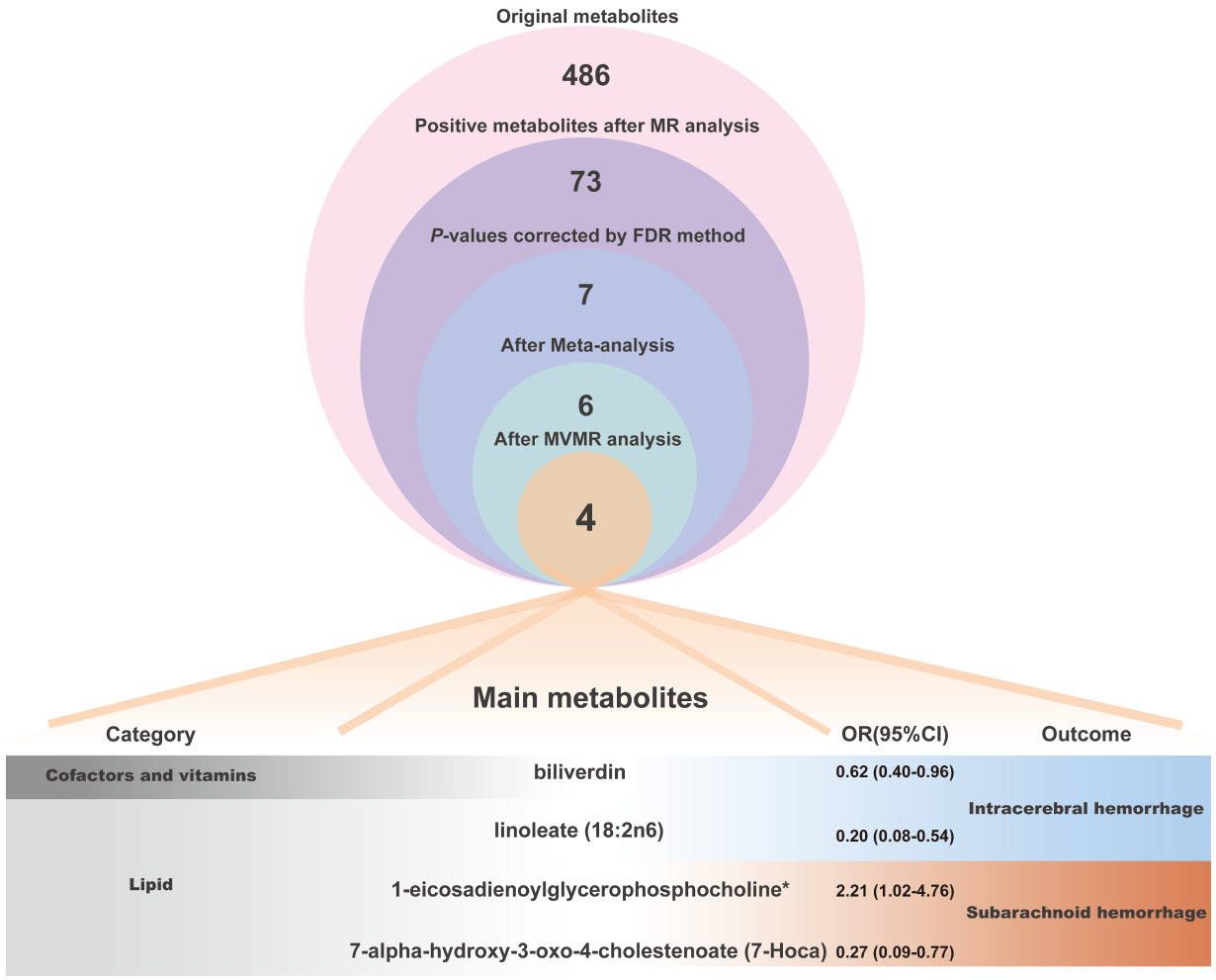

FIGURE 7
The analytical procedure and detailed information (category, OR values and outcome of action) of the 4 main metabolites were eventually obtained.

exploration of the causal relationship between serum metabolites and various subtypes of stroke, including hemorrhagic and ischemic stroke (41). While existing studies lack in-depth studies on each of these subtypes, our research focusing on hemorrhagic stroke fills this gap. We used multiple versions rather than a single version of the ending data to comprehensively analyze the causality, then combined the results of the individual versions utilizing meta-analysis, followed by the MVMR method to remove the interference of common confounders associated with HS, and the interlocking analyses led us to obtain a wealthy and robust causal relationship between CSMs and HS. We believe that the circulating serum metabolites discovered in this comprehensive study can offer assistance in the prevention, treatment, and deeper mechanistic investigation of hemorrhagic stroke.

Recently, a large cohort study that explored the association of L-alpha glycerylphosphorylcholine (α-GPC) with the risk of subsequent stroke at 10 years noted a higher hazard of hemorrhagic stroke in α-GPC users compared to non-users, after adjusting for traditional cerebrovascular risk factors (42). This indicates that exogenous metabolites can influence the occurrence of HS in the form of altered intake in a dose–response manner. In a meta-analysis of 26 prospective cohort studies and 12 randomized controlled trials, fish and long chain omega 3 fatty acids intake were found to be moderately negatively related to cerebrovascular risk (43). Fish can supply a wealth of diverse nutrients which, upon entering the body, make their transformation into a variety of metabolites entering the circulatory system and thereby intervening in the occurrence of cerebrovascular events, suggesting that HS is also capable of being interfered with by variations in the categories and concentrations of circulating metabolites due to food intake. As for endogenous circulating metabolites, current findings demonstrate that greater circulating concentrations of vitamin D correlate with a lower incidence of cerebrovascular disease, whereas higher levels of circulating calcium relate to an increased risk of cerebrovascular disease (44). Conversely, the post-HS CSMs also altered correspondingly. Reduced plasma concentrations of L-arginine in patients early after intracerebral hemorrhage were identified as an independent risk factor for poor outcomes (45). Meanwhile, following subarachnoid hemorrhage, nitric oxide metabolites nitrite and nitrate levels are also markedly elevated (46–48). The aforementioned discoveries confirm that CSMs and HS share a reciprocal impact. During our study, we initially identified 73 CSMs that were causally associated with HS; combined with reverse MR, we found similar mannose (carbohydrate), taurochenodeoxycholate (lipid), and tetradecanedioate (lipid), three metabolites that are capable of interfering with ICH. Mannose and

taurochenodeoxycholate serve as potential protective factors for ICH, and tetradecanedioate is a potentially hazardous element in ICH. Following the occurrence of ICH, the level of all three rises. Mannose synthesizes glycoproteins and participates in immunomodulation as a widely distributed monosaccharide in body fluids and tissues (49). Hence, it is upregulated after the onset of ICH as a timely energy supplier and immunomodulator. Taurochenodeoxycholate has been linked to the inhibition of cell death (50) and, in turn, may act as a neuroprotective factor that is activated upon the rise of stress following the development of ICH. Regarding tetradecanedioate, the pathway mediating FA β-oxidation, peroxisomal FA β-oxidation or FA α-oxidation may damage vascular components contributing to ICH (51), Whereas, once ICH occurs, it might remain persistently elevated owing to its complex biological functions for example *in vivo* transporter protein assessment of biomarkers (52).

We further adjusted for common confounders of hemorrhagic stroke via multivariate MR analysis, which ultimately identified four metabolites having significant causal effects. To begin with, biliverdin (cofactors and vitamins) was characterized as an ICH protective element. It acts as a by-product of heme degradation, and numerous studies have confirmed that its biological functions are tightly linked to anti-inflammatory, anti-apoptotic, and anti-oxidative stress (53). Moreover, it also inhibits the expression of the pro-inflammatory cytokines interleukin 1β, tumor necrosis factor α, and interleukin 6 to achieve an anti-inflammatory role (54). Studies have shown that the anti-oxidative stress effect of biliverdin (cofactors and vitamins) can be accomplished by scavenging superoxide (55); meanwhile, biliverdin protects vascular tissue from vessel damage by reducing c-Jun NH2 terminal kinase activation and preventing endothelial cell apoptosis (56); additionally, it regulates the Nrf2/A20/eEF1A2 axis to suppress cellular death and thereby attenuates cerebral ischemia–reperfusion injury (57). However, the main mechanisms involved in the pathogenesis of ICH include damage to the cerebral vascular wall, vitellosis, and lipid deposition (4); in the latest study, oxidative stress erythrocyte-associated erythrocyte-brain endothelial interactions that can induce microglia activation *in vivo* also lead to cerebral hemorrhage (58). In summary, biliverdin probably blocks the occurrence and progression of ICH by decreasing vascular inflammation and cellular pyroptosis caused by the release of cellular inflammatory factors, preventing vascular endothelial apoptosis and oxidative stress in erythrocytes. Linoleate (18:2n6) (lipid) is likewise recognized as a protection factor for ICH by us, and it is an n-6 polyunsaturated fatty acid essential for average growth and development. It is found in low concentrations within the brain (<2% of total fatty acids). It constitutes a necessary precursor to benign fatty acids and arachidonic acid in the brain, which has important implications for neurodevelopment and the regulation of pain and inflammatory signaling in peripheral tissues (59). The bio function of linoleate (18:2n6) is more sophisticated. There is a belief that long-term consumption of a low-level linoleate diet might protect the brain from inflammation. It has been found that a dietary structure in which linoleate is completely deprived for an extended period leads to a rapid loss of the beneficial components of ceruloplasmin in the rat brain and, conversely, an accumulation of anti-inflammatory lipids in the rat brain following low intake of linoleate. In contrast, excessive intake promotes neuroinflammation in the rats (60, 61). The genotype is closely related to how linoleate exerts inflammatory and metabolic responses in the human body (62). Briefly, linoleate (18:2n6) may act as an ICH protective factor through an anti-inflammatory mechanism of action, but long-term low-level intake is required to fulfill this conclusion. When ingested in excess over time, it could become a risk factor for ICH by enhancing the inflammatory response. Therefore, more in-depth mechanisms need to be investigated further.

SAH usually occurs in association with aneurysm rupture, and the mechanisms behind it are primarily hemodynamic stress and vascular wall injury with inhibition of its repair (5). Apart from the significant discovery of ICH and circulating serum metabolites, we have also identified circulating serum metabolites relevant to SAH. Our analysis showed that 1-eicosadienoylglycerophosphocholine* (lipid) promoted SAH. 1-eicosadienoylglycerophosphocholine*, alias lysophosphatidylcholine (20:2), a cleavage product of phosphatidylcholine, and in addition, lysophosphatidylcholine (20:2) (LPC) plays a critical role in promoting the progression of atherosclerosis and other cardiovascular diseases by affecting endothelial cells, vascular smooth muscle cells, and arteries (63). LPC is recognized as a significant component of oxidatively damaged low-density lipoprotein (oxLDL), which induces migration of lymphocytes and macrophages, increases the production of pro-inflammatory cytokines, and can aggregate inflammation, trigger oxidative stress, and promote apoptosis. On the other hand, it activates NLRP3 and NLRC4 inflammatory vesicles in microglia and astrocytes. It also synergizes with Procaspase-1 to induce activation of the ROS promoter CYP1B1 and a robust inflammatory response in human arterial endothelial cells (64, 65). Furthermore, lysophosphatidylcholine (20:2), besides inducing oxidative stress in human endothelial cells through NOX5-mediated increases in intracellular calcium (66), also activated voltage-dependent calcium channels to increase calcium influx and enhanced 5-HT-induced contraction of vascular smooth muscle cells in umbilical arteries (67). These micro-mechanisms provide more evidence that LPC can result in cerebral neurovascular inflammatory injury, oxidative stress, and rapid hemodynamic changes, consistent with our results. Hence, elevated levels of 1-eicosadienoylglycerophosphocholine* are likely to be the mechanism behind the development of SAH. 7-Hoca is a naturally existing cholesterol metabolite in human blood, produced by the metabolism of 7α-hydroxy-4-cholestene-3-one and 27-hydroxycholesterol in the brain. It is also an intermediate metabolite in the synthesis of bile acids (BA) (68). A significant rise in the concentration of 7-Hoca after SAH was observed (69); while the conversion of 27-hydroxycholesterol to 7-Hoca is an essential mechanism for the elimination of preoxidized sterols of the brain, 27-hydroxycholesterol has been implicated in the protection of both brain and cognition after injury (70). From this, the increase in 7-Hoca after SAH may indicate accelerated metabolism of 27-hydroxycholesterol to mediate cerebral protection. BA, a downstream product of 7-Hoca, could lower plasma triglycerides by inhibiting hepatic SREBP-1c expression or modulating glucose-induced adipogenesis. Meanwhile, BA's activation of the farnesoid X receptor (FXR) improved dyslipidemia in mice (71). So, 7-Hoca might be a metabolite acting as a cerebroprotective agent. Therefore, we consider that 7-Hoca exerts a potential protective function in SAH primarily via abolishing 27-hydroxycholesterol and facilitating BA as a downstream product, thereby mediating lipid regulation. Yet more direct mechanisms of action require more thorough exploration.

Although we have done complete and systematic research, some limitations remain. Firstly, the sources we chose for the dataset are all European, with results that are not guaranteed in terms of population generalizability. Secondly, to obtain a sufficient number of SNPs for MR analysis of the exposure data, we slightly liberalized the filtering criteria; this may have made the IVs less effective, although it is common practice among other studies, And the fact that the IVs we got are all strong instrumental variables and the directionality test has no wrong causal direction also strengthens the credibility of our results in some extent. Lastly, we have examined many metabolites of recognized functional structure, yet many unknown circulating serum metabolites could not be researched. Nevertheless, we went through a series of rigorous and comprehensive MR analyses, which led to the identification of a reliable causal relationship, which can provide a high reference value for carrying out more in-depth interaction research between CSMs and HS.

5 Conclusion

In conclusion, we comprehensively and systematically evaluated the causality among circulating serum metabolites and hemorrhagic stroke utilizing MR analysis. Four circulating serum metabolites with statistically significant and robust causal effects with hemorrhagic stroke were eventually identified. Of these, biliverdin and linoleate (18:2n6) are capable of decreasing the risk of ICH, 1-eicosadienoylglycerophosphocholine* is a hazard factor for SAH and 7-Hoca is a protective element for SAH, the mediation of inflammation, oxidative stress, apoptosis, lipid homeostasis and hemodynamics are the likely mechanisms for the action of these metabolites. Additionally, another ten notable metabolic pathways have been characterized. These results suggest that these metabolites might be considered biomarkers for HS prevention and monitoring and also provide some references and assistance for future research on the selection of circulating metabolites and the exploration of the mechanism of preventive and curative targets.

Data availability statement

The original contributions presented in the study are included in the article/Supplementary material, further inquiries can be directed to the corresponding authors.

Author contributions

YW: Conceptualization, Investigation, Visualization, Writing – original draft, Writing – review & editing. YS: Data curation, Software, Visualization, Writing – original draft, Writing – review & editing. QL: Resources, Software, Writing – review & editing. HX: Data curation, Investigation, Resources, Writing – review & editing. AG: Data curation, Investigation, Methodology, Writing – original draft. KL: Conceptualization, Investigation, Software, Writing – review & editing. YR: Data curation, Methodology, Resources, Writing – review & editing. SG: Methodology, Resources, Writing – review & editing. HL: Funding acquisition, Supervision, Writing – review & editing. XZ: Funding acquisition, Supervision, Writing – review & editing.

Funding

The author(s) declare financial support was received for the research, authorship, and/or publication of this article. This work was supported by the National Natural Science Foundations of China (nos. 82271340, 82071368) and the Outstanding Youth Funding of Harbin Medical University (no. HYD2020JQ0016).

Acknowledgments

We thank the researchers and volunteers who participated in the study, FinnGen, EBI, and all the joint studies for making their data publicly available.

Conflict of interest

The authors declare that the research was conducted in the absence of any commercial or financial relationships that could be construed as a potential conflict of interest.

Publisher's note

Supplementary material

The Supplementary material for this article can be found online at: https://www.frontiersin.org/articles/10.3389/fnut.2024.1376889/full#supplementary-material

References

1. Campbell BCV, Khatri P. Stroke. *Lancet (London, England)*. (2020) 396:129–42. doi: 10.1016/S0140-6736(20)31179-X

2. Owolabi MO, Thrift AG, Mahal A, Ishida M, Martins S, Johnson WD, et al. Primary stroke prevention worldwide: translating evidence into action. *Lancet Public Health*. (2022) 7:e74–85. doi: 10.1016/S2468-2667(21)00230-9

3. Ohashi SN, DeLong JH, Kozberg MG, Mazur-Hart DJ, van Veluw SJ, Alkayed NJ, et al. Role of inflammatory processes in hemorrhagic stroke. *Stroke*. (2023) 54:605–19. doi: 10.1161/STROKEAHA.122.037155

4. Sheth KN. Spontaneous intracerebral hemorrhage. *N Engl J Med*. (2022) 387:1589–96. doi: 10.1056/NEJMra2201449

5. Claassen J, Park S. Spontaneous subarachnoid haemorrhage. *Lancet (London, England)*. (2022) 400:846–62. doi: 10.1016/S0140-6736(22)00938-2

6. Diener C, Dai CL, Wilmanski T, Baloni P, Smith B, Rappaport N, et al. Genome-microbiome interplay provides insight into the determinants of the human blood metabolome. *Nat Metab*. (2022) 4:1560–72. doi: 10.1038/s42255-022-00670-1

7. Johnson CH, Ivanisevic J, Siuzdak G. Metabolomics: beyond biomarkers and towards mechanisms. *Nat Rev Mol Cell Biol*. (2016) 17:451–9. doi: 10.1038/nrm.2016.25

8. Hu JR, Coresh J, Inker LA, Levey AS, Zheng Z, Rebholz CM, et al. Serum metabolites are associated with all-cause mortality in chronic kidney disease. *Kidney Int*. (2018) 94:381–9. doi: 10.1016/j.kint.2018.03.008

9. Nathan JA. Metabolite-driven antitumor immunity. *Science (New York, NY)*. (2022) 377:1488–9. doi: 10.1126/science.ade3697

10. Floegel A, Kühn T, Sookthai D, Johnson T, Prehn C, Rolle-Kampczyk U, et al. Serum metabolites and risk of myocardial infarction and ischemic stroke: a targeted metabolomic approach in two German prospective cohorts. *Eur J Epidemiol*. (2018) 33:55–66. doi: 10.1007/s10654-017-0333-0

11. Crunkhorn S. Lipid metabolite triggers neural repair. *Nat Rev Drug Discov*. (2023) 22:787. doi: 10.1038/d41573-023-00142-5

12. Liu P, Li R, Antonov AA, Wang L, Li W, Hua Y, et al. Discovery of metabolite biomarkers for acute ischemic stroke progression. *J Proteome Res*. (2017) 16:773–9. doi: 10.1021/acs.jproteome.6b00779

13. Vojinovic D, Kalaoja M, Trompet S, Fischer K, Shipley MJ, Li S, et al. Association of circulating metabolites in plasma or serum and risk of stroke: meta-analysis from seven prospective cohorts. *Neurology*. (2020) 96:e1110–23. doi: 10.1212/WNL.0000000000011236

14. Kimberly WT, Wang Y, Pham L, Furie KL, Gerszten RE. Metabolite profiling identifies a branched chain amino acid signature in acute cardioembolic stroke. *Stroke*. (2013) 44:1389–95. doi: 10.1161/STROKEAHA.111.000397

15. Larsson SC, Butterworth AS, Burgess S. Mendelian randomization for cardiovascular diseases: principles and applications. *Eur Heart J*. (2023) 44:4913–24. doi: 10.1093/eurheartj/ehad736

16. Emdin CA, Khera AV, Kathiresan S. Mendelian randomization. *JAMA*. (2017) 318:1925–6. doi: 10.1001/jama.2017.17219

17. Skrivankova VW, Richmond RC, Woolf BAR, Yarmolinsky J, Davies NM, Swanson SA, et al. Strengthening the reporting of observational studies in epidemiology using Mendelian randomization: the STROBE-MR statement. *JAMA*. (2021) 326:1614–21. doi: 10.1001/jama.2021.18236

18. Shin S-Y, Fauman EB, Petersen A-K, Krumsiek J, Santos R, Huang J, et al. An atlas of genetic influences on human blood metabolites. *Nat Genet*. (2014) 46:543–50. doi: 10.1038/ng.2982

19. Sakaue S, Kanai M, Tanigawa Y, Karjalainen J, Kurki M, Koshiba S, et al. A cross-population atlas of genetic associations for 220 human phenotypes. *Nat Genet*. (2021) 53:1415–24. doi: 10.1038/s41588-021-00931-x

20. Sanna S, van Zuydam NR, Mahajan A, Kurilshikov A, Vich Vila A, Võsa U, et al. Causal relationships among the gut microbiome, short-chain fatty acids and metabolic diseases. *Nat Genet*. (2019) 51:600–5. doi: 10.1038/s41588-019-0350-x

21. Long Y, Tang L, Zhou Y, Zhao S, Zhu H. Causal relationship between gut microbiota and cancers: a two-sample Mendelian randomisation study. *BMC Med*. (2023) 21:66. doi: 10.1186/s12916-023-02761-6

22. Gu Y, Jin Q, Hu J, Wang X, Yu W, Wang Z, et al. Causality of genetically determined metabolites and metabolic pathways on osteoarthritis: a two-sample mendelian randomization study. *J Transl Med*. (2023) 21:357. doi: 10.1186/s12967-023-04165-9

23. Pierce BL, Burgess S. Efficient design for Mendelian randomization studies: subsample and 2-sample instrumental variable estimators. *Am J Epidemiol*. (2013) 178:1177–84. doi: 10.1093/aje/kwt084

24. Bowden J, Davey Smith G, Haycock PC, Burgess S. Consistent estimation in Mendelian randomization with some invalid instruments using a weighted median estimator. *Genet Epidemiol*. (2016) 40:304–14. doi: 10.1002/gepi.21965

25. Hartwig FP, Davey Smith G, Bowden J. Robust inference in summary data Mendelian randomization via the zero modal pleiotropy assumption. *Int J Epidemiol*. (2017) 46:1985–98. doi: 10.1093/ije/dyx102

26. Hemani G, Zheng J, Elsworth B, Wade KH, Haberland V, Baird D, et al. The MR-base platform supports systematic causal inference across the human phenome. *eLife*. (2018) 7:7. doi: 10.7554/eLife.34408

27. Bowden J, Davey Smith G, Burgess S. Mendelian randomization with invalid instruments: effect estimation and bias detection through Egger regression. *Int J Epidemiol*. (2015) 44:512–25. doi: 10.1093/ije/dyv080

28. Chen X, Kong J, Diao X, Cai J, Zheng J, Xie W, et al. Depression and prostate cancer risk: a Mendelian randomization study. *Cancer Med*. (2020) 9:9160–7. doi: 10.1002/cam4.3493

29. Storey JD, Tibshirani R. Statistical significance for genomewide studies. *Proc Natl Acad Sci USA*. (2003) 100:9440–5. doi: 10.1073/pnas.1530509100

30. Cohen JF, Chalumeau M, Cohen R, Korevaar DA, Khoshnood B, Bossuyt PM. Cochran's Q test was useful to assess heterogeneity in likelihood ratios in studies of diagnostic accuracy. *J Clin Epidemiol*. (2015) 68:299–306. doi: 10.1016/j.jclinepi.2014.09.005

31. Verbanck M, Chen CY, Neale B, Do R. Detection of widespread horizontal pleiotropy in causal relationships inferred from Mendelian randomization between complex traits and diseases. *Nat Genet*. (2018) 50:693–8. doi: 10.1038/s41588-018-0099-7

32. Ye X, Liu B, Bai Y, Cao Y, Lin S, Lyu L, et al. Genetic evidence strengthens the bidirectional connection between gut microbiota and periodontitis: insights from a two-sample Mendelian randomization study. *J Transl Med*. (2023) 21:674. doi: 10.1186/s12967-023-04559-9

33. O'Connor LJ, Price AL. Distinguishing genetic correlation from causation across 52 diseases and complex traits. *Nat Genet*. (2018) 50:1728–34. doi: 10.1038/s41588-018-0255-0

34. Hindy G, Engström G, Larsson SC, Traylor M, Markus HS, Melander O, et al. Role of blood lipids in the development of ischemic stroke and its subtypes: a Mendelian randomization study. *Stroke*. (2018) 49:820–7. doi: 10.1161/STROKEAHA.117.019653

35. Xia J, Psychogios N, Young N, Wishart DS. MetaboAnalyst: a web server for metabolomic data analysis and interpretation. *Nucleic Acids Res*. (2009) 37:W652–60. doi: 10.1093/nar/gkp356

36. Arya S, Schwartz TA, Ghaferi AA. Practical guide to Meta-analysis. *JAMA Surg*. (2020) 155:430–1. doi: 10.1001/jamasurg.2019.4523

37. D'Urso S, Arumugam P, Weider T, Hwang LD, Bond TA, Kemp JP, et al. Mendelian randomization analysis of factors related to ovulation and reproductive function and endometrial cancer risk. *BMC Med*. (2022) 20:419. doi: 10.1186/s12916-022-02585-w

38. Yavorska OO, Burgess S. MendelianRandomization: an R package for performing Mendelian randomization analyses using summarized data. *Int J Epidemiol*. (2017) 46:1734–9. doi: 10.1093/ije/dyx034

39. Bertrand A, Kostine M, Barnetche T, Truchetet ME, Schaeverbeke T. Immune related adverse events associated with anti-CTLA-4 antibodies: systematic review and meta-analysis. *BMC Med*. (2015) 13:211. doi: 10.1186/s12916-015-0455-8

40. Wang Q, Dai H, Hou T, Hou Y, Wang T, Lin H, et al. Dissecting causal relationships between gut microbiota, blood metabolites, and stroke: a Mendelian randomization study. *Journal of stroke*. (2023) 25:350–60. doi: 10.5853/jos.2023.00381

41. Zhang T, Cao Y, Zhao J, Yao J, Liu G. Assessing the causal effect of genetically predicted metabolites and metabolic pathways on stroke. *J Transl Med*. (2023) 21:822. doi: 10.1186/s12967-023-04677-4

42. Lee G, Choi S, Chang J, Choi D, Son JS, Kim K, et al. Association of L-α Glycerylphosphorylcholine with subsequent stroke risk after 10 years. *JAMA Netw Open*. (2021) 4:e2136008. doi: 10.1001/jamanetworkopen.2021.36008

43. Chowdhury R, Stevens S, Gorman D, Pan A, Warnakula S, Chowdhury S, et al. Association between fish consumption, long chain omega 3 fatty acids, and risk of cerebrovascular disease: systematic review and meta-analysis. *BMJ*. (2012) 345:e6698. doi: 10.1136/bmj.e6698

44. Chowdhury R, Stevens S, Ward H, Chowdhury S, Sajjad A, Franco OH. Circulating vitamin D, calcium and risk of cerebrovascular disease: a systematic review and meta-analysis. *Eur J Epidemiol*. (2012) 27:581–91. doi: 10.1007/s10654-012-9729-z

45. Mader MM, Böger R, Appel D, Schwedhelm E, Haddad M, Mohme M, et al. Intrathecal and systemic alterations of L-arginine metabolism in patients after intracerebral hemorrhage. *J Cereb. Blood Flow Metab.* (2021) 41:1964–77. doi: 10.1177/0271678X20983216

46. Suzuki M, Asahara H, Endo S, Inada K, Doi M, Kuroda K, et al. Increased levels of nitrite/nitrate in the cerebrospinal fluid of patients with subarachnoid hemorrhage. *Neurosurg Rev*. (1999) 22:96–8. doi: 10.1007/s101430050038

47. Sadamitsu D, Kuroda Y, Nagamitsu T, Tsuruta R, Inoue T, Ueda T, et al. Cerebrospinal fluid and plasma concentrations of nitric oxide metabolites in postoperative patients with subarachnoid hemorrhage. *Crit Care Med*. (2001) 29:77–9. doi: 10.1097/00003246-200101000-00018

48. Suzuki Y, Osuka K, Noda A, Tanazawa T, Takayasu M, Shibuya M, et al. Nitric oxide metabolites in the cisternal cerebral spinal fluid of patients with subarachnoid hemorrhage. *Neurosurgery*. (1997) 41:807–12. doi: 10.1097/00006123-199710000-00008

49. Wei Z, Huang L, Cui L, Zhu X. Mannose: good player and assister in pharmacotherapy. *Biomed. Pharmacother*. (2020) 129:110420. doi: 10.1016/j.biopha.2020.110420

50. Zhao Q, Dai MY, Huang RY, Duan JY, Zhang T, Bao WM, et al. *Parabacteroides distasonis* ameliorates hepatic fibrosis potentially via modulating intestinal bile acid metabolism and hepatocyte pyroptosis in male mice. *Nat Commun*. (2023) 14:1829. doi: 10.1038/s41467-023-37459-z

51. Wanders RJ, Komen J, Kemp S. Fatty acid omega-oxidation as a rescue pathway for fatty acid oxidation disorders in humans. *FEBS J*. (2011) 278:182–94. doi: 10.1111/j.1742-4658.2010.07947.x

52. Müller F, Sharma A, König J, Fromm MF. Biomarkers for in vivo assessment of transporter function. *Pharmacol Rev*. (2018) 70:246–77. doi: 10.1124/pr.116.013326

53. Ayer A, Zarjou A, Agarwal A, Stocker R. Heme Oxygenases in cardiovascular health and disease. *Physiol Rev*. (2016) 96:1449–508. doi: 10.1152/physrev.00003.2016

54. Fondevila C, Shen XD, Tsuchiyashi S, Yamashita K, Csizmadia E, Lassman C, et al. Biliverdin therapy protects rat livers from ischemia and reperfusion injury. *Hepatology (Baltimore, Md)*. (2004) 40:1333–41. doi: 10.1002/hep.20480

55. Vasavda C, Kothari R, Malla AP, Tokhunts R, Lin A, Ji M, et al. Bilirubin links Heme metabolism to neuroprotection by scavenging superoxide. *Cell Chem. Biol.* (2019) 26:1450–60.e7. doi: 10.1016/j.chembiol.2019.07.006

56. Nakao A, Murase N, Ho C, Toyokawa H, Billiar TR, Kanno S. Biliverdin administration prevents the formation of intimal hyperplasia induced by vascular injury. *Circulation*. (2005) 112:587–91. doi: 10.1161/CIRCULATIONAHA.104.509778

57. Bai W, Huo S, Zhou G, Li J, Yang Y, Shao J. Biliverdin modulates the Nrf2/A20/eEF1A2 axis to alleviate cerebral ischemia-reperfusion injury by inhibiting pyroptosis. *Biomed Pharmacother*. (2023) 165:115057. doi: 10.1016/j.biopha.2023.115057

58. Zhang H, Sumbria RK, Chang R, Sun J, Cribbs DH, Holmes TC, et al. Erythrocyte-brain endothelial interactions induce microglial responses and cerebral microhemorrhages in vivo. *J Neuroinflammation*. (2023) 20:265. doi: 10.1186/s12974-023-02932-5

59. Taha AY. Linoleic acid-good or bad for the brain? *NPJ Sci Food*. (2020) 4:1. doi: 10.1038/s41538-019-0061-9

60. Taha AY, Blanchard HC, Cheon Y, Ramadan E, Chen M, Chang L, et al. Dietary linoleic acid lowering reduces lipopolysaccharide-induced increase in brain arachidonic acid metabolism. *Mol Neurobiol*. (2017) 54:4303–15. doi: 10.1007/s12035-016-9968-1

61. Lin LE, Chen CT, Hildebrand KD, Liu Z, Hopperton KE, Bazinet RP. Chronic dietary n-6 PUFA deprivation leads to conservation of arachidonic acid and more rapid loss of DHA in rat brain phospholipids. *J Lipid Res*. (2015) 56:390–402. doi: 10.1194/jlr.M055590

62. Lankinen MA, Fauland A, Shimizu BI, Ågren J, Wheelock CE, Laakso M, et al. Inflammatory response to dietary linoleic acid depends on FADS1 genotype. *Am J Clin Nutr*. (2019) 109:165–75. doi: 10.1093/ajcn/nqy287

63. Liu P, Zhu W, Chen C, Yan B, Zhu L, Chen X, et al. The mechanisms of lysophosphatidylcholine in the development of diseases. *Life Sci*. (2020) 247:117443. doi: 10.1016/j.lfs.2020.117443

64. Freeman L, Guo H, David CN, Brickey WJ, Jha S, Ting JP. NLR members NLRC4 and NLRP3 mediate sterile inflammasome activation in microglia and astrocytes. *J Exp Med*. (2017) 214:1351–70. doi: 10.1084/jem.20150237

65. Lu Y, Nanayakkara G, Sun Y, Liu L, Xu K, Ct D, et al. Procaspase-1 patrolled to the nucleus of proatherogenic lipid LPC-activated human aortic endothelial cells induces ROS promoter CYP1B1 and strong inflammation. *Redox Biol*. (2021) 47:102142. doi: 10.1016/j.redox.2021.102142

66. da Silva JF, Alves JV, Silva-Neto JA, Costa RM, Neves KB, Alves-Lopes R, et al. Lysophosphatidylcholine induces oxidative stress in human endothelial cells via NOX5 activation - implications in atherosclerosis. *Clin Sci (Lond)*. (2021) 135:1845–58. doi: 10.1042/CS20210468

67. Okatani Y, Wakatsuki A, Watanabe K, Taniguchi K, Fukaya T. Melatonin counteracts potentiation by lysophosphatidylcholine of serotonin-induced vasoconstriction in human umbilical artery: relation to calcium influx. *J Pineal Res*. (2001) 30:116–22. doi: 10.1034/j.1600-079X.2001.300207.x

68. Saeed AA, Edström E, Pikuleva I, Eggertsen G, Björkhem I. On the importance of albumin binding for the flux of 7α-hydroxy-3-oxo-4-cholestenoic acid in the brain. *J Lipid Res*. (2017) 58:455–9. doi: 10.1194/jlr.P073403

69. Nagata K, Seyama Y, Shimizu T. Changes in the level of 7 alpha-hydroxy-3-oxo-4-cholestenoic acid in cerebrospinal fluid after subarachnoid hemorrhage. *Neurol Med Chir*. (1995) 35:294–7. doi: 10.2176/nmc.35.294

70. Meaney S, Heverin M, Panzenboeck U, Ekström L, Axelsson M, Andersson U, et al. Novel route for elimination of brain oxysterols across the blood-brain barrier: conversion into 7alpha-hydroxy-3-oxo-4-cholestenoic acid. *J Lipid Res*. (2007) 48:944–51. doi: 10.1194/jlr.M600529-JLR200

71. Lefebvre P, Cariou B, Lien F, Kuipers F, Staels B. Role of bile acids and bile acid receptors in metabolic regulation. *Physiol Rev*. (2009) 89:147–91. doi: 10.1152/physrev.00010.2008

frontiers | Frontiers in Nutrition

TYPE Clinical Trial
PUBLISHED 08 July 2024
DOI 10.3389/fnut.2024.1420087

OPEN ACCESS

EDITED BY
Julius Liobikas,
Lithuanian University of Health Sciences, Lithuania

REVIEWED BY
Cecilia Zanin Palchetti,
University of São Paulo, Brazil
Xu Zhu,
Hunan University of Chinese Medicine, China

*CORRESPONDENCE
Zhengyuan Cao
✉ 18985172332@163.com

RECEIVED 19 April 2024
ACCEPTED 26 June 2024
PUBLISHED 08 July 2024

CITATION
Liu Y, Zhou C, Shen R, Wang A, Zhang T and Cao Z (2024) Dietary folate intake and serum klotho levels in adults aged 40–79 years: a cross-sectional study from the national health and nutrition examination survey 2007–2016. *Front. Nutr.* 11:1420087. doi: 10.3389/fnut.2024.1420087

Dietary folate intake and serum klotho levels in adults aged 40–79 years: a cross-sectional study from the national health and nutrition examination survey 2007–2016

Yang Liu[1], Chunhuan Zhou[1], Rongjun Shen[2], Anxian Wang[1], Tingting Zhang[3] and Zhengyuan Cao[1]*

[1]Department of Medical Laboratory, Guihang 300 Hospital Affiliated to Zunyi Medical University, Guiyang, China, [2]Hospital Infection Control Department, Guihang 300 Hospital Affiliated to Zunyi Medical University, Guiyang, China, [3]Department of Endocrinology, Guihang 300 Hospital Affiliated to Zunyi Medical University, Guiyang, China

Objective: This study aims to explore the relationship between dietary folate intake and serum Klotho levels in adults from aged 40 to 79 years in the United States, seeking to elucidate the intricacies of their interaction.

Methods: Analyzing data from the National Health and Nutrition Examination Survey (NHANES) spanning 2007 to 2016. The survey research determined folate intake through a 24-h dietary recall and nutrient density modeling, and assessed Klotho levels using enzyme-linked immunosorbent assay (ELISA). The relationship between folate intake and Klotho levels was evaluated using weighted linear regression, and complemented by analysis via smoothed curve models for nuanced understanding.

Results: The study encompassed 10,278 participants, with an average age of 57.64 years, revealing a noteworthy positive correlation between dietary folate and serum Klotho levels. The regression coefficient stood at 0.11 (95% confidence interval, 0.05, 0.18) post-adjustment for various covariates. When dietary folate intake was categorized into quartiles, the second, third, and fourth quartiles exhibited statistically significant differences compared to the lowest quartile. This indicates that higher folate intake correlates with increased serum Klotho levels. These findings underscore the potential benefits of elevating folate intake to enhance serum Klotho levels. Stratified analysis indicated that this association was more pronounced among males aged 60 years or older and individuals with hypertension.

Conclusion: The findings suggest a significant correlation between increased dietary folate intake and elevated serum Klotho levels in adults aged 40–79 years. Hinting at the potential nutritional influences on the aging process and associated health conditions. This calls for further exploration into the mechanisms and broader implications of this association.

KEYWORDS

klotho, folate, dietary, intake, aging, NHANES

1 Introduction

Aging is universally recognized as a multifaceted process influenced by an intricate interplay of genetic, environmental, and lifestyle determinants (1–3). This phenomenon spans a comprehensive spectrum of biological transformations, including diminished cellular functionality (4), the accumulation of DNA damage (5), and anomalies in amino acid metabolism (6). These transformations transcend singular biological levels, engaging in complex interactions that cumulatively precipitate the deterioration of tissue and organ function, thereby impacting the organism's health and longevity. Consequently, it is crucial to thoroughly understand these processes. Effective interventions can slow down the aging process and enhance quality of life.

Since 1997, the Klotho protein has emerged as a focal point in anti-aging research (7, 8). It is predominantly expressed in the kidneys (9) and found in other tissues including the brain (10). Klotho plays a pivotal role in fostering longevity and health. It does so by modulating calcium and phosphorus metabolism, contributing to the antioxidant defense, and impacting critical cellular signaling pathways, notably Wnt/β-catenin and insulin-like growth factor-1 (IGF-1) (11, 12). A decline in Klotho gene expression is intricately linked to various aging-associated diseases, such as cardiovascular disease (13), osteoporosis (14), and chronic kidney disease (15). Research demonstrates that enhancing Klotho protein levels exogenously or activating its signaling pathways can mitigate these conditions and potentially slow the aging process (13, 16–19). Therefore, Klotho proteins not only serve as crucial markers for deciphering the mechanisms underlying aging, but also offer promising avenues for developing novel anti-aging therapies (8).

Folate, a critical component of the B-vitamin family, occupies a pivotal role in processes such as cell division and growth (20, 21), DNA synthesis and repair (22), and the metabolism of amino acids (23). Its significance is particularly pronounced during the initial stages of development, where it is indispensable in forestalling congenital disorders, including neural tube defects (24). Furthermore, a deficiency in folate intake can precipitate a range of health issues, encompassing anemia, cardiovascular diseases, and even cognitive impairments (25, 26). Ongoing scientific investigation continues to unveil the advantages of folate in supporting cardiovascular health, enhancing cognitive function, and contributing to anti-aging benefits (27). Therefore, it is essential to supplement folate for promoting health and preventing disease in pregnant women, those planning pregnancy, and individuals at risk of folate deficiency. However, high-dose supplementation is unnecessary for healthy individuals with normal folate levels (28).

Recent research has elucidated that particular dietary practices and the intake of specific types of food are closely linked to fluctuations in klotho protein levels (29, 30). Considering the pivotal roles that both klotho protein and folate occupy in fostering health and decelerating the aging process, understanding the dynamics of their interplay is of paramount importance.

2 Materials and methods

2.1 Study population

This investigation drew upon data from five successive cycles of the National Health and Nutrition Examination Survey (NHANES) spanning from 2007 to 2016, encompassing 87,719 participants. Following the exclusion of subjects due to incomplete data on serum Klotho levels ($n = 36,824$), Dietary energy ($n = 38,432$), dietary folate intake ($n = 804$), and other covariates ($n = 1,381$). the study's final cohort consisted of 10,278 individuals (Figure 1). The NHANES employed a sophisticated multistage probability sampling technique, orchestrated by the National Center for Health Statistics (NCHS). Informed Consent was signed by each participant, and the methodology of data collection received approval from an ethics committee, ensuring the protection of participants. Comprehensive details regarding the survey are accessible on the NHANES website.[1]

2.2 Measurement of dietary folate intake

In this study, the 24-h dietary recall was conducted using a combination of face-to-face and telephone interviews. The initial interview was carried out at the Mobile Examination Center (MEC), followed by subsequent interviews conducted via telephone 3 to 10 days later. This approach employed the USDA's Automated Multiple-Pass Method (AMPM),[2] which precisely recorded the types and quantities of foods and beverages consumed by participants within the 24 h prior to the interview. The nutrient content of these consumables was then assessed through a comprehensive dietary survey. The nutrient calculations used the USDA's Food and Nutrient Database for Dietary Studies (FNDDS 4.1; see Footnote 2). Moreover, the average of the two dietary recalls was taken, reflecting only the actual intake levels, not the habitual intake of the population. To minimize the measurement errors associated with self-reported dietary assessment tools, we standardized nutrient intake relative to total energy intake and accounted for variations in individual energy needs. The adjusted intake formula is: dietary folate intake / energy intake * 1000 (31). This method, commonly referred to as nutrient density model, allows for a more precise evaluation of dietary folate intake across diverse energy requirements.

Additionally, in sensitivity analyses, we extended this method to assess folate from natural foods, folic acid from fortified foods and supplements, and dietary vitamin B12. Each nutrient's intake was similarly adjusted for energy, ensuring robustness in our analyses across different dietary sources and intake patterns.

2.3 Serum klotho levels

Blood samples from participants were transported to the Northwest Laboratory for Lipid Metabolism and Diabetes Research, adhering to predefined protocols, and subsequently preserved at −80°C for analysis. The measurement of Klotho levels was conducted utilizing an ELISA kit produced ("IBL International," Japan). In a bid to uphold laboratory standards and mitigate potential detection bias attributable to random variance, the samples underwent duplicate analyses. The mean of these analyses was accepted contingent upon compliance with the in-lot quality control criteria. Samples

1 https://www.cdc.gov/nchs/nhanes/about_nhanes.htm
2 http://www.ars.usda.gov/ba/bhnrc/fsrg

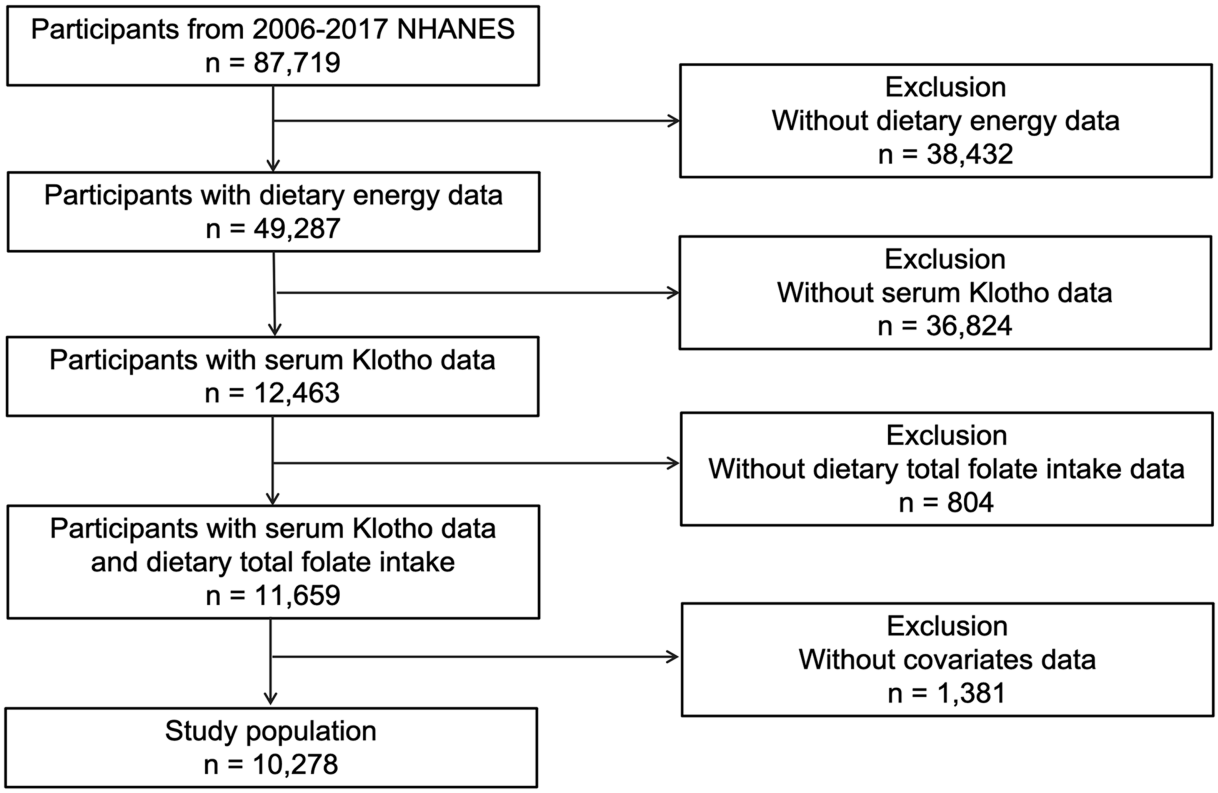

FIGURE 1
Flowchart of the study population.

demonstrating a variance exceeding 10% between the two measurements were subjected to reevaluation and duly documented.

2.4 Assessment of covariates

The study incorporated a comprehensive set of covariates, totaling 11 which included both continuous and categorical variables. These covariates are as follows: sex (categorized as male or female), age, racial/ethnic background (categorized as non-Hispanic white, non-Hispanic black, Mexican American, or other, which includes multiracial and other Latino identities), marital status (categorized as married, not currently partnered, or cohabiting with a partner), and household income relative to the poverty threshold (categorized into three groups: ≤1.30, 1.31–3.50, and > 3.50 based on the poverty income ratio [PIR]). The poor income ratio was determined based on Federal Poverty Level (FPL) information, which considers factors such as inflation and family size.[3] The Body Mass Index (BMI) is calculated as weight (in kilograms) divided by the square of height (in meters; kg/m^2). According to the World Health Organization (WHO), BMI is categorized into four groups: underweight (less than 18.5 kg/m^2), normal weight (18.5 to less than 25 kg/m^2), overweight (25 to less than 30 kg/m^2), and obese (30 kg/m^2 or greater).[4] Hypertension was defined as having an average systolic blood pressure greater than 140 mmHg, an average diastolic blood pressure greater than 90 mmHg, a history of being diagnosed with high blood pressure, or current use of prescription medication for high blood pressure, with at least one of these criteria being met. Diabetes status was determined based on a doctor's diagnosis. Heart disease identification relied on four indicators: a history of congestive heart failure, coronary artery disease, angina pectoris, or a heart attack, with any one of these conditions affirming the presence of heart disease. The Urine Albumin to Creatinine Ratio (UACR) was categorized as <30 mg/g for normal individuals and ≥ 30 mg/g indicating abnormal proteinuria. Glycosylated hemoglobin (HbA1c) levels were also considered, serving as an indicator of long-term glycemic control.

2.5 Statistical analysis

To obtain more representative estimates, this study applied the MEC weights recommended by the NHANES database in all analyses. All data collection and statistical analyses were performed using R4.2.0[5] and Empower Stats.[6]

3 https://aspe.hhs.gov/prior-hhs-poverty-guidelines-and-federal-register-references

4 https://www.who.int/data/gho/data/themes/topics/topic-details/GHO/body-mass-index

5 http://www.r-project.org

6 http://www.empowerstats.com

TABLE 1 Characteristic of the study population in NHANES 2007–2016.

Variables	Total	Dietary folate intake (μg/1000 kcal)				
		Q1 (41.83–147.61)	Q2 (147.62–186.00)	Q3 (186.03–239.11)	Q4 (239.2–1291.04)	*p*-value
N (%)	10,278	2,569 (25.00%)	2,570 (25.00%)	2,569 (25.00%)	2,570 (25.00%)	
Serum Klotho quartiles (pg/mL)	856.03 ± 311.67	846.83 ± 327.15	860.78 ± 320.93	856.29 ± 301.48	860.22 ± 296.04	0.018
Age (years)	57.64 ± 10.82	56.11 ± 10.54	57.47 ± 10.80	58.25 ± 10.97	58.73 ± 10.81	<0.001
UACR(mg/g)	47.67 ± 359.83	48.62 ± 374.18	41.86 ± 286.60	53.26 ± 398.82	46.95 ± 369.89	0.046
HbA1c (%)	5.94 ± 1.15	5.94 ± 1.19	5.94 ± 1.16	5.94 ± 1.15	5.94 ± 1.10	0.953
Gender (%)						<0.001
Male	4,908 (47.75%)	1,371 (53.37%)	1,221 (47.51%)	1,156 (45.00%)	1,160 (45.14%)	
Female	5,370 (52.25%)	1,198 (46.63%)	1,349 (52.49%)	1,413 (55.00%)	1,410 (54.86%)	
Ethnicity/Race (%)						<0.001
Non-Hispanic White	1,486 (14.46%)	314 (12.22%)	388 (15.10%)	404 (15.73%)	380 (14.79%)	
Non-Hispanic Black	1,096 (10.66%)	194 (7.55%)	264 (10.27%)	321 (12.50%)	317 (12.33%)	
Mexican American	4,832 (47.01%)	1,226 (47.72%)	1,228 (47.78%)	1,168 (45.47%)	1,210 (47.08%)	
Other Race - Including Multi-Racial	2001 (19.47%)	721 (28.07%)	535 (20.82%)	415 (16.15%)	330 (12.84%)	
Other Hispanic	863 (8.40%)	114 (4.44%)	155 (6.03%)	261 (10.16%)	333 (12.96%)	
Marital (%)						<0.001
Married	6,260 (60.91%)	1,468 (57.14%)	1,541 (59.96%)	1,596 (62.13%)	1,655 (64.40%)	
Currently in a relationship	478 (4.65%)	155 (6.03%)	128 (4.98%)	106 (4.13%)	89 (3.46%)	
Not currently in a partner	3,540 (34.44%)	946 (36.82%)	901 (35.06%)	867 (33.75%)	826 (32.14%)	
Poor income ratio (%)						<0.001
<1.3	2,896 (28.18%)	784 (30.52%)	735 (28.60%)	673 (26.20%)	704 (27.39%)	
1.3–3.5	3,740 (36.39%)	983 (38.26%)	954 (37.12%)	915 (35.62%)	888 (34.55%)	
≥3.5	3,642 (35.43%)	802 (31.22%)	881 (34.28%)	981 (38.19%)	978 (38.05%)	
BMI (%)						<0.001
Underweight (<18.5 kg/m2)	101 (0.98%)	32 (1.25%)	25 (0.97%)	28 (1.09%)	16 (0.62%)	
Normal weight (18.5–24.9 kg/m2)	2,323 (22.60%)	487 (18.96%)	542 (21.09%)	627 (24.41%)	667 (25.95%)	
Overweight (25–29.9 kg/m2)	3,496 (34.01%)	849 (33.05%)	875 (34.05%)	872 (33.94%)	900 (35.02%)	
Obese (≥30 kg/m2)	4,358 (42.40%)	1,201 (46.75%)	1,128 (43.89%)	1,042 (40.56%)	987 (38.40%)	
Hypertension (%)						0.433
No	5,524 (53.75%)	1,404 (54.65%)	1,363 (53.04%)	1,399 (54.46%)	1,358 (52.84%)	
Yes	4,754 (46.25%)	1,165 (45.35%)	1,207 (46.96%)	1,170 (45.54%)	1,212 (47.16%)	

(Continued)

10.3389/fnut.2024.1420087

TABLE 1 (Continued)

Variables	Total	Dietary folate intake (μg/1000 kcal)				
		Q1 (41.83–147.61)	Q2 (147.62–186.00)	Q3 (186.03–239.11)	Q4 (239.2–1291.04)	*p*-value
Diabetes (%)						0.009
Yes	1769 (17.21%)	384 (14.95%)	454 (17.67%)	447 (17.40%)	484 (18.83%)	
No	8,206 (79.84%)	2,113 (82.25%)	2032 (79.07%)	2054 (79.95%)	2007 (78.09%)	
Borderline	303 (2.95%)	72 (2.80%)	84 (3.27%)	68 (2.65%)	79 (3.07%)	
CVD (%)						0.115
No	8,970 (87.27%)	2,235 (87.00%)	2,243 (87.28%)	2,274 (88.52%)	2,218 (86.30%)	
Yes	1,308 (12.73%)	334 (13.00%)	327 (12.72%)	295 (11.48%)	352 (13.70%)	

Mean +/− SD for: age, dietary folate intake, UACR, HbA1c. % for: gender, race, marital, poor income ratio, BMI, hypertension, diabetes, CVD.

TABLE 2 Association between dietary folate intake and serum klotho levels among adults in NHANES 2007–2016.

Dietary folate intake (μg/1000 kcal)	Model 1		Model 2		Model 3	
	β (95%CI)	*p*-value	β (95%CI)	*p*-value	β (95%CI)	*p*-value
Continuous	0.09 (0.02, 0.15)	0.0079	0.11 (0.05, 0.18)	0.0005	0.11 (0.05, 0.18)	0.0009
Quartiles						
Q1(41.83–147.61)	Reference		Reference		Reference	
Q2(147.62–186.00)	27.34 (11.27, 43.41)	0.0009	30.58 (14.59, 46.57)	0.0002	29.79 (13.84, 45.75)	0.0003
Q3(186.03–239.11)	18.69 (2.54, 34.84)	0.0234	23.36 (7.18, 39.53)	0.0047	21.17 (5.01, 37.34)	0.0103
Q4(239.2–1291.04)	24.17 (8.05, 40.29)	0.0033	31.13 (14.96, 47.30)	0.0002	30.15 (13.94, 46.37)	0.0003
p for trend		0.0240		0.0022		0.0035

Model 1: no cofounder. Model 2: adjusted for age, gender, race. Model 3: adjusted for age, gender, race, marital, BMI, poor income ratio, hypertension, diabetes, CVD, HbA1c and UACR. CI, confidence interval.

10.3389/fnut.2024.1420087

The relationship between dietary folate intake and serum Klotho levels was examined using multivariate linear regression analysis, which facilitated the computation of beta values and 95% confidence intervals. This analysis was structured into three distinct models: Model 1, which did not adjust for any variables; Model 2, which adjusted for sex, age, and race; and Model 3, which incorporated adjustments for additional covariates. Serum Klotho levels were analyzed both as a continuous independent variable and categorically, divided into quartiles, to evaluate trends. To visually represent this relationship, a smoothed curve-fitting model was employed. The study also conducted stratified and interaction analyses to investigate how this association might differ across subgroups defined by each covariate. Specifically, analyses were stratified by age (comparing those under 60 years to those 60 years and older), sex, and the presence of hypertension across varying dietary folate intake.

Further, sensitivity analyses were carried out on distinct population subsets: those consuming only naturally occurring folate in foods, those whose intake included only dietary folic acid from fortified food [calculated as μg of DFEs provided = μg of natural food folate + (1.7 × μg of folic acid)] (32), and those consuming folate exclusively through supplements. The characteristics of these populations are detailed in Supplementary Table S1. These analyses aimed to assess the impact of potential outliers on the findings. To ensure the stability of the outcomes, the study excluded data points representing extreme values, this included individuals with Klotho levels above 2,500 pg./mL, those with dietary folate intake exceeding 500 μg/1000 kcal or below 100 μg/1000 kcal after energy adjustment, and individuals with energy-adjusted vitamin B12 levels greater than 6.0 μg/1000 kcal. Additionally, individuals categorized as "obese" by BMI, as well as those diagnosed with hypertension, diabetes, or heart disease, and those with a urine albumin/creatinine ratio (UACR) greater than 30 mg/g were also excluded.

3 Results

3.1 Baseline characteristics of all participants

This study enrolled a total of 10,278 participants, of whom 47.75% were male and 52.25% were female. The age range of participants spanned from 40 to 79 years, with a mean age of 57.64 years (standard deviation ±10.82 years). Participants were stratified based on the quartiles of serum Klotho levels, and the baseline characteristics are delineated in Table 1. Significant differences were observed across the quartiles of Dietary folate intake in terms of age, gender, race, marital status, Poor income ratio, body mass index (BMI), diabetes mellitus, urinary albumin-to-creatinine ratio (UACR), and glycosylated hemoglobin levels.

3.2 Association between dietary folate intake and serum klotho levels

In the multivariate regression analysis detailed in Table 2, an association was observed between dietary folate intake and serum Klotho levels. Specifically, in both Model 2 and Model 3, each 1 μg/1000 kcal increase in energy-adjusted dietary folate intake was associated with a 0.11 pg./mL increase in serum Klotho levels. Subgroup analyses in Models 2 and 3 showed significant associations for Groups Q2, Q3, and Q4 compared to Group Q1, with *p*-values less than 0.05 for each group. The trend difference between the groups in both Model 2 and Model 3 was significant, with *p*-values for trend less than 0.0022 and 0.0035, respectively.

We used smoothed curve fitting to show the complex, non-linear relationship between folate intake and Klotho levels in the blood (Figure 2). This technique helps highlight how these two variables interact beyond straightforward linear patterns.

3.3 Subgroup analysis and sensitivity analysis

In the subgroup analysis examining the relationship between dietary folate intake and Klotho levels (Table 3), the study population was stratified into quartiles based on their dietary folate intake. Following adjustments for potential confounding variables, the correlation appeared to be more pronounced among individuals aged 60 years or older, within the male demographic, and among participants with a history of hypertension.

Furthermore, extensive sensitivity analyses were conducted in this study to assess the stability of the results (refer to Table 4): (1) only samples deriving from natural food folate intake were included; (2) Inclusion was limited to samples containing dietary folic acid from fortified foods; (3) the analysis included only samples with intake of folate supplements; (4) samples exhibiting Klotho levels >2,500 pg./mL were excluded; (5) Excluding samples with dietary folate intake exceeding 500 μg/1000 kcal; (6) exclusion of samples with <100 μg/1000 kcal of dietary folate intake; (7) samples with dietary vitamin B12 intake >6.0 μg/1000 kcal were also excluded; (8) given the potential influence of hyperlipidemia on Klotho levels, samples with a BMI categorization of "obese" were excluded (33); (9) considering the association of hypertension prevalence with lower Klotho levels, samples with a hypertension status of "yes" were excluded (34); (10) due to the nonlinear relationship between serum Klotho levels and the prevalence of diabetes mellitus, samples with a diabetes mellitus status of "yes" were excluded (35); (11) recognizing the significant correlations of serum Klotho with heart failure (36) and myocardial infarction (37), samples with a cardiac status of "yes" were excluded; (12) considering the

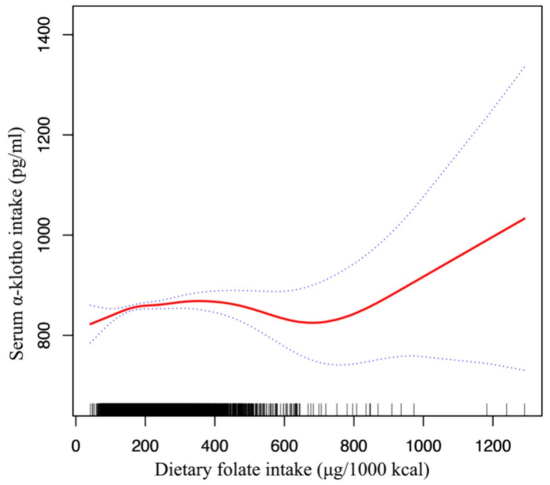

FIGURE 2
Association between dietary folate intake and serum Klotho levels adjusted for age, gender, race, marital, body mass index, poor income ratio, hypertension, diabetes, CVD, HbA1c and UACR.

association between Klotho levels and urinary albumin excretion rate (38) as well as chronic kidney disease albuminuria (15) samples with UACR results ≥30 were excluded. These results imply that folate intake from natural sources significantly impacts serum Klotho levels, whereas factors such as dietary fortification with folic acid and the prevalence of hypertension appear to have a negligible influence on this relationship.

4 Discussion

In our study, we explored the relationship between dietary folate intake and serum Klotho levels, finding a nuanced interplay. This connection was stronger in individuals over 60, males, and those with hypertension, highlighting folate's role in regulating the anti-aging factor Klotho. After adjusting for energy intake, each additional unit of dietary folate intake was associated with a 0.11 pg./mL increase in Klotho levels. This correlation may play a positive role in promoting healthy aging and preventing age-related diseases. Additionally, it lays the foundation for pioneering new health strategies focused on dietary interventions.

Folate intake has been found to exert significant effects on multiple signaling pathways, notably the mTOR pathway, the insulin/IGF-1 signaling pathway, and the Wnt/β-catenin signaling pathway. For instance, the research conducted by Fredrick J. Rosario and colleagues

TABLE 3 Stratified analyses of association between dietary folate intake and serum klotho levels in NHANES 2007–2016.

Variable	Dietary folate intake (μg/1000 kcal), β (95%CI)		*p*-value	*P* for interaction
Age subgroup				0.0742
<60 years	41.83–147.61	Reference		
	147.62–186.00	8.76 (−13.09, 30.60)	0.4321	
	186.03–239.11	11.92 (−10.58, 34.42)	0.2992	
	239.2–1291.04	16.46 (−6.04, 38.95)	0.1517	
	P for trend		0.1614	
≥60 years	41.83–147.61	Reference		
	147.62–186.00	64.30 (41.09, 87.51)	<0.0001	
	186.03–239.11	38.36 (15.52, 61.20)	0.0010	
	239.2–1291.04	51.37 (28.36, 74.39)	<0.0001	
	P for trend		0.0036	
Gender subgroup				0.1776
Male	41.83–147.61	Reference		
	147.62–186.00	26.54 (5.60, 47.48)	0.0130	
	186.03–239.11	3.29 (−18.37, 24.94)	0.7660	
	239.2–1291.04	37.55 (15.88, 59.21)	0.0007	
	P for trend		0.0047	
Female	41.83–147.61	Reference		
	147.62–186.00	33.65 (9.66, 57.64)	0.0060	
	186.03–239.11	37.52 (13.60, 61.45)	0.0021	
	239.2–1291.04	26.73 (2.74, 50.71)	0.0290	
	P for trend		0.1116	
Hypertension subgroup				0.3968
No	41.83–147.61	Reference		
	147.62–186.00	49.02 (27.29, 70.75)	<0.0001	
	186.03–239.11	27.55 (5.67, 49.44)	0.0136	
	239.2–1291.04	30.01 (7.83, 52.19)	0.0080	
	P for trend		0.1055	
Yes	41.83–147.61	Reference		
	147.62–186.00	−0.97 (−24.54, 22.60)	0.9357	
	186.03–239.11	9.40 (−14.69, 33.48)	0.4444	
	239.2–1291.04	26.95 (3.18, 50.72)	0.0263	
	P for trend		0.0114	

Adjusted for age, gender, race, marital, BMI, poor income ratio, hypertension, diabetes, CVD, HbA1c and UACR except the subgroup variable.

TABLE 4 Inclusion and exclusion criteria.

	β (95% CI)	*p*-value
Only folate intake from natural foods was included (μg/1000 kcal)	0.24 (0.14, 0.34)	<0.0001
Only dietary folic acid from fortified food (DFE μg/1000 kcal)	0.02 (−0.06, 0.10)	0.7025
Only folic acid supplement intake was included (DFE μg/1000 kcal)	−0.01 (−0.03, 0.01)	0.4292
Samples with klotho level > 2,500 pg./mL were excluded	0.12 (0.06, 0.18)	0.0002
Samples with dietary folate intake >500 (μg/1000 kcal) were excluded	0.15 (0.07, 0.23)	0.0001
Samples with dietary folate intake <100 (μg/1000 kcal) were excluded	0.10 (0.03, 0.17)	0.0040
Samples with dietary vitb12 > 6.0 (μg/1000 kcal) were excluded	0.18 (0.10, 0.25)	<0.0001
Exclusion of obese people	0.13 (0.04, 0.21)	0.0032
Excluding people with hypertension	0.13 (0.04, 0.22)	0.0042
Exclusion of people with diabetes	0.13 (0.06, 0.20)	0.0004
Excluding people with heart disease	0.12 (0.05, 0.19)	0.0007
People with UACR≥30 mg/g were excluded	0.13 (0.06, 0.19)	0.0004

illustrates that maternal folate deficiency can impair fetal growth by inhibiting placental mTOR signaling, thereby establishing a direct connection between folate levels and mTOR signaling (39). Furthermore, Elena Silva's studies have shown that folate deficiency influences cellular functions through innovative sensing mechanisms, which in turn activate the mTOR signaling pathway, affecting processes such as nutrient transport and protein synthesis (40). Additionally, Andrea Annibal and co-authors have discovered through high-resolution mass spectrometry analysis of the metabolome of the nematode Cryptomeria hidrobatidis, that one-carbon metabolism and the folate cycle are integral in jointly regulating lifespan, with insulin/IGF signaling playing a comparable regulatory role across different species' longevity models. This suggests that certain metabolic nodes are pivotal in promoting healthy aging (41). Meanwhile, research by Wen-Chi L. Chang and others on the impact of folic acid supplementation in the development of colitis-associated colorectal cancer indicated that high doses of folic acid can encourage cancer formation by modifying the epigenetic field effects of the Wnt/β-catenin and MAPK signaling pathways (42). Despite the compelling evidence linking folate intake with mechanisms of anti-aging, a gap remains in the direct, controlled trials demonstrating a connection with Klotho, highlighting a promising avenue for future research.

The primary dietary sources of folate include green leafy vegetables (for instance, spinach and broccoli), citrus fruits, legumes, nuts, and whole grain products (43–47). To alleviate health issues caused by folate deficiency, since 1998, the United States and Canada have mandated the addition of dietary folic acid from fortified food to flour and grain products. Common foods containing fortified folic acid include flour, bread, breakfast cereals, pasta, and cornmeal (48–50). Our sensitivity analysis unveiled a noteworthy observation: a significant correlation was identified exclusively between folate intake from natural sources and serum Klotho levels, whereas folic acid obtained through fortified foods and supplements did not exhibit a similar association, paralleling the discoveries of Mengyi Liu et al. (51). This prompts us to suggest that there exists an "optimal" range for folate intake, with the intake of folate from natural foods generally falling precisely within this range (52). The excessive intake of folic acid may precipitate adverse effects, notably when surpassing the recommended daily allowance (53). Such overconsumption bears the risk of concealing the diagnosis of vitamin B12 deficiency and merely ameliorating anemia symptoms without addressing the potential for neurological harm (54–56). Furthermore, certain research suggests that a long-term, high-dose regimen of folic acid could correlate with an elevated risk of specific cancers (57). Consequently, it is imperative to regulate folic acid intake meticulously to prevent excessive ingestion (58).

Subgroup analyses have elucidated a broad decline in metabolic function and nutrient absorption capabilities as individuals age (59–61). Notably, research focusing on adults aged 60 and above has highlighted a correlation between folate intake and serum Klotho levels, particularly pronounced among those seniors with elevated folate intake ($p < 0.0001$, trend p-value = 0.0036). These findings underscore the significance of maintaining a moderate intake of folate within aging populations to support cardiovascular health, bone integrity, and other health facets (62, 63). Conversely, in individuals younger than 60 years, the link between folate intake and Klotho levels did not prove to be significant. This suggests that the demand for folate, along with its contribution to physical well-being, assumes greater importance as one ages, highlighting the potential benefits of targeted nutritional supplementation to meet the specific needs posed by aging (2, 26).

Moreover, we observed pronounced differences between genders regarding the association between dietary folate intake and serum Klotho levels among men and women (64). In men, a notable correlation was observed between folate intake and serum Klotho levels, particularly within the moderate to high folate intake category (p-values = 0.0007 and a trend p-value of 0.0047). Similarly, in females, dietary folate intake was significantly associated with serum Klotho levels (p-values ranging from 0.0021 to 0.0290, trend p-value = 0.1116). Although some literature suggests the potential influence of testosterone levels on Klotho protein expression in men (65–67), our current dataset does not directly investigate this hypothesis at either a physiological or molecular level. Thus, these findings underscore the critical need for subsequent research to more comprehensively explore how gender differences affect the interplay between folate intake and Klotho levels.

The potential beneficial impact of folate on the expression and functionality of Klotho proteins assumes critical importance, particularly in light of Klotho's pivotal role in preserving vascular health and regulating the equilibrium of blood pressure (20, 62). This mode of action not only underscores the profound importance of folate in combating cardiovascular diseases but also illuminates its prospective utility in the realm of anti-aging (41).

This study is subject to certain limitations. Firstly, the NHANES cohort might not accurately reflect the global population, particularly in countries and regions where food is not fortified with folic acid. Thus, incorporating additional samples from a variety of centers could enhance the study's validity. Secondly, like all dietary assessment methods, the 24-h dietary recall used in this study has inherent limitations. These include recall bias, as it relies on participants' ability to accurately remember and report their food intake, and response bias, where participants might alter their reported intake to align with perceived social norms or to avoid negative judgment. Additionally, the 24-h recall provides a snapshot of a single day's intake, which may not accurately represent usual dietary patterns. Moreover, while data from cross-sectional studies can establish associations, they are insufficient for determining causality, necessitating further evidence to elucidate the cause-and-effect relationship.

5 Conclusion

In summary, among a nationally representative population of American adults, our study identified a significant association between dietary folate intake and serum Klotho levels, especially prominent in men, individuals aged 60 and above, and those with hypertension. These findings suggest a potential role for dietary folate in supporting healthy aging and underscore the need for further research to understand its mechanisms and broader health implications.

Data availability statement

Publicly available datasets were analyzed in this study. This data can be found at: https://wwwn.cdc.gov/nchs/nhanes/Default.aspx.

Ethics statement

The studies involving humans were approved by NCHS Ethics Review Board (ERB) Approval. The studies were conducted in accordance with the local legislation and institutional requirements. The participants provided their written informed consent to participate in this study.

Author contributions

YL: Data curation, Writing – original draft, Writing – review & editing. CZ: Conceptualization, Writing – review & editing. RS: Data curation, Writing – review & editing. AW: Conceptualization, Writing – review & editing. TZ: Writing – review & editing. ZC: Conceptualization, Writing – review & editing.

Funding

The author(s) declare that no financial support was received for the research, authorship, and/or publication of this article.

Acknowledgments

We sincerely thank the NHANES team and participants for their dedication and contributions, essential to the success of this study.

Conflict of interest

The authors declare that the research was conducted in the absence of any commercial or financial relationships that could be construed as a potential conflict of interest.

Publisher's note

Supplementary material

The Supplementary material for this article can be found online at: https://www.frontiersin.org/articles/10.3389/fnut.2024.1420087/full#supplementary-material

References

1. Bjørklund G, Shanaida M, Lysiuk R, Butnariu M, Peana M, Sarac I, et al. Natural compounds and products from an anti-aging perspective. *Molecules*. (2022) 27:7084. doi: 10.3390/molecules27207084

2. Yousefzadeh M, Henpita C, Vyas R, Soto-Palma C, Robbins P, Niedernhofer L. DNA damage-how and why we age? *eLife*. (2021) 10:10. doi: 10.7554/eLife.62852

3. Benayoun BA, Pollina EA, Brunet A. Epigenetic regulation of ageing: linking environmental inputs to genomic stability. *Nat Rev Mol Cell Biol*. (2015) 16:593–610. doi: 10.1038/nrm4048

4. Castaldi A, Dodia RM, Orogo AM, Zambrano CM, Najor RH, Gustafsson ÅB, et al. Decline in cellular function of aged mouse C-kit(+) cardiac progenitor cells. *J Physiol*. (2017) 595:6249–62. doi: 10.1113/jp274775

5. Schumacher B, Pothof J, Vijg J, Hoeijmakers JHJ. The central role of DNA damage in the ageing process. *Nature*. (2021) 592:695–703. doi: 10.1038/s41586-021-03307-7

6. Johnson AA, Cuellar TL. Glycine and aging: evidence and mechanisms. *Ageing Res Rev*. (2023) 87:101922. doi: 10.1016/j.arr.2023.101922

7. Kuro-o M, Matsumura Y, Aizawa H, Kawaguchi H, Suga T, Utsugi T, et al. Mutation of the mouse klotho gene leads to a syndrome resembling ageing. *Nature*. (1997) 390:45–51. doi: 10.1038/36285

8. Abraham CR, Li A. Aging-suppressor klotho: prospects in diagnostics and therapeutics. *Ageing Res Rev*. (2022) 82:101766. doi: 10.1016/j.arr.2022.101766

9. Buchanan S, Combet E, Stenvinkel P, Shiels PG. Klotho, aging, and the failing kidney. *Front Endocrinol (Lausanne)*. (2020) 11:560. doi: 10.3389/fendo.2020.00560

10. Semba RD, Moghekar AR, Hu J, Sun K, Turner R, Ferrucci L, et al. Klotho in the cerebrospinal fluid of adults with and without Alzheimer's disease. *Neurosci Lett*. (2014) 558:37–40. doi: 10.1016/j.neulet.2013.10.058

11. Miao J, Liu J, Niu J, Zhang Y, Shen W, Luo C, et al. Wnt/B-catenin/Ras signaling mediates age-related renal fibrosis and is associated with mitochondrial dysfunction. *Aging Cell*. (2019) 18:e13004. doi: 10.1111/acel.13004

12. Sopjani M, Rinnerthaler M, Kruja J, Dermaku-Sopjani M. Intracellular signaling of the aging suppressor protein klotho. *Curr Mol Med*. (2015) 15:27–37. doi: 10.2174/1566524015666150114111258

13. Chen K, Wang S, Sun QW, Zhang B, Ullah M, Sun Z. Klotho deficiency causes heart aging via impairing the Nrf2-gr pathway. *Circ Res*. (2021) 128:492–507. doi: 10.1161/circresaha.120.317348

14. Torres PU, Prié D, Molina-Blétry V, Beck L, Silve C, Friedlander G. Klotho: an antiaging protein involved in mineral and vitamin D metabolism. *Kidney Int*. (2007) 71:730–7. doi: 10.1038/sj.ki.5002163

15. Zhang J, Zhang A. Relationships between serum klotho concentrations and cognitive performance among older chronic kidney disease patients with albuminuria in Nhanes 2011-2014. *Front Endocrinol (Lausanne)*. (2023) 14:1215977. doi: 10.3389/fendo.2023.1215977

16. Zhou H, Pu S, Zhou H, Guo Y. Klotho as potential autophagy regulator and therapeutic target. *Front Pharmacol*. (2021) 12:755366. doi: 10.3389/fphar.2021.755366

17. Yi YY, Chen H, Zhang SB, Xu HW, Fang XY, Wang SJ. Exogenous klotho ameliorates extracellular matrix degradation and angiogenesis in intervertebral disc degeneration via inhibition of the Rac1/Pak1/Mmp-2 signaling Axis. *Mech Ageing Dev*. (2022) 207:111715. doi: 10.1016/j.mad.2022.111715

18. Castner SA, Gupta S, Wang D, Moreno AJ, Park C, Chen C, et al. Longevity factor klotho enhances cognition in aged nonhuman Primates. *Nat Aging*. (2023) 3:931–7. doi: 10.1038/s43587-023-00441-x

19. Kale A, Sankrityayan H, Anders HJ, Gaikwad AB. Epigenetic and non-epigenetic regulation of klotho in kidney disease. *Life Sci*. (2021) 264:118644. doi: 10.1016/j.lfs.2020.118644

20. Zheng Y, Cantley LC. Toward a better understanding of folate metabolism in health and disease. *J Exp Med*. (2019) 216:253–66. doi: 10.1084/jem.20181965

21. Clare CE, Brassington AH, Kwong WY, Sinclair KD. One-carbon metabolism: linking nutritional biochemistry to epigenetic programming of long-term development. *Annu Rev Anim Biosci*. (2019) 7:263–87. doi: 10.1146/annurev-animal-020518-115206

22. Koury MJ, Ponka P. New insights into erythropoiesis: the roles of folate, vitamin B12, and Iron. *Annu Rev Nutr*. (2004) 24:105–31. doi: 10.1146/annurev.nutr.24.012003.132306

23. Stanhewicz AE, Kenney WL. Role of folic acid in nitric oxide bioavailability and vascular endothelial function. *Nutr Rev*. (2017) 75:61–70. doi: 10.1093/nutrit/nuw053

24. Copp AJ, Greene ND. Neural tube defects: prevention by folic acid and other vitamins. *Indian J Pediatr*. (2000) 67:915–21. doi: 10.1007/bf02723958

25. Tamura T, Picciano MF. Folate and human reproduction. *Am J Clin Nutr*. (2006) 83:993–1016. doi: 10.1093/ajcn/83.5.993

26. Liu Y, Geng T, Wan Z, Lu Q, Zhang X, Qiu Z, et al. Associations of serum folate and vitamin B12 levels with cardiovascular disease mortality among patients with type 2 diabetes. *JAMA Netw Open*. (2022) 5:e2146124. doi: 10.1001/jamanetworkopen.2021.46124

27. Ashraf MJ, Cook JR, Rothberg MB. Clinical utility of folic acid testing for patients with Anemia or dementia. *J Gen Intern Med*. (2008) 23:824–6. doi: 10.1007/s11606-008-0615-z

28. Paniz C, Bertinato JF, Lucena MR, De Carli E, Amorim P, Gomes GW, et al. A daily dose of 5 mg folic acid for 90 days is associated with increased serum Unmetabolized folic acid and reduced natural killer cell cytotoxicity in healthy Brazilian adults. *J Nutr*. (2017) 147:1677–85. doi: 10.3945/jn.117.247445

29. Wu SE, Chen YJ, Chen WL. Adherence to Mediterranean diet and soluble klotho level: the value of food synergy in aging. *Nutrients*. (2022) 14:3910. doi: 10.3390/nu14193910

30. Liu S, Wu M, Wang Y, Xiang L, Luo G, Lin Q, et al. The association between dietary Fiber intake and serum klotho levels in Americans: a cross-sectional study from the National Health and nutrition examination survey. *Nutrients*. (2023) 15:3147. doi: 10.3390/nu15143147

31. Willett WC, Howe GR, Kushi LH. Adjustment for Total energy intake in epidemiologic studies. *Am J Clin Nutr*. (1997) 65:1220S–8S. doi: 10.1093/ajcn/65.4.1220S

32. Institute of Medicine Standing Committee on the Scientific Evaluation of Dietary Reference I, its Panel on Folate OBV, Choline. Dietary Reference Intakes for Thiamin, Riboflavin, Niacin, Vitamin B(6), Folate, Vitamin B(12), Pantothenic Acid, Biotin, and Choline. Washington (DC): National Academies Press (1998).

33. Yan S, Luo W, Lei L, Zhang Q, Xiu J. Association between serum klotho concentration and hyperlipidemia in adults: a cross-sectional study from Nhanes 2007-2016. *Front Endocrinol (Lausanne)*. (2023) 14:1280873. doi: 10.3389/fendo.2023.1280873

34. Yan Y, Chen J. Association between serum klotho concentration and all-cause and cardiovascular mortality among American individuals with hypertension. *Front Cardiovasc Med*. (2022) 9:1013747. doi: 10.3389/fcvm.2022.1013747

35. Wang K, Mao Y, Lu M, Liu X, Sun Y, Li Z, et al. Association between serum klotho levels and the prevalence of diabetes among adults in the United States. *Front Endocrinol (Lausanne)*. (2022) 13:1005553. doi: 10.3389/fendo.2022.1005553

36. Cai J, Zhang L, Chen C, Ge J, Li M, Zhang Y, et al. Association between serum klotho concentration and heart failure in adults, a cross-sectional study from Nhanes 2007-2016. *Int J Cardiol*. (2023) 370:236–43. doi: 10.1016/j.ijcard.2022.11.010

37. Xu JP, Zeng RX, He MH, Lin SS, Guo LH, Zhang MZ. Associations between serum soluble A-klotho and the prevalence of specific cardiovascular disease. *Front Cardiovasc Med*. (2022) 9:899307. doi: 10.3389/fcvm.2022.899307

38. Chang K, Li Y, Qin Z, Zhang Z, Wang L, Yang Q, et al. Association between serum soluble A-klotho and urinary albumin excretion in middle-aged and older us adults: Nhanes 2007-2016. *J Clin Med*. (2023) 12:637. doi: 10.3390/jcm12020637

39. Rosario FJ, Nathanielsz PW, Powell TL, Jansson T. Maternal folate deficiency causes inhibition of Mtor signaling, Down-regulation of placental amino acid transporters and fetal growth restriction in mice. *Sci Rep*. (2017) 7:3982. doi: 10.1038/s41598-017-03888-2

40. Silva E, Rosario FJ, Powell TL, Jansson T. Mechanistic target of rapamycin is a novel molecular mechanism linking folate availability and cell function. *J Nutr*. (2017) 147:1237–42. doi: 10.3945/jn.117.248823

41. Annibal A, Tharyan RG, Schonewolff MF, Tam H, Latza C, Auler MMK, et al. Regulation of the one carbon folate cycle as a shared metabolic signature of longevity. *Nat Commun*. (2021) 12:3486. doi: 10.1038/s41467-021-23856-9

42. Chang WL, Ghosh J, Cooper HS, Vanderveer L, Schultz B, Zhou Y, et al. Folic acid supplementation promotes Hypomethylation in both the inflamed colonic mucosa and colitis-associated dysplasia. *Cancers (Basel)*. (2023) 15:2949. doi: 10.3390/cancers15112949

43. Morris MC, Wang Y, Barnes LL, Bennett DA, Dawson-Hughes B, Booth SL. Nutrients and bioactives in green leafy vegetables and cognitive decline: prospective study. *Neurology*. (2018) 90:e214–22. doi: 10.1212/wnl.0000000000004815

44. Saini RK, Nile SH, Park SW. Carotenoids from fruits and vegetables: chemistry, analysis, occurrence, bioavailability and biological activities. *Food Res Int*. (2015) 76:735–50. doi: 10.1016/j.foodres.2015.07.047

45. Miles EA, Calder PC. Effects of Citrus fruit juices and their bioactive components on inflammation and immunity: a narrative review. *Front Immunol*. (2021) 12:712608. doi: 10.3389/fimmu.2021.712608

46. Thomas PM, Flanagan VP, Pawlosky RJ. Determination of 5-Methyltetrahydrofolic acid and folic acid in Citrus juices using stable isotope dilution-mass spectrometry. *J Agric Food Chem*. (2003) 51:1293–6. doi: 10.1021/jf020902e

47. Liang Q, Wang K, Shariful I, Ye X, Zhang C. Folate content and retention in wheat grains and wheat-based foods: effects of storage, processing, and cooking methods. *Food Chem*. (2020) 333:127459. doi: 10.1016/j.foodchem.2020.127459

48. Crider KS, Bailey LB, Berry RJ. Folic acid food fortification-its history, effect, concerns, and future directions. *Nutrients*. (2011) 3:370–84. doi: 10.3390/nu3030370

49. Centeno Tablante E, Pachón H, Guetterman HM, Finkelstein JL. Fortification of wheat and maize flour with folic acid for population health outcomes. *Cochrane Database Syst Rev*. (2019) 7:CD012150. doi: 10.1002/14651858.CD012150.pub2

50. Wang A, Rose CE, Qi YP, Williams JL, Pfeiffer CM, Crider KS. Impact of voluntary folic acid fortification of corn Masa flour on Rbc folate concentrations in the U.S. (Nhanes 2011-2018). *Nutrients*. (2021) 13:1325. doi: 10.3390/nu13041325

51. Liu M, Ye Z, Yang S, Zhang Y, Zhang Y, He P, et al. Relationship of dietary intake of food folate and synthetic folic acid intake from fortified foods with all-cause mortality in individuals with chronic kidney disease. *Food Funct*. (2024) 15:559–68. doi: 10.1039/d3fo03927g

52. Gomes S, Lopes C, Pinto E. Folate and folic acid in the Periconceptional period: recommendations from official health organizations in thirty-six countries worldwide and who. *Public Health Nutr*. (2016) 19:176–89. doi: 10.1017/s1368980015000555

53. Patel KR, Sobczyńska-Malefora A. The adverse effects of an excessive folic acid intake. *Eur J Clin Nutr*. (2017) 71:159–63. doi: 10.1038/ejcn.2016.194

54. Henry CJ, Nemkov T, Casás-Selves M, Bilousova G, Zaberezhnyy V, Higa KC, et al. Folate dietary insufficiency and folic acid supplementation similarly impair metabolism and compromise hematopoiesis. *Haematologica*. (2017) 102:1985–94. doi: 10.3324/haematol.2017.171074

55. Zhao G, Deng J, Shen Y, Zhang P, Dong H, Xie Z, et al. Hyperhomocysteinemia is key for increased susceptibility to Pnd in aged mice. *Ann Clin Transl Neurol*. (2019) 6:1435–44. doi: 10.1002/acn3.50838

56. Gil Martínez V, Avedillo Salas A, Santander BS. Vitamin supplementation and dementia: a systematic review. *Nutrients*. (2022) 14:1033. doi: 10.3390/nu14051033

57. Vegrim HM, Dreier JW, Alvestad S, Gilhus NE, Gissler M, Igland J, et al. Cancer risk in children of mothers with epilepsy and high-dose folic acid use during pregnancy. *JAMA Neurol*. (2022) 79:1130–8. doi: 10.1001/jamaneurol.2022.2977

58. Fardous AM, Heydari AR. Uncovering the hidden dangers and molecular mechanisms of excess folate: a narrative review. *Nutrients*. (2023) 15:4699. doi: 10.3390/nu15214699

59. Mattson MP, Arumugam TV. Hallmarks of brain aging: adaptive and pathological modification by metabolic states. *Cell Metab*. (2018) 27:1176–99. doi: 10.1016/j.cmet.2018.05.011

60. Xie S, Xu SC, Deng W, Tang Q. Metabolic landscape in cardiac aging: insights into molecular biology and therapeutic implications. *Signal Transduct Target Ther*. (2023) 8:114. doi: 10.1038/s41392-023-01378-8

61. López-Otín C, Blasco MA, Partridge L, Serrano M, Kroemer G. The hallmarks of aging. *Cell*. (2013) 153:1194–217. doi: 10.1016/j.cell.2013.05.039

62. Zhou YH, Tang JY, Wu MJ, Lu J, Wei X, Qin YY, et al. Effect of folic acid supplementation on cardiovascular outcomes: a systematic review and Meta-analysis. *PLoS One*. (2011) 6:e25142. doi: 10.1371/journal.pone.0025142

63. Fratoni V, Brandi ML. B vitamins, homocysteine and bone health. *Nutrients*. (2015) 7:2176–92. doi: 10.3390/nu7042176

64. Espuch-Oliver A, Vázquez-Lorente H, Jurado-Fasoli L, de Haro-Muñoz T, Díaz-Alberola I, López-Velez MDS, et al. References values of soluble A-klotho serum levels using an enzyme-linked immunosorbent assay in healthy adults aged 18-85 years. *J Clin Med*. (2022) 11:2415. doi: 10.3390/jcm11092415

65. Hsu SC, Huang SM, Lin SH, Ka SM, Chen A, Shih MF, et al. Testosterone increases renal anti-aging klotho gene expression via the androgen receptor-mediated pathway. *Biochem J*. (2014) 464:221–9. doi: 10.1042/bj20140739

66. Dote-Montero M, Amaro-Gahete FJ, De-la OA, Jurado-Fasoli L, Gutierrez A, Castillo MJ. Study of the Association of Dheas, testosterone and cortisol with S-klotho plasma levels in healthy sedentary middle-aged adults. *Exp Gerontol*. (2019) 121:55–61. doi: 10.1016/j.exger.2019.03.010

67. Zhang Z, Qiu S, Huang X, Jin K, Zhou X, Lin T, et al. Association between testosterone and serum soluble A-klotho in U.S. males: a cross-sectional study. *BMC Geriatr*. (2022) 22:570. doi: 10.1186/s12877-022-03265-3

frontiers | Frontiers in Nutrition

TYPE Original Research
PUBLISHED 22 July 2024
DOI 10.3389/fnut.2024.1410811

OPEN ACCESS

EDITED BY
Jagannath Misra,
Indiana University, Purdue University Indianapolis, United States

REVIEWED BY
Mithun Rudrapal,
Vignan's Foundation for Science, Technology and Research, India
Vishakha Dey,
Indiana University School of Medicine, United States

*CORRESPONDENCE
Khadijeh Mirzaei
✉ Zahra_roomi@yahoo.com

RECEIVED 23 April 2024
ACCEPTED 10 July 2024
PUBLISHED 22 July 2024

CITATION
Roumi Z, Mirzababaei A, Abaj F, Davaneghi S, Aali Y and Mirzaei K (2024) The interaction between polyphenol intake and genes (MC4R, Cav-1, and Cry1) related to body homeostasis and cardiometabolic risk factors in overweight and obese women: a cross-sectional study.
Front. Nutr. 11:1410811.
doi: 10.3389/fnut.2024.1410811

The interaction between polyphenol intake and genes (MC4R, Cav-1, and Cry1) related to body homeostasis and cardiometabolic risk factors in overweight and obese women: a cross-sectional study

Zahra Roumi[1], Atieh Mirzababaei[1,2], Faezeh Abaj[3], Soheila Davaneghi[4], Yasaman Aali[1,2], and Khadijeh Mirzaei[1]*

[1]Department of Nutrition, Science and Research Branch, Islamic Azad University, Tehran, Iran, [2]Department of Community Nutrition, School of Nutritional Sciences and Dietetics, Tehran University of Medical Sciences (TUMS), Tehran, Iran, [3]Department of Nutrition, Dietetics and Food, School of Clinical Sciences at Monash Health, Monash University, Clayton, VIC, Australia, [4]MSC, School of Nutrition and Food Sciences, Tabriz University of Medical Sciences, Tabriz, Iran

Background: Cardiovascular disease (CVD), which is an important global health challenge, is expanding. One of the main factors in the occurrence of CVD is a high genetic risk. The interaction between genetic risk in CVD and nutrition is debatable. Polyphenols are one of the important dietary components that may have a protective role in people who have a high genetic risk score (GRS) for cardiometabolic risk factors. This study, conducted in overweight and obese women, examines the interaction between polyphenol intake and specific genes (MC4r, Cav-1, and Cry1) related to maintaining body balance and their interaction with cardiometabolic risk factors.

Methods: This cross-sectional study included 391 women who were overweight or obese, aged 18 to 48 years, with a body mass index (BMI) between 25 and 40 kg/m^2. Body composition was measured using the InBody 770 scanner. Total dietary polyphenol intake (TDPI) was assessed with a validated 147-item food frequency questionnaire (FFQ), and polyphenol intakes were determined using the Phenol-Explorer database. Serum samples underwent biochemical tests. The Genetic Risk Score (GRS) was calculated based on the risk alleles of three genes: MC4r, Cav-1, and Cry1.

Results: The mean±standard deviation (SD) age and BMI of women were 36.67 (9.1) years and 30.98 (3.9) kg/m^2, respectively. The high GRS and high TDPI group had a significant negative interaction with fasting blood glucose (FBS) ($p = 0.01$). Individuals who had a high GRS and a high phenolic acid intake were found to have a significant negative interaction with Triglyceride ($p = 0.04$). Similarly, individuals with high GRS and a high intake of flavonoids had a significant negative interaction with TG ($p < 0.01$) and a significant positive interaction with High-density lipoprotein (HDL) ($p = 0.01$) in the adjusted model.

10.3389/fnut.2024.1410811

Conclusion: According to our findings, those with a high GRS may have a protective effect on cardiometabolic risk factors by consuming high amounts of polyphenols. Further studies will be necessary in the future to validate this association.

KEYWORDS

cardiometabolic risk factors, genetic risk score, homeostasis, obesity, polyphenols

Introduction

Cardiovascular disease (CVD), which is the leading cause of death and a global health challenge, is becoming more prevalent (1–3). It is projected that by 2030, the number of deaths from this disease will reach 23.6 million (4). The rate of CVD in women is reported to be 1 in every 3 women, with 45% of women over the age of 20 affected (5, 6). Cardiometabolic risk factors like obesity, high blood pressure, dyslipidemia, and inflammation play a role in the development of CVD (7, 8).

Genetic background plays an important role in CVD (9). CVD is greatly influenced by the genetic predisposition of individuals (10). Research has shown that having a genetic risk for developing cardiometabolic risk factors increases the likelihood of certain health problems, emphasizing the importance of genetic factors in understanding cardiometabolic diseases (11). A genetic risk score (GRS) is an estimate of an individual's genetic predisposition to a specific outcome, such as disease susceptibility. The combination of multiple genetic markers enables the prediction of disease risk based on an individual's genetic profile (12). Genes play a crucial role in maintaining body homeostasis by regulating various metabolic processes. The research suggests that gene expression is closely connected to metabolite homeostasis, influencing adaptations in response to environmental changes and influencing energy efficiency and product formation (13).

Genetic mutations, like the Melanocortin 4 receptor (MC4R) gene mutation, can lead to obesity (14). This gene is situated in the hypothalamus (15, 16) and its mutation may indirectly contribute to a higher risk of mortality from CVD (17). The MC4R gene (rs17782313) not only influences obesity but is also associated with other risk factors for CVD, including hypertension (HTN) (18). Inactivation of the MC4R gene has been shown to reduce blood pressure independently of obesity in previous studies (19).

CAV-1, also known as Caveolin-1, is a protein that has been related to different biological processes and diseases. Research has found that CAV-1 levels are increased in individuals with metabolic syndrome (20). Studies reported that CAV-1 might have a role in the impairment of endothelial function, which is a fundamental anomaly in the development of hypertension, atherosclerosis, and coronary artery disease (21).

Moreover, the presence of CAV-1 in the cells lining the blood vessels can be affected by various factors including green tea polyphenols. The presence of CAV-1 in individuals with metabolic syndrome, a disease linked to insulin resistance (IR), high blood glucose levels, hypertension, abnormal lipid levels, obesity, and increased WC, has been observed (20, 22).

The Cryptochrome 1 (Cry1) gene is a molecular clock gene that plays a role in generating circadian rhythms (23). Evidence suggests a potential association between CRY1 (rs10861688) polymorphism, obesity and related cardiovascular risk factors (24). Research has shown that CRY1 is associated with components of metabolic syndrome, such as hypertension and triglyceride (25) levels, as well as obesity and insulin resistance (IR) (26, 27). Furthermore, recent research has suggested that variations and genetic differences in the human genome, including different forms of the Cry1 gene, could have an effect on energy expenditure and body weight (28).

Nutrition is a factor that influences GRS on the incidence of cardiometabolic diseases (29). Polyphenols, chemical compounds present in plants such as fruits, vegetables, and tea, have been shown in studies to be effective in decreasing the risk factors associated with CVD (30, 31). Previous studies have discussed various types of polyphenols, including flavonoids, stilbenes, phenolic acids, and lignans (32). Numerous research studies have examined the potential benefits of polyphenols in preventing obesity, and there is evidence to suggest that plant polyphenols have the potential to be effective in this area (33). In a cohort study, researchers discovered that elevated levels of flavanones and lignans were correlated with adult body composition, including BMI and waist circumference (WC) (34). Furthermore, a separate study conducted on women showed that polyphenols were linked to decreased fasting blood sugar (FBS) and blood pressure levels. Moreover, there was a significant correlation between elevated levels of high-density lipoprotein (HDL) cholesterol (35, 36).

The GRS allows us to explore how various genes related to cardiometabolic diseases interact with dietary intake to influence cardiometabolic risk factors. In this study, we aim to examine how a high consumption of polyphenols affects cardiometabolic risk factors in individuals with a high GRS, to determine if consuming high levels of polyphenols is beneficial in improving these risk factors.

Method

Study population

In this cross-sectional study, 391 overweight or obese women, aged between 18 and 48 years and with a body mass index (BMI) between 25 and 40 kg/m^2 participated. These women were selected from people who visited 20 different health centers in Tehran using random sampling. Individuals with a prior medical history of cardiovascular or thyroid disease, malignancies, liver or kidney diseases, types of diabetes, acute or chronic diseases, pregnancy, lactation, or menopause, adherence to a specific diet or weight loss

supplements, consumption of glucose and lipid lowering drugs and blood pressure medications within the past year, and smoking were not included in the study. Before the study, all participants were required to sign a written informed consent form. The study protocol received ethics approval from the Human Ethics Committee of Tehran University of Medical Sciences, with the ethics number IR.TUMS.MEDICINE.REC.1402.636. The procedures were conducted in compliance with applicable guidelines and regulations.

Evaluation of dietary intake

The participants' nutritional status, including energy intake, macronutrients, and micronutrients, was assessed using the food frequency questionnaire (FFQ) consisting of 147 items. Previous studies have confirmed the validity of this questionnaire for the Iranian population (37). A trained nutritionist conducted interviews with women to complete this questionnaire. The data were then analyzed using version 7 of the NUTRITIONIST 4 software, after being converted to grams using household measure servings (38).

Evaluation of dietary polyphenol intake (DPI)

The Phenol-Explorer database (www.phenol explorer.eu/contents) was used to gather data on the overall polyphenol content in various foods (39). The total polyphenol content was determined either through the Folin Ciocalteu assay or by calculating the sum of four main subgroups, which include flavonoids, phenolic acids, stilbenes, lignans, and other polyphenols.

Measurement of anthropometric indicators

Participants' height was measured using a Seca stadiometer with an accuracy of 0.1 cm, and their weight was measured with a Seca digital scale (Hamburg, Germany) with an accuracy of 0.1 kg. To measure these two indicators, the participants must be without shoes and in the lightest clothes. BMI was calculated from the ratio of weight (kg) to the square of height (m^2). In addition, to measure abdominal obesity, WC in the smallest circumference and hip circumference (HC) in the largest circumference were measured with an accuracy of 0.1 cm (40). Waist-to-hip ratio (WHR) was also calculated.

Assessment of body composition

The InBody 770 Scanner, a multi-frequency bioelectrical impedance analyzer, was used to measure body composition parameters such as the amount and proportion of visceral fat level (VFL) and obesity degree (3). The measurements were taken in the morning while participants were in a fasted state and wearing light clothing. Participants were instructed to refrain from exercising, carrying electrical devices, and to urinate before the analysis to ensure accuracy. Following the manufacturer's instructions, participants stood on the scale barefoot and held the machine's handles for 20 s, after which the results were printed (41).

Biochemical assessments

To assess the levels of biochemical factors (such as glucose and lipids) in the participants, blood samples were collected after a period of fasting and the serum was separated using a centrifuge. The serum was then divided into smaller portions and stored at −80°C until it could be analyzed. All blood parameters were measured in the Bionanotechnology Laboratory of the Endocrine and Metabolism Research Institute of Tehran University of Medical Sciences and analyzed using an exclusive assay based on the instructions provided by the manufacturer. All calculations were performed using a package from Randox Laboratories (Hitachi 902). The GPO-PAP method was employed to determine the levels of TG, while enzymatic and clearance endpoint assays were utilized to measure the total cholesterol (TC) and HDL cholesterol, respectively, in this research (42). Alanine aminotransferase (4) and aspartate aminotransferase (AST) were measured via standard protocols.

Measurement of genetic risk score (GRS)

The DNA was obtained from whole blood samples through salting out techniques (43). The quality and quantity of the extracted DNA were evaluated using 1% agarose gel and the Nanodrop 8000 Spectrophotometer, respectively. TaqMan Open Array was used to genotype single nucleotide polymorphisms (SNPs), including CAV-1 (rs3807992), Cry1 (rs2287161), and MC4R (rs17782313) (44). These SNPs have been associated with obesity-related traits in previous studies (45–47). The GRS was computed by summing up the scores of the three SNPs, which were coded as 0, 1, or 2 based on their association with higher BMI. The unweighted GRS ranges from 0 to 6, with higher scores indicating a greater genetic predisposition to high BMI (48).

Measurement of blood pressure

Systolic blood pressure (SBP) and diastolic blood pressure (DBP) were measured using standard sphygmomanometer and cuff through auscultation. After each subject had sat for at least 5 min, two consecutive blood pressure measurements were taken. Systolic blood pressure (SBP) and diastolic blood pressure (DBP) were measured with a standard mercury sphygmomanometer using the first and fifth Korotkoff sounds, to within 2 mmHg. If the difference between the two systolic or diastolic blood pressures was more than 5 mmHg, an additional measurement was performed.

Assessment of other variables

Trained nutritionists filled out a demographic questionnaire that consisted of information regarding job, education, marital, and economic status. The present study measured PA as a confounding variable using the International Physical Activity Questionnaire (IPAQ). The data obtained from this questionnaire was measured on a scale of metabolic hours per week (MET. h $week^{-1}$) (49).

Statistical analysis

In the present study, cardiometabolic risk factors were determined based on biochemical, anthropometric and body composition criteria. The statistical analyses were performed using the IBM SPSS Statistics 23 software, with a significance level of less than 0.05. The normality of the distribution of the quantitative data of the study was performed by the Kolmogorov–Smirnov test. In this study, qualitative variables (Marriage, Education, Job and Economic Status) were described as numbers/percentages and quantitative variables (demographic variables, anthropometric measurements, body composition, blood parameters and blood pressure) were described as mean ± standard deviation (SD). The characteristics of the study participants among the tertile of GRS were compared with ANOVA and the characteristics of the study participants among the total dietary polyphenols index (TDPI) were compared with the independent t-test. To eliminate any confounding outcomes, ANCOVA was utilized. Both the crude and adjusted models employed a generalized linear model (GLM) to evaluate the interactions between metabolic factors and GRS, phenolic acid, lignans, flavonoids, and polyphenol. The outcomes were adjusted for age, energy intake, and PA.

Results

Study population characteristic

Our study was conducted on 391 overweight or obese women. The mean (± SD) age, weight, BMI and WC of participants were 36.67 (9.1) years, 80.28 (11.05) kg, 30.98 (3.9) kg/m^2 and 99.16 (9.42) cm, respectively. Most of the participants were married (70.8%) and had no academic education (51%). They were also in a Moderate economic situation (45.5%).

Characteristics of the study participants among tertile of GRS

The baseline characteristics of the study participants were presented in Table 1, categorized based on tertiles of their GRS. According to the table, in crude model there were a significant difference in mean values among the GRS tertiles for weight ($p = 0.03$), height ($p = 0.03$), WC ($p = 0.03$), and WHR ($p = 0.03$). There was also a marginally significant difference for TG ($p = 0.06$) among the GRS tertiles. After adjusting for confounding factors such as age, PA, and energy intake, the VFL ($p = 0.03$), SBP ($p = 0.01$), FBS ($p = 0.02$), and LDL ($p = 0.01$) became significantly different among the GRS tertiles. Additionally, there was a significant difference in height ($p = 0.005$), WC ($p = 0.04$), and WHR ($p = 0.02$), and a marginally significant difference for weight ($p = 0.06$) and TC ($p = 0.08$) among the GRS tertiles.

Characteristics of the study participants among intake of TDPI

In Table 2, the characteristics of the participants are compared based on receiving low and high TDPI. The results showed that in the crude model, there is a significant difference between the two groups (low and high TDPI) in terms of job ($p = 0.02$), However in the adjusted model (age, PA, and energy intake), in addition to job ($p = 0.01$), the participants also had significant differences in terms of FBS ($p < 0.001$), TC ($p = 0.01$), and LDL ($p < 0.001$). Also a marginal difference for WC ($p = 0.08$) and WHR ($p = 0.09$) between the low intake and high intake groups of TDPI.

The interaction between GRS, TDPI, stilbenes, phenolic acid, lignans, flavonoids and polyphenol on cardiometabolic risk factors

The findings on the interaction between GRS, TDPI, and stilbenes on cardiometabolic risk factors are presented in Table 3. The crude and adjusted models showed a significant negative interaction between high GRS and high intake TDPI with FBS (crude: 95%CI = −20.39, −3.28, $p < 0.001$; adjusted: 95%CI = −19.95, −1.8, $p = 0.01$).

The findings also showed that the significant negative interaction between moderate GRS and high intake TDPI with BMI (95%CI = −5.05, −1.03, $p < 0.001$), WC (95%CI = −12.53, −2.33, $p < 0.001$), VFL (95%CI = −3.88, −0.33, $p = 0.02$), FBS (95%CI = −20.39, −3.28, $p < 0.001$) and LDL (95% CI = −28.75, 0.028, $p = 0.05$) in the crude model. After adjusting for age, IPAC and total energy intake in model 1, the interaction between moderate GRS and high intake TDPI with BMI (95% CI = −4.55, −0.46, $p = 0.01$), WC (95% CI = −12.51, −2.38, $p < 0.001$), VFL (95% CI = −3.85, −0.26, $p = 0.02$) and FBS (95% CI = −13.38, −1.63, $p = 0.01$) remained negative. The interaction between TDPI and GRS on BMI, WC, VFL and FBS is shown in Figure 1.

Furthermore, there was no significant interaction found between moderate/high GRS and stilbenes with cardiometabolic risk factors in both the crude and adjusted models.

The interaction between GRS, phenolic acid and lignans on cardiometabolic risk factors were presented in Table 4. In the crude model, a significant positive interaction was observed between high GRS and high intake phenolic acid on HDL (95%CI = 0.16, 19.23, $p = 0.04$) But in adjusted model, this interaction was not reported. However, a significant negative interaction was observed between high GRS and high intake phenolic acid on TG (95%CI = −115.66, −2.42, $p = 0.04$). Interaction between Phenolic acid and GRS on TG is shown in Figure 2.

Furthermore, there was no significant interaction found between moderate/high GRS and lignans with cardiometabolic risk factors in both the crude and adjusted models.

The interaction between GRS, flavonoids and polyphenol on cardiometabolic risk factors were presented in Table 5. The crude and adjusted models showed a significant negative interaction between high GRS and high intake flavonoids with TG (crude: 95%CI = −137.58, −31.2, $p < 0.001$; adjusted: 95%CI = −135.52, −22.69, $p < 0.001$). Also, a significant positive interaction was observed between high GRS and high intake flavonoids with HDL (95%CI = 2.47, 22.65, $p = 0.01$) in the adjusted model.

The findings also showed that the significant negative interaction between moderate GRS and high intake flavonoids with BMI

10.3389/fnut.2024.1410811

TABLE 1 Characteristics of the study participants among tertile of genetic risk score (GRS).

Variables		GRS				
		Low risk <3 (n = 164)	Moderate risk (3&4) (n = 97)	High risk ≥5 (n = 130)	p-value	p-value*
Demographic variables						
Age (years)		36.02 ± 8.78	36.53 ± 8.15	36.08 ± 8.61	0.91	0.89
PA (MET-minutes/week)		1052.27 ± 1116.01	1353.96 ± 2742.28	1389.51 ± 2576.15	0.61	0.58
Anthropometric measurements						
Weight (kg)		79.31 ± 9.79	76.9903 ± 10.29312	82.47 ± 9.33	**0.03**	0.06
Height (cm)		162.46 ± 5.41	160.26 ± 5.93	161.41 ± 4.45	**0.03**	**0.005**
BMI (kg/m^2)		29.98 ± 3.31	30.09 ± 3.5	31.44 ± 3.32	0.16	0.22
WC (cm)		97.39 ± 8.62	96.4 ± 8.56	101.42 ± 9.03	**0.03**	**0.04**
WHR		0.92 ± 0.05	0.92 ± 0.04	0.95 ± 0.05	**0.03**	**0.02**
Body composition						
VFL (cm^2)		14.9 ± 3.15	15 ± 3.07	16.16 ± 2.98	0.19	**0.03**
OD (%)		139.37 ± 15.47	139.91 ± 16.32	146.25 ± 15.54	0.16	0.22
Blood pressure						
SBP (mmHg)		111.24 ± 12.06	111.26 ± 15.38	113.08 ± 14.57	0.83	**0.01**
DBP (mmHg)		77.14 ± 10.08	77.44 ± 9.51	77.58 ± 11.04	0.97	0.16
Blood parameters						
FBS (mg/dL)		87.32 ± 9.2	86.46 ± 10.32	88.7 ± 9.82	0.57	**0.02**
TC (mg/dL)		186.41 ± 33.3	182.95 ± 37.7	179.83 ± 35.46	0.68	0.08
TG (mg/dL)		120.83 ± 57.88	108.35 ± 53.01	136.91 ± 75.67	0.06	0.11
HDL (mg/dL)		47.35 ± 9.69	47.59 ± 11.62	46.87 ± 11.6	0.95	0.98
LDL (mg/dL)		96.96 ± 21.67	95.12 ± 25.51	90.45 ± 25.82	0.51	**0.01**
AST (IU/L)		17.51 ± 6.9	17.97 ± 8.08	17.91 ± 8.56	0.92	0.79
ALT (IU/L)		18.16 ± 14.02	18.77 ± 13.31	20.25 ± 13.68	0.8	0.53
Qualitative variable N (%)						
Marriage status	Single	29 (49.2)	25 (42.4)	5 (8.5)	0.16	0.18
	Married	69 (35.9)	96 (50)	27 (14.1)		
Education levels	Non academic	49 (76.8)	62 (88.4)	22 (34.9)	0.3	0.32
	Academic	49 (42.2)	57 (49.1)	10 (8.6)		
Job	Unemployed	52 (34.7)	77 (51.3)	21 (14)	0.16	0.18
	Employed	45 (46.9)	40 (41.7)	11 (11.5)		
Economic status	Poor	19 (34.5)	27 (49.1)	9 (16.4)	0.77	0.77
	Moderate	46 (39.3)	56 (47.9)	15 (12.8)		
	Good	28 (43.8)	30 (46.9)	6 (9.4)		

BMI, Body mass index; WC, waist circumference; WHR, waist height ratio; FBS, fasting blood sugar; Chol, Cholesterol; TG, Triglyceride; HDL, High density lipoprotein; LDL, Low density lipoprotein; SBP, Systolic Blood Pressure; DBP, Diastolic Blood Pressure; OD, Obesity degree; VFL, Visceral fat level; TC, total cholesterol.
Quantitative variable: Mean ± SD (Standard deviation), Qualitative variable: N (%) Number (Percentage).
p-values < 0.05 are in bold.
p-value calculated by analysis of variance (ANOVA).
*p-value was found by ANCOVA, and adjusted for age, IPAC and total energy intake.

(95%CI = −5.44, −1.49, p < 0.001), WC (95%CI = −12.48, −2.39, p < 0.001), VFL (95%CI = −3.96, −0.46, p = 0.01) and OD (95%CI = −24.62, −1.47, p = 0.02) in the crude model. After adjusting for age, IPAC, and total energy intake in model 1, the interaction between moderate GRS and high intake flavonoids with BMI (95%CI = −4.59, −0.52, p = 0.01), WC (95%CI = −10.79, −0.56, p = 0.03) and OD (95%CI = −22.67, 0.27, p = 0.05) remained negative. Interaction between Flavonoids and GRS on BMI, WC, OD, TG and HDL is shown in Figure 3.

Furthermore, there was no significant interaction found between moderate/high GRS and polyphenol with cardiometabolic risk factors in both the crude and adjusted models.

10.3389/fnut.2024.1410811

TABLE 2 Characteristics of the study participants among intake of total dietary polyphenols index (TDPI).

Quantitative variables		TDPI			
		Low intake (n = 196)	High intake (n = 195)	p-value	p-value *
Demographic variables					
Age (years)		35.44 ± 8.58	36.77 ± 8.42	0.23	0.31
PA(MET-minutes/week)		1086.64 ± 2159.97	1292.74 ± 2061.70	0.44	0.21
Anthropometric measurements					
BMI (kg/m^2)		30.6 ± 4.06	30.29 ± 3.4	0.53	0.43
Weight (kg)		80.51 ± 11.04	79.73 ± 10.56	0.48	0.21
Height (cm)		160.82 ± 6.31	161.25 ± 5.31	0.47	0.35
WC (cm)		98.17 ± 9.06	97.32 ± 9.24	0.48	0.08
WHR		0.93 ± 0.046	0.92 ± 0.05	0.45	0.09
Body composition					
VFL (cm^2)		15.32 ± 3.3	15.06 ± 3.3	0.55	0.45
OD (%)		142.21 ± 18.98	140.88 ± 15.84	0.56	0.43
Blood parameters					
FBS (mg/dL)		88.19 ± 11.18	86.77 ± 8.4	0.27	**<0.001**
TC (mg/dL)		186.86 ± 40.29	182.19 ± 32.73	0.33	**0.01**
TG (mg/dL)		116.29 ± 56.32	118.61 ± 60.03	0.76	0.31
HDL (mg/dL)		46.63 ± 11.28	47.39 ± 10.35	0.59	0.73
LDL (mg/dL)		94.68 ± 24.53	95.55 ± 23.98	0.78	**<0.001**
AST (IU/L)		17.97 ± 6.37	17.68 ± 8.11	0.76	0.81
ALT (IU/L)		18.68 ± 10.33	19.38 ± 14.93	0.68	0.48
Qualitative variable					
Marriage status	Single	58 (52.7)	52 (47.3)	0.29	0.36
	Married	138 (49.1)	143 (50.9)		
Education	Nonacademic	97 (49.5)	107 (55.4)	0.26	0.14
	Academic	99 (50.5)	86 (44.6)		
Job	Unemployed	105 (46.3)	122 (53.7)	**0.02**	**0.01**
	Employed	90 (57)	68 (43)		
Economic status	Poor	42 (47.7)	46 (52.3)	0.18	0.17
	Moderate	86 (47.3)	96 (52.7)		
	Good	62 (57.9)	45 (42.1)		

BMI, Body mass index; WC, waist circumference; WHR, waist height ratio; FBS, fasting blood sugar; Chol, Cholesterol; TG, Triglyceride; HDL, High density lipoprotein; LDL, Low-density lipoprotein; OD, Obesity degree; VFL, Visceral fat level; TC, total cholesterol.
TDPI Low intake < 2060.65 (mg/day), TDPI High intake ≥ 2060.65(mg/day).
p-values < 0.05 are in bold.
Quantitative variable: Mean ± SD (Standard deviation).
Qualitative variable N (%): N (%) Number (Percentage).
p-value calculated by analysis of independent sample t-test.
p-value *Adjusted for age, IPAC, and total energy intake calculated by analysis of covariance (ANCOVA).

Discussion

The purpose of this cross-sectional study was to investigate the relationship between polyphenol consumption and genes (MC4r, Cav-1, and Cry1) and cardiometabolic risk factors in overweight and obese Iranian women.

The findings of our study revealed a significant negative interaction between high GRS and high intake TDPI with FBS in both crude and adjusted models. Also, a significant negative interaction was observed between high GRS and high intake of phenolic acid on TG in the adjusted model. Moreover, a significant negative interaction was observed between high GRS and high intake flavonoids with TG, and a significant positive interaction was observed between high GRS and high intake flavonoids with HDL in the adjusted model. Furthermore, a significant negative interaction between moderate GRS and high intake TDPI on BMI, WC, VLF and FBS levels. According to our results, high intake of TDPI is associated with significant interaction with decreased levels of BMI, WC, VLF, and FBS in participants at moderate risk of GRS. In addition, in this study reported a significant negative interaction between moderate GRS and flavonoid on BMI, WC and OD levels.

10.3389/fnut.2024.1410811

TABLE 3 The interaction between GRS, TDPI and stilbenes on cardiometabolic risk factors.

Variables	GRS	TDPI							Stilbenes						
		Low intake < 2060.65 (mg/day)	High intake						Low intake < 0.49 (mg/day)	High intake					
			Crude			Adjust				Crude			Adjust		
			β	95% CI	*p*	β	95% CI	*p*		β	95% CI	*p*	β	95% CI	*p*
Anthropometric factors															
BMI (kg/m^2)	Low risk	Reference	Reference						Reference	Reference					
	Moderate risk	–	−3.04	−5.05 to −1.03	**<0.001**	−2.50	−4.55 to −0.46	**0.01**	–	0.48	−1.49 to 2.47	0.62	0.12	−1.89 to 2.14	0.9
	High risk	–	−1.81	−4.96 to 1.34	0.26	−1.79	−5.01 to 1.42	0.27	–	−1.16	−4.13 to 1.8	0.44	−0.43	−3.47 to 2.59	0.77
WC (cm)	Low risk	Reference	Reference						Reference	Reference					
	Moderate risk	–	−7.43	−12.53 to −2.33	**<0.001**	−7.45	−12.51 to −2.38	**<0.001**	–	3.27	−1.73 to 8.29	0.2	2.68	−2.36 to 7.73	0.29
	High risk	–	−5.29	−13.12 to 2.53	0.18	−5.59	−13.32 to 2.14	0.15	–	−2.35	−9.8 to 5.09	0.53	−1.21	−8.72 to 6.29	0.75
WHR	Low risk	Reference	Reference						Reference	Reference					
	Moderate risk	–	−0.01	−0.048 to 0.008	0.17	−0.02	−0.052 to 0.004	0.09	–	0.02	0.001–0.056	0.06	0.02	−0.005 to 0.05	0.1
	High risk	–	−0.02	−0.056 to 0.031	0.56	<0.001	−0.051 to 0.035	0.71	–	−0.01	−0.051 to 0.03	0.61	<0.001	−0.05 to 0.32	0.68
Body composition															
VFL (cm^2)	low risk	Reference	Reference						Reference	Reference					
	Moderate risk	–	−2.11	−3.88 to −0.33	**0.02**	−2.06	−3.85 to −0.26	**0.02**	–	0.89	−1.66 to 1.83	0.92	−0.23	−2.02 to 1.55	0.79
	High risk	–	−1.02	−3.76 to 1.71	0.46	−0.82	−3.58 to 1.93	0.55	–	−0.96	−3.56 to 1.64	0.47	−0.31	−2.98 to 2.34	0.81
OD (%)	Low risk	Reference	Reference						Reference	Reference					
	Moderate risk	–	−6.70	−18.47 to 5.06	0.26	−6.77	−18.37 to 4.82	0.25	–	2.17	−9.32 to 13.67	0.71	−2.32	−13.78 to 9.13	0.69
	High risk	–	−8.52	−26.69 to 9.65	0.35	−9.56	−27.36 to 8.23	0.29	–	−7.73	−24.85 to 9.39	0.37	−4.72	−21.77 to 12.32	0.58
Biochemical variables															
FBS (mg/dL)	Low risk	Reference	Reference						Reference	Reference					
	Moderate risk	–	−9.16	−14.74 to −3.58	**<0.001**	−7.51	−13.38 to −1.63	**0.01**	–	3.06	−2.41 to 8.53	0.27	3.48	−2.29 to 9.17	0.24
	High risk	–	−11.83	−20.39 to −3.28	**<0.001**	−10.88	−19.95 to −1.8	**0.01**	–	2.58	−5.68 to 10.85	0.54	4.09	−4.66 to 12.84	0.36

(Continued)

10.3389/fnut.2024.1410811

TABLE 3 (Continued)

Variables	GRS	TDPI							Stilbenes						
		Low intake < 2060.65 (mg/day)	High intake						Low intake < 0.49 (mg/day)	High intake					
			Crude			Adjust				Crude			Adjust		
			β	95% CI	*p*	β	95% CI	*p*		β	95% CI	*p*	β	95% CI	*p*
TC (mg/dL)	Low risk	Reference	Reference						Reference	Reference					
	Moderate risk	–	−25.02	−46.51 to −3.54	0.22	−18.77	−40.94 to 3.39	0.09	–	1.51	−19.24 to 22.28	0.88	−3.86	−25.18 to 17.44	0.72
	High risk	–	−21.92	−54.89 to 11.04	0.19	−18.74	−52.97 to 15.49	0.28	–	3.88	−27.47 to 35.24	0.8	17.08	−15.44 to 49.62	0.3
TG (mg/dL)	Low risk	Reference	Reference						Reference	Reference					
	Moderate risk	–	−7.63	−44.58 to 29.23	0.68	0.45	−38.6 to 39.52	0.98	–	18.50	−16.65 to 53.67	0.3	14.71	−22.49 to 51.91	0.43
	High risk	–	−23.11	−81.29 to 35.06	0.43	−21.68	−83.49 to 40.12	0.49	–	4.36	−49.41 to 58.13	0.87	14.59	−42.95 to 72.15	0.61
HDL (mg/dL)	Low risk	Reference	Reference						Reference	Reference					
	Moderate risk	–	−1.42	−8.12 to 5.26	0.67	1.23	−5.8 to 8.26	0.73	–	0.30	−5.97 to 6.58	0.92	0.51	−6.12 to 7.14	0.88
	High risk	–	2.73	−7.53 to 13	0.6	1.09	−9.76 to 11.95	0.84	–	2.71	−6.7 to 12.26	0.56	4.77	−5.35 to 14.89	0.35
LDL (mg/dL)	Low risk	Reference	Reference						Reference	Reference					
	Moderate risk	–	−14.36	−28.75 to 0.028	**0.05**	−6.08	−21.04 to 8.87	0.42	–	6.25	−7.41 to 19.91	0.37	7.05	−7.12 to 21.24	0.33
	High risk	–	−20.03	−42.11 to 2.049	0.07	−21.10	−44.2 to 1.99	0.07	–	6.39	−14.24 to 27.03	0.54	12.57	−9.08 to 34.22	0.25
AST (IU/L)	Low risk	Reference	Reference						Reference	Reference					
	Moderate risk	–	−0.50	−5.05 to 4.038	0.82	0.83	−3.91 to 5.59	0.72	–	0.52	−3.8 to 4.86	0.81	1.94	−2.58 to 6.47	0.4
	High risk	–	−4.80	−11.78 to 2.16	0.17	−3.90	−11.25 to 3.43	0.29	–	−3.69	−10.51 to 2.57	0.23	−3.76	−10.68 to 3.14	0.28
ALT (IU/L)	Low risk	Reference	Reference						Reference	Reference					
	Moderate risk	–	−3.25	−11.27 to 4.76	0.42	−1.39	−9.92 to 7.14	0.74	–	0.64	−7.01 to 8.29	0.86	3.00	−5.14 to 11.14	0.47
	High risk	–	−5.93	−18.23 to 6.37	0.34	−4.02	−17.2 to 9.15	0.54	–	−2.71	−14.27 to 8.85	0.64	−0.96	−13.39 to 11.46	0.87

B, Standard Error; GRS, Genetic risk score; BMI, Body mass index; WC, waist circumference; WHR, waist height ratio; FBS, fasting blood sugar; TG, Triglyceride; LDL, Low density lipoprotein; HDL, High density lipoprotein; OD Obesity degree; VFL, Visceral fat level; TC, total cholesterol.

TDPI High intake ≥ 2060.65 (mg/day), Stilbenes High intake ≥ 0.49(mg/day).

p-values < 0.05 are in bold.

Adjust = adjusted for potential confounding factors including (age, IPAC and total energy intake).

Low Risk: 0,1,2 Risk alleles, Moderate Risk: 3,4 Risk allele, High Risk: 5,6 Risk allele.

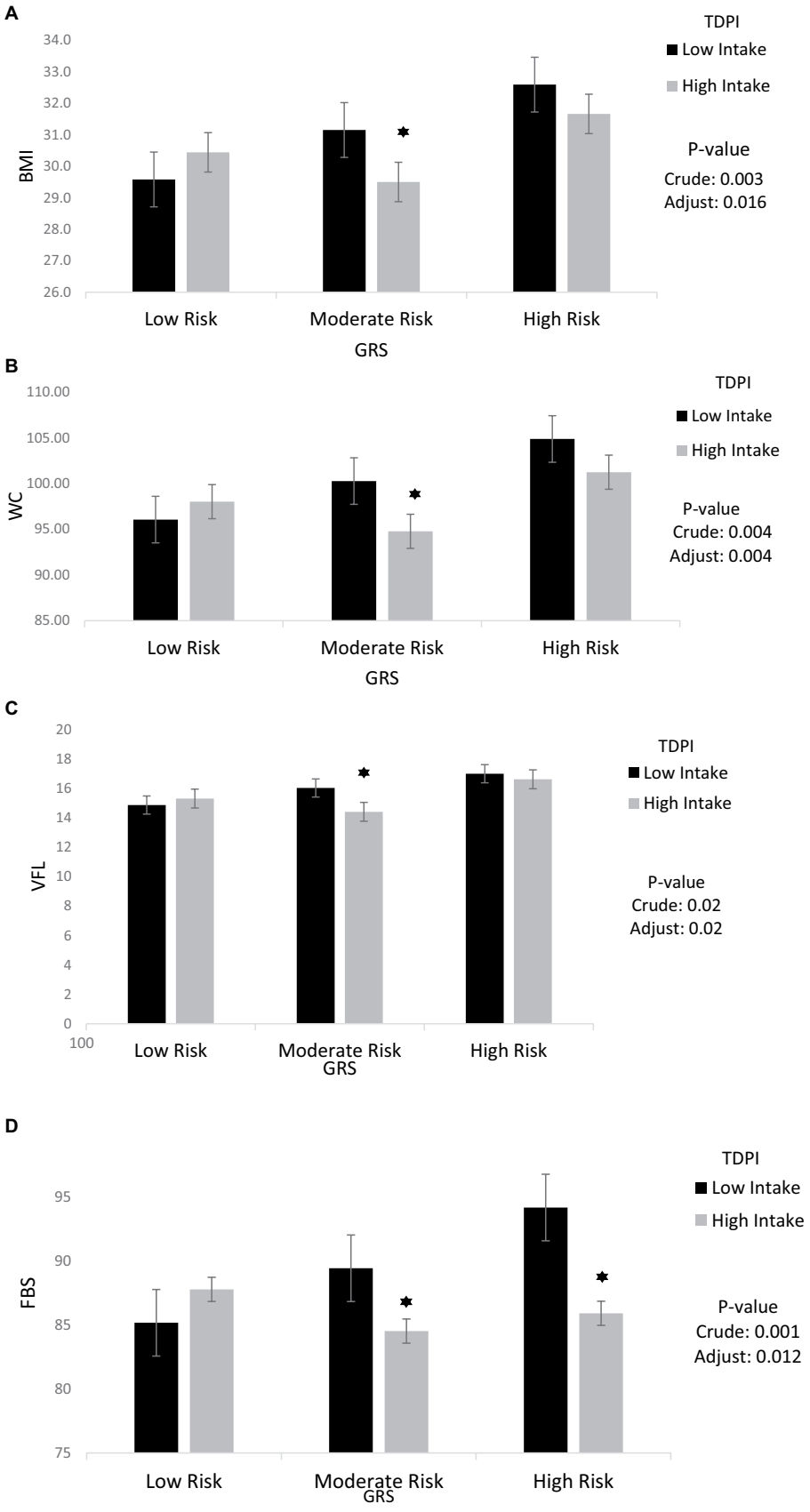

FIGURE 1
Interaction between TDPI and GRS on **(A)** BMI, **(B)** WC, **(C)** VFL, **(D)** FBS. The interaction between low and high intake of TDPI and GRS. Data shown are mean ± standard error of the mean. BMI, Body mass index; WC, Waist circumference; VFL, Visceral fat level; FBS, Fasting Blood Sugar; GRS, genetic risk score; TDPI, total dietary polyphenol intake. Adjust = adjusted for potential confounding factors including (age, IPAC and total energy intake). The asterisk (*) represents the *p*-value of the statistical test. The asterisk means that the *p*-value is less than 0.05.

10.3389/fnut.2024.1410811

TABLE 4 The interaction between GRS, phenolic acid and Lignans on cardiometabolic risk factors.

Variables	GRS	Phenolic acid							Lignans						
		Low intake < 55.95 (mg/day)	High intake						Low intake < 0.0065 (mg/day)	High intake					
			Crude			Adjust				Crude			Adjust		
			β	95% CI	*p*	β	95% CI	*p*		β	95% CI	*p*	β	95% CI	*p*
Anthropometric factors															
BMI (kg/m^2)	Low risk	Reference	Reference						Reference	Reference					
	Moderate risk	–	−0.83	−2.83 to 1.16	0.41	−0.60	−2.62 to 1.41	0.55	–	−0.30	−2.29 to 1.69	0.76	0.48	−1.54 to 2.52	0.63
	High Risk	–	−0.59	−3.56 to 2.37	0.69	−1.26	−4.29 to 1.77	0.41	–	−1.08	−4.04 to 1.88	0.47	−0.60	−3.65 to 2.44	0.69
WC (cm)	Low Risk	Reference	Reference						Reference	Reference					
	Moderate Risk	–	0.33	−4.74 to 5.4	0.89	−0.06	−5.15 to 5.01	0.97	–	−0.69	−5.76 to 4.38	0.78	1.05	−4.03 to 6.15	0.68
	High Risk	–	2.09	−5.38 to 9.56	0.58	<0.001	−7.55 to 7.53	0.99	–	−3.52	−11 to 3.95	0.35	−2.20	−9.8 to 5.39	0.56
WHR	Low Risk	Reference	Reference						Reference	Reference					
	Moderate Risk	–	0.01	−0.01 to 0.04	0.35	0.01	−0.01 to 0.03	0.43	–	<0.001	−0.03 to 0.02	0.67	−2.24	−0.02 to 0.02	0.99
	High Risk	–	0.03	−0.009 to 0.072	0.12	0.02	−0.01 to 0.06	0.21	–	−0.01	−0.05 to 0.02	0.52	<0.001	−0.04 to 0.03	0.86
Body composition															
VFL (cm^2)	Low risk	Reference	Reference						Reference	Reference					
	Moderate risk	–	−0.66	−2.42 to 1.09	0.45	−0.66	−2.44 to 1.12	0.46	–	0.57	−1.17 to 2.33	0.51	0.92	−0.86 to 2.72	0.31
	High risk	–	0.07	−2.51 to 2.67	0.95	−0.24	−2.89 to 2.41	0.85	–	−0.83	−3.42 to 1.76	0.39	0.03	−2.64 to 2.7	0.98
OD (%)	Low risk	Reference	Reference						Reference	Reference					
	Moderate risk	–	2.99	−8.57 to 14.56	0.61	0.25	−11.18 to 11.69	0.96	–	3.79	−7.58 to 15.54	0.5	5.08	−6.4 to 16.57	0.38
	High Risk	–	0.27	−16.82 to 17.37	0.97	−4.73	−21.75 to 12.28	0.58	–	−7.17	−24.29 to 9.94	0.41	−5.25	−22.42 to 11.9	0.54
Biochemical variables															
FBS (mg/dL)	Low risk	Reference	Reference						Reference	Reference					
	Moderate risk	–	0.45	−5.03 to 5.94	0.87	0.30	−5.45 to 6.05	0.91	–	1.19	−4.34 to 6.72	0.67	1.03	−4.78 to 6.84	0.72
	High risk	–	−2.71	−10.97 to 5.55	0.52	−3.39	−12.21 to 5.41	0.45	–	0.37	−7.96 to 8.7	0.93	0.41	−8.7 to 9.54	0.92
TC (mg/dL)	Low risk	Reference	Reference						Reference	Reference					
	Moderate risk	–	0.65	−20.11 to 21.42	0.95	−3.75	−24.96 to 17.45	0.72	–	16.88	−3.92 to 37.68	0.11	12.40	−8.99 to 33.81	0.25
	T3	–	−11.81	−43.07 to 19.44	0.45	−21.04	−53.54 to 11.45	0.2	–	4.59	−26.73 to 35.93	0.77	14.60	−18.97 to 48.18	0.39

(Continued)

10.3389/fnut.2024.1410811

TABLE 4 (Continued)

Variables	GRS	Phenolic acid							Lignans						
		Low intake < 55.95 (mg/day)	High intake						Low intake < 0.0065 (mg/day)	High intake					
			Crude			Adjust				Crude			Adjust		
			β	95% CI	*p*	β	95% CI	*p*		β	95% CI	*p*	β	95% CI	*p*
TG (mg/dL)	Low Risk	Reference	Reference						Reference	Reference					
	Moderate risk	–	31.83	−2.74 to 66.41	0.07	28.60	−7.62 to 64.82	0.12	–	1.96	−33.53 to 37.45	0.91	−9.24	−46.61 to 28.13	0.62
	High risk	–	−39.54	−92.26 – 13.17	0.14	−59.04	−115.66 to −2.42	**0.04**	–	16.72	−37.22 to 70.67	0.54	28.58	−30.54 to 87.7	0.34
HDL (mg/dL)	Low risk	Reference	Reference						Reference	Reference					
	Moderate risk	–	3.10	−3.23 to 9.44	0.33	2.87	−3.77 to 9.52	0.39	–	−0.13	−6.56 to 6.3	0.96	2.13	−4.6 to 8.87	0.53
	High risk	–	9.70	0.16–19.23	**0.04**	7.89	−2.3 to 18.08	0.12	–	1.85	−7.83 to 11.54	0.7	7.02	−3.55 to 17.59	0.19
LDL (mg/dL)	Low risk	Reference	Reference						Reference	Reference					
	Moderate risk	–	6.33	−7.48 to 20.14	0.36	9.11	−5.01 to 23.25	0.2	–	9.69	−4.22 to 23.61	0.17	11.26	−3.14 to 25.66	0.12
	High risk	–	−7.33	−28.12 to 13.45	0.48	−13.89	−35.54 to 7.76	0.2	–	0.19	−20.76 to 21.16	0.98	3.34	−19.24 to 25.9	0.77
AST (IU/L)	Low risk	Reference	Reference						Reference	Reference					
	Moderate risk	–	−2.93	−7.25 to 1.37	0.18	−2.68	−7.19 to 1.83	0.24	–	−2.01	−6.39 to 2.36	0.36	−0.54	−5.13 to 4.04	0.81
	High risk	–	−2.31	−8.8 to 4.17	0.48	−1.86	−8.78 to 5.05	0.59	–	−1.35	−7.95 to 5.23	0.68	2.03	−5.16 to 9.23	0.58
ALT (IU/L)	Low risk	Reference	Reference						Reference	Reference					
	Moderate risk	–	−6.83	−14.38 to 0.71	0.07	−5.45	−13.49 to 2.59	0.18	–	−7.23	−14.9 to 0.43	0.06	−4.59	−12.79 to 3.59	0.27
	High Risk	–	−0.28	−11.64 to 11.07	0.96	−0.12	−12.45 to 12.2	0.98	–	−3.70	−15.26 to 7.84	0.52	1.02	−11.83 to 13.87	0.87

B, Standard Error; GRS, Genetic risk score; BMI, Body mass index; WC, waist circumference; WHR, waist height ratio; FBS, fasting blood sugar; TG, Triglyceride; LDL, Low-density lipoprotein; HDL, High-density lipoprotein; OD, Obesity degree; VFL, Visceral fat level; TC, total cholesterol.
Phenolic acid High intake ≥ 55.95(mg/day), Lignans High intake ≥ 0.0065(mg/day).
p-values < 0.05 are in bold.
Adjust = adjusted for potential confounding factors including (age, IPAC and total energy intake).
Low Risk: 0,1,2 Risk alleles, Moderate Risk: 3,4 Risk allele, High Risk: 5,6 Risk allele.

However, there was no significant interaction found between moderate/high GRS and high intake stilbenes, polyphenols, and lignans with cardiometabolic risk factors in both the crude and adjusted models. In a study, there was no significant association total polyphenol and stilbenes with FBS, TG, HDL in participants. Also, there was no association between lignans with cholesterol, TG, HDL, DBP (50). The another study after adjusted for age, BMI, physical activity, and total energy intake, there was no association between Cry1 genotypes with cholesterol, TG, HDL, LDL, SBP, DBP (51). There was no association between Cav-1 rs3807992 genotypes with FBS, insulin, TC, TG (52).

Polyphenols are effective in cardiovascular health due to their antioxidant, blood sugar control, anti-inflammatory, and lipid profile control effects (25, 53, 54). In a study, it was discovered that a better diet quality, which might include polyphenol-rich foods, was significantly linked to a reduction in cardiometabolic risk factors (55). Furthermore, a cohort study spanning 10 years and involving more than 450,000 participants across 10 European countries revealed that

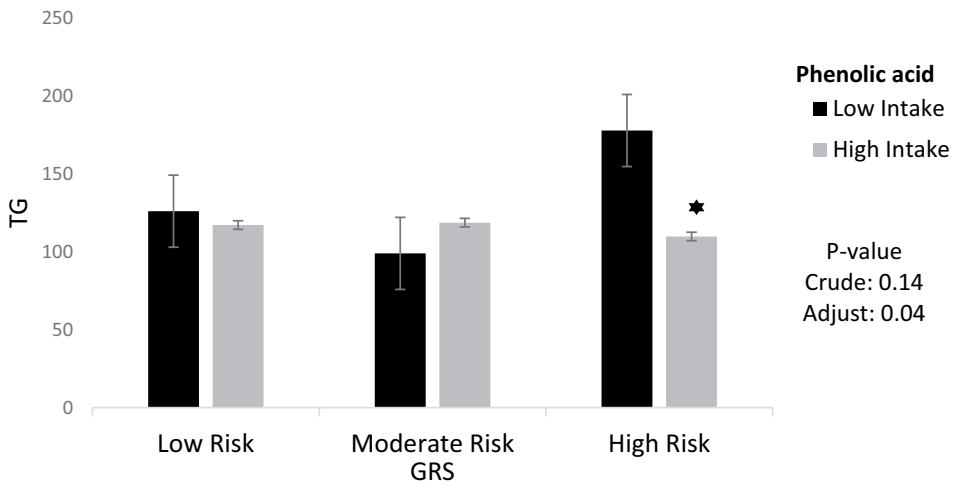

FIGURE 2
Interaction between phenolic acid and GRS on TG. The interaction between low and high intake of phenolic acid and GRS on Triglycerides. Data shown are mean ± standard error of the mean. TG, Triglycerides; GRS, genetic risk score. Adjust = adjusted for potential confounding factors including (age, IPAC and total energy intake). The asterisk (*) represents the *p*-value of the statistical test. The asterisk means that the *p*-value is less than 0.05.

higher diet quality index (DQI) scores were linked to a reduced risk of CVD mortality and its associated risk factors, such as dyslipidemia and hyperglycemia (56).

GRS play a key role in comprehending various aspects of body homeostasis, especially with respect to conditions such as type 2 diabetes (T2DM) and cardiometabolic risk factors (9, 57). It seems that the effects of MC4R, Cav-1 and Cry1 genes on body composition and metabolic parameters may depend on the quality of the diet (58). Polyphenols have antioxidant and anti-inflammatory properties that can improve the quality of food. Based on the evidence, these compounds have the ability to influence the interaction and interactions between diet, genes, and metabolic parameters (59, 60). Polyphenols and their various types play a role in this interaction by either activating or deactivating genes that are associated with obesity. The precise molecular and cellular mechanism behind this process is still not entirely comprehended (36). Previous research has shown that gene-diet interactions have an impact on metabolic factors, and our study's findings are consistent with this. A cross-sectional study found a relationship between the dietary inflammatory index (DII) and the rs17782313 mutation, which influences body composition (61). Hianza et al. conducted a study on individuals with a genetic predisposition to obesity and discovered that adopting a healthy diet led to a decrease in risk factors associated with CVD (62).

A study conducted by Aali et al. has significantly validated the findings of our study. Both studies have found a negative correlation between the consumption of polyphenols and its various forms with indicators of body composition (such as WC, WHR, WHtR) and metabolic parameters such as glycemia (FBG, HOMA-IR) and lipids (CHOL, TG). Also, Aali's study has reported a positive correlation with HDL cholesterol. However, our study did not find any significant correlation between the consumption of lignans and stilbenes with body composition and CVD risk factors, Aali's study did report such a correlation, which is the only point of difference between the two studies (50).

Numerous studies have confirmed that GRS increases the risk of CVD (9), the exact way in which food compounds like polyphenols can mitigate this effect remains unclear. The statistical power of the analysis can be affected by factors such as sample size, food components used, genetic variations, and gender, which can cause discrepancies in study findings. Evidence shows that polyphenols and its types reduce TG accumulation, increase lipolysis, decrease lipogenesis, and increase energy consumption, which may be an acceptable reason to justify the negative interaction between the consumption of polyphenols and GRS on body composition and some of the risk factors of CVD (63). Polyphenols play a crucial role in regulating blood sugar levels and improving the body's ability to respond to insulin by decreasing the production of specific hormones (64). Moreover, these compounds have the ability to control the process of lipolysis by activating hormone-sensitive lipase (65). Polyphenols enhance the body's antioxidant system, reduce fat oxidation, and enhance the activity of antioxidant enzymes (66, 67). Therefore, it is anticipated that enhancing the consumption of a diet rich in polyphenols and their various forms will result in enhanced body composition and a reduction in certain risk factors associated with CVD (68). These results are confirmed by our study.

The present study is one of the first studies to examine the interaction of polyphenol intake with GRS on metabolic parameters, which is one of the strengths of this study. Some limitations of this research include the cross-sectional design of the study, the lack of investigation into causal interactions, the use of memory-based tools such as FFQ, and the inability to generalize the results to men's gender.

Conclusion

Our findings indicate that individuals who consume high GRS and polyphenols have a significant negative effect on FBS and TG levels, as well as a significant positive effect on HDL. Therefore, a high intake of polyphenols in individuals with high GRS may have a protective effect on cardiometabolic risk. This finding indicates that the interaction of dietary components, such as polyphenols, with genetic risk factors over cardiometabolic risk factors is of great

TABLE 5 The interaction between GRS, flavonoids and polyphenol on cardiometabolic risk factors.

Variables	GRS	Flavonoids							Polyphenol						
		Low intake < 81.55 (mg/day)	High intake ≥81.55(mg/day)						Low intake < 62.59 (mg/day)	High intake ≥62.59(mg/day)					
			Crude			Adjust				Crude			Adjust		
			β	95% CI	*p*	β	95% CI	*p*		β	95% CI	*p*	β	95% CI	*p*
Anthropometric factors															
BMI (kg/m^2)	Low risk	Reference	Reference						Reference	Reference					
	Moderate risk	–	−3.46	−5.44 to −1.49	**<0.001**	−2.56	−4.59 to −0.52	**0.01**	–	0.26	−1.7 to 2.23	0.79	0.43	−1.56 to 2.44	0.66
	High risk	–	−0.91	−3.84 to 2.02	0.54	−0.27	−3.28 to 2.73	0.85	–	−0.66	−3.66 to 2.34	0.66	0.62	−2.45 to 3.69	0.69
WC (cm)	Low risk	Reference	Reference						Reference	Reference					
	Moderate risk	–	−7.43	−12.48 to −2.39	**<0.001**	−5.67	−10.79 to −0.56	**0.03**	–	0.82	−4.17 to 5.81	0.74	2.53	−2.48 to 7.54	0.32
	High risk	–	−0.82	−8.22 to 6.58	0.82	0.65	−6.78 to 8.08	0.86	–	−3.08	−10.67 to 4.5	0.42	1.60	−6.04 to 9.26	0.68
WHR	Low risk	Reference	Reference						Reference	Reference					
	Moderate risk	–	−0.01	−0.043 to 0.013	0.29	<0.001	−0.033 to 0.023	0.71	–	0.00	−0.02 to 0.03	0.85	0.01	−0.014 to 0.041	0.34
	High risk	–	0.02	−0.016 to 0.066	0.23	0.03	−0.007 to 0.075	0.1	–	<0.001	−0.051 to 0.032	0.65	0.01	−0.023 to 0.061	0.37
Body composition															
VFL (cm^2)	Low risk	Reference	Reference						Reference	Reference					
	Moderate risk	–	−2.21	−3.96 to −0.46	**0.01**	−1.61	−3.4 to 0.17	0.07	–	0.10	−1.63 to 1.83	0.91	0.87	−0.87 to 2.63	0.32
	High risk	–	0.57	−2 to 3.15	0.66	1.44	−1.15 to 4.05	0.27	–	−0.00	−2.65 to 2.64	0.99	1.67	−1.01 to 4.36	0.22
OD (%)	Low risk	Reference	Reference						Reference	Reference					
	Moderate risk	–	−13.04	−24.62 to −1.47	**0.02**	−11.20	−22.67 to 0.27	**0.05**	–	−4.03	−15.45 to 7.38	0.48	0.85	−10.48 to 12.18	0.88
	High risk	–	−3.69	−20.75 to 13.36	0.67	−1.25	−17.99 to 15.47	0.88	–	−8.65	−26.06 to 8.76	0.33	−0.90	−18.24 to 16.43	0.91
Biochemical variables															
FBS (mg/dL)	Low risk	Reference	Reference						Reference	Reference					
	Moderate risk	–	−0.85	−6.43 to 4.72	0.76	0.07	−5.82 to 5.97	0.98	–	−0.09	−5.53 to 5.34	0.97	0.86	−4.82 to 6.56	0.76
	High risk	–	−3.58	−11.92 to 4.75	0.4	−2.92	−11.71 to 5.86	0.51	–	−0.76	−9.2 to 7.68	0.86	−0.12	−9.15 to 8.91	0.97

(Continued)

10.3389/fnut.2024.1410811

TABLE 5 (Continued)

Variables	GRS	Flavonoids							Polyphenol						
		Low intake < 81.55 (mg/day)	High intake ≥81.55(mg/day)						Low intake < 62.59 (mg/day)	High intake ≥62.59(mg/day)					
			Crude			Adjust				Crude			Adjust		
			β	95% CI	*p*	β	95% CI	*p*		β	95% CI	*p*	β	95% CI	*p*
TC (mg/dL)	Low risk	Reference	Reference						Reference	Reference					
	Moderate risk	–	−13.03	−34.14 to 8.08	0.22	−7.61	−29.5 to 14.26	0.49	–	−3.11	−23.63 to 17.39	0.76	2.69	−18.31 to 23.71	0.8
	High risk	–	−16.48	−48.02 to 15.06	0.3	−4.17	−36.79 to 28.43	0.8	–	−10.82	−42.67 to 21.02	0.5	−11.42	−44.78 to 21.93	0.5
TG (mg/dL)	Low risk	Reference	Reference						Reference	Reference					
	Moderate risk	–	−5.96	−41.06 to 29.12	0.73	2.96	−34.27 to 40.21	0.87	–	4.04	−30.93 to 39.01	0.82	9.17	−27.45 to 45.79	0.62
	High risk	–	−84.30	−137.58 to −31.02	**<0.001**	−79.11	−135.52 to −22.69	**<0.001**	–	8.23	−47.21 to 63.68	0.77	15.75	−44.36 to 75.86	0.6
HDL (mg/dL)	Low risk	Reference	Reference						Reference	Reference					
	Moderate risk	–	1.75	−4.72 to 8.22	0.59	3.94	−2.82 to 10.71	0.25	–	−4.03	−10.35 to 2.28	0.21	−2.17	−8.8 to 4.44	0.51
	High risk	–	8.39	−1.28 to 18.06	0.08	12.56	2.47–22.65	**0.01**	–	−7.74	−17.56 to 2.06	0.12	−7.31	−17.82 to 3.19	0.17
LDL (mg/dL)	Low risk	Reference	Reference						Reference	Reference					
	Moderate risk	–	−2.68	−16.77 to 11.39	0.7	3.94	−10.74 to 18.63	0.59	–	0.95	−10.35 to 2.28	0.21	3.46	−8.8 to 4.44	0.51
	High Risk	–	−11.13	−32.18 to 9.91	0.3	−4.83	−26.72 to 17.06	0.66	–	−16.77	−17.56 to 2.06	0.12	−22.00	−17.82 to 3.19	0.17
AST (IU/L)	Low risk	Reference	Reference						Reference	Reference					
	Moderate risk	–	−2.14	−6.57 to 2.28	0.34	−1.86	−6.51 to 2.79	0.43	–	0.70	−3.61 to 5.03	0.74	1.15	−3.36 to 5.67	0.61
	High risk	–	−0.78	−5.83 to 7.4	0.81	2.35	−4.58 to 9.29	0.5	–	−0.79	−7.5 to 5.9	0.81	1.25	−5.91 to 8.42	0.73
ALT (IU/L)	Low risk	Reference	Reference						Reference	Reference					
	Moderate risk	–	−7.02	−14.74 to 0.69	0.07	−5.31	−13.58 to 2.96	0.2	–	0.83	−6.77 to 8.43	0.83	2.34	−5.72 to 10.42	0.56
	High risk	–	3.75	−7.78 to 15.28	0.52	6.04	−6.28 to 18.37	0.33	–	−5.77	−17.58 to 6.02	0.33	−2.46	−15.27 to 10.34	0.7

B, Standard Error; GRS, Genetic risk score; BMI, Body mass index; WC, waist circumference; WHR, waist height ratio; FBS, fasting blood sugar; TG, Triglyceride; LDL, Low density lipoprotein; HDL, High density lipoprotein; OD, Obesity degree; VFL, Visceral fat level.
Flavonoids High intake ≥ 81.55(mg/day), Polyphenol High intake ≥ 62.59(mg/day).
p-values < 0.05 are in bold.
Adjust = adjusted for potential confounding factors including (age, IPAC and total energy intake).
Low Risk: 0,1,2 Risk allele, Moderate Risk: 3,4 Risk allele, High Risk: 5,6 Risk allele.

10.3389/fnut.2024.1410811

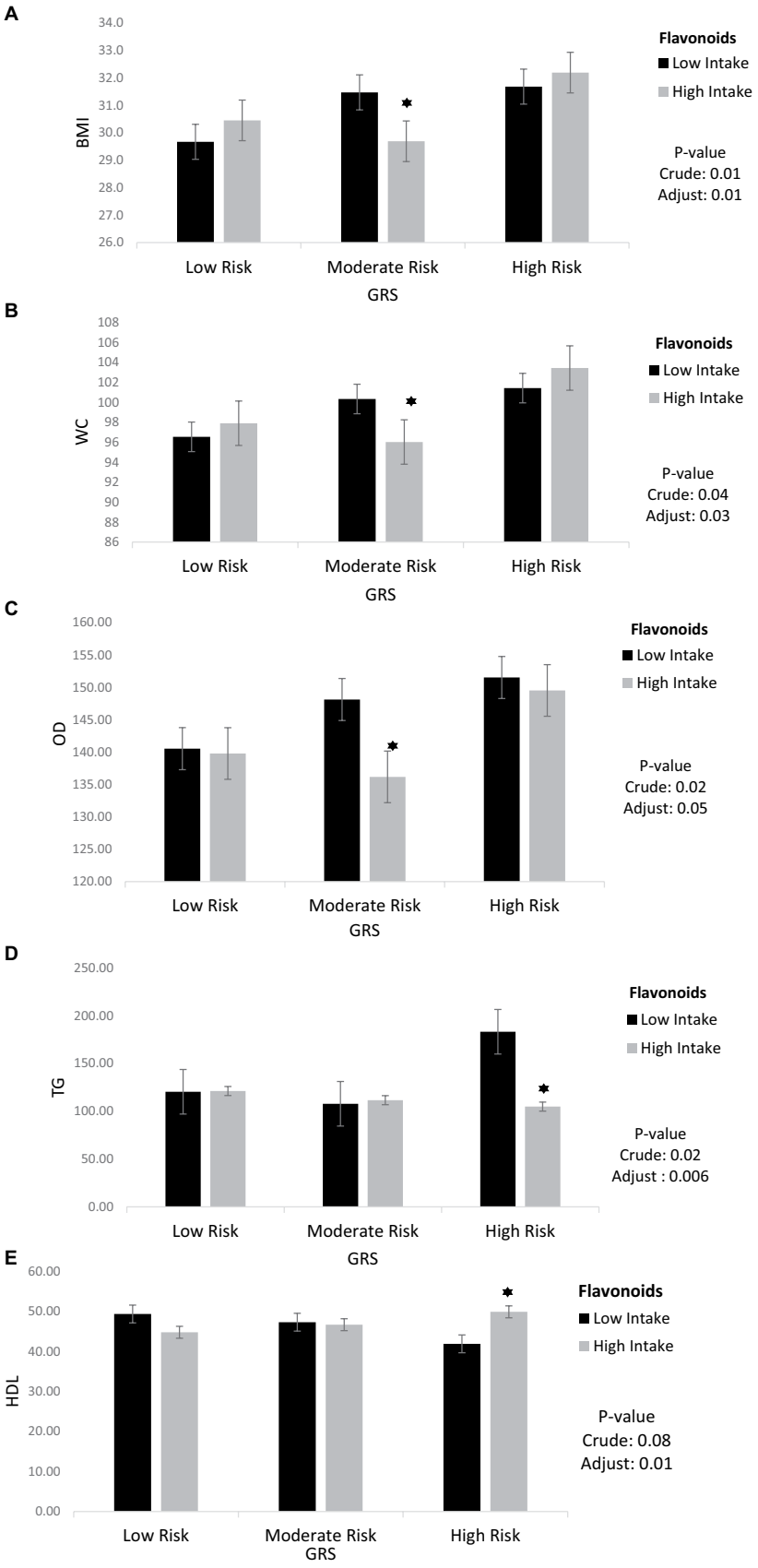

FIGURE 3
Interaction between flavonoids and GRS on **(A)** BMI, **(B)** WC, **(C)** OD, **(D)** TG, **(E)** HDL. The interaction between low and high intake of Flavonoids and GRS on BMI, WC, OD, TG, HDL. Data shown are mean ± standard error of the mean. BMI, Body mass index; WC, Waist circumference; OD, Obesity degree; TG, Triglycerides; HDL, High density lipoprotein; GRS, genetic risk score. Adjust = adjusted for potential confounding factors including (age, IPAC and total energy intake). The asterisk (*) represents the *p*-value of the statistical test. The asterisk means that the *p*-value is less than 0.05.

importance. Further research is necessary in the future to validate this association.

Data availability statement

The raw data supporting the conclusions of this article will be made available by the authors, without undue reservation.

Ethics statement

The studies involving humans were approved by the authors and the Ethics Committee of Tehran University of Medical Sciences (IR.TUMS.MEDICINE.REC.1402.636) have received approval for the method and protocol of the current study. The studies were conducted in accordance with the local legislation and institutional requirements. The participants provided their written informed consent to participate in this study.

Author contributions

ZR: Writing – original draft, Writing – review & editing. AM: Investigation, Validation, Writing – review & editing. FA: Data curation, Formal analysis, Methodology, Software, Writing – review & editing. SD: Conceptualization, Writing – original draft. YA: Methodology, Writing – review & editing. KM: Funding acquisition, Visualization, Writing – review & editing.

Funding

The author(s) declare financial support was received for the research, authorship, and/or publication of this article. The study was supported by the Tehran University of Medical Sciences Grant (No: 1402-4-212-66522).

Acknowledgments

The researchers expressed their gratitude to all the individuals who participated in the research, as well as the Faculty of Nutrition and Dietetics at Tehran University of Medical Sciences.

Conflict of interest

The authors declare that the research was conducted in the absence of any commercial or financial relationships that could be construed as a potential conflict of interest.

Publisher's note

All claims expressed in this article are solely those of the authors and do not necessarily represent those of their affiliated organizations, or those of the publisher, the editors and the reviewers. Any product that may be evaluated in this article, or claim that may be made by its manufacturer, is not guaranteed or endorsed by the publisher.

References

1. Benjamin EJ, Virani SS, Callaway CW, Chamberlain AM, Chang AR, Chang S, et al. Correction to: heart disease and stroke Statistics-2018 update: a report from the American Heart Association. *Circulation*. (2018) 137:e493–2. doi: 10.1161/CIR.0000000000000573

2. Gaziano TA, Bitton A, Anand S, Abrahams-Gessel S, Murphy A. Growing epidemic of coronary heart disease in low-and middle-income countries. *Curr Probl Cardiol*. (2010) 35:72–115. doi: 10.1016/j.cpcardiol.2009.10.002

3. Roger VL, Go AS, Lloyd-Jones DM, Adams RJ, Berry JD, Brown TM, et al. Heart disease and stroke statistics—2011 update: a report from the American Heart Association. *Circulation*. (2011) 123:e18–e209. doi: 10.1161/CIR.0b013e3182009701

4. World Health Organization. Global status report on noncommunicable diseases 2014 World Health Organization (2014). Regions: Africa Americas, Europe, Eastern Mediterranean Western Pacific.

5. Mozaffarian D, Benjamin EJ, Go AS, Arnett DK, Blaha MJ, Cushman M, et al. AHA statistical update: Heart disease and stroke statistics AHA (2015).

6. Cho L, Davis M, Elgendy I, Epps K, Lindley KJ, Mehta PK, et al. Summary of updated recommendations for primary prevention of cardiovascular disease in women: JACC state-of-the-art review. *J Am Coll Cardiol*. (2020) 75:2602–18. doi: 10.1016/j.jacc.2020.03.060

7. McMillan DC, Sattar N, Lean M, McArdle CS. Obesity and cancer. *BMJ*. (2006) 333:1109–11. doi: 10.1136/bmj.39042.565035.BE1

8. Must A, Spadano J, Coakley EH, Field AE, Colditz G, Dietz WH, et al. The disease burden associated with overweight and obesity. *JAMA*. (1999) 282:1523–9. doi: 10.1001/jama.282.16.1523

9. Gholami F, Rasaei N, Samadi M, Yekaninejad MS, Keshavarz SA, Javdan G, et al. The relationship of genetic risk score with cardiometabolic risk factors: a cross-sectional study. *BMC Cardiovasc Disord*. (2022) 22:459. doi: 10.1186/s12872-022-02888-z

10. Hruby A, Hu FB. The epidemiology of obesity: a big picture. *PharmacoEconomics*. (2015) 33:673–89. doi: 10.1007/s40273-014-0243-x

11. Xiao B, Velez Edwards DR, Lucas A, Drivas T, Gray K, Keating B, et al. Inference of causal relationships between genetic risk factors for cardiometabolic phenotypes and female-specific health conditions. *J Am Heart Assoc*. (2023) 12:e026561. doi: 10.1161/JAHA.121.026561

12. Igo RP Jr, Kinzy TG, Cooke Bailey JN. Genetic risk scores. *Curr Protoc Hum Genet*. (2019) 104:e95. doi: 10.1002/cphg.95

13. Rothman DL, Stearns SC, Shulman RG. Gene expression regulates metabolite homeostasis during the Crabtree effect: Implications for the adaptation and evolution of Metabolism. *Proc Natl Acad Sci U S A*. (2021) 118:e2014013118. doi: 10.1073/pnas.2014013118

14. Grant SF, Bradfield JP, Zhang H, Wang K, Kim CE, Annaiah K, et al. Investigation of the locus near MC4R with childhood obesity in Americans of European and African ancestry. *Obesity*. (2009) 17:1461–5. doi: 10.1038/oby.2009.53

15. Schmid PM, Heid I, Buechler C, Steege A, Resch M, Birner C, et al. Expression of fourteen novel obesity-related genes in Zucker diabetic fatty rats. *Cardiovasc Diabetol*. (2012) 11:48–11. doi: 10.1186/1475-2840-11-48

16. Cone RD. The central melanocortin system and energy homeostasis. *Trends Endocrinol Metab*. (1999) 10:211–6. doi: 10.1016/S1043-2760(99)00153-8

17. Jee SH, Sull JW, Park J, Lee SY, Ohrr H, Guallar E, et al. Body-mass index and mortality in Korean men and women. *N Engl J Med*. (2006) 355:779–87. doi: 10.1056/NEJMoa054017

18. Sun Y, Sun J, Wu J, Yang M. Combined effects of FTO rs9939609 and MC4R rs17782313 on elevated nocturnal blood pressure in the Chinese Han population: cardiovascular topics. *Cardiovasc J Afr*. (2016) 27:21–4. doi: 10.5830/CVJA-2015-064

19. Greenfield JR, Miller JW, Keogh JM, Henning E, Satterwhite JH, Cameron GS, et al. Modulation of blood pressure by central melanocortinergic pathways. *N Engl J Med*. (2009) 360:44–52. doi: 10.1056/NEJMoa0803085

20. de Souza GM, de Albuquerque Borborema ME, de Lucena TMC, da Silva Santos AF, de Lima BR, de Oliveira DC, et al. Caveolin-1 (CAV-1) up regulation in metabolic syndrome: all roads leading to the same end. *Mol Biol Rep*. (2020) 47:9245–50. doi: 10.1007/s11033-020-05945-y

21. Jia G, Sowers JR. Caveolin-1 in cardiovascular disease: a double-edged sword. *Diabetes*. (2015) 64:3645–7. doi: 10.2337/dbi15-0005

22. Voghel G, Thorin-Trescases N, Farhat N, Mamarbachi M, Villeneuve L, Perrault LP, et al. Replicative senescence of vascular endothelial cells isolated from coronary patients is worsened by oxidative stress associated with risk factors for cardiovascular disease. *FASEB J*. (2008) 22. doi: 10.1096/fasebj.22.1_supplement.964.24

23. Fourier C, Ran C, Sjöstrand C, Waldenlind E, Steinberg A, Belin AC. The molecular clock gene cryptochrome 1 (CRY1) and its role in cluster headache. *Cephalalgia*. (2021) 41:1374–81. doi: 10.1177/03331024211024165

24. Ye D, Cai S, Jiang X, Ding Y, Chen K, Fan C, et al. Associations of polymorphisms in circadian genes with abdominal obesity in Chinese adult population. *Obes Res Clin Pract*. (2016) 10:S133–41. doi: 10.1016/j.orcp.2016.02.002

25. Lanuza F, Zamora-Ros R, Bondonno NP, Meroño T, Rostgaard-Hansen AL, Riccardi G, et al. Dietary polyphenols, metabolic syndrome and cardiometabolic risk factors: an observational study based on the DCH-NG subcohort. *Nutr Metab Cardiovasc Dis*. (2023) 33:1167–78. doi: 10.1016/j.numecd.2023.02.022

26. Lemmer B, Oster H. The role of circadian rhythms in the hypertension of diabetes mellitus and the metabolic syndrome. *Curr Hypertens Rep*. (2018) 20:1–9. doi: 10.1007/s11906-018-0843-5

27. Dashti HS, Smith CE, Lee YC, Parnell LD, Lai CQ, Arnett DK, et al. CRY1 circadian gene variant interacts with carbohydrate intake for insulin resistance in two independent populations: Mediterranean and north American. *Chronobiol Int*. (2014) 31:660–7. doi: 10.3109/07420528.2014.886587

28. Mirzababaei A, Daneshzad E, Shiraseb F, Pourreza S, Setayesh L, Clark CCT, et al. Variants of the cry 1 gene may influence the effect of fat intake on resting metabolic rate in women with overweight of obesity: a cross-sectional study. *BMC Endocr Disord*. (2021) 21:196. doi: 10.1186/s12902-021-00860-0

29. Gholami F, Samadi M, Rasaei N, Yekaninejad MS, Keshavarz SA, Javdan G, et al. Interactions between genetic risk score and healthy plant diet index on Cardiometabolic risk factors among obese and overweight women. *Clin Nutr Res*. (2023) 12:199–217. doi: 10.7762/cnr.2023.12.3.199

30. Adriouch S, Lampuré A, Nechba A, Baudry J, Assmann K, Kesse-Guyot E, et al. Prospective association between total and specific dietary polyphenol intakes and cardiovascular disease risk in the Nutrinet-Santé French cohort. *Nutrients*. (2018) 10:1587. doi: 10.3390/nu10111587

31. Ponzo V, Goitre I, Fadda M, Gambino R, de Francesco A, Soldati L, et al. Dietary flavonoid intake and cardiovascular risk: a population-based cohort study. *J Transl Med*. (2015) 13:1–13. doi: 10.1186/s12967-015-0573-2

32. Pandey KB, Rizvi SI. Plant polyphenols as dietary antioxidants in human health and disease. *Oxidative Med Cell Longev*. (2009) 2:270–8. doi: 10.4161/oxim.2.5.9498

33. Aloo SO, Ofosu FK, Kim NH, Kilonzi SM, Oh DH. Insights on dietary polyphenols as agents against metabolic disorders: obesity as a target disease. *Antioxidants (Basel)*. (2023) 12. doi: 10.3390/antiox12020416

34. Adriouch S, Kesse-Guyot E, Feuillet T, Touvier M, Olié V, Andreeva V, et al. Total and specific dietary polyphenol intakes and 6-year anthropometric changes in a middle-aged general population cohort. *Int J Obes*. (2018) 42:310–7. doi: 10.1038/ijo.2017.227

35. Zujko ME, Waśkiewicz A, Witkowska AM, Szcześniewska D, Zdrojewski T, Kozakiewicz K, et al. Dietary total antioxidant capacity and dietary polyphenol intake and prevalence of metabolic syndrome in polish adults: a nationwide study. *Oxidative Med Cell Longev*. (2018) 2018:1–10. doi: 10.1155/2018/7487816

36. Grosso G, Stepaniak U, Micek A, Stefler D, Bobak M, Pająk A. Dietary polyphenols are inversely associated with metabolic syndrome in polish adults of the HAPIEE study. *Eur J Nutr*. (2017) 56:1409–20. doi: 10.1007/s00394-016-1187-z

37. Rezazadeh A, Omidvar N, Tucker KL. Food frequency questionnaires developed and validated in Iran: a systematic review. *Epidemiol Health*. (2020) 42:e2020015. doi: 10.4178/epih.e2020015

38. Ghaffarpour M., Houshiar-Rad A., Kianfar H., The manual for household measures, cooking yields factors and edible portion of foods. Tehran: Nashre Olume Keshavarzy, (1999). *7*: p. 42–58.

39. Neveu V, Perez-Jimenez J, Vos F, Crespy V, du Chaffaut L, Mennen L, et al. Phenol-explorer: an online comprehensive database on polyphenol contents in foods. *Database*. (2010) 2010:bap024. doi: 10.1093/database/bap024

40. Fidanza F. Nutritional status assessment: A manual for population studies. United kingdom: Springer (2013).

41. Yarizadeh HSL, Roberts C, Yekaninejad MS, Mirzaei K. Nutrient pattern of unsaturated fatty acids and vitamin E increase resting metabolic rate of overweight and obese women. *Int J Vitam Nutr Res*. (2022) 92:214–22. doi: 10.1024/0300-9831/a000664

42. Penumarthy S, Penmetsa GS, Mannem S. Assessment of serum levels of triglycerides, total cholesterol, high-density lipoprotein cholesterol, and low-density lipoprotein cholesterol in periodontitis patients. *J Indian Soc Periodontol*. (2013) 17:30–5. doi: 10.4103/0972-124X.107471

43. MWer S, Dykes D, Polesky H. A simple salting out procedure for extracting DNA from human nucleated cells. *Nucleic Acids Res*. (1988) 16:1215. doi: 10.1093/nar/16.3.1215

44. Myakishev MV, Khripin Y, Hu S, Hamer DH. High-throughput SNP genotyping by allele-specific PCR with universal energy-transfer-labeled primers. *Genome Res*. (2001) 11:163–9. doi: 10.1101/gr.157901

45. Abaj F, Koohdani F, Rafiee M, Alvandi E, Yekaninejad MS, Mirzaei K. Interactions between Caveolin-1 (rs3807992) polymorphism and major dietary patterns on cardio-metabolic risk factors among obese and overweight women. *BMC Endocr Disord*. (2021) 21:138. doi: 10.1186/s12902-021-00800-y

46. Yu K, Li L, Zhang L, Guo L, Wang C. Association between MC4R rs17782313 genotype and obesity: a meta-analysis. *Gene*. (2020) 733:144372. doi: 10.1016/j.gene.2020.144372

47. Tangestani H, Emamat H, Yekaninejad MS, Keshavarz SA, Mirzaei K. Variants in circadian rhythm gene Cry1 interacts with healthy dietary pattern for serum leptin levels: a cross-sectional study. *Clin Nutr Res*. (2021) 10:48–58. doi: 10.7762/cnr.2021.10.1.48

48. Miranda AM, Steluti J, Norde MM, Fisberg RM, Marchioni DM. The association between genetic risk score and blood pressure is modified by coffee consumption: gene–diet interaction analysis in a population-based study. *Clin Nutr*. (2019) 38:1721–8. doi: 10.1016/j.clnu.2018.07.033

49. Ainsworth BE, Haskell WL, Whitt MC, Irwin ML, Swartz AM, Strath SJ, et al. Compendium of physical activities: an update of activity codes and MET intensities. *Med Sci Sports Exerc*. (2000) 32:S498–516. doi: 10.1097/00005768-200009001-00009

50. Aali Y, Ebrahimi S, Shiraseb F, Mirzaei K. The association between dietary polyphenol intake and cardiometabolic factors in overweight and obese women: a cross-sectional study. *BMC Endocr Disord*. (2022) 22:120. doi: 10.1186/s12902-022-01025-3

51. Firouzabadi FD, Mirzababaei A, Shiraseb F, Tangestani H, Mirzaei K. The interaction between CRY1 polymorphism and alternative healthy eating index (AHEI) on cardiovascular risk factors in overweight women and women with obesity: a cross-sectional study. *BMC Endocr Disord*. (2023) 23:172. doi: 10.1186/s12902-023-01429-9

52. Abaj F, Mirzababaei A, Hosseininasab D, Bahrampour N, Clark CCT, Mirzaei K. Interactions between Caveolin-1 polymorphism and plant-based dietary index on metabolic and inflammatory markers among women with obesity. *Sci Rep*. (2022) 12:9088. doi: 10.1038/s41598-022-12913-y

53. Haș IM, Teleky BE, Vodnar DC, Ștefănescu BE, Tit DM, Nițescu M. Polyphenols and Cardiometabolic health: knowledge and concern among Romanian people. *Nutrients*. (2023) 15:2281. doi: 10.3390/nu15102281

54. Wang S, du Q, Meng X, Zhang Y. Natural polyphenols: a potential prevention and treatment strategy for metabolic syndrome. *Food Funct*. (2022) 13:9734–53. doi: 10.1039/D2FO01552H

55. Mohamadi A, Shiraseb F, Mirzababaei A, AkbarySedigh A, Ghorbani M, Clark CCT, et al. The association between adherence to diet quality index and cardiometabolic risk factors in overweight and obese women: a cross-sectional study. *Front Public Health*. (2023) 11:11. doi: 10.3389/fpubh.2023.1169398

56. Lassale C, Gunter MJ, Romaguera D, Peelen LM, van der Schouw YT, Beulens JWJ, et al. Diet quality scores and prediction of all-cause, cardiovascular and cancer mortality in a pan-European cohort study. *PLoS One*. (2016) 11:e0159025. doi: 10.1371/journal.pone.0159025

57. Norris JM, Rich SS. Genetics of glucose homeostasis: implications for insulin resistance and metabolic syndrome. *Arterioscler Thromb Vasc Biol*. (2012) 32:2091–6. doi: 10.1161/ATVBAHA.112.255463

58. Hosseininasab D, Mirzababaei A, Abaj F, Firoozi R, Clark CCT, Mirzaei K. Are there any interactions between modified Nordic-style diet score and MC4R polymorphism on cardiovascular risk factors among overweight and obese women? A cross-sectional study. *BMC Endocr Disord*. (2022) 22:221. doi: 10.1186/s12902-022-01132-1

59. Barth SW, Koch TCL, Watzl B, Dietrich H, Will F, Bub A. Moderate effects of apple juice consumption on obesity-related markers in obese men: impact of diet–gene interaction on body fat content. *Eur J Nutr*. (2012) 51:841–50. doi: 10.1007/s00394-011-0264-6

60. Soyalan B, Minn J, Schmitz HJ, Schrenk D, Will F, Dietrich H, et al. Apple juice intervention modulates expression of ARE-dependent genes in rat colon and liver. *Eur J Nutr*. (2011) 50:135–43. doi: 10.1007/s00394-010-0124-9

61. Yarizadeh H, Mirzababaei A, Ghodoosi N, Pooyan S, Djafarian K, Clark CCT, et al. The interaction between the dietary inflammatory index and MC4R gene variants on cardiovascular risk factors. *Clin Nutr*. (2021) 40:488–95. doi: 10.1016/j.clnu.2020.04.044

62. Heianza Y, Zhou T, Sun D, Hu FB, Qi L. Healthful plant-based dietary patterns, genetic risk of obesity, and cardiovascular risk in the UK biobank study. *Clin Nutr*. (2021) 40:4694–701. doi: 10.1016/j.clnu.2021.06.018

63. Boccellino M, D'Angelo S. Anti-obesity effects of polyphenol intake: current status and future possibilities. *Int J Mol Sci*. (2020) 21:5642. doi: 10.3390/ijms21165642

64. Dao T-MA, Waget A, Klopp P, Serino M, Vachoux C, Pechere L, et al. Resveratrol increases glucose induced GLP-1 secretion in mice: a mechanism which contributes to the glycemic control. *PLoS One*. (2011) 6:e20700. doi: 10.1371/journal.pone.0020700

65. Nakazato K, Song H, Waga T. Effects of dietary apple polyphenol on adipose tissues weights in Wistar rats. *Exp Anim*. (2006) 55:383–9. doi: 10.1538/expanim.55.383

66. Dembinska-Kiec A, Mykkänen O, Kiec-Wilk B, Mykkänen H. Antioxidant phytochemicals against type 2 diabetes. *Br J Nutr*. (2008) 99:ES109. doi: 10.1017/S000711450896579X

67. Crespy V, Williamson G. A review of the health effects of green tea catechins in in vivo animal models. *J Nutr*. (2004) 134:3431S–40S. doi: 10.1093/jn/134.12.3431S

68. Wang S, Moustaid-Moussa N, Chen L, Mo H, Shastri A, Su R, et al. Novel insights of dietary polyphenols and obesity. *J Nutr Biochem*. (2014) 25:1–18. doi: 10.1016/j.jnutbio.2013.09.001

10.3389/fnut.2024.1410811

Glossary

ALT	Alanine aminotransferase
AST	Aspartate aminotransferase
CVD	Cardiovascular diseases
BMI	Body mass index
WC	Waist circumference
DPI	Dietary polyphenols intake
FBS	Fasting blood glucose
FPG	Fasting plasma glucose
MC4R	Melanocortin 4 receptor
Cry1	Cryptochrome 1 gene
CAV1	Caveolin-1
FFQ	Food frequency questionnaire
DQI	diet quality index
PA	Physical activity
IPAQ	International physical activity questionnaire-short form
HC	Hp circumference
WHR	Waist-to-hip ratio
VFL	Visceral fat level
OD	Obesity degree
GOD-PAP	Glucose oxidase-phenol 4-aminoantipyrine peroxidase
GPOPAP	Glycerol-3-phosphate oxidase–phenol 4-aminoantipyrine peroxidase
TG	Triglyceride
HDL	High-density lipoprotein
LDL	Low-density lipoprotein
SBP	Systolic blood pressure
DBP	Diastolic blood pressure
GRS	Genetic risk score
TC	Total cholesterol
TDPI	Total dietary polyphenols index
SLM	Soft lean mass
FFM	Fat-free mass
SMM	Skeletal muscle mass
DII	Dietary inflammatory index

frontiers | Frontiers in Nutrition

TYPE Original Research
PUBLISHED 01 August 2024
DOI 10.3389/fnut.2024.1443895

OPEN ACCESS

EDITED BY
Julius Liobikas,
Lithuanian University of Health Sciences, Lithuania

REVIEWED BY
Irmak Ferah Okkay,
Atatürk University, Türkiye
Çevik Gürel,
Harran University, Türkiye
Uche Okuu Arunsi,
Georgia Institute of Technology, United States

*CORRESPONDENCE
Adeyemi Fatai Odetayo
✉ adeyemiodetayo@gmail.com;
✉ adeyemi.odetayo@fuhsi.edu.ng

RECEIVED 05 June 2024
ACCEPTED 19 July 2024
PUBLISHED 01 August 2024

CITATION
Odetayo AF, Akhigbe RE, Hamed MA, Balogun ME, Oluwole DT and Olayaki LA (2024) Omega-3 fatty acids abrogates oxido-inflammatory and mitochondrial dysfunction-associated apoptotic responses in testis of tamoxifen-treated rats. *Front. Nutr.* 11:1443895. doi: 10.3389/fnut.2024.1443895

Omega-3 fatty acids abrogates oxido-inflammatory and mitochondrial dysfunction-associated apoptotic responses in testis of tamoxifen-treated rats

Adeyemi Fatai Odetayo[1]*, Roland Eghoghosoa Akhigbe[2,3], Moses Agbomhere Hamed[4,5], Morufu Eyitayo Balogun[1], David Tolulope Oluwole[6] and Luqman Aribidesi Olayaki[7]

[1]Department of Physiology, Faculty of Basic Medical Sciences, Federal University of Health Sciences, Ila Orangun, Nigeria, [2]Reproductive Biology and Toxicology Research Laboratory, Oasis of Grace Hospital, Osogbo, Nigeria, [3]Department of Physiology, Ladoke Akintola University of Technology, Ogbomoso, Nigeria, [4]Department of Medical Laboratory Science, Afe Babalola University, Ado Ekiti, Nigeria, [5]The Brainwill Laboratories and Biomedical Services, Osogbo, Nigeria, [6]Department of Physiology, Crescent University, Abeokuta, Nigeria, [7]Department of Physiology, University of Ilorin, Ilorin, Nigeria

Background: Tamoxifen (TAM) is a widely used drug in patients with gynecomastia and breast cancer. TAM exerts its anticancer effects via its antiestrogenic activities. Unfortunately, TAM has been reported to exert gonadotoxic effects on male testes. Therefore, this study was designed to explore the possible associated mechanisms involved in TAM-induced testicular dysfunction and the possible ameliorative effects of omega-3 fatty acids (O3FA).

Methodology: Animals were randomly divided into control, O3FA, TAM, and TAM + O3FA. All treatment lasted for 28 days.

Results: TAM exposure impaired sperm qualities (count, motility, and normal morphology) and decreased testicular 3β-HSD and 17β-HSD. It was accompanied by a decline in serum testosterone and an increase in estradiol, luteinizing and follicle-stimulating hormones. These observed alterations were associated with an increase in testicular injury markers, oxido-inflammatory response, and mitochondria-mediated apoptosis. These observed alterations were ameliorated by O3FA treatments.

Conclusions: O3FA ameliorated TAM-induced testicular dysfunction in male Wistar rats by modulating XO/UA and Nrf2/NF-kb signaling and cytochrome c-mediated apoptosis in TAM-treated rats.

KEYWORDS

anticancer drugs, nuclear factor erythroid 2-related factor 2 (Nrf2) and nuclear factor-kappa B (NF-κB) signaling, selective estrogen receptor modulators, testicular function, cytochrome c

Introduction

Tamoxifen (TAM; Z-1-[4-(2-dimethylaminoethoxy)-phenyl]-1,2-diphenyl-1-butene) is a synthetic nonsteroidal estrogen agonist-antagonist antineoplastic agent (1, 2). TAM is the major anti-estrogen therapy for the management of hormone receptor-positive breast cancer in pre-menopausal women (3). TAM has also been recommended for the

management of gynecomastia in males (4). In fact, TAM is recommended for pubertal gynecomastia once it is accompanied by significant pain, irrespective of the disc size (5). TAM is believed to majorly act through its inhibitory effect on estradiol binding at the ligand-binding domain of the estrogen receptor (ER) alpha and blockage of estrogen receptor interaction with co-activator proteins (6, 7). However, TAM has also been shown to act as an estrogen agonist. These dual actions on estrogen could depend on the type of species, cell types, tissue, and organs (8, 9). In humans and rats, TAM primarily exhibits antiestrogenic activities with residual estrogenic effects (10). Apart from these estrogenic effects, TAM also acts via different signaling proteins such as protein kinase C, mitogen-activated protein kinases, and c-jun N-terminal kinase (JNK) and also distorts bcl-2-like protein 4 (BAX)/B-cell lymphoma 2 (BCL-2) ratio. Furthermore, TAM stimulates the mitochondrial permeability transition and cytochrome C release, which eventually results in increased apoptosis (11). With the increasing usage of TAM for the management of gynecomastia (4) and possibly benign prostatic hyperplasia (12), attention has been drawn to its possible testicular toxic effects.

TAM has been shown to impair spermatogenesis and steroidogenesis (13). TAM administration has also been shown to disrupt the hypothalamic-pituitary-gonadal (HPG)-axis (14) responsible for maintaining testicular functions. TAM-induced testicular toxicities could be associated with reactive oxygen species (ROS) generation (15), which are capable of reacting with the cellular DNA, proteins, and lipids to form DNA-adducts, protein crosslink, and lipid peroxidation products (16) in the testis. As a result, these activities can create oxidative stress (redox imbalance), inflammatory response, mitochondrial dysfunction, uncontrolled cell death, and impair testicular cells integrity and functionality. Hence, this study sought to establish a supplement for managing TAM-induced gonadotoxicity in patients who require TAM treatment.

Nutritional supplements can be recommended for the prevention and management of toxicants-induced health disorders. Omega-3 fatty acids (O3FA) is one of these natural supplements that has been shown to possess various pharmacological and biological activities (17, 18). O3FA are essential fatty acids commonly found in plants and marine life. They are referred to as essential fatty acids because they cannot be synthesized in the body; they can only be obtained from diets. O3FA are required for different functions such as growth, brain development, vision, and fertility enhancement (19). O3FA might be performing these functions via its anti-inflammatory (20), anti-oxidant (21, 22), and anti-apoptotic (23) activities.

Despite O3FA's established protective activities, no study has explored its possible ameliorative role on TAM-induced testicular injury. Hence, we hypothesize that O3FA might attenuate TAM-induced testicular toxicity in male Wistar rats. The findings from this study will establish O3FA as a supplement that can be introduced as an adjunct therapy together with TAM.

Materials and methods

Chemicals/reagents

TAM 20 mg was purchased from Milpharm, Ltd, UK, while O3FA was procured from Gujarat Liqui Pharmacaps Pvt. Ltd. Vadodara, Gujarat, India. Each of the O3FA capsules consists of eicosapentaenoic acid (EPA) and docosahexaenoic acid (DHA) in 3:2. All other chemicals used in this study except otherwise stated were of analytical grades and were procured from Sigma (MS, USA).

Ethical consideration

The animals were humanly handled in accordance with the Guidelines for Laboratory Animal Care published by the National Institute of Health (NIH). The experimental protocol complied with the US NAS guidelines, and ethical approval was obtained from the Institutional Ethical Review Committee (UERC/ASN/2022/2396).

Animals

Twenty-four (24) male Wistar rats (aged 10–12 weeks and weighing 180–200 g) were purchased from the Biochemistry Department, University of Ilorin, and housed in standard ventilated cages. The rats were allowed free access to feed and water under a normal 12-h light and darkness cycle.

Experimental procedure

The animals were allowed to acclimatize for 2 weeks before they were randomly divided into 4 groups ($n = 6$ groups): Group 1: Control (Cntrl), vehicle-treated animals with 0.5 ml of corn oil, Group 2: animals treated with 300 mg/kg of O3FA, Group 4: animals exposed to 0.4 mg/kg of TAM, Group 5: animals co-treated with 0.4 mg/kg of TAM and 300 mg/kg of O3FA. All treatments were via oral gavage and lasted for 28 days. The dose of 0.4 mg/kg used in this study has been earlier reported as the most effective dosage of TAM for antifertility studies (7) and is similar to that of Motrich et al. (1) and Lee et al. (15), while the 300 mg/kg of O3FA was the most effective dosage based on the reports from our previous findings (19, 22).

The study was terminated 24 h after the last treatment, and animals were sacrificed via an intraperitoneal administration of ketamine (40 mg/kg) and xylazine (4 mg/kg) (24). Blood samples were obtained via cardiac puncture and put into plain bottles. The obtained blood samples were centrifuged at 3,000 rpm for 10 min, and the obtained serum was used for hormonal assay. Both testes were removed, and the surrounding tissues were separated. The left testes were homogenized in phosphate buffer for biochemical

assays, while the right testes were preserved with bouin solution for histology.

Sperm analysis

Caudal epididymis was meticulously cut into a clean petri dish, and sperm count, motility, and abnormal sperm morphology were estimated based on previous methods (25, 26). Briefly, for sperm motility, cauda epididymis was cut with surgical blade; the spermatozoa released onto a sterile glass slide and then diluted with pre-warmed 2.9% sodium citrate dehydrate solution. The glass slide was covered with a coverslip, and sperm motility was evaluated under microscope by examining at least ten microscopic fields at ×40 magnification. For sperm count, the cauda epididymis was gently crushed in normal saline and filtered with a nylon mesh to obtain the sperm suspension. Five μL of the sperm suspension was mixed with 95 μl of 0.35% formalin containing 0.25% trypan blue and 5% NaHCO3. A fraction (10 μl) of the diluted spermatozoa was placed on the haemocytometer, allowed to sediment for 5 min, and then counted using the Improved Neubauer chamber and a light microscope at ×40. For sperm morphology, The abnormalities in the head, middle-piece and tail (tailless head, bent mid piece, curved mid-piece, headless tail, bent tail, curved tail, looped tail) were counted and classified as documented by Bloom (27) and Parkinson (28).

Steroidogenic enzymes

Testicular 3 beta-hydroxysteroid (3β-HSD) (29, 30) and 17 beta-hydroxysteroid (17 β-HSD) dehydrogenase (30, 31) were estimated as previously established respectively. "For 3β-HSD, testicular tissue was homogenized, and the supernatant was carefully separated. 1 ml of the supernatant was mixed with 1 ml of 100 μmol sodium pyrophosphate buffer (pH 8.9), 30 μg of dehydroepiandrosterone in 40 μl of ethanol, and 960 μl of 25% BSA. The mixture was then incubated and 0.5 μmol of NAD was added. The absorbance was read spectrophotometrically at a wavelength of 340 nm using a blank as reference. For testicular 17β-HSD, 1 ml of the supernatant obtained from the testicular sample was mixed with 1 ml of 440 μmol sodium pyrophosphate buffer (pH 10.2), 40 μl of ethanol containing 0.3 μmol of testosterone, and 960 μl of 25% BSA. The mixture was incubated and 1.1 μmol of NAD was added in a U 2,000 spectrophotometer cuvette at 340 nm against a blank."

Reproductive hormones

The serum levels of luteinizing hormone (LH), follicle-stimulating hormone (FSH), testosterone, and estradiol (Bio-Inteco, UK) were determined using an ELISA method according to the manufacturer's description.

Testicular histology

Histology was performed according to the established method (32, 33). The preserved testis in bouin solution was dehydrated using ethanol series and cleared with toluene. The cleared testes were embedded and blocked in paraffin wax. After that, 5 μm thick paraffin sections were stained with hematoxylin and eosin (H&E). Testicular biopsy/Johnsen score was estimated as previously described (30, 34).

Testicular injury markers

Testicular lactate dehydrogenase (LDH) and Gamma-glutamyl transferase (GGT) activities were determined as described by the manufacturer (Agape Diagnostics Ltd.). Additionally, testicular lactate concentration was evaluated based on the manufacturer's guideline (EnzyChrom, ELAC-100).

Oxidative stress markers

Testicular malondialdehyde (MDA) level was assayed as previously reported (35, 36). In addition, testicular glutathione (GSH), glutathione peroxidase (GPx), Glutathione-S-transferase (GST), superoxide dismutase (SOD), and catalase (CAT) activities were assayed based on established methods (30, 37, 38).

"Malondialdehyde (MDA), a marker of oxidative stress, was determined as previously documented based on the generated amount of thiobarbituric acid reactive substance (TBARS) during lipid peroxidation. This method involves the reaction between 2- thiobarbituric acid (TBA) and malondialdehyde, a byproduct of lipid peroxidation, by analyzing the pink chromogen complex [(TBA) 2-malondialdehyde adduct] formed upon heating at acidic pH. The sample (200 μl) was first treated with 500 μl of Trichloroacetic acid (TCA) to remove proteins and centrifuged at 3,000 rpm for 10 min. Next, 1 ml of 0.75% TBA was added to 0.1 ml of the supernatant and heated in a water bath at 100°C for 20 min, then cooled with ice water. The absorbance of the sample/standard was then read at 532 nm using a spectrophotometer and compared to a blank. The concentration of TBARS was determined by extrapolating from a standard curve.

For GSH, an aliquot of the sample was deproteinized by adding an equal volume of 4% sulfosalicylic acid, and was centrifuged at 4,000 rpm for 5 min. 0.5 ml of the supernatant was then added to 4.5 ml of Ellman's reagent. A blank was prepared by mixing 0.5 ml of the diluted precipitating agent with 4.5 ml of Ellman's reagent. The level of GSH was calculated by measuring the absorbance at 412 nm.

For catalase, 1:29 dilution of the sample was made by mixing 1 ml of the supernatant of the testicular homogenate with 19 ml of diluted water. 4 ml of H2O2 solution (800 μmoles) and 5 ml of phosphate buffer were added to a 10 ml flat bottom flask. 1 ml of the diluted enzyme preparation was mixed into the reaction mixture by gentle swirling at 37°C. Samples of the reaction mixture were withdrawn at 60 s intervals, and the H_2O_2 content was determined by blowing 1 ml of the sample into 2 ml

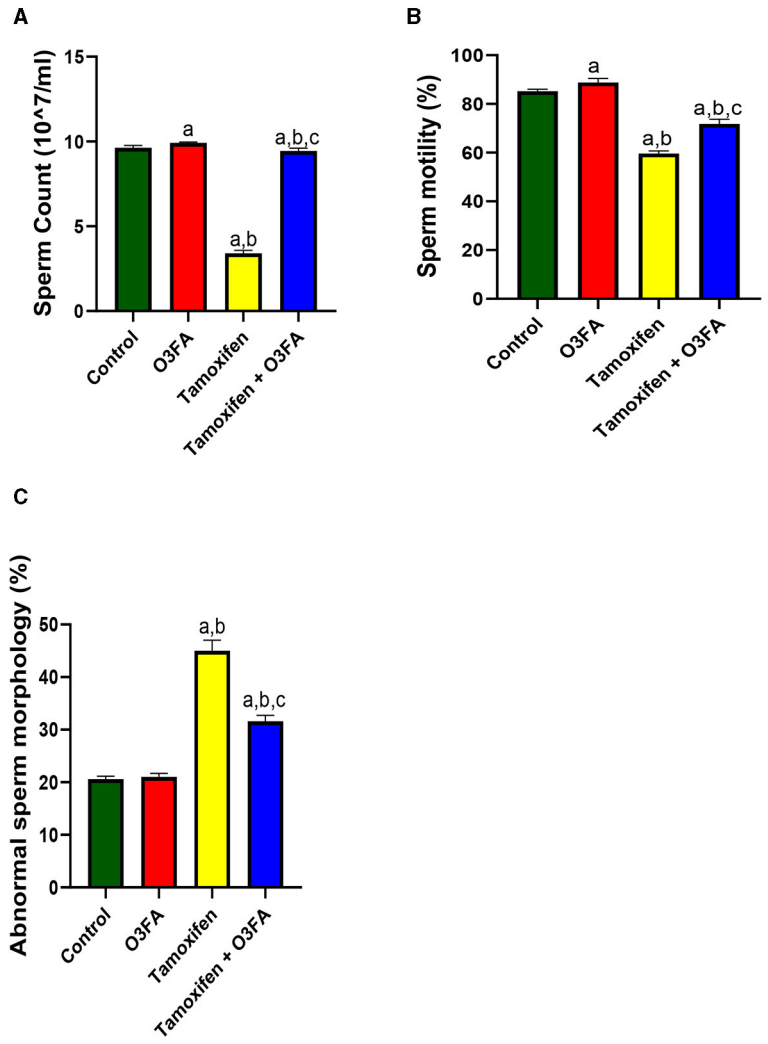

FIGURE 1
Effect of O3FA on sperm **(A)** count **(B)** motility **(C)** abnormal morphology in TAM exposed rats. $^{a}P < 0.05$ vs. control, $^{b}P < 0.05$ vs. O3FA; $^{c}P < 0.05$ vs. TAM. Data were analyzed by one way ANOVA and Tukey's *post-hoc* test. O3FA, Omega-3 fatty acids; TAM, Tamoxifen.

dichromate/acetic acid reagent. Catalase levels in the sample were determined by comparing the absorbance at 653 nm to that of a certified catalase standard.

For GPx, the sample was incubated at 37°C for 3 min, then 0.5 ml of 10% trichloroacetic acid (TCA) was added and the mixture was centrifuged at 3,000 rpm for 5 min. The supernatant was then mixed with 2 ml of phosphate buffer and 1 ml of 5′- 5′- dithiobis-2-dinitrobenzoic acid (DTNB) solution, and the absorbance was measured at 412 nm using a blank as reference. The GPx activity was determined by plotting a standard curve and determining the concentration of remaining GSH from the curve.

The activity of glutathione-S-transferase in testicles was also measured. This method utilizes the enzyme's high activity with 1-chloro-2,4-dinitrobenzene as a substrate. The assay was performed at 37°C for 60 s and the absorbance was read at 340 nm after comparing it with a blank sample.

For SOD, a 1:10 dilution of the sample was made using 1 ml of sample and 9 ml of distilled water. 0.2 ml of the diluted sample was added to 2.5 ml of 0.05 M carbonate buffer (pH 10.2) and the reaction was initiated by adding 0.3 ml of freshly prepared 0.3 mM adrenaline. The mixture was mixed and the increase in absorbance was monitored at 480 nm every 30 s for 150 s using a spectrophotometer. A reference cuvette containing 2.5 ml buffer, 0.3 ml substrate (adrenaline), and 0.2 ml water was also used."

Inflammatory markers

Testicular tumor necrotic factor-alpha (TNF-α) and interleukin 6 (IL-6) were assayed using ELISA kits (Solarbio, China). Also, testicular myeloperoxidase (MPO) was estimated according to previously reported methods (30, 39), while testicular nitric oxide (NO) concentration was determined based on the Griess reaction (40).

Briefly, "the method for measuring MPO is based on the ability of myeloperoxidase to catalyze the oxidation of guaiacol to oxidized guaiacol in the presence of hydrogen peroxide. The oxidized form of guaiacol has a brown color, which is measured

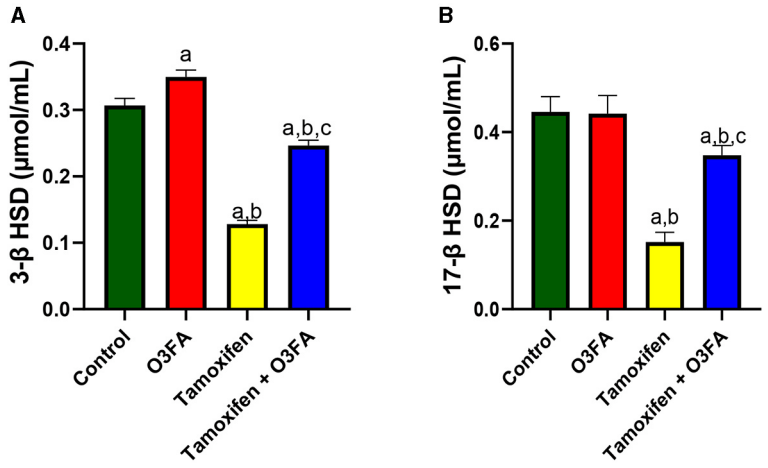

FIGURE 2
Effect of O3FA on testicular **(A)** 3β-HSD **(B)** 17β-HSD in TAM exposed rats. [a]$P < 0.05$ vs. control, [b]$P < 0.05$ vs. O3FA; [c]$P < 0.05$ vs. TAM. Data were analyzed by one way ANOVA and Tukey's *post-hoc* test. O3FA, Omega-3 fatty acids; TAM Tamoxifen; 3β-HSD, 3 beta-hydroxysteroid dehydrogenase; 17β-HSD, 17 beta-hydroxysteroid dehydrogenase.

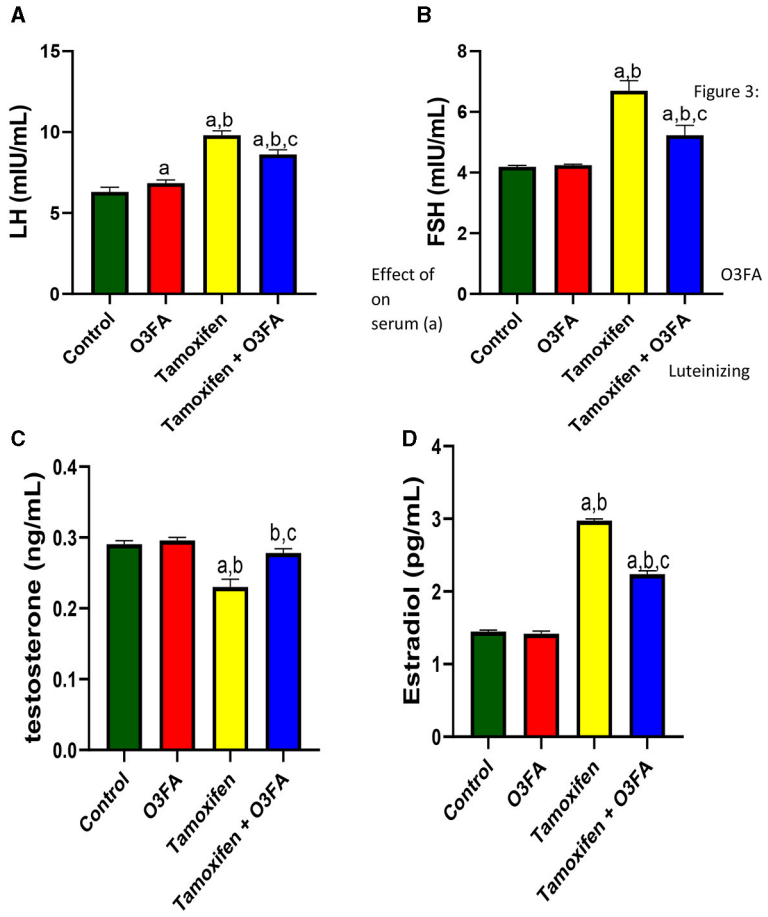

FIGURE 3
Effect of O3FA on serum **(A)** Luteinizing hormone (LH) **(B)** Follicle stimulating hormone (FSH) **(C)** testosterone **(D)** estradiol in TAM exposed rats. [a]$P < 0.05$ vs. control, [b]$P < 0.05$ vs. O3FA; [c]$P < 0.05$ vs. TAM. Data were analyzed by one way ANOVA and Tukey's *post-hoc* test. O3FA, Omega-3 fatty acids; TAM, Tamoxifen.

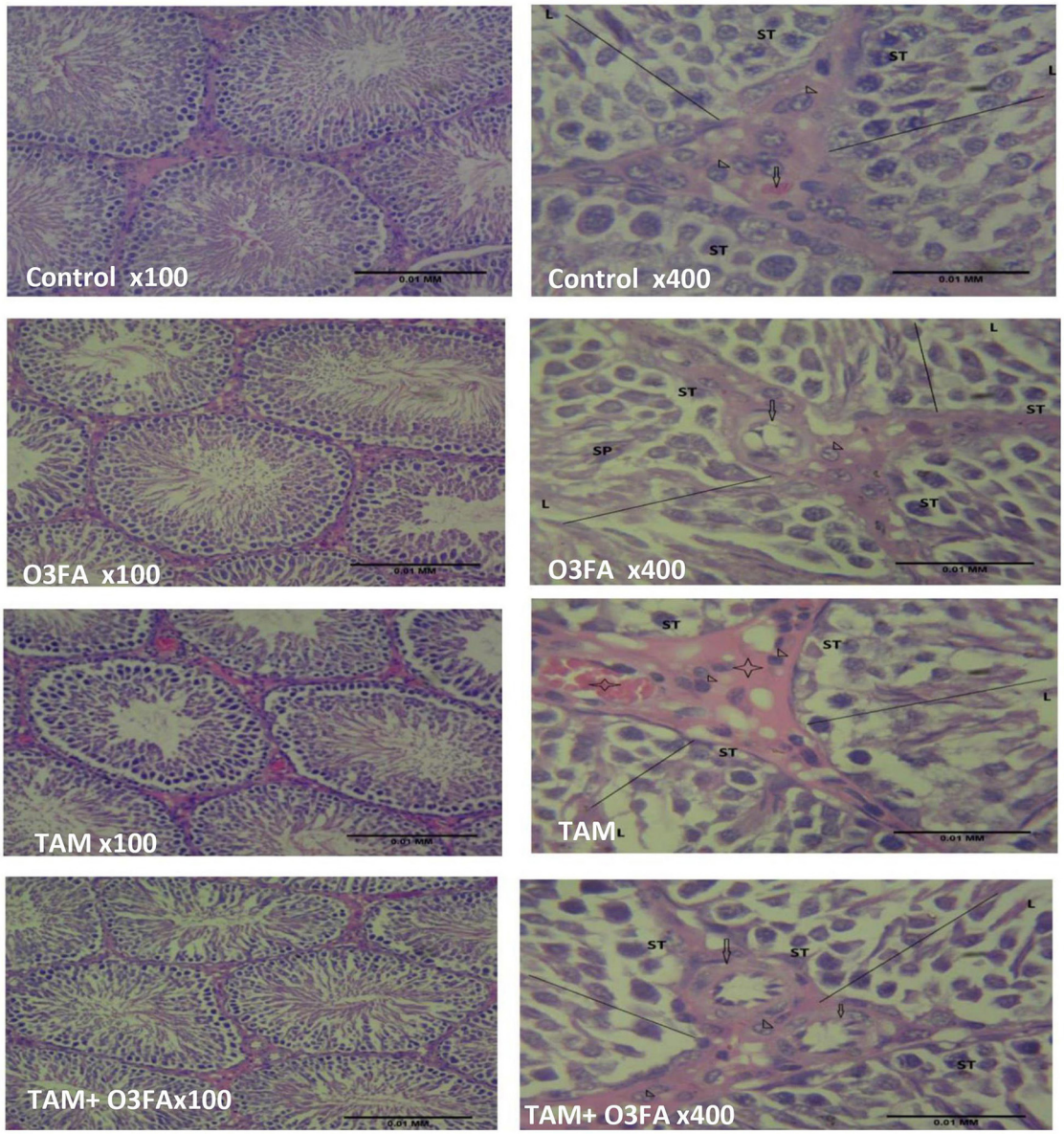

FIGURE 4
Testicular histology. Control, O3FA, and TAM + O3FA: section shows the testicular tissue composed of coils of seminiferous tubules (ST) with a defined lumen (L) containing sperm cells (SP), the seminiferous tubules contained germinal epithelium with germ cells at varying degree of maturation (line). The interstitium, contained blood vessel (arrow) which is free of collection and contained interstitial cells of Leydig (arrow head) appearing unremarkable. TAM, The blood vessels (black star) within the interstitium (plain star) appeared congested, and the interstitial cells of Leydig (arrow head) appears unremarkable.

spectrophotometrically at a wavelength of 470 nm. The intensity of the color produced is proportional to the concentration of oxidized guaiacol produced in the reaction, thus providing a measure of myeloperoxidase activity.

For NO, a mixture of 100 µl of Griess reagent, 300 µl of a nitrate-containing testicular homogenate, and 2.6 ml of deionized water were incubated for 30 min at room temperature in a spectrophotometer cuvette. A blank was prepared by mixing 100 µl of Griess reagent and 2.9 ml of deionized water. The absorbance of the nitrate-containing sample was measured at 548 nm in relation to the reference sample."

Xanthine oxidase/uric acid

The activities of testicular xanthine oxidase (XO) were determined based on the method of Zahide and Bahad (41), while a colorimetric method was used for uric acid (UA) concentration (Precision, UK).

Transcriptional factors

Testicular nuclear factor kappa B (NFkB) and nuclear factor erythroid 2-related factor 2 (Nrf2) levels were

determined using the ELISA method (Elabscience Biotechnology Inc., USA).

Apoptotic markers

Testicular BCl-2, cytochrome C, and caspase 3 activities were determined by an ELISA method as described by the manufacturer (Elabscience Biotechnology Inc., USA). At the same time, the testicular DNA Fragmentation Index (DFI) was estimated according to the method of Perandones et al. (42). Five ml each of testicular homogenate supernatant and pellet were treated with 3 ml of freshly prepared diphenylamine (DPA) reagent for color development. The solution was incubated at 37°C for 16 to 24h. The absorbance of light green/yellowish-green supernatant was read spectrophotometrically at 620 nm. The percentage of fragmented DNA was calculated by dividing the absorbance of the homogenate supernatant by the sum of the absorbance of the pellet and the absorbance of the supernatant.

Statistical analysis

Data were analyzed using a one-way analysis of variance (ANOVA) followed by Tukey's *post hoc* test using GraphPad PRISM 5 software, and they were reported as mean ± standard deviation. Also, all P values below 0.05 were classified as statistically significant.

Results

As shown in Figure 1, TAM exposure led to a significant decrease in sperm count ($p < 0.0001$), motility ($p < 0.0001$), and an increase in abnormal morphology ($p < 0.0001$) compared with the control and O3FA groups. These impaired sperm qualities were ameliorated by O3FA treatment.

In the same vein, TAM administration impaired steroidogenic enzymatic activities, evidenced by a significant decrease in 3β-HSD ($p < 0.0001$) and 17β-HSD ($p < 0.0001$) compared with the control and O3FA groups (Figure 2). These observed decreases were abrogated in animals in the TAM+ O3FA group.

Furthermore, compared with the control groups, animals administered with TAM had a significant increase in serum LH ($p < 0.0001$), FSH ($p < 0.0001$), and estradiol and a decrease in testosterone (Figure 3). TAM and O3FA co-administration blunted these observed hormonal imbalances.

Histopathological findings revealed features consistent with normal testicular tissue of animals in the control, O3FA, and TAM + O3FA groups, while their counterparts in the TAM group exhibited histological features that suggest cellular reaction to injury and inflammatory response (Figure 4). Also, a decrease in Johnsen score was observed in TAM-exposed animals compared with the controls (Figure 5). This alteration was ameliorated in animals that received TAM and O3FA co-treatment.

Additionally, TAM administration led to a significant increase in testicular lactate, LDH, and GGT and a decrease in testicular SDH (Figure 6) compared with the controls. These observed increases in testicular injury markers were ameliorated in animals treated with TAM and O3FA.

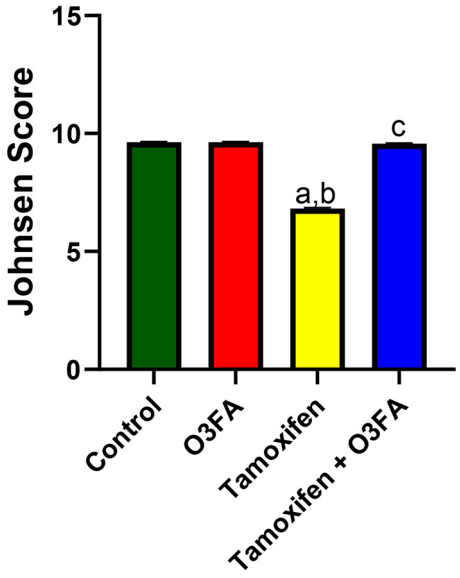

FIGURE 5
Effect of O3FA on Johnsen Score in TAM exposed rats. $^{a}P < 0.05$ vs. control, $^{b}P < 0.05$ vs. O3FA; $^{c}P < 0.05$ vs. TAM. Data were analyzed by one way ANOVA and Tukey's *post-hoc* test. O3FA, Omega 3 fatty acids; TAM, Tamoxifen.

Also, Figure 7 showed that TAM administration led to a significant increase in testicular MDA and a decrease in testicular SOD, CAT, GSH, GPX, and GST. This observed redox imbalance was abrogated in animals that received O3FA and TAM co-treatment.

Similarly, TAM treatment significantly led to an increase in testicular TNF-α, IL-6, MPO, and NO compared with the control groups (Figure 8). These observed TAM-induced inflammatory responses were ameliorated in animals treated with TAM and O3FA.

Furthermore, testicular XO and UA were significantly elevated in animals treated with TAM compared with the control (Figure 9). These observed TAM-induced XO/UA signaling distortions were blunted in animals treated with TAM and O3FA.

Additionally, TAM administration led to a significant decrease in testicular Nrf2 and an increase in testicular Nf-κB compared with the control groups (Figure 10). This observed TAM-induced Nrf2/Nf-κB signaling distortion in TAM-treated animals was ameliorated in their counterparts treated with TAM and O3FA.

Finally, TAM exposure led to a significant increase in testicular cytochrome C, BCl-2, caspase 3, and DFI compared with the animals in the control group (Figure 11). TAM and O3FA co-treatment blunted this observed increase in apoptotic markers.

Discussion

It has been sufficiently established that estrogen plays a major role in male reproductive system development and maintenance. In fact, the presence of ER α and β in the testicular (43, 44)

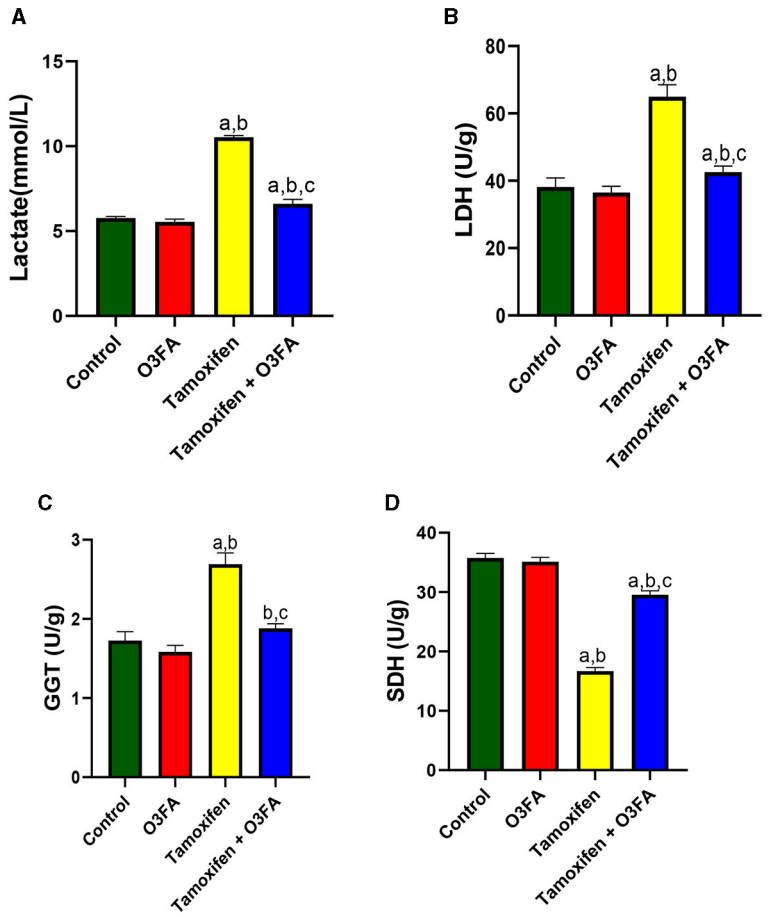

FIGURE 6
Effect of O3FA on testicular **(A)** lactate **(B)** lactate dehydrogenase (LDH) **(C)** Gamma-glutamyl transferase (GGT) **(D)** sorbitol dehydrogenase (SDH) in TAM exposed rats. $^{a}P < 0.05$ vs. control, $^{b}P < 0.05$ vs. O3FA; $^{c}P < 0.05$ vs. TAM. Data were analyzed by one way ANOVA and Tukey's *post-hoc* test. O3FA, Omega 3 fatty acids; TAM, Tamoxifen.

and sperm cells (45, 46) indicates the cognate role of estrogen in testicular functions. Supportively, Korach (47) reported impaired testicular functions in ER α and β knockout mice. TAM is a potent nonsteroidal antiestrogen that has been recommended for managing breast cancer and gynecomastia. In fact, it has been recommended for treating idiopathic oligospermia despite insufficient data on its effectiveness (48, 49). However, these authors did not compare their findings with a placebo control, which is a fundamental aspect to consider when testing the real therapeutic effect of a drug. In fact, Rolf et al. (50) concluded that the beneficial role of TAM may not justify its side effects in healthy males after reviewing 29 clinical trials involving 1,586 patients. TAM has been reported to negatively impact male fertility status in different strains, including rats, monkeys, and dogs (1). Although different studies have studied the antiestrogenic and estrogenic effects of TAM, information on its effect on oxido-inflammatory response and apoptosis on testicular tissue is still lacking. Hence, we investigated the putative gonadotoxic effects of TAM and the possible role of redox imbalance, inflammation, and apoptotic response in TAM-induced testicular dysfunction. Also, we explored the possible ameliorative effect of O3FA on TAM-induced gonadotoxicity.

Our findings revealed that O3FA treatment inhibited the impaired sperm quality, steroidogenesis, HPG-axis, and surge in testicular injury markers following TAM exposure. These histological and biochemical events were accompanied by O3FA-induced amelioration of TAM-mediated distortion of Nrf2/Nf-κb signaling and the consequent redox balance, the suppression of inflammatory response, and cytochrome C-mediated apoptosis.

In this study, TAM administration led to a significant decrease in sperm motility, count, and normal morphology. This impaired sperm quality was accompanied by a significant decline in serum testosterone and steroidogenic enzymatic activities, which are in tandem with previous reports (13). Different mechanisms might be responsible for the observed spermatogenesis and steroidogenesis impairment. TAM might impair testicular function by disrupting the HPG axis activities or via direct testicular damage. In male reproduction, the hypothalamus is responsible for secreting GnRH, which stimulates LH and FSH secretion from the pituitary gland, which also stimulates the testis. The secreted LH stimulates steroidogenesis (testosterone and estrogen secretion), while FSH stimulates spermatogenesis. Additionally, testosterone and estrogen also play a dominant role in spermatogenesis. Testosterone and estrogens,

10.3389/fnut.2024.1443895

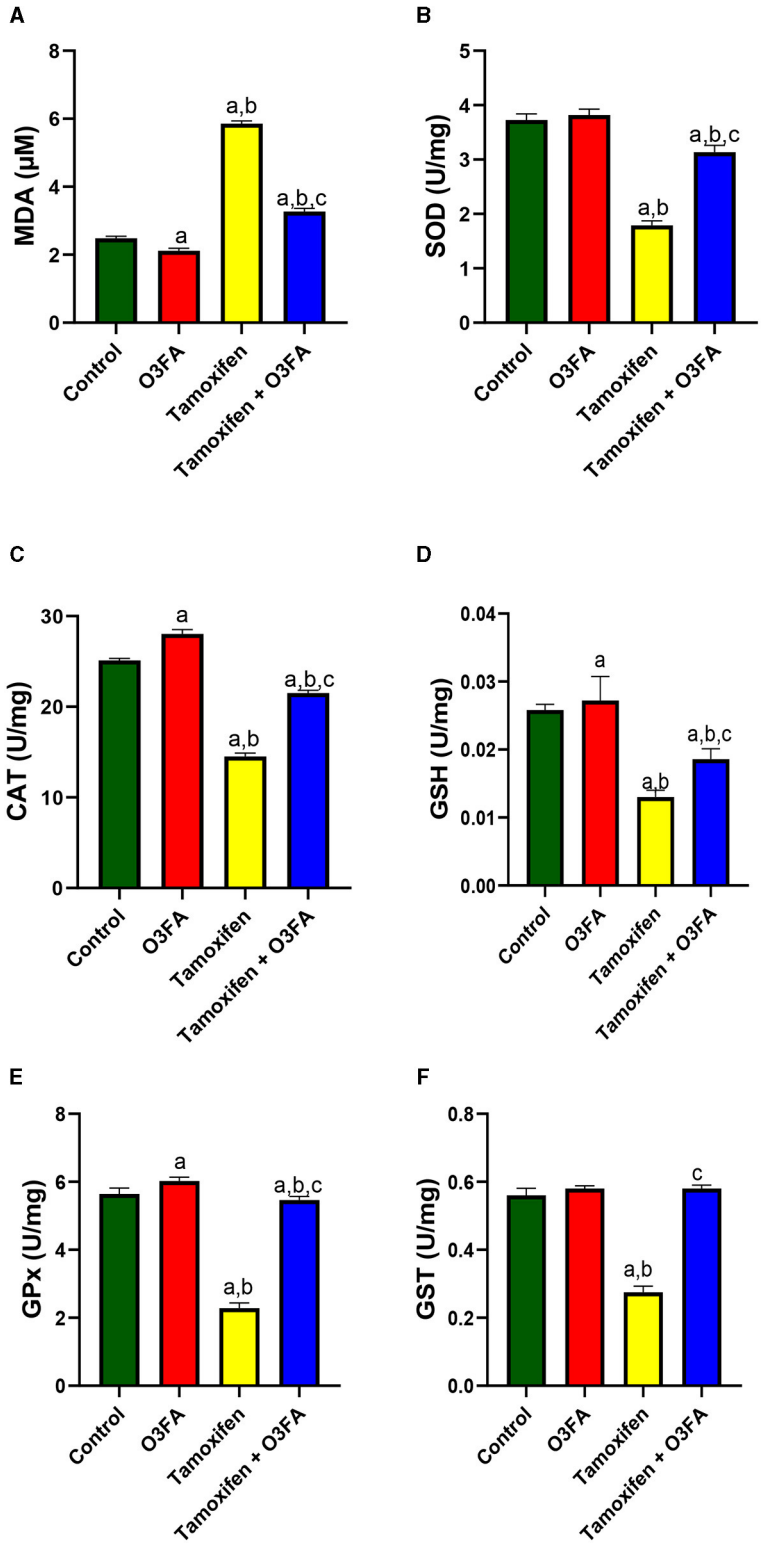

FIGURE 7
Effect of O3FA on testicular **(A)** malondialdehyde (MDA) **(B)** superoxide dismutase (SOD) **(C)** catalase (CAT) **(D)** glutathione (GSH) **(E)** glutathione peroxidase (GPx) **(F)** Glutathione-S-transferase (GST) in TAM exposed rats. $^{a}P < 0.05$ vs. control, $^{b}P < 0.05$ vs. O3FA; $^{c}P < 0.05$ vs. TAM. Data were analyzed by one way ANOVA and Tukey's *post-hoc* test. O3FA, Omega 3 fatty acids; TAM, Tamoxifen.

in turn, inhibit the synthesis of the gonadotropins at the level of the pituitary or directly inhibit GnRH secretion from the hypothalamus (51). Thus, the disruption of the HPG axis activities at any level will directly impair testicular functions (spermatogenesis and steroidogenesis). The fact that TAM exposure led to a significant increase in gonadotropins (LH and FSH) might suggest that

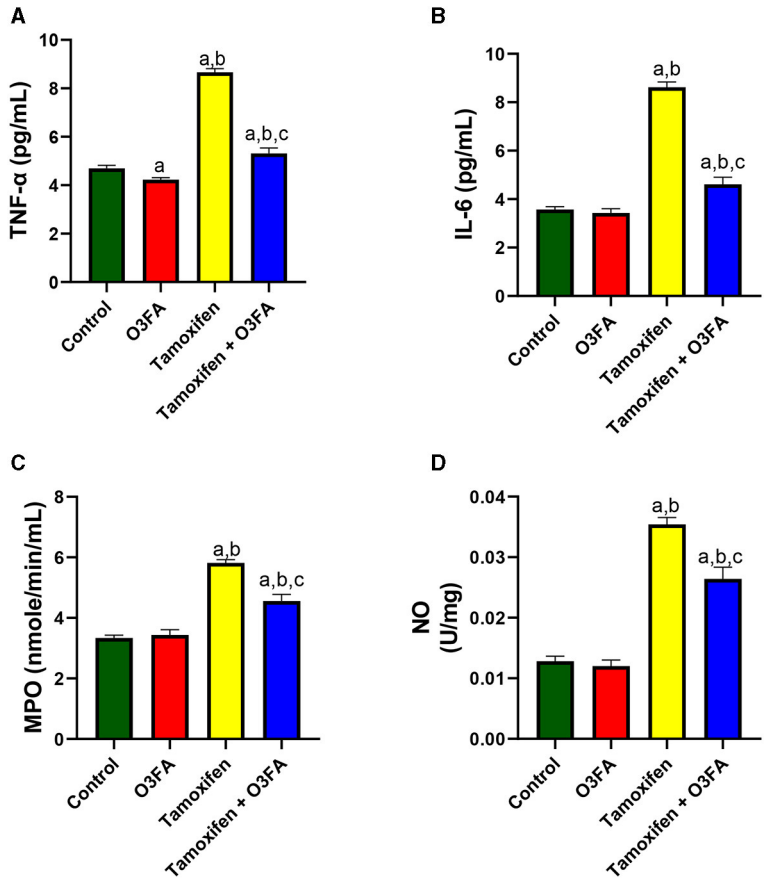

FIGURE 8
Effect of O3FA on testicular **(A)** tumor necrotic factor-alpha (TNF-α) **(B)** interleukin 6 (IL-6) **(C)** myeloperoxidase (MPO) **(D)** nitric oxide (NO) in TAM exposed rats. $^{a}P < 0.05$ vs. control, $^{b}P < 0.05$ vs. O3FA; $^{c}P < 0.05$ vs. TAM. Data were analyzed by one way ANOVA and Tukey's *post-hoc* test. O3FA, Omega 3 fatty acids; TAM, Tamoxifen.

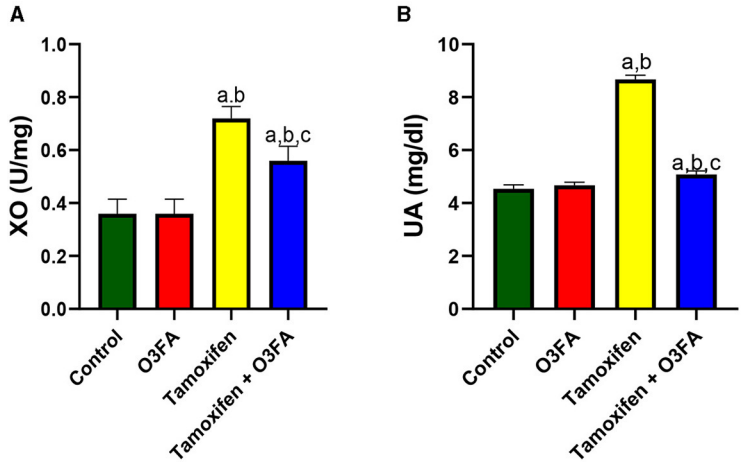

FIGURE 9
Effect of O3FA on testicular **(A)** Xanthine oxidase (XO) **(B)** uric acid (UA) in TAM exposed rats. $^{a}P < 0.05$ vs. control, $^{b}P < 0.05$ vs. O3FA; $^{c}P < 0.05$ vs. TAM. Data were analyzed by one way ANOVA and Tukey's *post-hoc* test. O3FA, Omega 3 fatty acids; TAM, Tamoxifen.

TAM-induced testicular dysfunction could be independent of the HPG axis activities rather than via direct testicular damage since circulatory LH was unable to stimulate the gonad (testis) to synthesize testosterone.

The fact that TAM exposure disrupted the normal testicular cytoarchitecture supports our claim that TAM might impair testicular function via direct testicular damage. Also, the increase in testicular injury markers (Lactate, LDH, GGT, and SDH) following

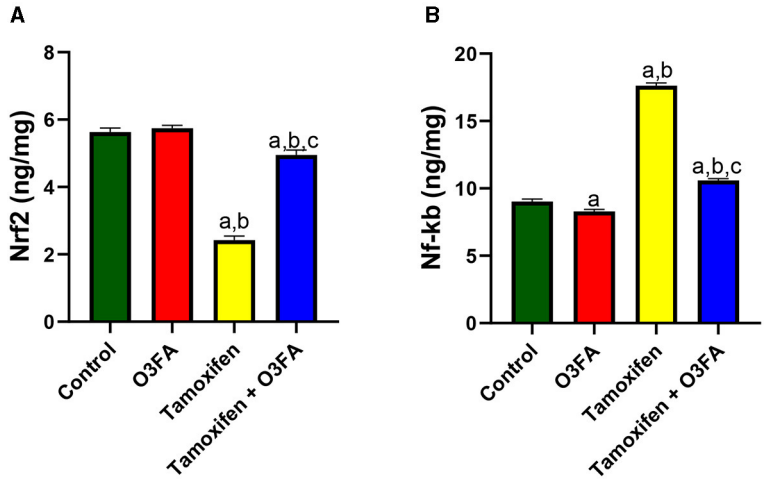

FIGURE 10
Effect of O3FA on testicular **(A)** Nrf2 **(B)** Nf-kb in TAM exposed rats. $^{a}P < 0.05$ vs. control, $^{b}P < 0.05$ vs. O3FA; $^{c}P < 0.05$ vs. TAM. Data were analyzed by one way ANOVA and Tukey's *post-hoc* test. O3FA, Omega 3 fatty acids; TAM, Tamoxifen.

TAM exposure further substantiates our claim. Additionally, spermatogenesis is a complex process that requires energy balance (52). Unfortunately, the observed increase in lactate is a marker of energy imbalance (53), which is an indication of impaired spermatogenesis and testicular degeneration (22). These findings corroborated previous findings of Marek et al. (54), who reported that TAM activities are associated with energy imbalance and an increase in lactate.

This direct testicular damage could result from oxidative stress or redox imbalance, which plays a key role in testicular functions (55, 56). Oxidative stress occurs when there is an imbalance between pro-oxidant generation and antioxidant activities. Oxidative stress, on the other hand, can stimulate different transcription factors to activate inflammatory pathways (57, 58). TAM treatment could impair testicular function via its oxido-inflammatory activities evidenced by an increase in testicular MDA, IL-6, TnF-a, MPO, and NO and a decrease in CAT, SOD, GSH, GST, and GPx. These observed TAM-induced oxido-inflammatory responses could be mediated by the increase in XO/UA signaling. An increase in XO and the consequent increase in UA has been implicated in lipid peroxidation (59). Although UA is an antioxidant, it becomes a pro-oxidant once produced in excess (60), thereby generating excessive ROS. Excessive ROS can overwhelm Nrf2 activities, the endogenous transcription factor responsible for maintaining redox balance (35). The consequent redox imbalance might activate Nf-κb, responsible for increasing pro-inflammatory gene induction, leading to an inflammatory response (61). The increase in Nf-κb will further inhibit Nrf2 activities, thereby leading to a further decline in the endogenous antioxidant activities. This observed XO/UA and Nrf2/Nf-κb-mediated oxido-inflammatory response following tamoxifen exposure agreed with the study of Ahmed et al. (62) and Schieber and Chandel (63), who reported that TAM can impair cellular functions via oxidative stress.

Additionally, excessive oxidative stress and inflammatory response can collaborate to stimulate apoptosis (64), which is another key factor that can be responsible for TAM-induced testicular dysfunction. The observed increase in testicular cytochrome c following TAM exposure could account for the observed TAM-induced apoptotic response. In mammals, the cytochrome c-initiated pathway is a key caspase activation pathway (65). Various apoptotic stimuli can stimulate the release of cytochrome c from the mitochondria, leading to a series of biochemical reactions that activate caspase and the consequent cell death. Mitochondria plays a major role in the redistribution of cytochrome c (66). Also, the anti-apoptotic protein (BCl-2) located predominantly at the outer mitochondria membrane assists in blocking $\Delta\psi m$ reduction and cytochrome c release (67). Hence, during mitochondrial dysfunction, there is a leakage of cytochrome c from the mitochondria and a decrease in BCl-2 (66), thereby leading to caspase 3- 3-mediated apoptosis (68). Hence, it is plausible that the observed increase in testicular caspase 3 and DFI and decrease in testicular BCl-2 might be associated with the leakage of cytochrome c from the mitochondria of TAM-treated rats. Our guess that TAM disrupts testicular function via mitochondria dysfunction-mediated apoptosis corroborates the findings of Unten et al. (69) and Nazarewicz et al. (70).

Another key finding from this study is the therapeutic potential of O3FA against TAM-induced testicular dysfunction. This study revealed that O3FA ameliorated TAM-induced testicular dysfunction by decreasing testicular injury markers and oxido-inflammatory and apoptotic response, thus improving spermatogenesis, sperm quality, hormone synthesis, and testicular histoarchitecture. These findings agreed with previous studies that established the antioxidant (71), anti-inflammatory (22), and anti-apoptotic (72) effects of O3FA. Hence, it is safe to infer that the increase in testicular SOD, CAT, GSH, GPX, and GST and decrease in TNF-a, IL-6, MPO, and NO of TAM exposed rats showed that O3FA –driven repression UA release via XO activities downregulation probably modulated the Nrf2/Nf-κb signaling, thereby inhibiting the transcription of genes responsible for encoding pro-inflammatory

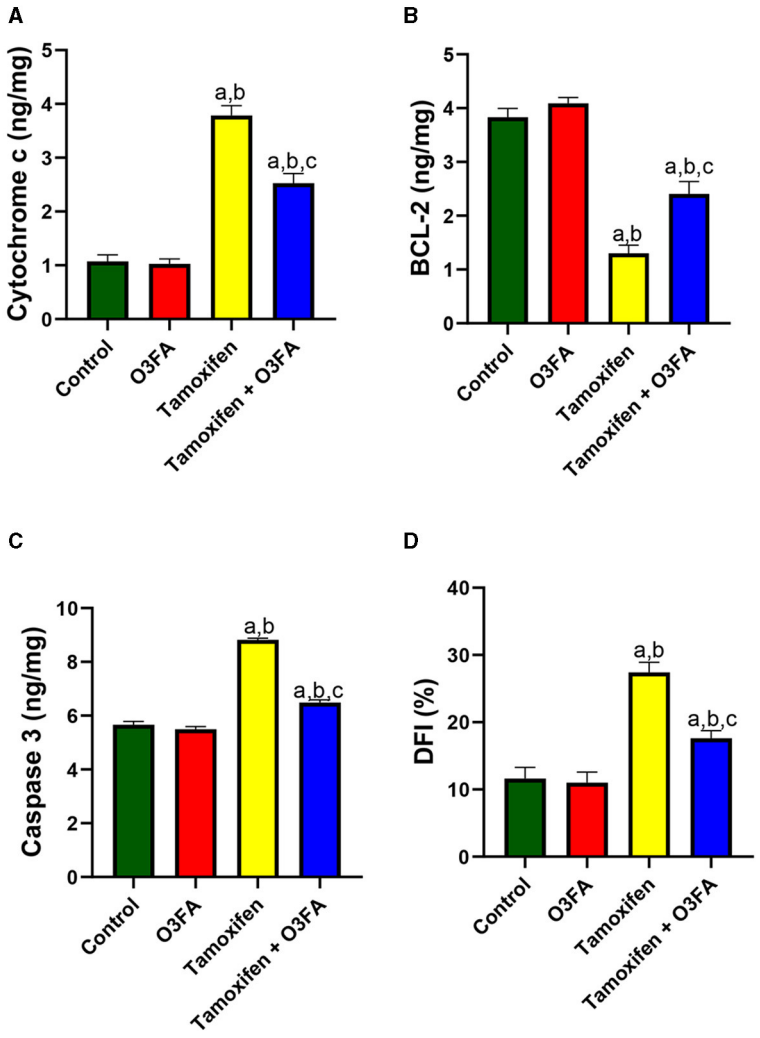

FIGURE 11
Effect of O3FA on testicular **(A)** cytochrome c **(B)** B-cell lymphoma 2 (BCl-2) **(C)** caspase 3 **(D)** DNA fragmentation index (DFI) in TAM exposed rats. [a]$P < 0.05$ vs. control, [b]$P < 0.05$ vs. O3FA; [c]$P < 0.05$ vs. TAM. Data were analyzed by one way ANOVA and Tukey's *post-hoc* test. O3FA, Omega 3 fatty acids; TAM, Tamoxifen.

cytokines and oxidative response. Furthermore, the observed increase in BCl-2 and decrease in caspase 3 and DFI in O3FA and TAM co-treated rats could also be associated with O3FA-associated decline in cytochrome c release from the mitochondria.

Conclusion

The findings from this study revealed that O3FA ameliorated impaired sperm quality, hormonal imbalance, oxido-inflammatory response, and apoptosis by modulating XO/UA and Nrf2/NF-kb signaling and cytochrome c-mediated apoptosis in TAM-treated rats. These findings suggests the combination therapy with TAM and O3FA in the management of gynecomastia and breast cancer, since O3FA can help alleviate the side effects associated with TAM with respect to male fertility.

Limitations

This study was conducted in healthy animals and we suggest a replica of it in gynecomastia subjects receiving TAM treatment. Additionally, downstream target genes responsible for maintain oxido-inflammatory response and apoptosis were not estimated using real-time PCR, western blot, immunohistochemistry, or TUNEL analysis (for apoptosis). However, the observed modulation of XO/UA and Nrf2/NF-kb and cytochrome c-mediated apoptosis accompanied by oxido-inflammatory response suggests the involvement of these pathways in TAM-induced testicular dysfunction.

Data availability statement

The raw data supporting the conclusions of this article will be made available by the authors, without undue reservation.

Ethics statement

The animal study was approved by the University of Ilorin Ethical Review Committee. The study was conducted in accordance with the local legislation and institutional requirements.

Author contributions

AO: Conceptualization, Data curation, Formal analysis, Funding acquisition, Investigation, Methodology, Project administration, Resources, Software, Supervision, Validation, Visualization, Writing – original draft, Writing – review & editing. RA: Formal analysis, Investigation, Methodology, Project administration, Supervision, Validation, Visualization, Writing – review & editing. MH: Formal analysis, Funding acquisition, Investigation, Methodology, Project administration, Resources, Supervision, Validation, Visualization, Writing – review & editing. MB: Methodology, Project administration, Supervision, Validation, Visualization, Writing – review & editing. DO: Methodology, Project administration, Supervision, Visualization, Writing – review & editing. LO: Methodology, Project administration, Resources, Supervision, Validation, Visualization, Writing – review & editing.

Funding

The author(s) declare that no financial support was received for the research, authorship, and/or publication of this article.

Conflict of interest

The authors declare that the research was conducted in the absence of any commercial or financial relationships that could be construed as a potential conflict of interest.

Publisher's note

All claims expressed in this article are solely those of the authors and do not necessarily represent those of their affiliated organizations, or those of the publisher, the editors and the reviewers. Any product that may be evaluated in this article, or claim that may be made by its manufacturer, is not guaranteed or endorsed by the publisher.

References

1. Motrich RD, Ponce AA, Rivero VE. Effect of tamoxifen treatment on the semen quality and fertility of the male rat. *Fertil Steril.* (2007) 88:452–61. doi: 10.1016/j.fertnstert.2006.11.196

2. Kavishahi NN, Rezaee A, Jalalian S. The impact of miRNAs on the efficacy of tamoxifen in breast cancer treatment: a systematic review. *Clin Breast Cancer.* (2024) 24:341–50. doi: 10.1016/j.clbc.2024.01.015

3. De Oliveira Andrade F, Yu W, Zhang X, Carney E, Hu R, Clarke R, et al. Effects of Jaeumkanghwa-tang on tamoxifen responsiveness in preclinical ER+ breast cancer model. *Endocr Relat Cancer.* (2019) 26:339–53. doi: 10.1530/ERC-18-0393

4. Senkoro E, Varadarajan M, Candela C, Gebreselassie A, Antoniadi C, Boffito M. Anastrozole as a therapeutic option for gynecomastia in a person receiving antiretroviral therapy: Case report. *Br J Clin Pharmacol.* (2024) 90:350–3. doi: 10.1111/bcp.15951

5. Sabanci E, Pehlivantürk-Kizilkan M, Akgül S, Derman O, Kanbur N. Tamoxifen treatment for pubertal gynecomastia: when to start and how long to continue. *Breast Care.* (2023) 18:249–55. doi: 10.1159/000530408

6. Singh B, Bhat NK, Bhat HK. Partial inhibition of estrogen-induced mammary carcinogenesis in rats by tamoxifen: balance between oxidant stress and estrogen responsiveness. *PLoS ONE.* (2011) 6:e25125. doi: 10.1371/journal.pone.0025125

7. Gill-Sharma M, Balasinor N, Parte P, Aleem M, Juneja H. Effects of tamoxifen metabolites on fertility of male rat. *Contraception.* (2001) 63:103–9. doi: 10.1016/S0010-7824(01)00178-0

8. Hoffmann B, Schuler G. Receptor blockers - general aspects with respect to their use in domestic animal reproduction. *Animal Reproduction Sci.* (2000) 60:295–312. doi: 10.1016/S0378-4320(00)00129-9

9. Corrada Y, Arias D, Rodríguez R, Spaini E, Fava F, Gobello C. Effect of tamoxifen citrate on reproductive parameters of male dogs. *Theriogenology.* (2004) 61:1327–41. doi: 10.1016/j.theriogenology.2003.07.020

10. Furr BJA, Jordan VC. The pharmacology and clinical uses of tamoxifen. *Pharmacol Ther.* (1984) 25:127–205. doi: 10.1016/0163-7258(84)90043-3

11. Owumi SE, Anaikor RA, Arunsi UO, Adaramoye OA, Oyelere AK. Chlorogenic acid co-administration abates tamoxifen-mediated reproductive toxicities in male rats: An experimental approach. *J Food Biochem.* (2021) 45:e13615. doi: 10.1111/jfbc.13615

12. Chen B, Bai JL, Zhang SS, Fu W. An experimental study of the inhibition of tamoxifen on rat model of benign prostatic hyperplasia. *National J Androl.* (2002) 8:98–102.

13. Verma R, Krishna A. Effect of tamoxifen on spermatogenesis and testicular steroidogenesis. *Biochem Biophys Res Commun.* (2017) 486:36–42. doi: 10.1016/j.bbrc.2017.02.092

14. Mitwally M, Casper R, Diamond M. Oestrogen-selective modulation of FSH and LH secretion by pituitary gland. *Br J Cancer.* (2005) 92:416–7. doi: 10.1038/sj.bjc.6602292

15. Lee S, Lee MS, Park J, Zhang JY, Jin DI. Oxidative stress in the testis induced by tamoxifen and its effects on early embryo development in isogenic mice. *J Toxicol Sci.* (2012) 37:675–9. doi: 10.2131/jts.37.675

16. Blair IA. DNA adducts with lipid peroxidation products. *J Biol Chem.* (2008) 283:15545–9.

17. Oktar S, Karadeniz M, Acar M, Zararsiz I. The effects of omega-3 fatty acids on antioxidant enzyme activities and nitric oxide levels in the cerebral cortex of rats treated ethanol. *Biomed Khim.* (2024) 70:83–8. doi: 10.18097/pbmc20247002083

18. Xia Y, Zhang Y, Li Y, Li X, Wu Y, Yao Q. Omega-3 polyunsaturated fatty acids play a protective role in a mouse model of Parkinson's disease by increasing intestinal inducible Treg cells. *Cell Mol Biol.* (2024) 70:107–12. doi: 10.14715/cmb/2024.70.4.17

19. Odetayo AF, Olayaki LA. Omega-3 fatty acid improves sexual and erectile function in BPF-treated rats by upregulating NO/cGMP signaling and steroidogenic enzymes activities. *Sci Rep.* (2023) 13:18060. doi: 10.1038/s41598-023-45344-4

20. Akhigbe RE, Hamed MA, Odetayo AF, Akhigbe TM, Ajayi AF, Ajibogun F. Omega-3 fatty acid rescues ischaemia/perfusion-induced testicular and sperm damage via modulation of lactate transport and xanthine oxidase/uric acid signaling. *Biomed Pharmacother.* (2021) 142:111975. doi: 10.1016/j.biopha.2021.111975

21. Tian A, Zheng Y, Li H, Zhang Z, Du L, Huang X, et al. Eicosapentaenoic acid activates the P62/KEAP1/NRF2 pathway for the prevention of diabetes-associated cognitive dysfunction. *Food Funct.* (2024) 15:5251–71. doi: 10.1039/D4FO00774C

22. Odetayo AF, Adeyemi WJ, Olayaki LA. Omega-3 fatty acid ameliorates bisphenol F-induced testicular toxicity by modulating Nrf2/NFkB pathway and apoptotic signaling. *Front Endocrinol.* (2023) 14:1256154. doi: 10.3389/fendo.2023.1256154

23. Elsafty M, Abdeen A, Aboubakr M. Allicin and Omega-3 fatty acids attenuates acetaminophen mediated renal toxicity and modulates oxidative stress, and cell apoptosis in rats. *Naunyn-Schmiedeberg's Arch Pharmacol.* (2024) 397:317–28. doi: 10.1007/s00210-023-02609-z

24. Okesina KB, Odetayo AF, Adeyemi WJ, Ajibare AJ, Okesina AA, Olayaki LA. Naringin from sweet orange peel improves testicular function in high fat diet-induced diabetic rats by modulating xanthine oxidase/uric acid signaling and maintaining redox balance. *Lab Anim Res.* (2024) 40:5. doi: 10.1186/s42826-024-00188-5

25. Akhigbe RE, Hamed MA, Odetayo AF. HAART and anti-Koch's impair sexual competence, sperm quality and offspring quality when used singly and in combination in male Wistar rats. *Andrologia.* (2021) 53:e13951. doi: 10.1111/and.13951

26. Fatai OA, Aribidesi OL. Effect of bisphenol F on sexual performance and quality of offspring in Male Wistar rats. *Ecotoxicol Environ Saf.* (2022) 244:114079. doi: 10.1016/j.ecoenv.2022.114079

27. Bloom E. The ultrastructure of some characteristic sperm defects. *Nord Vet Med.* (1973) 12:125–39.

28. Parkinson T. Fertility and infertility in male animals. In: Noakes DE, Parkinson TJ, England GCW. editors *Arthur's Veterinary Reproduction andObstetrics,* 8th ed. Saunders Publishers (2001). p. 695–750. doi: 10.1016/B978-070202556-3.50034-7

29. Talalay P. Enzymatic analysis of steroid hormone methods. *Biochem Anal.* (1960) 8:119. doi: 10.1002/9780470110249.ch3

30. Odetayo AF, Adeyemi WJ, Olayaki LA. In vivo exposure to bisphenol F induces oxidative testicular toxicity: role of Erβ and p53/Bcl-2 signaling pathway. *Front Reprod Health.* (2023) 5:1204728. doi: 10.3389/frph.2023.1204728

31. Jarabak J, Adams JA, Williams-Ashman HG, Talalay PJ. Purification of a 17betahydroxysteroid dehydrogenase of human placenta and studies on its transhydrogenase function. *Biol Chem.* (1962) 237:345–335. doi: 10.1016/S0021-9258(18)93926-8

32. Oluwasola A, Ayoola OE, Odetayo AF, Saa'du G, Olayaki LA. Ameliorative effect of melatonin on reproductive hormones in ethanol extracts of cannabis sativa-treated female wistar Rats. *Soc Exp Biol Nigeria.* (2023) 22:53–8.

33. Ulusoy E, Cayan S, Yilmaz N, Aktaş S, Acar D, Doruk E. Interferon alpha-2b may impair testicular histology including spermatogenesis in a rat model. *Arch Androl.* (2004) 50:379–85. doi: 10.1080/01485010490474823

34. Johnsen SG. Testicular biopsy score count–a method for registration of spermatogenesis in human testes: normal values and results in 335 hypogonadal males. *Hormones.* (1970) 1:2–25. doi: 10.1159/000178170

35. Ajibare AJ, Odetayo AF, Akintoye OO, Olayaki LA. Zinc ameliorates acrylamide-induced oxidative stress and apoptosis in testicular cells via Nrf2/HO-1/NfkB and Bax/Bcl2 signaling pathway. *Redox Rep.* (2024) 29:2341537. doi: 10.1080/13510002.2024.2341537

36. Afolabi OA, Anyogu DC, Hamed MA, Odetayo AF, Adeyemi DH, Akhigbe RE. Glutamine prevents upregulation of NF-kB signaling and caspase 3 activation in ischaemia/reperfusion-induced testicular damage: an animal model. *Biomed Pharmacother.* (2022) 150:113056. doi: 10.1016/j.biopha.2022.113056

37. Hamed MA, Akhigbe RE, Aremu AO, Odetayo AF. Zinc normalizes hepatic lipid handling via modulation of ADA/XO/UA pathway and caspase 3 signaling in highly active antiretroviral therapy-treated Wistar rats. *Chem Biol Interact.* (2022) 368:110233. doi: 10.1016/j.cbi.2022.110233

38. Olayaki LA, Okesina KB, Jesubowale JD, Ajibare AJ, Odetayo AF. Orange peel extract and physical exercise synergistically ameliorate type 2 diabetes mellitus-induced dysmetabolism by upregulating GLUT4 concentration in male wistar rats. *J Med Food.* (2023) 26:470–9. doi: 10.1089/jmf.2023.0061

39. Desser RK, Himmelhoch SR, Evans WH, Januska M, Mage M, Shelton E. Guinea pig heterophil and eosinophil peroxidase. *Arch Biochem Biophys.* (1972) 148:452–65. doi: 10.1016/0003-9861(72)90164-6

40. Ridnour LA, Sim JE, Hayward MA, Wink DA, Martin SM, Buettner GR, et al. A spectrophotometric method for the direct detection and quantitation of nitric oxide, nitrite, and nitrate in cell culture media. *Anal Biochem.* (2000) 281:223–9. doi: 10.1006/abio.2000.4583

41. Zahide ED, Bahad OA. Modified xanthine oxidase activity method based on uric acid absorption. *ChemXpress.* (2014) 6:09–13.

42. Perandones CE, Illera VA, Peckham D, Stunz LL, Ashman RF. Regulation of apoptosis in vitro in mature murine spleen T cells. *J Immunol.* (1993) 151:3521–9. doi: 10.4049/jimmunol.151.7.3521

43. Liguori G, Tafuri S, Pelagalli A, Ali S, Russo M, Mirabella N, et al. G protein-coupled estrogen receptor (GPER) and ERs are modulated in the testis-epididymal complex in the normal and cryptorchid dog. *Veter Sci.* (2024) 11:21. doi: 10.3390/vetsci11010021

44. Pelletier G, El-Alfy M. Immunocytochemical localization of estrogen receptors alpha and beta in the human reproductive organs. *J Clin Endocrinol Metab.* (2000) 85:4835–40. doi: 10.1210/jcem.85.12.7029

45. Dewaele A, Dujardin E, André M, Albina A, Jammes H, Giton F, et al. Absence of testicular estrogen leads to defects in spermatogenesis and increased semen abnormalities in male rabbits. *Genes.* (2022) 13:2070. doi: 10.3390/genes13112070

46. Solakidi S, Psarra AG, Nikolaropoulos S, Sekeris CE. Estrogen receptors α and β (ERα and ERβ) and androgen receptor (AR) in human sperm: localization of ERβ and AR in mitochondria of the midpiece. *Hum Reprod.* (2005) 20:3481–7. doi: 10.1093/humrep/dei267

47. Korach KS. Estrogen receptor knock-out mice: molecular and endocrine phenotypes. *J Soc Gynecol. Investig.* (2000) 7:S16–S17. doi: 10.1177/1071557600007001S06

48. Cavallini G. Male idiopathic oligoasthenoteratozoospermia. *Asian J Androl.* (2006) 8:143–57. doi: 10.1111/j.1745-7262.2006.00123.x

49. Vandekerckhove P, Lilford R, Vail A, Hughes E. Clomiphene or tamoxifen for idiopathic oligo/asthenospermia. *Cochr Datab System Rev.* (2000) 1996:CD000151. doi: 10.1002/14651858.CD000151

50. Rolf C, Behre HM, Nieschlag E. Tamoxifen bei männlicher Infertilität. Analyse einer fragwürdigen Therapie [Tamoxifen in male infertility Analysis of a questionable therapy]. *Deutsche medizinische Wochenschrift.* (1996) 121:33–9. doi: 10.1055/s-2008-1042969

51. Odetayo AF, Akhigbe RE, Bassey GE, Hamed MA, Olayaki LA. Impact of stress on male fertility: role of gonadotropin inhibitory hormone. *Front Endocrinol.* (2024) 14:1329564. doi: 10.3389/fendo.2023.1329564

52. Oliveira PF, Sousa M, Silva BM, Monteiro MP, Alves MG. Obesity, energy balance and spermatogenesis. *Reproduction.* (2017) 153:R173–85. doi: 10.1530/REP-17-0018

53. Allen MO, Salman TM, Alada A, Odetayo AF, Patrick EB, Salami SA. Effect of the beta-adrenergic blockade on intestinal lactate production and glycogen concentration in dogs infused with hexoses. *J Complem Integr Med.* (2021) 19:287–96. doi: 10.1515/jcim-2021-0062

54. Marek CB, Peralta RM, Itinose AM, Bracht A. Influence of tamoxifen on gluconeogenesis and glycolysis in the perfused rat liver. *Chem Biol Interact.* (2011) 193:22–33. doi: 10.1016/j.cbi.2011.04.010

55. Hussain T, Kandeel M, Metwally E, Murtaza G, Kalhoro DH, Yin Y, et al. Unraveling the harmful effect of oxidative stress on male fertility: a mechanistic insight. *Front Endocrinol.* (2023) 14:1070692. doi: 10.3389/fendo.2023.1070692

56. Odetayo AF, Abdulrahim HA, Fabiyi OT, Adewole TA, Ajiboye BE, Omeiza AN, et al. Synergistic effects of vitamin D and exercise on diabetes-induced gonadotoxicity in male wistar rats: role of xanthine oxidase/uric acid and Nrf2/NfkB signaling. *Cell Biochem Biophy.* (2024) 2024:1–13. doi: 10.1007/s12013-024-01313-w

57. Scarian E, Viola C, Dragoni F, Di Gerlando R, Rizzo B, Diamanti L, et al. New insights into oxidative stress and inflammatory response in neurodegenerative diseases. *Int J Mol Sci.* (2024) 25:2698. doi: 10.3390/ijms25052698

58. Hussain T, Tan B, Yin Y, Blachier F, Tossou MC, Rahu N. Oxidative stress and inflammation: what polyphenols can do for us? *Oxid Med Cell Longev.* (2016) 2016:7432797. doi: 10.1155/2016/7432797

59. Chen C, Lü JM, Yao Q. Hyperuricemia-related diseases and xanthine oxidoreductase (XOR) inhibitors: an overview. *Med Sci Monitor.* (2016) 22:2501–12. doi: 10.12659/MSM.899852

60. Liu N, Xu H, Sun Q, Yu X, Chen W, Wei H, et al. The role of oxidative stress in hyperuricemia and xanthine oxidoreductase (XOR) inhibitors. *Oxid Med Cell Longev.* (2021) 2021:1470380. doi: 10.1155/2021/1470380

61. Guo Q, Jin Y, Chen X, Ye X, Shen X, Lin M, et al. NF-κB in biology and targeted therapy: new insights and translational implications. *Signal Transd Targ Ther.* (2024) 9:53. doi: 10.1038/s41392-024-01757-9

62. Ahmed NS, Samec M, Liskova A, Kubatka P, Saso L. Tamoxifen and oxidative stress: an overlooked connection. *Disc Oncol.* (2021) 12:17. doi: 10.1007/s12672-021-00411-y

63. Schieber M, Chandel NS, ROS. function in redox signaling and oxidative stress. *Current Biol.* (2014) 24:R453–62. doi: 10.1016/j.cub.2014.03.034

64. Kumar S, Saxena J, Srivastava VK, Kaushik S, Singh H, Abo-El-Sooud K, et al. The interplay of oxidative stress and ROS scavenging: antioxidants as a therapeutic potential in sepsis. *Vaccines.* (2022) 10:1575. doi: 10.3390/vaccines10101575

65. Jiang X, Wang X. Cytochrome C-mediated apoptosis. *Annu Rev Biochem.* (2004) 73:87–106. doi: 10.1146/annurev.biochem.73.011303.073706

66. Chen Q, Gong B, Almasan A. Distinct stages of cytochrome c release from mitochondria: evidence for a feedback amplification loop linking caspase activation to mitochondrial dysfunction in genotoxic stress induced apoptosis. *Cell Death Differ.* (2000) 7:227–33. doi: 10.1038/sj.cdd.4400629

67. Yang J, Liu X, Bhalla K, Kim C, Ibrado A-M, Cai J, et al. Prevention of apoptosis by Bcl-2: release of cytochrome c from mitochondria blocked. *Science.* (1997) 275:1129–32. doi: 10.1126/science.275.5303.1129

68. Yuan J, Murrell GA, Trickett A, Wang MX. Involvement of cytochrome c release and caspase-3 activation in the oxidative stress-induced apoptosis in human tendon fibroblasts. *Biochim Biophys Acta.* (2003) 1641:35–41. doi: 10.1016/S0167-4889(03)00047-8

69. Unten Y, Murai M, Koshitaka T, Kitao K, Shirai O, Masuya T, et al. Comprehensive understanding of multiple actions of anticancer drug tamoxifen in isolated mitochondria. *Biochim Biophys Acta Bioener.* (2022) 1863:148520. doi: 10.1016/j.bbabio.2021.148520

70. Nazarewicz RR, Zenebe WJ, Parihar A, Larson SK, Alidema E, Choi J, et al. Tamoxifen induces oxidative stress and mitochondrial apoptosis via stimulating mitochondrial nitric oxide synthase. *Cancer Res.* (2007) 67:1282–90. doi: 10.1158/0008-5472.CAN-06-3099

71. Meital LT, Windsor MT, Perissiou M, Schulze K, Magee R, Kuballa A, et al. Omega-3 fatty acids decrease oxidative stress and inflammation in macrophages from patients with small abdominal aortic aneurysm. *Sci Rep.* (2019) 9:12978. doi: 10.1038/s41598-019-49362-z

72. Sinha RA, Khare P, Rai A, Maurya SK, Pathak A, Mohan V, et al. Anti-apoptotic role of omega-3-fatty acids in developing brain: perinatal hypothyroid rat cerebellum as apoptotic model. *Int J Dev Neurosci.* (2009) 27:377–83. doi: 10.1016/j.ijdevneu.2009.02.003

frontiers | Frontiers in Nutrition

TYPE Original Research
PUBLISHED 23 October 2024
DOI 10.3389/fnut.2024.1454880

OPEN ACCESS

EDITED BY
Jagannath Misra,
Indiana University, Purdue University Indianapolis, United States

REVIEWED BY
Mithun Rudrapal,
Vignan's Foundation for Science, Technology and Research, India
Marcus Scotti,
Federal University of Paraíba, Brazil

*CORRESPONDENCE
Wenke Cheng
✉ cwk2517@163.com

RECEIVED 25 June 2024
ACCEPTED 09 October 2024
PUBLISHED 23 October 2024

CITATION
Yu W, Wang X, Du Z and Cheng W (2024) Association of triglyceride-glucose index and its combination with obesity indicators in predicting the risk of aortic aneurysm and dissection.
Front. Nutr. 11:1454880.
doi: 10.3389/fnut.2024.1454880

Association of triglyceride-glucose index and its combination with obesity indicators in predicting the risk of aortic aneurysm and dissection

Wangqin Yu[1], Xiaoling Wang[2], Zhongyan Du[3] and Wenke Cheng[4,5]*

[1]School of Basic Medical Sciences, Zhejiang Chinese Medical University, Hangzhou, China, [2]Department of Pharmacy, Lintong Rehabilitation and Recuperation Centre, Xi'an, China, [3]Zhejiang Key Laboratory of Blood-Stasis-Toxin Syndrome, Zhejiang Engineering Research Center for "Preventive Treatment" Smart Health of Traditional Chinese Medicine, School of Basic Medical Sciences, Zhejiang Chinese Medical University, Hangzhou, China, [4]Zhejiang Key Laboratory of Blood-Stasis-Toxin Syndrome, Zhejiang Chinese Medical University, Hangzhou, China, [5]Medical Faculty, University of Leipzig, Leipzig, Germany

Background: The association between the triglyceride-glucose (TyG) index and its combination with obesity indictors in aortic aneurysm and dissection (AAD) remains unclear. We aimed to investigate the association between TyG and TyG-body mass index (TyG-BMI), TyG-waist circumference (TyG-WC), TyG-waist height ratio (TyG-WHtR) and AAD risk.

Methods: This study included 387,483 baseline participants from the UK Biobank with complete data on TyG, TyG-BMI, TyG-WC and TyG-WHtR. Cox proportional hazard models evaluated the relationship between these four indicators and the risk of AAD occurrence. Restricted cubic spline (RCS) examined the non-linear relationship between these indicators and AAD risk, while receiver operating characteristic (ROC) curves assessed the predictive value of these four indicators for AAD risk.

Results: Over a median follow-up of 13.7 years, 3,041 AAD events were recorded. Multivariate Cox regression analysis indicated that for each standard deviation increase, the risk of AAD occurrence increased by 33% (HR: 1.33, 95%CI: 1.29–1.38), 25% (HR: 1.25, 95%CI: 1.21–1.29), 61% (HR: 1.61, 95%CI: 1.56–1.66) and 44% (HR: 1.44, 95%CI: 1.39–1.49) for TyG, TyG-BMI, TyG-WC and TyG-WHtR, respectively. RCS demonstrated a linear relationship between these indicators and AAD risk, with TyG-WC demonstrating the best performance in predicting AAD occurrence based on ROC curves.

Conclusion: The present study, based on a large prospective cohort design, showed that higher TyG index and its combination with obesity indices were significantly associated with the risk of AAD. Moreover, AFT models further showed that elevation of these indicators significantly advanced the onset of AAD. In addition, RCS analyses demonstrated a linear association between these indicators and the risk of AAD, and the TyG-WC showed higher predictive ability for AAD. These findings emphasize the potential application of the TyG index and its combination with obesity indicators in the early identification of AAD.

KEYWORDS

TyG, TyG-BMI, TyG-WC, TyG-WHtR, aortic aneurysm and dissection, UK biobank

Introduction

Aortic aneurysm and dissection (AAD) poses a significant risk to cardiovascular health, with an extremely high mortality rate (1). Epidemiological data indicates an annual incidence of AAD ranging from 2 to 16 cases per 100,000 individuals, with a significant male predominance (2, 3). Statistics reveal that AAD claims over 150,000 lives annually (4). Currently, surgical intervention stands as the primary treatment, yet despite advancements, postoperative mortality rates persist above 10% (5). While medications like β-adrenergic receptor antagonists and angiotensin II receptor antagonists offer some control over aneurysm progression, the lack of precise biomarkers and effective therapeutic targets hampers prevention and treatment efforts (6, 7).

Previous research identifies smoking, hypertension, age and atherosclerosis as key AAD risk factors (8). Smoking is a well-established contributor, as it leads to chronic inflammation and weakening of the aortic wall, significantly increasing the risk of aneurysm formation (9). Hypertension, or high blood pressure, places additional stress on the aortic wall, which not only promotes the growth of aneurysms but also increases the risk of aortic dissection, where a tear in the inner layer of the aorta can occur (10). Age is another crucial factor, with the risk of both conditions increasing as the aorta becomes more fragile over time (11). Atherosclerosis, characterized by the accumulation of plaque in the arteries, can cause the stiffening and narrowing of the aorta, which further elevates the risk of aneurysm rupture and dissection by weakening the structural integrity of the arterial wall (12). Additionally, increasing evidence implicates diabetes and obesity in AAD development (13, 14). Insulin resistance (IR), a hallmark of diabetes and obesity, emerges as a pivotal contributor to various cardiovascular diseases (CVDs) (15). Furthermore, studies link higher IR markers with larger aneurysm diameters (16). IR disrupts metabolic processes and fuels inflammation, underscoring its potential significance in AAD onset and progression (17).

While the hyperinsulinemic-euglycemic clamp serves as the gold standard for IR measurement, its complexity including the need for specialized equipment, prolonged testing time, and skilled personnel limits its feasibility for routine clinical application (18). The triglyceride-glucose (TyG) emerges as a simpler, efficient alternative for early IR identification (19). Ahn et al. showed the potential efficacy of TyG in discerning prediabetes from diabetes in the general population (20). Moreover, it serves as a reliable indicator for various metabolic diseases, including stroke, CVD and metabolic syndrome (21–23). Furthermore, combining the TyG index with obesity indicators enhances diagnostic accuracy compared to TyG alone (24, 25).

To date, no study has explored the relationship between the TyG index, its combination with obesity indicators, and the risk of AAD. In summary, IR has been shown to increase the risk of AAD, and both the TyG index and obesity-related parameters hold promise as potential surrogates for IR. Therefore, we hypothesize that higher levels of the TyG index and its combinations with obesity parameters (TyG-BMI, TyG-WC, TyG-WHtR) are associated with an increased risk of AAD occurrence. In the present study, our aim was to investigate the associations between the TyG index, its combinations with obesity metrics, and the risk of AAD, as well as to compare the ability of these IR surrogates in predicting AAD occurrence.

Methods

The UKB constitutes a large-scale, prospective, community-based cohort study aimed at advancing biomedical research and informing public health policies. Between 2006 and 2010, the project recruited over 500,000 participants from 22 centers across the United Kingdom. All participants were registered with the National Health Service (NHS), the publicly funded healthcare system in the United Kingdom, ensuring they had comprehensive health records available for long-term follow-up and research purposes. At baseline, participants completed detailed touchscreen questionnaires covering demographics, health and lifestyle factors, alongside undergoing physical examinations, functional assessments and providing blood, urine and saliva samples. Comprehensive study protocols and descriptions have been previously reported (26), and all data collection and research in the UKB adhere to strict ethical and privacy standards, with participants providing written informed consent before enrolment. The study received approval from the North West Multi-Center Research Ethics Committee and aligns with the Declaration of Helsinki principles.

Ascertainment of exposures

Upon enrolment in the UKB, blood samples were randomly collected from participants with fasting times recorded prior to blood sampling. Given the logistic challenges of collecting fasting blood samples from a large, geographically dispersed population (27), biochemical measurements were conducted within 24 h on non-fasting serum samples, including triglycerides (TG), glucose, total cholesterol (TC), high (HDL)- and low-density lipoprotein cholesterol (LDL). The coefficients of variation for TG and glucose concentrations were both less than 3%. Physical measurements such as height, weight and WC were also ontained during baseline examinations. WHtR was computed as the ratio of WC to height (28). Four indices were calculated using the following formulas: TyG = ln [triglycerides (mg/dL) × glucose (mg/dL) / 2]; TyG-BMI = TyG * BMI; TyG-WC = TyG * WC; TyG-WHtR = TyG * WHtR (29, 30).

Assessment of outcome

The diagnosis of AAD relied on the International Classification of Diseases, Tenth Revision (ICD-10) codes I71.0-I71.9, with data sourced from hospital admissions and death registries within the UKB. Participants were followed from the date of their recruitment into the study until the first of the following events occurred: a confirmed AAD event, death, or the study cutoff date of 26 October 2022. The follow-up period ended at whichever of these events happened first for each individual.

Assessment of covariates

Baseline sociodemographic data encompassed sex, age, ethnicity, physical activity, smoking and drinking status, dietary habits, Townsend Deprivation Index (TDI), family history of CVD, medication usage and baseline history of chronic diseases, primarily cancer, heart diseases,

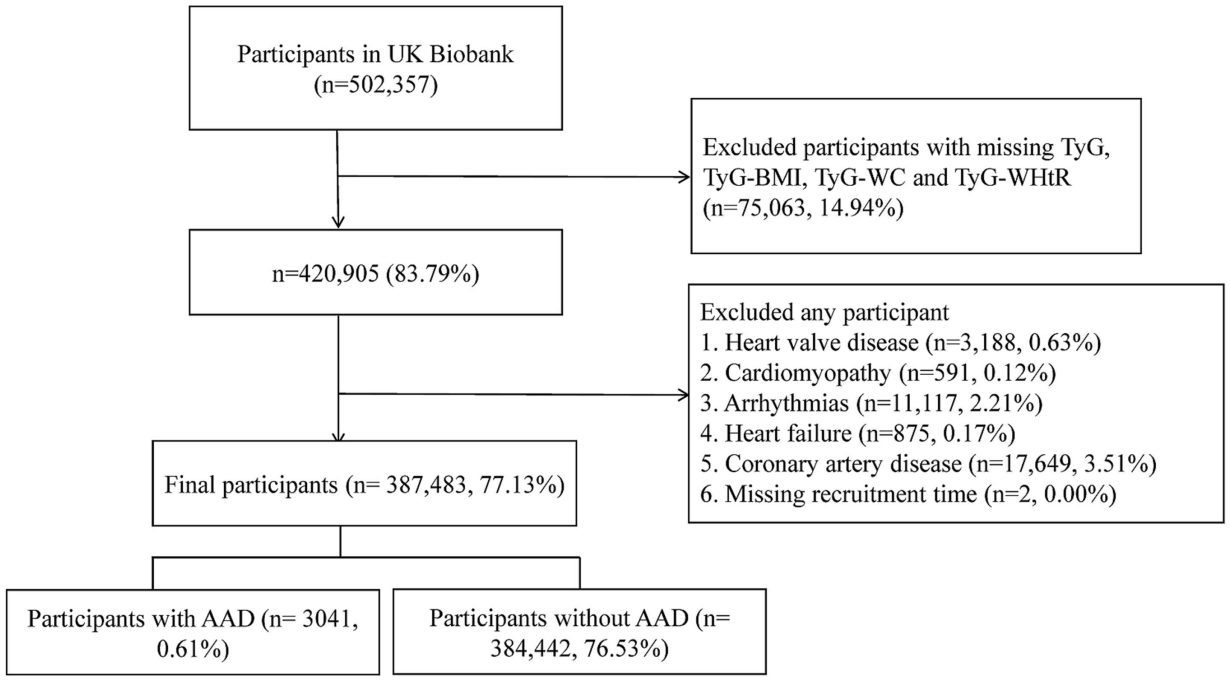

FIGURE 1
Flowchart of participant selection.

hypertension and diabetes. Physical activity levels were quantified using weekly metabolic equivalent (MET) minutes (31). TDI reflected participants' socioeconomic status at baseline (32). Dietary scores were derived from participants' reports of consumption of nine food items, with detailed scoring information reported elsewhere (32, 33). Family history of CVD herein referred to parental heart disease history collected through self-reports at baseline. Medication history primarily encompassed antihypertensive drugs, lipid-lowering drugs and insulin.

Selection criteria

We initially included 502,357 participants from UK Biobank. We then excluded the participants with any missing TyG, TyG-BMI, TyG-WC and TyG-WHtR data (n = 75,063). Subsequently, we excluded two participants with missing recruitment time records. Additionally, to mitigate confounding effects, participants with baseline CVDs including heart valve disease, cardiomyopathy, arrhythmias, heart failure or coronary artery disease (n = 33,420) were further excluded (Supplementary Table S1). Consequently, a total of 387,483 participants were retained for subsequent analysis (Figure 1).

Statistical analysis

Missing covariate values were imputed using multiple imputations via random forests, with one set of imputed data selected for analysis. Kolmogorov–Smirnov test was used to assess the distribution type of continuous variables. All continuous variables exhibited a skewed distribution. Baseline characteristics were stratified according to AAD and non-AAD groups, with continuous variables expressed as medians (interquartile ranges) and categorical variables presented as numbers and proportions (N, %). Comparisons between the two groups for continuous and categorical variables were conducted using the Mann–Whitney U test and Chi-square test, respectively Incidence of AAD across quartiles of TyG, TyG-BMI, TyG-WC and TyG-WHtR during the follow-up period was assessed using Kaplan–Meier (KM) curves, with significance evaluated by log-rank test. Cox proportional hazard models were employed to assess the association between TyG and its combination with obesity metrics and AAD risk across three Cox multivariable regression models. Model 1 lacked adjustments for any variables, while Model 2 adjusted for age, sex and race. Model 3 further adjusted for physical activity, smoking and drinking habits, diet score, TDI, fasting time, family history of CVD, usage of antihypertensive drugs, lipid-lowering drugs or insulin and baseline chronic diseases including cancer, hypertension and diabetes. The selection of confounders was determined using a directed acyclic graph (DAG)[1] (34), with the results depicted in Supplementary Figure S1. Each model categorized TyG, TyG-BMI, TyG-WC and TyG-WHtR into quartiles, with the first quartile (Q1) serving as a reference to evaluate AAD risk trends and calculate p-values. Subsequently, these four metrics were standardized using Z-scores to assess AAD risk changes per one standard deviation (SD) increase.

Restricted cubic spline (RCS) analysis with three knots (10, 50, 90th) were employed to evaluate the non-linear association between these four indicators and AAD risk, adjusting for Model 3 covariates, with nonlinearity assessed using the log-likelihood ratio test. Subsequently, the accelerated failure time (AFT) model investigated the impact of TyG, TyG-BMI, TyG-WC and TyG-WHtR levels on AAD event timings (35). Using the lowest quartile group (Q1) as the reference, we assessed the effect of increases in these indices on the timing of AAD onset. Receiver operating characteristic (ROC) curves and area under the curve (AUC) analyses evaluated the diagnostic and

1 http://www.dagitty.net

predictive capabilities of the four indicators in predicting the risk of AAD. To assess the stability of the model, we randomly split the dataset into 70% training and 30% testing sets. We then plotted ROC curves for both sets to evaluate the model's generalization ability on unseen data.

Additionally, subgroup analyses were conducted based on sex, age, BMI, smoking and alcohol consumption, fasting time, diet score, diabetes, hypertension, cancer, medication use and family history of CVD, with *p*-values for between-group interactions calculated via likelihood ratio tests. Finally, several sensitivity analyses were conducted to assess the robustness of our findings. (1) Participants who developed AAD within 2 years of the follow-up period were excluded to mitigate potential reverse causal effects. (2) Participants with any missing covariate values at baseline were excluded, and the main analysis was repeated. (3) To address the significant differences in sample sizes between the AAD and non-AAD groups, as well as differences in baseline characteristics, and avoid potential selection bias, propensity score matching (PSM) was employed in a 1:1 manner based on all Model 3 covariates. After calculating propensity scores, matching was performed using the nearest-neighbor matching algorithm with a caliper of 0.2 pooled SD (36). All analyses were performed using R (version 4.2.1), with statistical significance set at a two-sided *p*-value less than 0.05.

Results

Basic characteristics of participants

A total of 387,483 AAD-free participants, with a median age of 57 years and 44.6% males, were included. Table 1 illustrates baseline

TABLE 1 Baseline demographic and clinical characteristics.

Characteristic	Total	Non-AAD	AAD	*p*-value
	(*n* = 387,483)	(*n* = 384,442)	(n = 3,041)	
Age, years	57.0 (50.0–63.0)	57.0 (50.0–63.0)	63.0 (58.0–66.0)	<0.001
Male	172,711 (44.6%)	170,383 (44.3%)	2,328 (76.6%)	<0.001
White	366,889 (94.7%)	363,922 (94.7%)	2,967 (97.6%)	<0.001
Weight	76.0 (66.2–87.1)	76.0 (66.1–87.0)	83.0 (73.4–93.6)	<0.001
Height	168.0 (161.5–175.0)	168.0 (161.0–175.0)	173.0 (167.0–179.0)	<0.001
BMI	26.6 (24.1–29.7)	26.6 (24.1–29.7)	27.6 (25.1–30.6)	<0.001
WC	89.0 (80.0–98.0)	89.0 (80.0–98.0)	96.0 (88.5–104.0)	<0.001
MET	1800.0 (825.0–3573.0)	1800.0 (825.0–3572.0)	1815.0 (742.5–3767.5)	0.905
TDI	−2.2 (−3.7–0.4)	−2.2 (−3.7–0.4)	−2.1 (−3.6–0.6)	0.122
Fasting time	3.0 (2.0–4.0)	3.0 (2.0–4.0)	3.0 (3.0–4.0)	<0.001
Diet score	5.0 (4.0–6.0)	5.0 (4.0–6.0)	5.0 (4.0–6.0)	<0.001
DM	16,718 (4.3%)	16,547 (4.3%)	171 (5.6%)	<0.001
Hypertension	97,138 (25.1%)	95,802 (24.9%)	1,336 (43.9%)	<0.001
Cancer	34,108 (8.8%)	33,794 (8.8%)	314 (10.3%)	0.003
History of heart diseases family	149,648 (38.6%)	148,470 (38.6%)	1,178 (38.7%)	0.894
Lipid-lowering drugs	51,879 (13.4%)	51,056 (13.3%)	823 (27.1%)	<0.001
Antihypertensives	68,231 (17.6%)	67,187 (17.5%)	1,044 (34.3%)	<0.001
Insulin	3,363 (0.9%)	3,342 (0.9%)	21 (0.7%)	<0.001
Drinking status				<0.001
Never	16,552 (4.3%)	16,471 (4.3%)	81 (2.7%)	
Previous	12,995 (3.4%)	12,854 (3.3%)	141 (4.6%)	
Current	357,936 (92.4%)	355,117 (92.4%)	2,819 (92.7%)	
Smoking status				<0.001
Never	158,096 (40.8%)	157,362 (40.9%)	734 (24.1%)	
Previous	188,904 (48.8%)	187,306 (48.7%)	1,598 (52.5%)	
Current	40,483 (10.4%)	39,774 (10.3%)	709 (23.3%)	
TyG	8.7 (8.3–9.1)	8.7 (8.3–9.1)	8.8 (8.5–9.2)	<0.001
TyG-BMI	232.1 (203.7–265.7)	232.0 (203.6–265.6)	245.5 (217.3–277.8)	<0.001
TyG-WC	776.2 (676.1–878.6)	775.5 (675.5–877.9)	855.0 (763.0–948.5)	<0.001
TyG-WHtR	4.6 (4.1–5.2)	4.6 (4.1–5.2)	4.9 (4.4–5.5)	<0.001

AAD, aortic aneurysm and dissection; BMI, body mass index; WC, waist circumference; MET, metabolic equivalent task; TDI, Townsend deprivation index; DM, diabetes mellitus.

characteristics, categorized by AAD status. Compared to the non-AAD group, the AAD group exhibited higher age, BMI, WC, weight and height, alongside a higher proportion of male and white participants, and a higher prevalence of chronic diseases (all $p < 0.001$). Additionally, levels of TyG, TyG-BMI, TyG-WC and TyG-WHtR were significantly elevated in the AAD group compared to the non-AAD group (all $p < 0.001$).

The associations between TyG, TyG-BMI, TyG-WC, TyG-WHtR and the risk of AAD

During a median follow-up of 13.7 years, 3,041 AAD cases were identified. KM curves illustrated an escalating risk of AAD with increasing quartiles of TyG, TyG-BMI, TyG-WC and TyG-WHtR (all *p*-values <0.001; Figure 2). Consistent findings emerged from Cox models. In Model 1, lacking adjustments, there was an upward trend in the relative risk of AAD occurrence with increasing quartiles of TyG, TyG-BMI, TyG-WC and TyG-WHtR (all P for trend <0.001; Table 2). For each SD increase, the risk of AAD occurrence increased by 33% (HR: 1.33, 95%CI: 1.29–1.38), 25% (HR: 1.25, 95%CI: 1.21–1.29), 61% (HR: 1.61, 95%CI: 1.56–1.66) and 44% (HR: 1.44, 95%CI: 1.39–1.49) for TyG, TyG-BMI, TyG-WC and TyG-WHtR, respectively. These associations persisted in Model 2 after adjusting for age, sex and race. Furthermore, in Model 3, adjusting for additional covariates, the increased quartiles of these four indicators enhanced the risk of AAD occurrence compared to the Q1 group, especially in the Q4 group. Meanwhile, each SD increase in these four indicators increased the risk of AAD occurrence by 10% (HR: 1.10, 95%CI: 1.05–1.14), 13% (HR: 1.13, 95%CI: 1.09–1.18), 21% (HR: 1.21, 95%CI: 1.16–1.26) and 15% (HR: 1.15, 95%CI: 1.10–1.19), respectively (Table 2).

Subsequent RCS exhibited a linear dose-dependent relationship between all four indicators and AAD risk (all P for nonlinear >0.05; Figure 3).

Impact of TyG, TyG-BMI, TyG-WC and TyG-WHtR on time to AAD onset

AFT analysis revealed a decreasing time to AAD onset with increasing quartiles of TyG, TyG-BMI, TyG-WC and TyG-WHtR (all P for trend <0.05; Figure 4). Specifically, compared to the Q1 group, the median time to AAD onset in the Q2 to Q4 groups of the TyG index was advanced by 25.2 months, 54.6 months and 69.5 months, respectively. Similar trends were observed for TyG-BMI, TyG-WC and TyG-WHtR, particularly for TyG-WC, with the median time to AAD onset in the Q2 to Q4 groups advanced by 31.9 months, 58.2 months

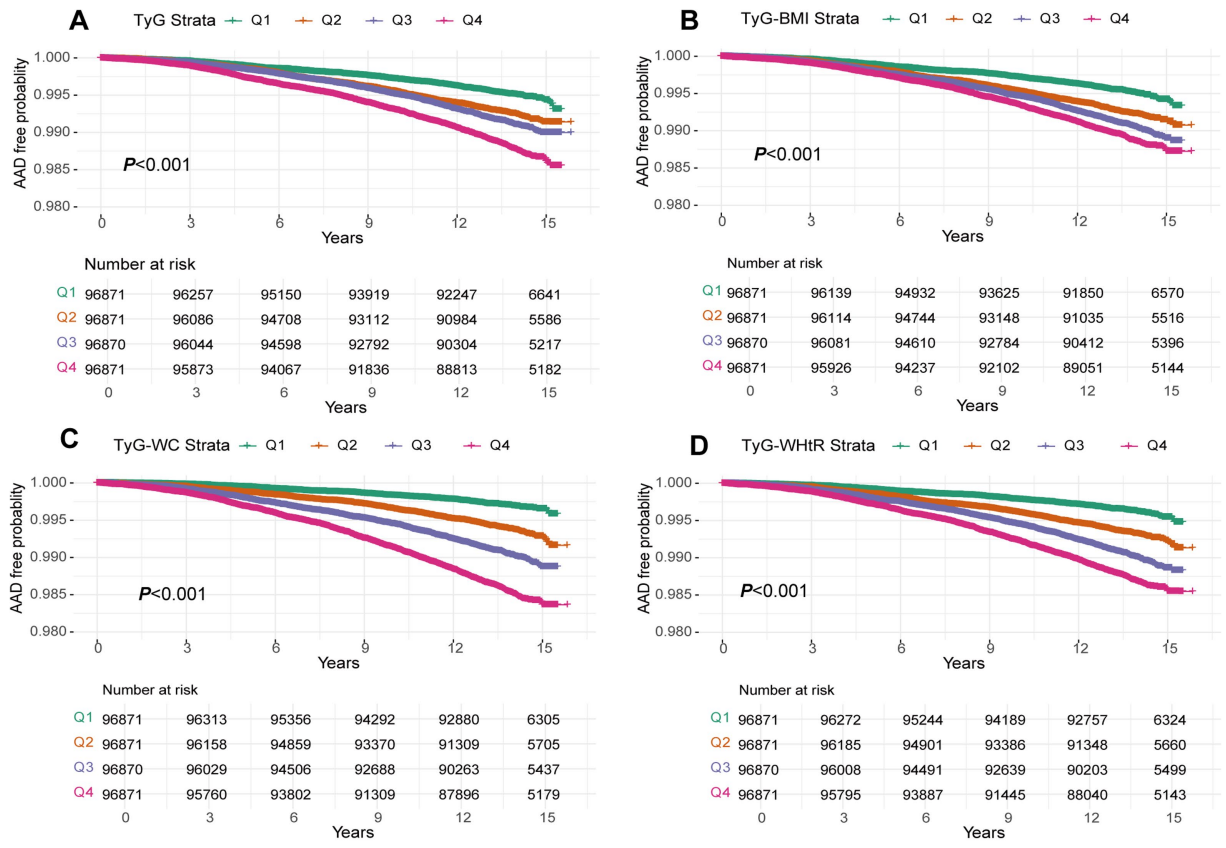

FIGURE 2
A Kaplan–Meier curves for AAD events in the TyG index **(A)**, TyG-BMI **(B)**, TyG-WC **(C)** and TyG-WHtR **(D)** quintile group. TyG index, triglyceride glucose index; TyG-BMI, triglyceride glucose index–body mass index; TyG-WC, triglyceride glucose index-waist circumference; TyG-WHtR, triglyceride glucose index-waist height ratio.

TABLE 2 The association between TyG, TyG-BMI, TyG-WC, TyG-WHtR and the risk of AAD.

Type	Model 1		Model 2		Model 3	
	HR (95%CI)	*p*	HR (95%CI)	*p*	HR (95%CI)	*p*
TyG						
Q1	Reference		Reference		Reference	
Q2	1.51 (1.34–1.7)	< 0.001	1.14 (1.01–1.28)	0.033	1.1 (0.98–1.24)	0.111
Q3	1.77 (1.57–1.98)	< 0.001	1.15 (1.03–1.29)	0.017	1.08 (0.96–1.21)	0.198
Q4	2.39 (2.14–2.67)	< 0.001	1.43 (1.28–1.6)	< 0.001	1.29 (1.15–1.44)	< 0.001
P for trend	< 0.001		< 0.001		< 0.001	
Per SD increase	1.33 (1.29–1.38)	< 0.001	1.14 (1.1–1.18)	< 0.001	1.1 (1.05–1.14)	< 0.001
TyG-BMI						
Q1	Reference		Reference		Reference	
Q2	1.56 (1.39–1.76)	< 0.001	1.08 (0.96–1.22)	0.183	1.07 (0.95–1.2)	0.291
Q3	1.93 (1.72–2.16)	< 0.001	1.19 (1.06–1.33)	0.003	1.11 (0.99–1.25)	0.073
Q4	2.28 (2.04–2.54)	< 0.001	1.54 (1.37–1.72)	< 0.001	1.36 (1.21–1.53)	< 0.001
P for trend	< 0.001		< 0.001		< 0.001	
Per SD increase	1.25 (1.21–1.29)	< 0.001	1.18 (1.14–1.23)	< 0.001	1.13 (1.09–1.18)	< 0.001
TyG-WC						
Q1	Reference		Reference		Reference	
Q2	2.06 (1.79–2.38)	< 0.001	1.19 (1.03–1.38)	0.02	1.13 (0.98–1.31)	0.1
Q3	3.19 (2.79–3.65)	< 0.001	1.38 (1.2–1.59)	< 0.001	1.25 (1.09–1.45)	0.002
Q4	4.86 (4.27–5.53)	< 0.001	1.86 (1.62–2.14)	< 0.001	1.58 (1.37–1.82)	< 0.001
P for trend	< 0.001		< 0.001		< 0.001	
Per SD increase	1.61 (1.56–1.66)	< 0.001	1.28 (1.23–1.33)	< 0.001	1.21 (1.16–1.26)	< 0.001
TyG-WHtR						
Q1	Reference		Reference		Reference	
Q2	1.8 (1.58–2.05)	< 0.001	1.09 (0.95–1.24)	0.021	1.04 (0.91–1.19)	0.57
Q3	2.59 (2.29–2.93)	< 0.001	1.28 (1.13–1.45)	< 0.001	1.15 (1.02–1.31)	0.027
Q4	3.42 (3.03–3.85)	< 0.001	1.64 (1.45–1.85)	< 0.001	1.38 (1.22–1.56)	< 0.001
P for trend	< 0.001		< 0.001		< 0.001	
Per SD increase	1.44 (1.39–1.49)	< 0.001	1.22 (1.18–1.27)	< 0.001	1.15 (1.1–1.19)	< 0.001

AAD, aortic aneurysm and dissection; Model 1 has no variables adjusted; Model 2 adjusted age, sex, and race; Model 3 further adjusted with physical activity, smoking and drinking status, diet score, TDI, fasting time, family history of CVD, usage of antihypertensive drugs, lipid-lowering drugs, and insulin, cancer, hypertension, and diabetes.

and 121.4 months, respectively (all P for trend <0.05; Figure 4; Supplementary Table S2).

Additionally, the ROC curve highlighted TyG-WC as the strongest predictor of AAD risk, with the highest AUC (AUC = 0.65, 95%CI: 0.64–0.66), followed by TyG-WHtR (AUC = 0.62, 95%CI: 0.61–0.63), TyG index (AUC = 0.59, 95%CI: 0.58–0.60) and TyG-BMI (AUC = 0.58, 95%CI: 0.57–0.59; Supplementary Figure S2). Notably, these results remained consistent across both the training and testing sets.

Subgroup analyses

Stratified analyses upheld the positive correlation between TyG, TyG-BMI, TyG-WC, TyG-WHtR and AAD risk across various subgroups, including age, medication use, diet score, family history of CVD and hypertension (Figures 5–8). Additionally, the association was more pronounced in male participants, individuals with BMI < 30 kg/m^2, Caucasians, current smokers, alcohol consumers, and those without a history of cancer. Furthermore, significant interactions were noted between TyG indices and AAD risk, particularly in relation to smoking status for TyG (P for interaction = 0.003; Figure 5) and gender for TyG-BMI (P for interaction = 0.004; Figure 6).

Sensitivity analyses

In sensitivity analyses, the exclusion of participants within 2 years of follow-up and those with missing baseline covariates yielded consistent results with the main findings (Supplementary Tables S3, S4). Additionally, PSM analysis effectively balanced baseline characteristics between AAD and non-AAD groups (Supplementary Table S5). Subsequent Cox proportional hazards

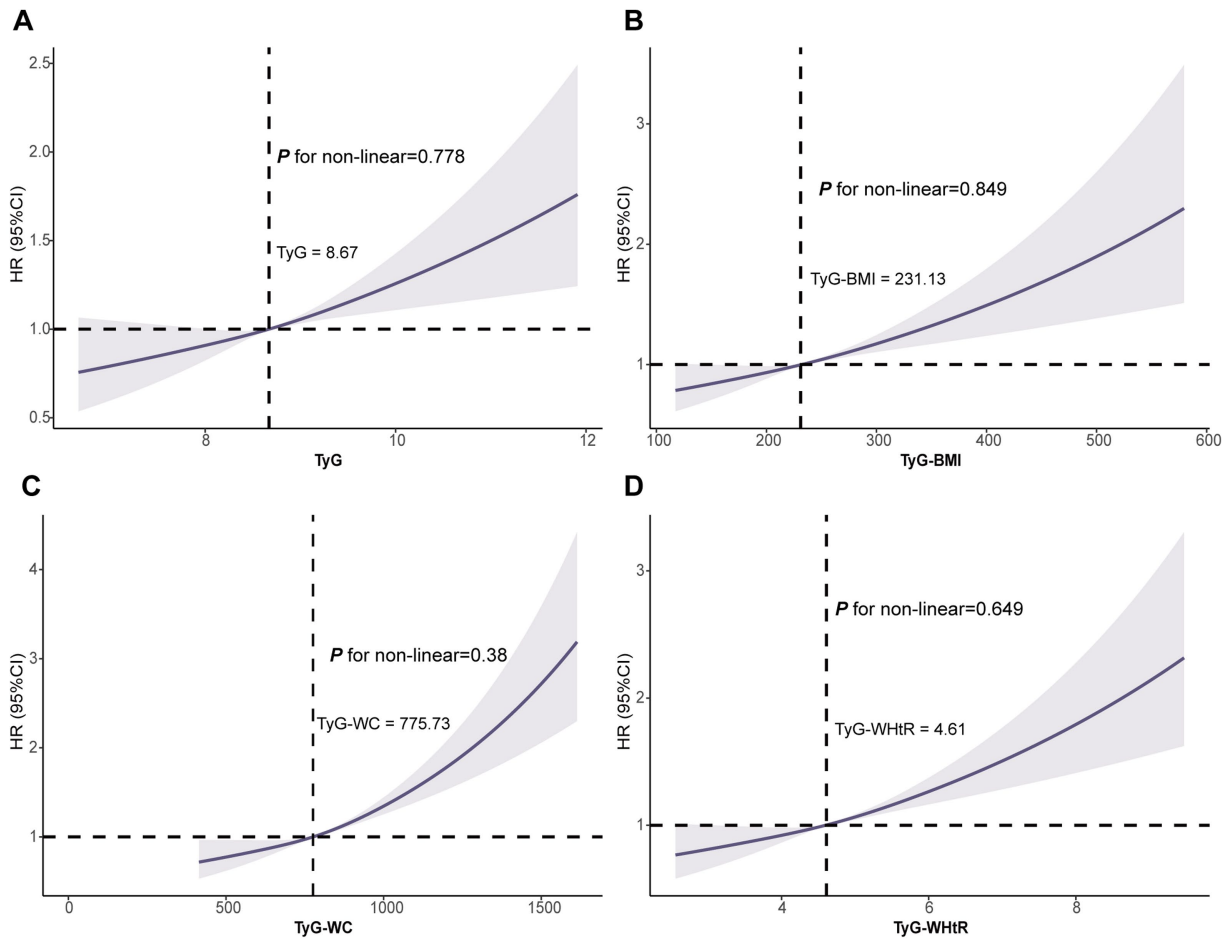

FIGURE 3
Association of the TyG **(A)**, TyG-BMI **(B)**, TyG-WC **(C)** and TyG-WHtR **(D)** with AAD using RCS. Models were fully adjusted with the maximum covariates in Model2. AAD, aortic aneurysm and dissection; RCS, Restricted cubic splines.

models post-PSM adjustment demonstrated consistent results (Supplementary Table S6).

Discussion

This large-scale prospective cohort study, to the best of our knowledge, represents the first investigation into the interplay between the TyG index, obesity indices and AAD risk. Our findings underscore a significant positive association between TyG, TyG-BMI, TyG-WC, TyG-WHtR and AAD risk, with a linear relationship observed. Furthermore, elevations in these indices significantly accelerated AAD occurrence. Among these indicators, TyG-WC exhibited the strongest association with AAD risk, as indicated by a larger AUC. Furthermore, the associations of the four indicators with AAD were particularly prominent among individuals with BMI < 30 kg/m^2, Caucasians, current smokers, alcohol consumers and those without a history of cancer.

The TyG index, serving as a surrogate marker for IR, has garnered attention owing to its convenience and high sensitivity and specificity (37). In a retrospective cohort study of individuals over 40 years old, Hong S et al. reported a 26% increased risk of stroke (HR: 1.26, 95% CI: 1.23–1.29) and a 31% increased risk of myocardial infarction (HR: 1.31, 95% CI: 1.28–1.35) among participants in the TyG Q4 group compared to the Q1 group (37, 38). Similarly, Wan Y et al. demonstrated a linear association between each unit increase in TyG and a 16% increase in CVD risk, consistent with our findings (39). Conversely, Che B et al. identified a nonlinear relationship between TyG and CVD risk (40).

TyG-BMI, TyG-WC and TyG-WHtR represent combinations of TyG with obesity metrics. A prospective cohort study revealed that each SD increase in TyG-BMI correlated with a 17% increase in CVD risk (HR: 1.17, 95% CI: 1.04–1.31). The linear relationship between TyG-BMI and CVD risk observed in this study aligns with our findings (41). Another subgroup cohort study investigating the association between TyG-BMI and prehypertension (pre-HTN) or hypertension (HTN) identified TyG-BMI as an independent risk factor for the development of pre-HTN and HTN, with a linear correlation between TyG-BMI and pre-HTN/HTN risk, particularly showing significant sex interaction (42). Consistent with our study, we also observed a significant sex interaction in the relationship between TyG-BMI and AAD risk.

TyG-WC and TyG-WHtR are two additional indices utilized in CVD identification. Dang K et al. demonstrated that elevated levels of

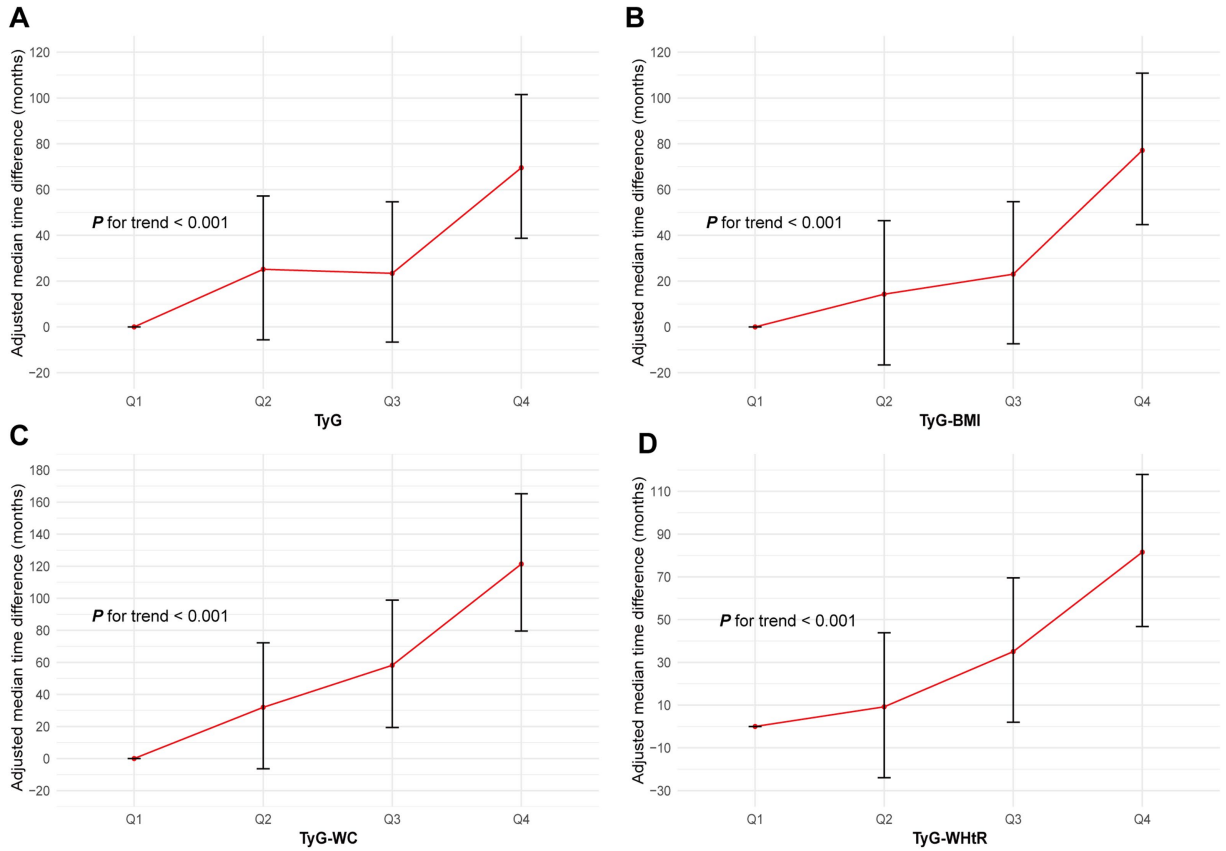

FIGURE 4
Association of the TyG **(A)**, TyG-BMI **(B)**, TyG-WC **(C)** and TyG-WHtR **(D)** with AAD using AFT. Models were fully adjusted with the maximum covariates in Model2. AAD, aortic aneurysm and dissection; TyG index, triglyceride glucose index; TyG-BMI, triglyceride glucose index–body mass index; TyG-WC, triglyceride glucose index-waist circumference; TyG-WHtR, triglyceride glucose index-waist height ratio; AFT, accelerated failure time.

TyG-WC and TyG-WHtR significantly increase the risk of CVD (24, 37). Furthermore, another study indicated that TyG-WC and TyG-WHtR exhibit a linear relationship with developing CVD risk, with TyG-WC (AUC = 0.63) and TyG-WHtR (AUC = 0.65) outperforming TyG (AUC = 0.59) and TyG-BMI (AUC = 0.58) in predicting CVD risk (43). Similarly, Miao H et al. found that TyG-WC and TyG-WHtR surpass TyG and TyG-BMI in predicting CVD, with TyG-WC showing the strongest predictive capability (44). In our study, we similarly observed that TyG-WC and TyG-WHtR were closely associated with AAD risk, displaying a linear relationship. Notably, TyG-WC exhibited the highest predictive performance for AAD, followed by TyG-WHtR, TyG and TyG-BMI. Although the AUC of TyG-WC was 0.65, it should be emphasized that this is only the predictive ability of a single indicator. The clinical symptoms of AAD are highly variable and the etiology of the disease is complex, which poses a diagnostic challenge. The accuracy of any single biomarker in predicting AAD is limited. In the future, the combination of TyG-WC with other markers should be considered to improve the predictive ability of AAD.

AAD represents a challenging medical event to predict in advance (45). Although factors such as male gender, older age, hypertension and a family history of aneurysms are associated with AAD risk, identifying high-risk populations remains difficult due to its low incidence rate (8). The occurrence of AAD may be linked to various cardiovascular-related conditions (46). In our study, to eliminate the potential confounding effects of heart disease on the study results, participants with a history of heart disease at baseline were excluded. Subgroup analysis revealed that TyG, TyG-BMI, TyG-WC and TyG-WHtR demonstrated a stronger impact on AAD occurrence in men, Caucasians, individuals with BMI < 30 kg/m^2, those without hypertension, diabetes, a history of cancer, and without a family history of cardiovascular disease.

The mechanisms underlying AAD development in relation to the TyG index and its derivatives, TyG-BMI, TyG-WC and TyG-WHtR, remain incompletely understood but likely involve several aspects. Firstly, the TyG index comprises lipid and glucose components. The lipid portion inhibits insulin secretion, leading to ectopic fat deposition in muscle cells and subsequent IR (47). The glucose component may elevate reactive oxygen species (ROS) levels, exerting toxic effects on pancreatic β-cells and impairing their function, thereby contributing to IR (48). TyG-BMI, TyG-WC and TyG-WHtR combined with obesity indicators, reflect the accumulation of visceral fat, further exacerbating IR and metabolic disturbances, which in turn mediate systemic inflammation, endothelial dysfunction and vascular remodeling, thereby promoting atherosclerosis (49). Previous studies have highlighted a strong correlation between the TyG index and atherosclerosis (50, 51). Atherosclerosis weakens the arterial wall, rendering it more susceptible to AAD under fluctuations in blood pressure or mechanical stress (52). Endothelial injury and

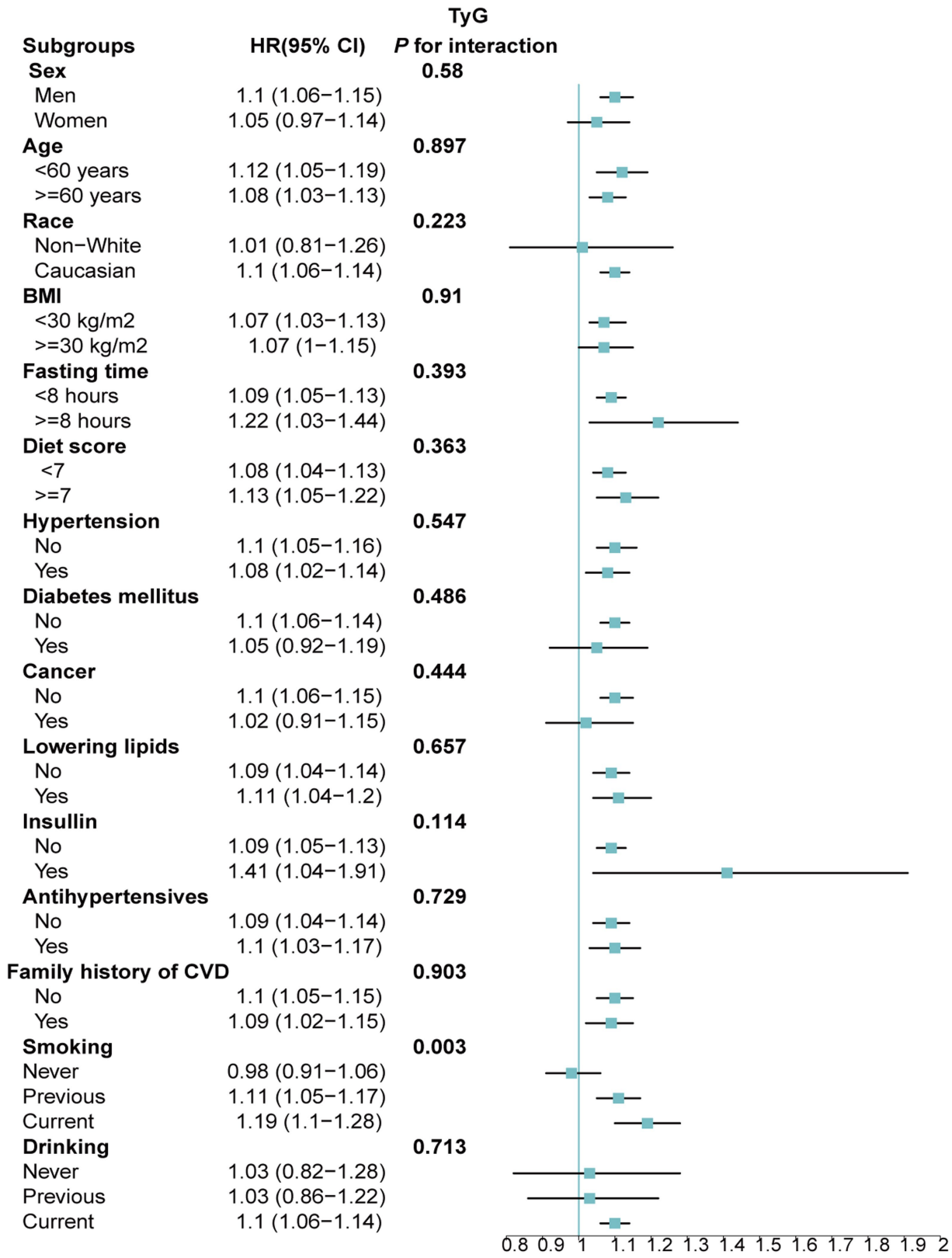

FIGURE 5
Association between each standard deviation increase in TyG and the risk of AAD stratified by different clinical characteristics. AAD, aortic aneurysm and dissection; TyG index, triglyceride glucose index.

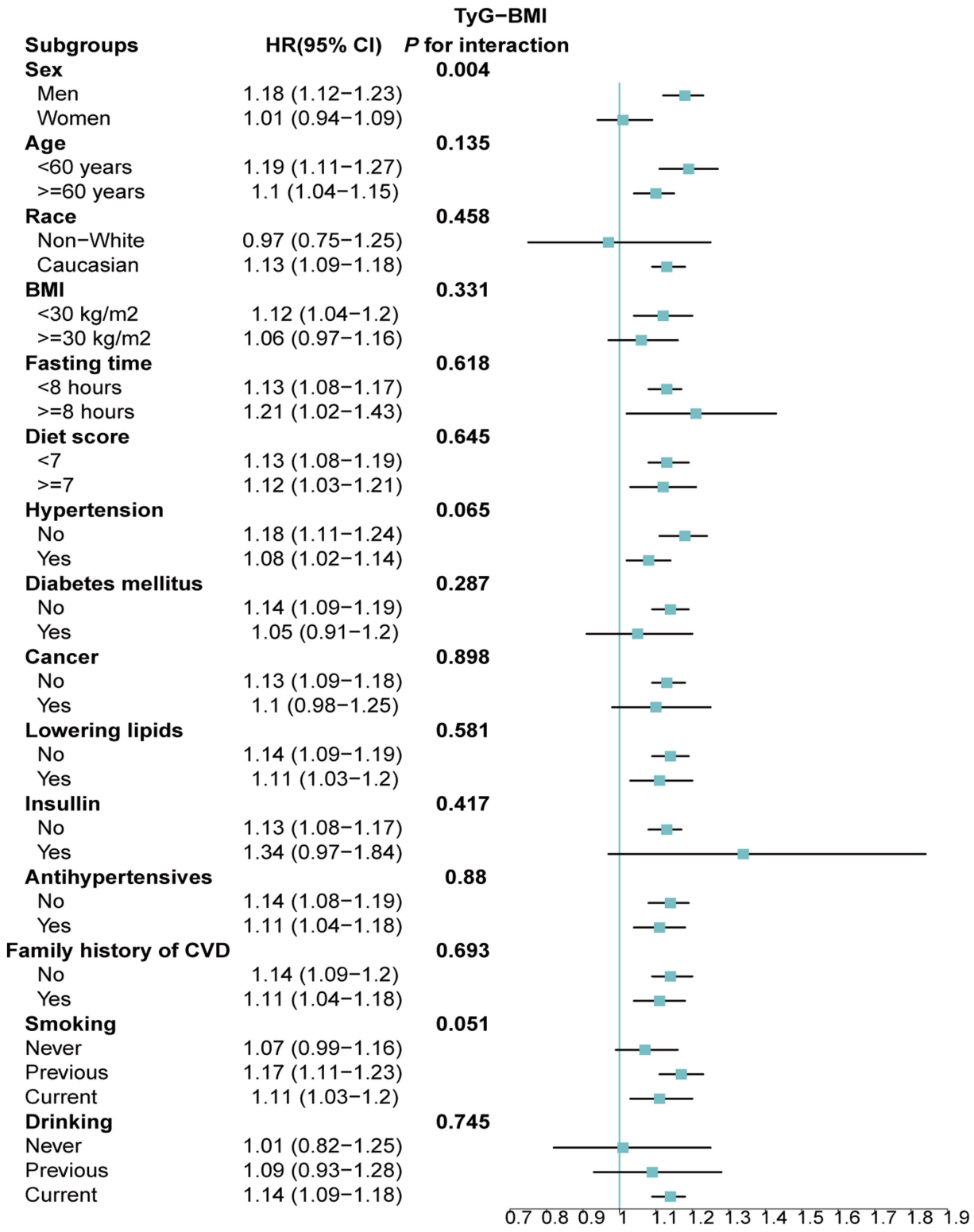

FIGURE 6
Association between each standard deviation increase in TyG-BMI and the risk of AAD stratified by different clinical characteristics. AAD, aortic aneurysm and dissection; TyG-BMI, triglyceride glucose index–body mass index.

inflammatory reactions further weaken the arterial wall, facilitating blood infiltration into the medial layer, ultimately resulting in AAD occurrence (52). Moreover, vascular endothelial secretion of inflammatory factors such as vascular cell adhesion molecule-1 (VCAM-1) and intercellular adhesion molecule-1 (ICAM-1) induces platelet adhesion and aggregation, promoting thrombus formation and vascular endothelial damage and increases the risk of dissection formation and extension (53–55).

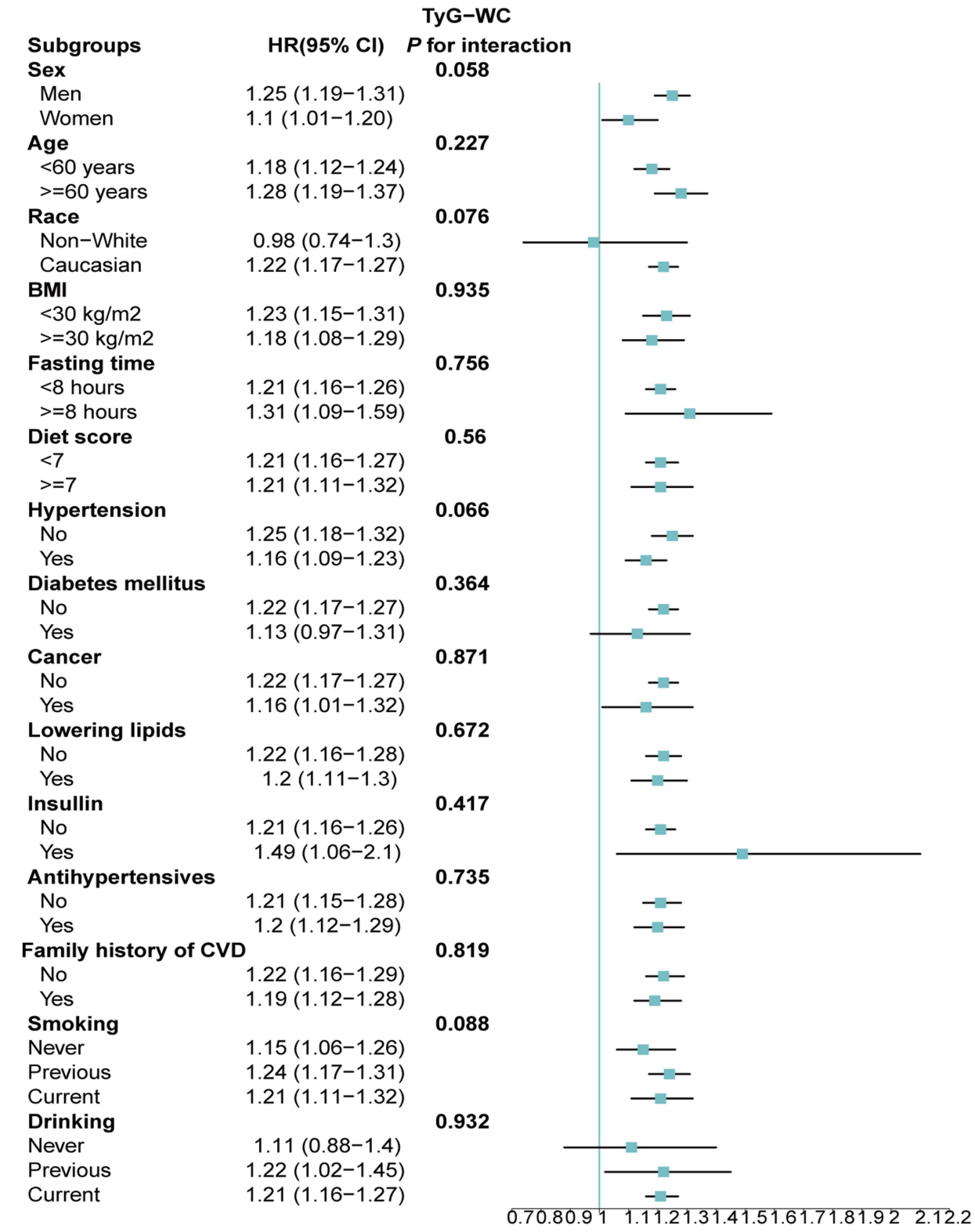

FIGURE 7
Association between each standard deviation increase in TyG-WC and the risk of AAD stratified by different clinical characteristics. AAD, aortic aneurysm and dissection; TyG-WC, triglyceride glucose index-waist circumference.

Our study boasts certain strengths. First, it is the first to explore the relationship between TyG and obesity-related indicators and the AAD risk using a prospective approach and comprehensive long-term follow-up data. Additionally, subgroup analysis identified high-risk populations for AAD, and sensitivity analysis enhanced the robustness of the results. However, several limitations should also be acknowledged. Firstly, data on TyG, TyG-BMI, TyG-WC and TyG-WHtR were collected only at baseline, preventing observation of

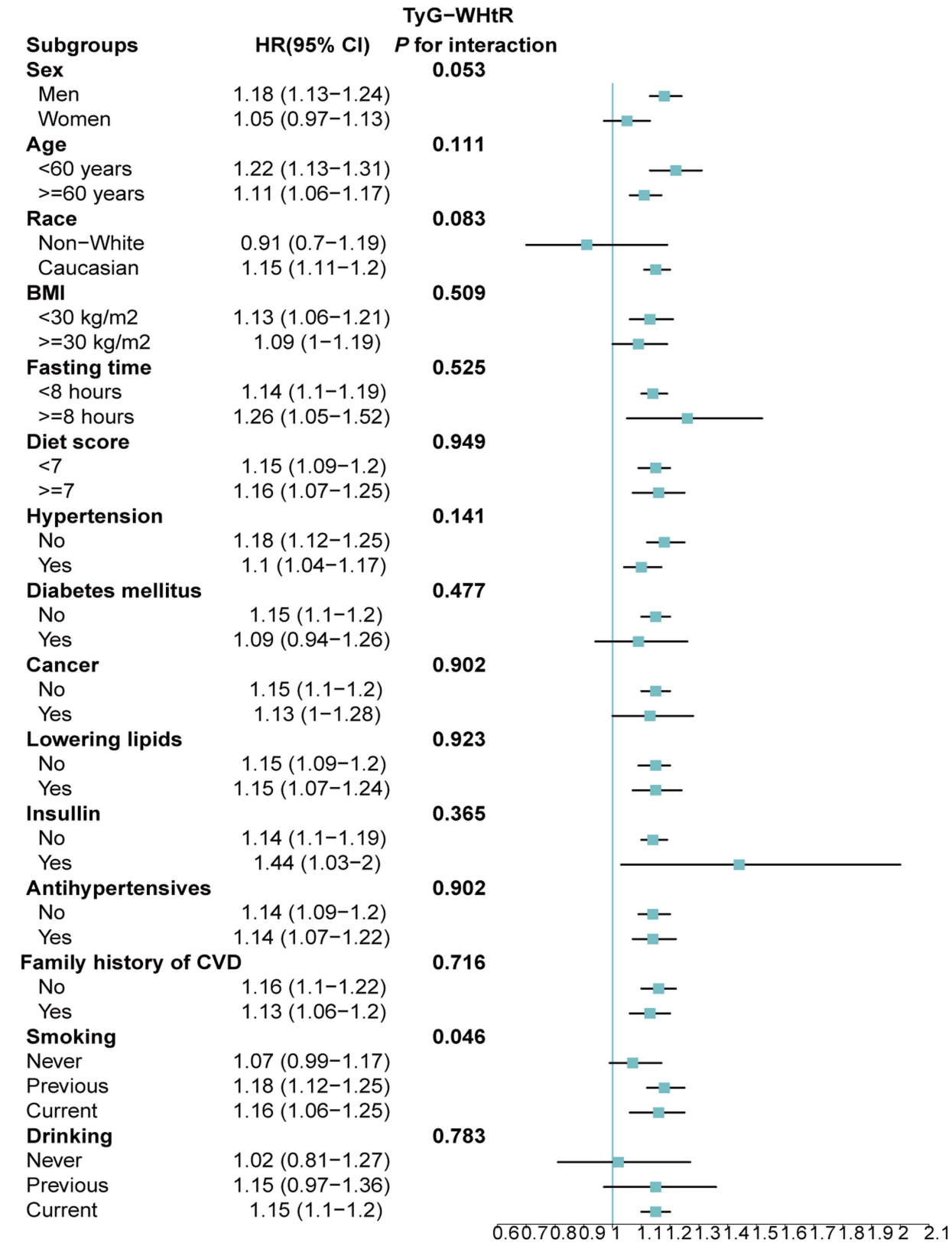

FIGURE 8
Association between each standard deviation increase in TyG-WHtR and the risk of AAD stratified by different clinical characteristics. AAD, aortic aneurysm and dissection; TyG-WHtR, triglyceride glucose index-waist height ratio.

dynamic changes during follow-up and their impact on AAD. Secondly, despite adjusting for known confounding factors, unmeasured variables may still influence outcomes due to the observational study design, precluding the establishment of causality. Thirdly, our study's predominantly middle-aged and older adults, along with a predominantly White population, may limit generalizability to other demographics. Lastly, the likelihood of healthy individuals participating during UKB recruitment may underestimate AAD incidence.

Conclusion

The present study, based on a large prospective cohort design, showed that higher TyG index and its combination with obesity indices were significantly associated with the risk of AAD. Moreover, AFT models further showed that elevation of these indicators significantly advanced the onset of AAD. In addition, RCS analyses demonstrated a linear association between these indicators and the risk of AAD, and the TyG-WC showed higher predictive ability for AAD. These findings emphasize the potential application of the TyG index and its combination with obesity indicators in the early identification of AAD.

Data availability statement

The datasets presented in this study can be found in online repositories. The names of the repository/repositories and accession number(s) can be found in the article/Supplementary material.

Ethics statement

The studies involving humans were approved by UK Biobank / North West Multi-Center Research Ethics Committee (REC reference: 11/NW/0382). The studies were conducted in accordance with the local legislation and institutional requirements. The participants provided their written informed consent to participate in this study.

Author contributions

WY: Conceptualization, Methodology, Software, Writing – original draft, Writing – review & editing. XW: Conceptualization, Writing – original draft, Writing – review & editing. ZD: Writing – original draft, Writing – review & editing. WC: Investigation, Resources, Supervision, Validation, Visualization, Writing – original draft, Writing – review & editing.

Funding

The author(s) declare that financial support was received for the research, authorship, and/or publication of this article. This work was supported by Natural Science Foundation of Zhejiang Province, United Foundation of Beijing Zhongwei (LBY21H270002). WC is funded by China Scholarship Council (CSC No. 202009370095).

Acknowledgments

We extend our deepest gratitude to the study participants and the members of the UK Biobank cohort. The establishment of the UK Biobank was made possible through the efforts of the Wellcome Trust, Medical Research Council, Department of Health, Scottish Government, and the Northwest Regional Development Agency. We thank my colleague Chuang Yang for censoring the data. This study was conducted using the UK Biobank Resource, Application Number: 107335. Besides, we thank Bullet Edits Limited for the linguistic editing and proofreading of the manuscript.

Conflict of interest

The authors declare that the research was conducted in the absence of any commercial or financial relationships that could be construed as a potential conflict of interest.

Publisher's note

Supplementary material

The Supplementary material for this article can be found online at: https://www.frontiersin.org/articles/10.3389/fnut.2024.1454880/full#supplementary-material

References

1. Takada M, Yamagishi K, Tamakoshi A, Iso H. Height and mortality from aortic aneurysm and dissection. *J Atheroscler Thromb*. (2022) 29:1166–75. doi: 10.5551/jat.62941

2. Isselbacher EM, Preventza O, Augoustides JG, Beck AW, Bolen MA, Braverman AC, et al. ACC/AHA guideline for the diagnosis and Management of Aortic Disease: A report of the American Heart Association/American College of Cardiology Joint Committee on clinical practice guidelines. *Circulation*. (2022) 146:e334–482. doi: 10.1161/CIR.0000000000001106

3. Gouveia E, Melo R, Mourão M, Caldeira D, Alves M, Lopes A, et al. A systematic review and meta-analysis of the incidence of acute aortic dissections in population-based studies. *J Vasc Surg*. (2022) 75:709–20. doi: 10.1016/j.jvs.2021.08.080

4. Aboyans V, Causes of Death Collaborators. Global, regional, and national age-sex specific all-cause and cause-specific mortality for 240 causes of death, 1990–2013: A systematic analysis for the global burden of disease study 2013. *Lancet (London, England)*. (2015) 385:117–71. doi: 10.1016/S0140-6736(14)61682-2

5. Conway BD, Stamou SC, Kouchoukos NT, Lobdell KW, Khabbaz KR, Murphy E, et al. Improved clinical outcomes and survival following repair of acute type A aortic dissection in the current era. *Interact Cardiovasc Thorac Surg*. (2014) 19:971–6. doi: 10.1093/icvts/ivu268

6. van Dorst DCH, De WNP, van der Pluijm I, Roos-Hesselink JW, Essers J, Danser AH. Transforming growth factor-β and the renin-angiotensin system in syndromic thoracic aortic aneurysms: implications for treatment. *Cardiovasc Drugs Ther*. (2021) 35:1233–52. doi: 10.1007/s10557-020-07116-4

7. Xu B, Xuan H, Iida Y, Miyata M, Dalman RL. Pathogenic and therapeutic significance of angiotensin II type I receptor in abdominal aortic aneurysms. *Curr Drug Targets*. (2018) 19:1318–26. doi: 10.2174/1389450119666180122155642

8. Gawinecka J, Schönrath F, Von EA. Acute aortic dissection: pathogenesis, risk factors and diagnosis. *Swiss Med Wkly*. (2017) 147:w14489. doi: 10.4414/smw.2017.14489

9. Wang H, Wang L, Wang J, Zhang L, Li C. The biological effects of smoking on the formation and rupture of intracranial aneurysms: A systematic review and Meta-analysis. *Front Neurol*. (2022) 13:862916. doi: 10.3389/fneur.2022.862916

10. Hibino M, Otaki Y, Kobeissi E, Pan H, Hibino H, Taddese H, et al. Blood pressure, hypertension, and the risk of aortic dissection incidence and mortality: results from the J-SCH study, the UK biobank study, and a Meta-analysis of cohort studies. *Circulation*. (2022) 145:633–44. doi: 10.1161/CIRCULATIONAHA.121.056546

11. Liu Z-L, Li Y, Lin Y-J, Shi M-M, Fu M-X, Li Z-Q, et al. Aging aggravates aortic aneurysm and dissection via miR-1204-MYLK signaling axis in mice. *Nat Commun*. (2024) 15:5985. doi: 10.1038/s41467-024-50036-2

12. Barbetseas J, Alexopoulos N, Brili S, Aggeli C, Chrysohoou C, Frogoudaki A, et al. Atherosclerosis of the aorta in patients with acute thoracic aortic dissection. *Circulation J Official J Japanese Circulation Society*. (2008) 72:1773–6. doi: 10.1253/circj.cj-08-0433

13. Prakash SK, Pedroza C, Khalil YA, Milewicz DM. Diabetes and reduced risk for thoracic aortic aneurysms and dissections: a nationwide case-control study. *J Am Heart Assoc*. (2012) 1:1. doi: 10.1161/JAHA.111.000323

14. Aizawa K, Sakano Y, Ohki S, Saito T, Konishi H, Misawa Y. Obesity is a risk factor of young onset of acute aortic dissection and postoperative hypoxemia. *Kyobu geka Japanese J Thoracic Surg*. (2013) 66:437–44.

15. Hill MA, Yang Y, Zhang L, Sun Z, Jia G, Parrish AR, et al. Insulin resistance, cardiovascular stiffening and cardiovascular disease. *Metab Clin Exp*. (2021) 119:154766. doi: 10.1016/j.metabol.2021.154766

16. Lareyre F, Moratal C, Zereg E, Carboni J, Panaïa-Ferrari P, Bayer P, et al. Association of abdominal aortic aneurysm diameter with insulin resistance index. *Biochem Med*. (2018) 28:30702. doi: 10.11613/BM.2018.030702

17. Zheng H, Qiu Z, Chai T, He J, Zhang Y, Wang C, et al. Insulin resistance promotes the formation of aortic dissection by inducing the phenotypic switch of vascular smooth muscle cells. *Front Cardiovascular Med*. (2021) 8:732122. doi: 10.3389/fcvm.2021.732122

18. Kim JK. Hyperinsulinemic-euglycemic clamp to assess insulin sensitivity in vivo. *Methods Molecular Biol (Clifton, NJ)*. (2009) 560:221–38. doi: 10.1007/978-1-59745-448-3_15

19. Du T, Yuan G, Zhang M, Zhou X, Sun X, Yu X. Clinical usefulness of lipid ratios, visceral adiposity indicators, and the triglycerides and glucose index as risk markers of insulin resistance. *Cardiovasc Diabetol*. (2014) 13:146. doi: 10.1186/s12933-014-0146-3

20. Ahn N, Baumeister SE, Amann U, Rathmann W, Peters A, Huth C, et al. Visceral adiposity index (VAI), lipid accumulation product (LAP), and product of triglycerides and glucose (TyG) to discriminate prediabetes and diabetes. *Sci Rep*. (2019) 9:9693. doi: 10.1038/s41598-019-46187-8

21. Yang Y, Huang X, Wang Y, Leng L, Xu J, Feng L, et al. The impact of triglyceride-glucose index on ischemic stroke: a systematic review and meta-analysis. *Cardiovasc Diabetol*. (2023) 22:2. doi: 10.1186/s12933-022-01732-0

22. Tao L-C, Xu J-N, Wang T-T, Hua F, Li J-J. Triglyceride-glucose index as a marker in cardiovascular diseases: landscape and limitations. *Cardiovasc Diabetol*. (2022) 21:68. doi: 10.1186/s12933-022-01511-x

23. Nabipoorashrafi SA, Seyedi SA, Rabizadeh S, Ebrahimi M, Ranjbar SA, Reyhan SK, et al. The accuracy of triglyceride-glucose (TyG) index for the screening of metabolic syndrome in adults: A systematic review and meta-analysis. *Nutr Metab Cardiovasc Dis*. (2022) 32:2677–88. doi: 10.1016/j.numecd.2022.07.024

24. Dang K, Wang X, Hu J, Zhang Y, Cheng L, Qi X, et al. The association between triglyceride-glucose index and its combination with obesity indicators and cardiovascular disease: NHANES 2003-2018. *Cardiovasc Diabetol*. (2024) 23:8. doi: 10.1186/s12933-023-02115-9

25. Zeng ZY, Liu SX, Xu H, Xu X, Liu XZ, Zhao XX. Association of triglyceride glucose index and its combination of obesity indices with prehypertension in lean individuals: A cross-sectional study of Chinese adults. *J Clin Hypertens (Greenwich)*. (2020) 22:1025–32. doi: 10.1111/jch.13878

26. Sudlow C, Gallacher J, Allen N, Beral V, Burton P, Danesh J, et al. UK biobank: an open access resource for identifying the causes of a wide range of complex diseases of middle and old age. *PLoS Med*. (2015) 12:e1001779. doi: 10.1371/journal.pmed.1001779

27. Elliott P, Peakman TC. The UK biobank sample handling and storage protocol for the collection, processing and archiving of human blood and urine. *Int J Epidemiol*. (2008) 37:234–44. doi: 10.1093/ije/dym276

28. Alshamiri MQ, Mohd A Habbab F, al-Qahtani SS, Alghalayini KA, al-Qattan OM, el-shaer F. Waist-to-height ratio (WHtR) in predicting coronary artery disease compared to body mass index and waist circumference in a single center from Saudi Arabia. *Cardiol Res Pract*. (2020) 2020:4250793–6. doi: 10.1155/2020/4250793

29. Fritz J, Bjørge T, Nagel G, Manjer J, Engeland A, Häggström C, et al. The triglyceride-glucose index as a measure of insulin resistance and risk of obesity-related cancers. *Int J Epidemiol*. (2020) 49:193–204. doi: 10.1093/ije/dyz053

30. Xing Y, Liu J, Gao Y, Zhu Y, Zhang Y, Ma H. Stronger associations of TyG index with diabetes than TyG-obesity-related parameters: more pronounced in Young, middle-aged, and women. *Diabetes, metabolic syndrome and obesity targets and therapy*. (2023) 16:3795–805. doi: 10.2147/DMSO.S433493

31. Craig CL, Marshall AL, Sjöström M, Bauman AE, Booth ML, Ainsworth BE, et al. International physical activity questionnaire: 12-country reliability and validity. *Med Sci Sports Exerc*. (2003) 35:1381–95. doi: 10.1249/01.MSS.0000078924.61453.FB

32. Shweikh Y, Ko F, Chan MP, Patel PJ, Muthy Z, Khaw PT, et al. Measures of socioeconomic status and self-reported glaucoma in the U.K. biobank cohort. *Eye (Lond)*. (2015) 29:1360–7. doi: 10.1038/eye.2015.157

33. Petermann-Rocha F, Ho FK, Foster H, Boopor J, Parra-Soto S, Gray SR, et al. Nonlinear associations between cumulative dietary risk factors and cardiovascular diseases, Cancer, and all-cause mortality: A prospective cohort study from UK biobank. *Mayo Clin Proc*. (2021) 96:2418–31. doi: 10.1016/j.mayocp.2021.01.036

34. Tennant PW, Murray EJ, Arnold KF, Berrie L, Fox MP, Gadd SC, et al. Use of directed acyclic graphs (DAGs) to identify confounders in applied health research: review and recommendations. *Int J Epidemiol*. (2021) 50:620–32. doi: 10.1093/ije/dyaa213

35. Pang M, Platt RW, Schuster T, Abrahamowicz M. Spline-based accelerated failure time model. *Stat Med*. (2021) 40:481–97. doi: 10.1002/sim.8786

36. Kane LT, Fang T, Galetta MS, Goyal DK, Nicholson KJ, Kepler CK, et al. Propensity score matching: A statistical method. *Clin Spine Surg*. (2020) 33:120–2. doi: 10.1097/BSD.0000000000000932

37. Guerrero-Romero F, Simental-Mendía LE, González-Ortiz M, Martínez-Abundis E, Ramos-Zavala MG, Hernández-González SO, et al. The product of triglycerides and glucose, a simple measure of insulin sensitivity. Comparison with the euglycemic-hyperinsulinemic clamp. *J Clin Endocrinol Metab*. (2010) 95:3347–51. doi: 10.1210/jc.2010-0288

38. Hong S, Han K, Park C-Y. The triglyceride glucose index is a simple and low-cost marker associated with atherosclerotic cardiovascular disease: a population-based study. *BMC Med*. (2020) 18:361. doi: 10.1186/s12916-020-01824-2

39. Wan Y, Zhang Z, Ling Y, Cui H, Tao Z, Pei J, et al. Association of triglyceride-glucose index with cardiovascular disease among a general population: a prospective cohort study. *Diabetol Metab Syndr*. (2023) 15:204. doi: 10.1186/s13098-023-01181-z

40. Che B, Zhong C, Zhang R, Pu L, Zhao T, Zhang Y, et al. Triglyceride-glucose index and triglyceride to high-density lipoprotein cholesterol ratio as potential cardiovascular disease risk factors: an analysis of UK biobank data. *Cardiovasc Diabetol*. (2023) 22:34. doi: 10.1186/s12933-023-01762-2

41. Li F, Wang Y, Shi B, Sun S, Wang S, Pang S, et al. Association between the cumulative average triglyceride glucose-body mass index and cardiovascular disease incidence among the middle-aged and older population: a prospective nationwide cohort study in China. *Cardiovasc Diabetol*. (2024) 23:16. doi: 10.1186/s12933-023-02114-w

42. Chen L, He L, Zheng W, Liu Q, Ren Y, Kong W, et al. High triglyceride glucose-body mass index correlates with prehypertension and hypertension in east Asian populations: A population-based retrospective study. *Front Cardiovascular Med*. (2023) 10:1139842. doi: 10.3389/fcvm.2023.1139842

43. Park H-M, Han T, Heo S-J, Kwon Y-J. Effectiveness of the triglyceride-glucose index and triglyceride-glucose-related indices in predicting cardiovascular disease in middle-aged and older adults: A prospective cohort study. *J Clin Lipidol*. (2024) 18:e70–9. doi: 10.1016/j.jacl.2023.11.006

44. Miao H, Zhou Z, Yang S, Zhang Y. The association of triglyceride-glucose index and related parameters with hypertension and cardiovascular risk: a cross-sectional study. *Hypertension Res Official J Japanese Society of Hypertension*. (2024) 47:877–86. doi: 10.1038/s41440-023-01502-9

45. Evangelista A, Isselbacher EM, Bossone E, Gleason TG, Di Eusanio M, Sechtem U, et al. Insights from the international registry of acute aortic dissection: A 20-year experience of collaborative clinical research. *Circulation*. (2018) 137:1846–60. doi: 10.1161/CIRCULATIONAHA.117.031264

46. Zhou Z, Cecchi AC, Prakash SK, Milewicz DM. Risk factors for thoracic aortic dissection. *Gene*. (2022) 13:13. doi: 10.3390/genes13101814

47. Athyros VG, Doumas M, Imprialos KP, Stavropoulos K, Georgianou E, Katsimardou A, et al. Diabetes and lipid metabolism. *Hormones (Athens)*. (2018) 17:61–7. doi: 10.1007/s42000-018-0014-8

48. Dong K, Ni H, Wu M, Tang Z, Halim M, Shi D. ROS-mediated glucose metabolic reprogram induces insulin resistance in type 2 diabetes. *Biochem Biophys Res Commun*. (2016) 476:204–11. doi: 10.1016/j.bbrc.2016.05.087

49. Owusu J, Barrett E. Early microvascular dysfunction: is the vasa Vasorum a "missing link" in insulin resistance and atherosclerosis. *Int J Mol Sci*. (2021) 22:7574. doi: 10.3390/ijms22147574

50. Zhao J, Fan H, Wang T, Yu B, Mao S, Wang X, et al. TyG index is positively associated with risk of CHD and coronary atherosclerosis severity among NAFLD patients. *Cardiovasc Diabetol*. (2022) 21:123. doi: 10.1186/s12933-022-01548-y

51. Lambrinoudaki I, Kazani MV, Armeni E, Georgiopoulos G, Tampakis K, Rizos D, et al. The TyG index as a marker of subclinical atherosclerosis and arterial stiffness in lean and overweight postmenopausal women. *Heart Lung Circ*. (2018) 27:716–24. doi: 10.1016/j.hlc.2017.05.142

52. Skotsimara G, Antonopoulos A, Oikonomou E, Papastamos C, Siasos G, Tousoulis D. Aortic Wall inflammation in the pathogenesis, diagnosis and treatment of aortic aneurysms. *Inflammation*. (2022) 45:965–76. doi: 10.1007/s10753-022-01626-z

53. Singh V, Kaur R, Kumari P, Pasricha C, Singh R. ICAM-1 and VCAM-1: gatekeepers in various inflammatory and cardiovascular disorders. *Clinica chimica acta; Int J Clin Chem*. (2023) 548:117487. doi: 10.1016/j.cca.2023.117487

54. Massberg S, Brand K, Grüner S, Page S, Müller E, Müller I, et al. A critical role of platelet adhesion in the initiation of atherosclerotic lesion formation. *J Exp Med*. (2002) 196:887–96. doi: 10.1084/jem.20012044

55. Zhang S, Qian H, Yang Q, Hu J, Gan C, Meng W. Relationship between the extent of dissection and platelet activation in acute aortic dissection. *J Cardiothorac Surg*. (2015) 10:162. doi: 10.1186/s13019-015-0351-5

frontiers | Frontiers in Nutrition

TYPE Original Research
PUBLISHED 06 December 2024
DOI 10.3389/fnut.2024.1485428

OPEN ACCESS

EDITED BY
Jagannath Misra,
Indiana University–Purdue University Indianapolis, United States

REVIEWED BY
Shokouh Attarilar,
Shanghai Jiao Tong University, China
Munkhtuya Tumurkhuu,
Wake Forest Baptist Medical Center, United States

*CORRESPONDENCE
Zhi Chen
✉ 810316156@qq.com

†These authors have contributed equally to this work

RECEIVED 23 August 2024
ACCEPTED 26 November 2024
PUBLISHED 06 December 2024

CITATION
Yuan W, Chen J, Sun J, Song C and Chen Z (2024) Association between oxidative balance score and serum cobalt level in population with metal implants: a cross-sectional study from NHANES 2015–2020.
Front. Nutr. 11:1485428.
doi: 10.3389/fnut.2024.1485428

Association between oxidative balance score and serum cobalt level in population with metal implants: a cross-sectional study from NHANES 2015–2020

Wenxiu Yuan[1†], Jing Chen[2†], Jun Sun[3], Chenyang Song[4] and Zhi Chen[4*]

[1]Postdoctoral Workstation, Fujian Key Laboratory of Oral Diseases, Fujian Provincial Engineering Research Center of Oral Biomaterial, Stomatological Key Lab of Fujian College and University, Department of Orthodontics, School and Hospital of Stomatology, Fujian Medical University, Fuzhou, China, [2]Department of Ophthalmology, Fujian Provincial Hospital, Fuzhou, Fujian, China, [3]Department of Emergency, Zhaotong Traditional Chinese Medicine Hospital, Zhaotong, Yunnan, China, [4]Department of Orthopedics, Fujian Medical University Union Hospital, Fuzhou, Fujian, China

Background: Growing evidence indicates that metal implants influence the body's oxidative stress status, which in turn affects the degradation and stability of metal implants. The oxidative balance score (OBS) is a composite indicator, reflecting the overall oxidative balance of pro-and antioxidants of the human body. However, the associations between OBS and the level of metal ions on the population with metal implants remain to be elucidated.

Methods: We conducted a cross-sectional study using data from 2015 to 2020 National Health and Nutrition Examination Survey (NHANES). Dietary and lifestyle factors closely associated with oxidative stress were quantified to calculate the OBS. Weighted multivariate logistic regression and smooth curve fittings were performed to examine the relationship between OBS and serum cobalt levels. Subgroup analyses were stratified by age and gender. In cases where non-linearity was detected, threshold effects were assessed using a two-piecewise linear regression model.

Results: A total of 549 participants were included in this analysis. The dietary OBS was negatively associated with serum cobalt level in fully adjusted model (β = −0.179, 95%CI: −0.358 to −0.001, *P*: 0.04918). Stratified by age and gender, negative correlation of OBS and dietary OBS with serum cobalt level was observed only in men and age over 70 years participants. Threshold effect analysis showed linear relationships between OBS, dietary OBS and cobalt level in males. There were non-linear relationships between OBS, dietary OBS and cobalt level in age over 70 years participants, with inflection points identified at 16.3 and 8.7 for OBS and dietary OBS, respectively.

Conclusion: Our study confirms the inverse relationships between oxidative stress and serum cobalt level in individuals with metal implants, highlighting the significance of optimizing OBS to mitigate the risk of metal ion toxicity. These findings emphasize the importance of maintaining an antioxidant diet and lifestyle, particularly as they offer greater protective effect for males and the elderly population.

KEYWORDS

metal implant, oxidative balance score, cobalt, NHANES, dietary

1 Introduction

Currently, the trend of global aging is becoming increasingly prominent due to persistently low birth rates and extended life expectancy. By 2050, it is projected that the population aged 65 and older will account for 20% of the global population (1), which suggests a significant rise in the incidence of degenerative diseases and related complications, such as osteoporosis, fractures, osteoarthritis (2). In patients with orthopedic diseases, the use of metal implants for fixation or replacement to relieve pain, correct deformities, and restore function has increased annually (2–6). It has been reported that over one million total hip and knee replacement are performed annually in the United States, with the cost exceeding $25 billion (7). However, the long-term survival rate of metal implants is not optimistic. Among younger patients undergoing total hip replacement, only 72% of the implants are able to last for 10 years (8). One of the challenges in the application of metal implants is the generation of metal debris and the release of metal ions. As is well known, these debris and ions can trigger localized adverse reactions, leading to the loosening and failure of the implants, and they may even enter the circulatory system, resulting in systemic damage (9). Numerous studies suggest that the accumulation of metal debris and ions can induce the formation of local pseudotumors (10, 11). Research conducted by Grammatopoulos et al. (12) found that out of 53 cases of metal-on-metal hip replacements, 16 required revision surgery due to the presence of pseudotumors. A prospective study carried out by British researchers revealed that, compared to preoperative values, patients who underwent metal-on-metal hip replacement experienced a significant increase in the incidence of chromosomal aneuploidy and translocations in peripheral blood, with rates rising 2-fold and 1.5-fold, respectively, within 2 years post-surgery (13). As our understanding of the adverse reactions caused by metal implants deepens, the prevention of these adverse effects has gradually become a focal point of research.

An increasing number of studies indicate that the integration process of metal implants with surrounding tissues may trigger a series of physiological and pathological changes (14). In the initial stage of implantation, the interaction between immune cells and the metal materials leads to the activation and secretion of various mediators, such as superoxide anions and hydroxyl radicals (15, 16). Additionally, metal particles generated due to fatigue, fretting, or corrosion can similarly stimulate local cells to produce excessive reactive oxygen species (ROS) (17–21). These intracellular and extracellular ROS may induce local inflammation and alter the chemical environment of the implants, thereby accelerating the degradation of metal implants and the release of metal ions. Metal micro-particles and ions not only cause localized harm but can also penetrate the bloodstream and lymphatic system, spreading throughout various tissues and organs, triggering systemic inflammatory responses and activating the immune system, resulting in tissue damage and functional impairment (22). Although existing research suggests that ROS are an important factor in the reduced stability of metal implants (5), there is currently a lack of reliable indicators to reflect the oxidative state after metal implantation and to elucidate the relationship between oxidative stress and the dissociation of metal ions.

The OBS is a comprehensive metric designed to assess the balance between oxidative stress and antioxidant capacity within the body (23–25). This indicator has been used to identify individuals at high risk for various chronic diseases, such as cardiovascular diseases, diabetes, and cancer, and to implement corresponding intervention measures. Additionally, it is considered an important monitoring indicator for evaluating treatment efficacy (24, 26–29). However, it remains unclear whether the oxidative stress status of patients with metal implants can be adequately assessed using the OBS, and whether this metric can effectively illustrate the relationship between oxidative stress and the dissociation of metal ions. Herein, we conducted a cross-sectional study to investigate the association between OBS and metal ion of the patients with metal implants using a large-scale, community population-based data from NHANES 2015–2020.

2 Materials and methods

2.1 Data source

The NHANES is a program in the United States designed to assess the health and nutritional status of adults and children. It involves a complex and comprehensive set of data methods, including physical examinations, laboratory tests, and questionnaires. The survey aims to monitor trends in various health indicators, such as diseases, nutritional deficiencies, and exposure to environmental contaminants. The National Center for Health Statistics Ethics Review Board has approved NHANES protocols, with all participants provided consenting to their data's use in research (30).

2.2 Study population

In this study, we analyzed NHANES data from three consecutive 2-year cycles spanning 2015–2020. We included participants with metal objects inside body, and had complete data of OBS components, serum cobalt, and serum chromium. We excluded participants without metal objects ($n = 32{,}360$), with missing data for cobalt ($n = 1{,}194$), chromium ($n = 2$), calcium ($n = 46$), cotinine ($n = 5$), Body mass index (BMI) ($n = 13$), with indication of infection (WBC $> 10 \times 10^9$/L; $n = 86$) and inflammation (CRP > 5 mg/L; $n = 173$). The participant screening processes is presented in Figure 1.

For each participant enrolled, data on OBS components, serum cobalt, and serum chromium, and covariates were extracted and analyzed.

2.3 Study variables

2.3.1 Independent variables

Based on prior research about the relationship of nutrients and lifestyle factors with oxidative stress, 16 nutrients and three lifestyle factors (alcohol consumption, smoking, and BMI) were collected to calculate OBS, including five pro-oxidants and 14 antioxidants (31, 32). Among the variables assessed, 16 nutrients and alcohol were derived from the mean of the various ingredients from the dietary interview on first day to determine the quantiles thresholds for scoring purposes. Smoking was estimated by serum cotinine, which was measured by an isotope dilution-high performance liquid chromatography/atmospheric pressure chemical ionization tandem mass spectrometry (ID HPLC-APCI MS/MS). The BMI (kg/m^2) was collected from body measures and calculated as weight in kilograms divided by height in meters square. We stratified all components into three distinct groups,

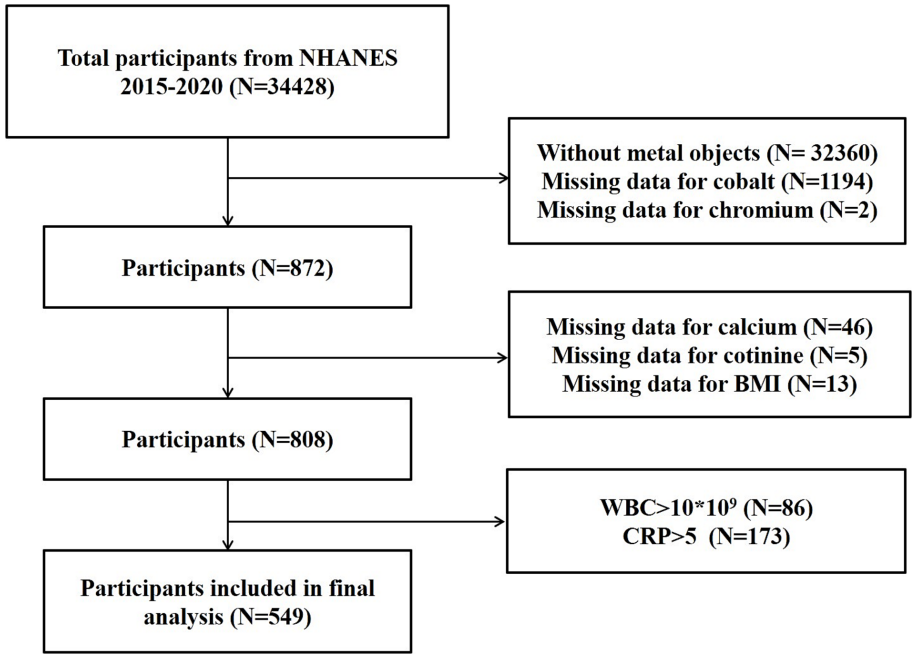

FIGURE 1
Flowchart diagram depicting the selection strategy of study participants.

corresponding to the first, second, and third tertiles, respectively. Antioxidants were allocated fractional values ranging from 0 to 2, whereas the scoring for pro-oxidants were inversely distributed. Finally, the OBS scores for each participant were aggregated to yield the individual final OBS values. Supplementary Table S1 shows the distribution scheme of OBS components.

2.3.2 Dependent variables

Whole blood specimens were processed, stored, and shipped to the Division of Laboratory Sciences, National Center for Environmental Health, Centers for Disease Control and Prevention, Atlanta, GA for analysis. The concentrations of cobalt (nmol/L) and chromium (nmol/L) in whole blood specimens were directly measured using inductively coupled plasma mass spectrometry (ICP-MS) (33).

2.3.3 Covariates

All covariates were identified based on findings from previous studies (22, 34). The demographic data, including age (year), gender (male/female), and ethnicity (Hispanic, non-Hispanic White, non-Hispanic Black, and Other Races), were collected. BMI was obtained from body measures. The criteria for identifying hypertension and diabetes were based on participants' self-reported medical diagnoses validated by a physician. Smoking status was ascertained through Questionnaire Data. Participants who had smoked fewer than 100 lifetime cigarettes were categorized as never smokers. Those who had smoked at least 100 cigarettes, but were not smoking at the time of the survey were classified as former smokers. Conversely, participants who had exceeded the 100 cigarette threshold and were actively smoking at the time of the survey were identified as current smokers (35). The neutrophil count (1,000 cells/μL), neutrophil percentage (%), lymphocyte count (1,000 cells/μL), monocyte number (1,000 cells/μL), and platelet count (1,000 cells/μL), were quantified utilizing the Complete Blood Count with a Five-Part Differential methodology. Blood urea nitrogen (mg/dL), iron (ug/dL), phosphorus (mg/dL), total protein (g/dL), albumin (g/dL), and uric acid (mg/dL) were assessed using Beckman UniCel® DxC800 Synchron. HDL-cholesterol (mg/dL) and total cholesterol (mg/dL) were quantified using Roche/Hitachi Modular P Chemistry Analyzer. The albumin in urine (mg/dL) was measured using a solid-phase fluorescent immunoassay by sequoia-Turner Digital Fluorometer, Model 450, urine creatinine (mg/dL) was determined by Enzymatic using Roche Cobas 6,000 Analyzer. Urinary albumin-creatinine ratio (UACR) was calculated by dividing urinary albumin by creatinine (36). Monocyte/HDL cholesterol ratio (MHR) was calculated as monocyte number divided by HDL cholesterol (37). Systemic immune-inflammation indicator (SII) was calculated by multiplying the platelet count by the neutrophil count and dividing by the lymphocyte count (38). Neutrophil percentage to albumin ratio (NPAR) was calculated as neutrophil percentage divided by albumin (39). The NHANES website provides full information on the laboratory procedures, data processing, quality control, and analytic notes.

2.4 Statistical analysis

The statistical software packages R 3.4.3[1] and EmpowerStats 2.0[2] were used to conduct data analysis, with $p < 0.05$ was considered statistically significant. All estimates were calculated with consideration of the NHANES sample weights. Continuous variables were compared using a weighted linear regression model, while

1 https://www.r-project.org/
2 http://www.empowerstats.com

categorical variables were assessed with a weighted chi-square test. Weighted multivariable linear regression analyses were performed to investigate the relationship of OBS with serum cobalt and chromium. Further investigation was conducted through subgroup analyses, stratified by age and gender. The presence of non-linear relationships was examined using generalized additive models and smooth curve fittings. When non-linearity was detected, a two-piecewise linear regression model was employed to analyze the threshold effect.

3 Results

3.1 Baseline characteristics

In accordance with the inclusion and exclusion criteria, a total of 549 participants were deemed eligible for inclusion in the definitive analysis. These participants were divided into four groups based on OBS levels. As the levels of OBS escalate, there is a progressive decline in the levels of serum cobalt, BMI, urine creatinine, and uric acid, as well as the incidence rates of diabetes and hypertension (Table 1).

3.2 Association between OBS, dietary OBS, lifestyle OBS, and serum cobalt

Multiple linear regression analyses were conducted to evaluate the correlations between OBS, dietary OBS, lifestyle OBS, and serum cobalt level. The unadjusted and adjusted outcomes of these analyses are presented in Table 2. In all models examined, no significant correlation was observed between OBS and lifestyle OBS with respect to serum cobalt levels. Dietary OBS was found negatively associated with serum cobalt levels in fully adjusted model (model 3: $\beta = -0.179$, 95%CI: −0.358 to −0.001, *P*: 0.04918), but not in unadjusted and partially adjusted model.

3.3 Subgroup analysis for the relationship of OBS, dietary OBS, lifestyle OBS, and serum cobalt

When stratified by gender, negative relationships of OBS (model 3: $\beta = -0.259$, 95%CI: −0.487 to −0.032, *P*: 0.02626) and dietary OBS (model 3: $\beta = -0.288$, 95%CI: −0.524 to −0.052, *P*: 0.01740) with serum cobalt were found to be statistically significant in males while not in females (Table 3).

In subgroup analysis stratified by age, we observed negative relationships of OBS (model 3: $\beta = -0.545$, 95%CI: −0.982 to −0.108, *P*: 0.01545) and dietary OBS (model 3: $\beta = -0.657$, 95%CI: −1.110 to −0.205, *P*: 0.00496) with serum cobalt only in ≥70 years old participants, but not in other age groups (Table 4).

3.4 Threshold effect analysis

The relationship between OBS and serum cobalt exhibited a non-linear pattern, as shown by smooth curve fitting (Figure 2A). When OBS < 19.7, a one-unit increase in OBS level was associated with 0.5 units decrease in serum cobalt level. When OBS was >19.7, no significant association was observed with serum cobalt (Figure 2A and Table 5).

Similarly, dietary OBS and serum cobalt exhibited a non-linear relationship as shown by smooth curve fitting (Figure 3A). When dietary OBS < 9.6, a one-unit increase in dietary OBS was associated with 2.225 units decrease in serum cobalt level. When OBS was >9.6, no significant association was observed with serum cobalt (Figure 3A and Table 5).

When stratified by gender, linear relationships of OBS and dietary OBS with serum cobalt were detected in males (Figures 2B, 3B). When stratified by age, non-linear relationships of OBS and dietary OBS with serum cobalt were observed in ≥70 years old participants (Figures 2C, 3C). When OBS < 16.3, a one-unit increase in OBS level was associated with 1.904 units decrease in serum cobalt level. When OBS was >16.3, no significant association was observed with serum cobalt. Similarly, when dietary OBS < 8.7, a one-unit increase in dietary OBS level was associated with 5.184 units decrease in serum cobalt level. When dietary OBS was >8.7, no significant association was observed with serum cobalt (Table 6).

4 Discussion

To investigate the association between oxidative stress and metal ion levels in patients with metal implants, we conducted a large-scale cross-sectional study involving 549 representative participants based on data from NHANES 2015–2020. Our results indicated that as the OBS increased, serum cobalt levels gradually decreased. These findings highlight the importance of managing OBS in individuals with metal implants. Elevated OBS and dietary OBS levels are indicative of lower cobalt levels, ultimately helping to minimize the impact of metal ions on health.

Aging is an irreversible trend that has led to a significant increase in orthopedic degenerative diseases and their complications among the elderly population, thereby resulting in a continuous rise in the demand for metal implants. Epidemiological studies indicate that the prevalence of chronic diseases, such as hypertension, coronary heart disease, and diabetes, is relatively high in this demographic. Therefore, it is crucial to explore the factors influencing the progression of chronic disease in patients who have undergone metal implantation. Oxidative stress refers to the imbalance between antioxidant defense mechanisms and the production of ROS, and it has been confirmed to be closely associated with various chronic diseases. Oxidative stress is considered a significant contributing factor to cardiovascular diseases like atherosclerosis, heart disease, and hypertension, and it also plays a vital role in the onset and progression of diabetes (40). Hyperglycemic states can trigger the production of ROS, leading to insulin resistance and β-cell dysfunction. Furthermore, oxidative stress is closely related to complications of diabetes, including cardiovascular diseases, kidney disease, and neuropathy (41). Our research has revealed that as OBS levels increase, the incidence of diabetes and hypertension gradually decreases, and renal function also shows improvement. This finding suggests that maintaining a healthy lifestyle and a diet rich in antioxidants can help mitigate the progression of chronic diseases in patients receiving metal implant therapy.

Mechanical wear and fluid corrosion have long been recognized as the primary factors leading to the generation of metallic particles and the release of metal ions (42, 43). In recent years, the role of oxidative stress in this process has garnered increasing attention. Research indicates that oxidative stress exacerbates the generation of metallic particles and the release of metal ions through various mechanisms,

TABLE 1 Baseline characteristics of study participants.

	OBS				
Characteristics	<10	≥10, <20	≥20, <30	≥30	*p*-value
n	66	203	225	55	
Age (years)	62.292 ± 12.112	64.521 ± 10.159	61.054 ± 12.267	61.236 ± 12.192	0.01531
BMI (kg/m^2)	31.124 ± 5.723	29.693 ± 5.075	29.545 ± 6.778	25.773 ± 3.402	<0.00001
Chromium (nmol/L)	9.512 ± 16.489	10.324 ± 9.739	8.210 ± 7.720	8.613 ± 7.542	0.13219
Cobalt (nmol/L)	10.269 ± 40.897	3.460 ± 7.514	4.370 ± 8.265	2.787 ± 1.290	0.01864
Urine creatinine (mg/dL)	122.523 ± 91.860	103.849 ± 62.542	98.079 ± 64.584	75.665 ± 48.977	0.00152
Blood urea nitrogen (mg/dL)	15.699 ± 7.220	16.286 ± 5.444	16.433 ± 4.857	16.791 ± 4.212	0.73797
Iron (μg/dL)	89.411 ± 26.580	85.607 ± 28.057	86.114 ± 33.064	86.230 ± 37.065	0.91010
Phosphorus (mg/dL)	3.673 ± 0.514	3.666 ± 0.494	3.709 ± 0.564	3.728 ± 0.514	0.77810
Total Protein (g/dL)	7.049 ± 0.413	6.971 ± 0.407	6.910 ± 0.361	7.055 ± 0.328	0.01160
Uric acid (mg/dL)	5.375 ± 1.360	5.591 ± 1.361	5.336 ± 1.362	4.750 ± 1.038	0.00016
Monocyte number (1,000 cells/μL)	0.626 ± 0.187	0.571 ± 0.163	0.574 ± 0.178	0.596 ± 0.298	0.31775
HDL-cholesterol (mg/dL)	55.236 ± 16.203	57.743 ± 22.547	56.273 ± 19.857	60.625 ± 16.961	0.39335
Total cholesterol (mg/dL)	186.738 ± 32.688	192.013 ± 43.755	193.473 ± 47.404	198.341 ± 32.718	0.55408
MHR	0.012 ± 0.005	0.012 ± 0.007	0.012 ± 0.006	0.011 ± 0.007	0.66601
UACR	0.520 ± 2.228	0.208 ± 1.025	0.559 ± 2.937	0.240 ± 0.622	0.34465
NPAR	0.949 ± 0.298	0.904 ± 0.262	0.951 ± 0.285	0.835 ± 0.283	0.01519
SII	464.666 ± 210.373	483.256 ± 250.736	520.514 ± 255.919	501.649 ± 215.223	0.33337
Dietary OBS	4.371 ± 1.365	11.350 ± 2.756	20.929 ± 3.131	26.585 ± 1.436	<0.00001
Lifestyle OBS	3.077 ± 1.120	3.397 ± 1.302	3.552 ± 1.349	4.979 ± 1.083	<0.00001
Gender					0.50096
Male	47.250	43.238	47.368	37.636	
Female	52.750	56.762	52.632	62.364	
Race					0.11863
Hispanic	9.240	9.561	7.862	4.006	
Non-Hispanic White	70.385	74.423	79.801	85.374	
Non-Hispanic Black	16.173	6.800	4.519	3.096	
Other	4.202	9.215	7.817	7.524	
Diabetes					0.02921
Yes	24.417	19.821	12.504	5.818	
No	74.145	77.318	85.133	93.695	
Borderline	1.438	2.861	2.364	0.487	
Hypertension					0.00271
Yes	68.423	53.094	45.113	36.083	
No	31.577	46.906	54.887	63.917	
Smoking					0.28010
Never	37.659	39.608	47.766	48.476	
Former	37.057	41.651	36.792	41.180	
Still	25.283	18.742	15.442	10.343	

MHR, monocyte/high density lipoprotein cholesterol ratio; UACR, urinary albumin/creatinine ratio; NPAR, neutrophil percentage to albumin ratio; SII, systemic immune-inflammation indicator. Mean ± SD for continuous variables: *P*-value was calculated by weighted linear regression model. Percent for categorical variables: *P*-value was calculated by weighted chi-square test.

such as enhancing the corrosion rate of metal implants, promoting inflammatory responses, intensifying cellular damage and apoptosis, and altering the surface characteristics of materials. The increase in ROS accelerates the degradation of implants while diminishing the tissue's ability to clear metal ions, thereby exacerbating the accumulation of metallic particles and ions in the surrounding environment (44–47). Xu et al. (44) observed extensive infiltration and accumulation of macrophages in the synovial tissue of patients with failed metal hip

TABLE 2 Relationships of OBS, dietary OBS, lifestyle OBS, and the cobalt level.

Outcome	Model 1		Model 2		Model 3	
	β (95%CI)	p-value	β (95%CI)	P-value	β (95%CI)	P-value
OBS	−0.100 (−0.256, 0.056)	0.20771	−0.086 (−0.246, 0.075)	0.29628	−0.155 (−0.328, 0.018)	0.07924
Dietary OBS	−0.129 (−0.292, 0.035)	0.12269	−0.109 (−0.278, 0.059)	0.20412	−0.179 (−0.358, −0.001)	0.04918
Lifestyle OBS	0.485 (−0.350, 1.320)	0.25504	0.390 (−0.473, 1.253)	0.37604	0.556 (−0.564, 1.676)	0.33119

Model 1: no covariates were adjusted.
Model 2: age, M-HDL, and UACR were adjusted.
Model 3: age, BMI (kg/m^2), diabetes, hypertension, smoking, urine creatinine (mg/dL), blood urea nitrogen (mg/dL), iron (μg/dL), phosphorus (mg/dL), total Protein (g/dL), uric acid (mg/dL), monocyte number (1,000 cells/μL), HDL-Cholesterol (mg/dL), total Cholesterol (mg/dL), M-HDL, UACR, NPAR, and SII were adjusted.

TABLE 3 Relationships of OBS, dietary OBS, lifestyle OBS, and the cobalt level stratified by gender.

Outcome	Male		Female	
	β (95%CI)	P-value	β (95%CI)	P-value
Model 1				
OBS	−0.153 (−0.356, 0.051)	0.14243	−0.054 (−0.288, 0.180)	0.65016
Dietary OBS	−0.186 (−0.398, 0.027)	0.08746	−0.076 (−0.322, 0.169)	0.54266
Lifestyle OBS	0.479 (−0.600, 1.558)	0.38494	0.442 (−0.822, 1.707)	0.49358
Model 2				
OBS	−0.124 (−0.328, 0.080)	0.23453	−0.046 (−0.289, 0.197)	0.71257
Dietary OBS	−0.154 (−0.368, 0.060)	0.16057	−0.063 (−0.318, 0.192)	0.62932
Lifestyle OBS	0.428 (−0.662, 1.517)	0.44209	0.332 (−0.981, 1.645)	0.62048
Model 3				
OBS	−0.259 (−0.487, −0.032)	0.02626	−0.102 (−0.376, 0.171)	0.46308
Dietary OBS	−0.288 (−0.524, −0.052)	0.01740	−0.122 (−0.403, 0.158)	0.39272
Lifestyle OBS	0.332 (−1.175, 1.839)	0.66641	0.528 (−1.167, 2.222)	0.54214

Model 1: no covariates were adjusted.
Model 2: age, M-HDL, and UACR were adjusted.
Model 3: age, BMI (kg/m^2), diabetes, hypertension, smoking, creatinine, urine (mg/dL), blood urea nitrogen (mg/dL), iron (μg/dL), phosphorus (mg/dL), total Protein (g/dL), uric acid (mg/dL), monocyte number (1,000 cells/μL), HDL-Cholesterol (mg/dL), total cholesterol (mg/dL), M-HDL, UACR, NPAR, and SII were adjusted.

prostheses. Their study revealed that cobalt released from the metal implants stimulate surrounding immune cells to produce ROS, which subsequently downregulate the RhoA signaling pathway in macrophages. This alteration results in increased formation of intracellular podosome-type adhesion structures and enhanced adhesion to the extracellular matrix, ultimately leading to decreased motility of the macrophages (44). Furthermore, Kim et al. (47) found that ROS induced by metal implants could trigger apoptosis in osteoblasts and gingival fibroblasts through the activation of the Nrf2/ARE pathway and the upregulation of heme oxygenase-1. What is even worse, the significant entry of metal ions into the bloodstream can provoke systemic toxic reactions, impacting the functionality of vital organs. Metals such as cobalt, chromium, nickel, and titanium, which are major components of metal implants, have gained increasing attention due to the health issues they may cause. In a prospective study involving 100 patients with metal implants, researcher Brodner evaluated the serum cobalt concentrations in patients following metal-on-metal total hip arthroplasty, finding that the serum cobalt levels exceeded the detection limit (48). Another study described a 70-year-old patient with cobalt toxicity, whose primary symptoms included progressive hearing and vision deterioration, cataracts, and axonal sensorimotor neuropathy (49). Signorello et al. (50) found that cobalt released from metal implants enters the bloodstream and ultimately accumulates in large amounts in the bladder, resulting in a significant increase in the incidence rate of bladder cancer among patients undergoing hip replacement surgeries. Building on this, Speer et al. (46) investigated the effects of cobalt on human urothelial cells and revealed that soluble cobalt induces cell cycle arrest, leading to cytotoxicity and genotoxicity. Moreover, elevated levels of serum cobalt have also been found to closely associated with increased risks of cardiovascular diseases, hormonal imbalances, immune system suppression, and reduced capacity for infection resistance (21, 51, 52). In this study, we observed a negative correlation between OBS, dietary OBS, and the serum cobalt levels in patients with metal implant. When OBS is less than 19.7, for every unit increase in OBS, the cobalt level decreased by 0.5 units. Similarly, when dietary OBS is less than 9.6, the cobalt levels reduced by 2.225 units as the unit dietary OBS raised. This suggests that maintaining a healthy lifestyle and dietary habits may be an effective strategy to reduce ion dissociation from metal implants, lower related complications, and improve the long-term survival rate of implants.

Previous studies have indicated that there are significant differences in the response to oxidative stress based on gender and age. Before puberty, girls appear to be more susceptible to metabolic dysfunction induced by oxidative stress, whereas elevated redox markers in boys seem to offer protection against arterial stiffness and maintain lipid homeostasis (53). This phenomenon suggests that sex may play a crucial

TABLE 4 Relationship of OBS, dietary OBS, lifestyle OBS, and the cobalt level stratified by age.

Outcome	<50		≥50, <60		≥60, <70		≥70	
	β (95%CI)	*P*-value	*β* (95%CI)	*P*-value	*β* (95%CI)	*P*-value	*β* (95%CI)	*P*-value
Model 1								
OBS	−0.032 (−0.028, 0.091)	0.30203	−0.019 (−0.147, 0.109)	0.77068	0.103 (−0.169, 0.375)	0.46034	−0.332 (−0.738, 0.075)	0.11123
Dietary OBS	0.019 (−0.043, 0.082)	0.54829	−0.031 (−0.168, 0.106)	0.65973	0.136 (−0.136, 0.409)	0.32842	−0.432 (−0.868, 0.004)	0.05367
Lifestyle OBS	0.384 (0.081, 0.688)	0.01522	0.231 (−0.460, 0.923)	0.51312	−1.001 (−2.502, 0.500)	0.19303	1.205 (−0.995, 3.404)	0.28423
Model 2								
OBS	0.026 (−0.032, 0.085)	0.37504	−0.025 (−0.158, 0.108)	0.71546	0.109 (−0.184, 0.403)	0.46614	−0.413 (−0.820, −0.005)	0.04846
Dietary OBS	0.016 (−0.045, 0.076)	0.61676	−0.036 (−0.178, 0.106)	0.61878	0.145 (−0.145, 0.436)	0.32802	−0.509 (−0.942, −0.077)	0.02212
Lifestyle OBS	0.337 (0.038, 0.637)	0.03006	0.201 (−0.516, 0.918)	0.58347	−1.184 (−2.798, 0.431)	0.15292	1.065 (−1.190, 3.321)	0.35565
Model 3								
OBS	0.022 (−0.039, 0.084)	0.48221	−0.098 (−0.266, 0.070)	0.25728	0.216 (−0.125, 0.558)	0.21683	−0.545 (−0.982, −0.108)	0.01545
Dietary OBS	0.019 (−0.043, 0.082)	0.54491	−0.114 (−0.291, 0.063)	0.20996	0.252 (−0.083, 0.586)	0.14332	−0.657 (−1.110, −0.205)	0.00496
Lifestyle OBS	0.144 (−0.257, 0.545)	0.48342	0.172 (−0.843, 1.187)	0.74097	−1.649 (−3.722, 0.424)	0.12152	2.836 (−0.191, 5.862)	0.06798

Model 1: no covariates were adjusted.
Model 2: M-HDL, and UACR were adjusted.
Model 3: BMI (kg/m^2), diabetes, hypertension, smoking, urine creatinine (mg/dL), blood urea nitrogen (mg/dL), iron (μg/dL), phosphorus (mg/dL), total Protein (g/dL), uric acid (mg/dL), monocyte number (1,000 cells/μL), HDL-Cholesterol (mg/dL), total Cholesterol (mg/dL), M-HDL, UACR, NPAR, and SII were adjusted.

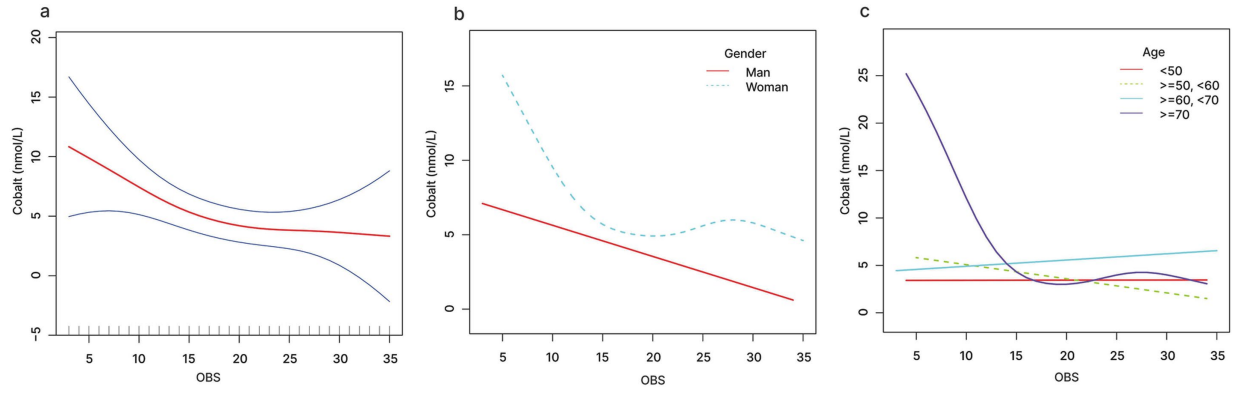

FIGURE 2
The relationship between OBS and serum cobalt **(A)**, stratified by gender **(B)**, stratified by age **(C)**.

role in regulating oxidative stress-related genes, such as NCF2 and NOX3. Furthermore, research has demonstrated that sex hormones can influence the expression and activity of NADPH oxidase genes and myeloperoxidase, resulting in differences in the response to oxidative stress between males and females (54). Antioxidant lifestyles have been shown to play a significant protective role in the prevention and treatment of depression in women (23). Additionally, Cao's research has found stronger protective effects of dietary antioxidants in women, suggesting that dietary changes can effectively prevent chronic kidney disease (55). This phenomenon may be attributed to the regulation of most proteins involved in redox status and mitochondrial function by sex hormones (56). The expression of mitochondrial related genes has been shown to be closely related to gender, suggesting a key role of sex hormone signaling in mitochondrial dynamics and cellular redox biology (57). When activated, estrogen-related receptors improve fatty acid oxidation, mitochondrial dynamics, and respiratory chain activity (58, 59). The results of our study indicate that the negative correlation between OBS and serum cobalt levels is pronounced in men but not as

evident in women. This discrepancy may be related to differences in hormone levels, as estrogen is known to combat oxidative stress. Itagaki et al. (60) have found that estradiol inhibits the production of ROS and MAPK signaling, thereby preventing the activation of transcription factors and inactivating the downstream transcription processes involved in the expression and activation of TGF-β. Additionally, Sun's research indicates that β-estradiol can enhance ROS generation and RUBICON expression, further promoting LC3B-associated phagocytosis in macrophages, which suggests a novel perspective for understanding the mechanism of trained immunity in gender differences during sepsis response (61). Furthermore, women tend to adopt healthier lifestyle choices compared to men, which may contribute to a lack of significant impact on their serum cobalt levels. Consequently, dietary modifications may be more beneficial for lowering serum cobalt levels in men.

Moreover, subgroup analyses reveal significant differences in the association between OBS and serum cobalt levels across various age groups. A notable negative correlation is observed in participants over the age of 70, while this correlation is less pronounced in other age groups. This finding is consistent with previous research by Qu, which highlighted a stronger negative correlation between OBS and periodontitis in the elderly (24). Xiao et al. (62) comprehensively identified redox-modified disease networks that are remodeled in aged mice, establishing a systemic molecular foundation for the complex links between redox dysregulation and tissue aging. They found that the bladders of aged mice exhibit baseline reactive oxygen species (ROS) accumulation and heightened oxidative stress. Mysorekar' team discovered that D-mannose treatment reversed autophagy flux, rescued the senescence-associated secretory phenotype, and alleviated ROS and the shedding of NLRP3/Gasdermin/IL-1β-driven pyroptotic epithelial cell in elderly animals (63). These phenomena may be associated with the decline in cellular repair capacity and the efficiency of antioxidant defense systems that often accompany aging. Therefore, it is crucial for older adults to improve their OBS in order to reduce serum cobalt levels and mitigate the toxic effects of cobalt.

TABLE 5 Threshold effect analysis of OBS and dietary OBS on the cobalt level using the two-piecewise linear regression model.

	Adjusted β (95%CI)	*P*-value
OBS infection point	19.7	
OBS < 19.7	−0.500 (−0.876, −0.125)	0.0093
OBS > 19.7	0.154 (−0.191, 0.499)	0.3818
Log likelihood ratio	0.039	
Dietary OBS infection point	9.6	
Dietary OBS < 9.6	−2.225 (−3.120, −1.329)	<0.0001
Dietary OBS > 9.6	0.161 (−0.067, 0.389)	0.1662
Log likelihood ratio	<0.001	

The age, BMI (kg/m^2), diabetes, hypertension, smoking, urine creatinine (mg/dL), blood urea nitrogen (mg/dL), iron (μg/dL), phosphorus (mg/dL), total Protein (g/dL), uric acid (mg/dL), monocyte number (1,000 cells/μL), HDL-Cholesterol (mg/dL), total Cholesterol (mg/dL), M-HDL, UACR, NPAR, and SII were adjusted.

This study exhibits prominent strengths. Firstly, the data from NHANES were obtained by a sophisticated, multi-stage probability sampling design, strictly adhered to comprehensive quality control to ensure the effectiveness and integrity of the dataset. Therefore, based on the database, our results are highly credible when extended to non-institutionalized populations, especially, the association was validated to be robust after the adjustment for various confounders. Second, an increasing number of studies have demonstrated a significant correlation between CRP levels and biomarkers associated with oxidative stress, indicating that inflammation and infection may be potential factors influencing oxidative stress. To mitigate this impact, we implemented stringent exclusion criteria to omit individuals with CRP levels exceeding 5 mg/L, thereby enhancing the reliability of our findings (64, 65). Third, the present study concentrated on the OBS, encompassing a composite indicator of antioxidant lifestyle and diet, rather than monitoring single component in isolation. This approach enables a more thoroughgoing understanding of the intricate interplay among diverse diet and lifestyle factors in the population with metal implants, as well as their association with the serum cobalt level. Fourth, our study found the association between OBS and serum cobalt level for the first time in population with metal implants and uncovered the gender-specific and age-specific effects of OBS on the serum cobalt level. Fifth, the use of an appropriate covariate adjustment increased the representativeness and reliability of our study. Therefore, the findings carry vital public health implications in the mitigation of the metal ions toxicity on human with metal implants.

Nevertheless, there were also a few limitations in this study. Firstly, the grading criteria for physical activity lack uniformity and

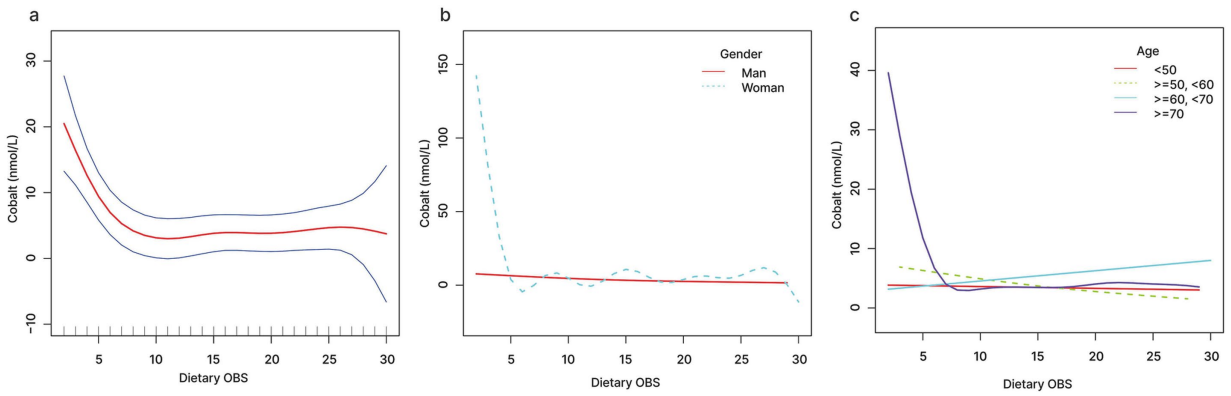

FIGURE 3
The relationship between dietary OBS and serum cobalt **(A)**, stratified by gender **(B)**, stratified by age **(C)**.

TABLE 6 Threshold effect analysis of OBS and dietary OBS on the cobalt level in ≥70 participants using the two-piecewise linear regression model.

	Adjusted β (95%CI)	*P*-value
OBS infection point	16.3	
OBS < 16.3	−1.904 (−3.261, −0.548)	0.0066
OBS > 16.3	0.060 (−0.660, 0.780)	0.8711
Log likelihood ratio	0.029	
Dietary OBS infection point	8.7	
Dietary OBS < 8.7	−5.184 (−7.497, −2.871)	<0.0001
Dietary OBS > 8.7	0.053 (−0.510, 0.615)	0.8548
Log likelihood ratio	<0.001	

The age, BMI (kg/m^2), diabetes, hypertension, smoking, creatinine, urine (mg/dL), blood urea nitrogen (mg/dL), iron (μg/dL), phosphorus (mg/dL), total Protein (g/dL), uric acid (mg/dL), monocyte number (1,000 cells/μL), HDL-Cholesterol (mg/dL), total Cholesterol (mg/dL), M-HDL, UACR, NPAR, and SII were adjusted.

certain essential data are inaccessible. Therefore, physical activity was excluded from the calculation of the OBS score. Second, our design of a cross-sectional survey restricts causal inferences between OBS and serum cobalt level. So further prospectively designed studies are needed to verify the causality between OBS and serum cobalt level in human with metal objects. Meanwhile, the biases of recall and reporting using self-reported questionnaires may compromise the accuracy of OBS calculations. Third, the level of metal ions in the human body is influenced by environment and occupation. However, due to privacy concerns, the NHANES database fail to get the geographical location and living status of participants, which makes it impossible to estimate the impact of environmental and occupational exposure on metal ions of human body. Moreover, the uncertainty of implantation type, quantity, reason, or duration, determined the highly heterogeneity of the included population. Finally, the level of metal ions may alter with prolonged postoperative time, so a longer follow-up is extremely needed to further clarify the relationship between the OBS and the serum cobalt level in the population with metal implants.

5 Conclusion

In conclusion, data from a nationally representative sample uncovers the significant negative association between OBS and the level of serum cobalt in the population with metal implants. This negative correlation has been corroborated across different gender and age subgroups. Notably, the protective effects of an antioxidant diet and healthy lifestyle are particularly pronounced among males and individuals aged over 70. For the population with metal implants, maintaining good dietary and lifestyle habits may help reduce the generation of metal particles and the dissociation of metal ions, thereby improving the survival rate of metal implants and decreasing the risk of related complications.

Data availability statement

The original contributions presented in the study are included in the article/Supplementary material, further inquiries can be directed to the corresponding author.

Ethics statement

The studies involving humans were approved by the National Center for Health Statistics ethics review board. The studies were conducted in accordance with the local legislation and institutional requirements. The human samples used in this study were acquired from NHANES. The National Center for Health Statistics ethics review board approved all NHANES protocols, and informed consent was obtained from every participant. Written informed consent for participation was not required from the participants or the participants' legal guardians/next of kin in accordance with the national legislation and institutional requirements.

Author contributions

WY: Conceptualization, Writing – original draft. JC: Investigation, Writing – original draft. JS: Methodology, Writing – original draft. CS: Methodology, Writing – original draft. ZC: Conceptualization, Validation, Writing – review & editing.

Funding

The author(s) declare that financial support was received for the research, authorship, and/or publication of this article. This research was supported by Postdoctoral Science Grant of School and Hospital of Stomatology Fujian Medical University (No. 202301), Startup Fund for Scientific Research, Fujian Medical University (No. 2023QH1146), and Fujian Medical University Union Hospital Talent Launch Fund Project (No. 2024XH017).

Conflict of interest

The authors declare that the research was conducted in the absence of any commercial or financial relationships that could be construed as a potential conflict of interest.

Publisher's note

Supplementary material

The Supplementary material for this article can be found online at: https://www.frontiersin.org/articles/10.3389/fnut.2024.1485428/full#supplementary-material

References

1. Ni J, Ling H, Zhang S, Wang Z, Peng Z, Benyshek C, et al. Three-dimensional printing of metals for biomedical applications. *Mater Today Bio*. (2019) 3:100024. doi: 10.1016/j.mtbio.2019.100024

2. Meng M, Wang J, Huang H, Liu X, Zhang J, Li Z. 3D printing metal implants in orthopedic surgery: methods, applications and future prospects. *J Orthop Translat*. (2023) 42:94–112. doi: 10.1016/j.jot.2023.08.004

3. Yin S, Lin S, Xu J, Yang G, Chen H, Jiang X. Dominoes with interlocking consequences triggered by zinc: involvement of microelement-stimulated MSC-derived exosomes in senile osteogenesis and osteoclast dialogue. *J Nanobiotechnol*. (2023) 21:346. doi: 10.1186/s12951-023-02085-w

4. Huang P, Xu J, Xie L, Gao G, Chen S, Gong Z, et al. Improving hard metal implant and soft tissue integration by modulating the "inflammatory-fibrous complex" response. *Bioact Mater*. (2023) 20:42–52. doi: 10.1016/j.bioactmat.2022.05.013

5. Dong J, Zhang L, Ruan B, Lv Z, Wang H, Wang Y, et al. NRF2 is a critical regulator and therapeutic target of metal implant particle-incurred bone damage. *Biomaterials*. (2022) 288:121742. doi: 10.1016/j.biomaterials.2022.121742

6. Huang XY, Chang LJ, Zhao H, Cai Z. Study on craniocerebral dynamics response and helmet protective performance under the blast waves. *Mater Des*. (2022) 224:111408. doi: 10.1016/j.matdes.2022.111408

7. Lee K, Goodman SB. Current state and future of joint replacements in the hip and knee. *Expert Rev Med Devices*. (2008) 5:383–93. doi: 10.1586/17434440.5.3.383

8. Puolakka TJ, Pajamäki KJ, Halonen PJ, Pulkkinen PO, Paavolainen P, Nevalainen JK. The Finnish arthroplasty register: report of the hip register. *Acta Orthop Scand*. (2001) 72:433–41. doi: 10.1080/000164701753532745

9. de Steiger RN, Hang JR, Miller LN, Graves SE, Davidson DC. Five-year results of the ASR XL acetabular system and the ASR hip resurfacing system: an analysis from the Australian Orthopaedic Association National Joint Replacement Registry. *J Bone Joint Surg Am*. (2011) 93:2287–93. doi: 10.2106/JBJS.J.01727

10. Freeman MA, Swanson SA, Heath JC. Study of the wear particles produced from cobalt-chromium-molybdenum-manganese total joint replacement prostheses. *Ann Rheum Dis*. (1969) 28:Suppl:29 PMID: 5379846

11. Cohen D. How safe are metal-on-metal hip implants? *BMJ*. (2012) 344:e1410. doi: 10.1136/bmj.e1410

12. Grammatopoulos G, Pandit H, Kwon YM, Gundle R, McLardy-Smith P, Beard DJ, et al. Hip resurfacings revised for inflammatory pseudotumour have a poor outcome. *J Bone Joint Surg Br*. (2009) 91-B:1019–24. doi: 10.1302/0301-620X.91B8.22562

13. Ladon D, Doherty A, Newson R, Turner J, Bhamra M, Case CP. Changes in metal levels and chromosome aberrations in the peripheral blood of patients after metal-on-metal hip arthroplasty. *J Arthroplast*. (2004) 19:78–83. doi: 10.1016/j.arth.2004.09.010

14. Kalbacova M, Roessler S, Hempel U, Tsaryk R, Peters K, Scharnweber D, et al. The effect of electrochemically simulated titanium cathodic corrosion products on ROS production and metabolic activity of osteoblasts and monocytes/macrophages. *Biomaterials*. (2007) 28:3263–72. doi: 10.1016/j.biomaterials.2007.02.026

15. Anderson JM, Miller KM. Biomaterial biocompatibility and the macrophage. *Biomaterials*. (1984) 5:5–10. doi: 10.1016/0142-9612(84)90060-7

16. Ingham E, Fisher J. The role of macrophages in osteolysis of total joint replacement. *Biomaterials*. (2005) 26:1271–86. doi: 10.1016/j.biomaterials.2004.04.035

17. Toledano-Serrabona J, Camps-Font O, de Moraes DP, Corte-Rodríguez M, Montes-Bayón M, Valmaseda-Castellón E, et al. Ion release and local effects of titanium metal particles from dental implants: an experimental study in rats. *J Periodontol*. (2023) 94:119–29. doi: 10.1002/JPER.22-0091

18. Nandra RS, Elnahal WA, Mayne A, Brash L, McBryde CW, Treacy RBC. Birmingham hip resurfacing at 25 years. *Bone Joint J*. (2024) 106-B:540–7. doi: 10.1302/0301-620X.106B6.BJJ-2023-1064.R1

19. Wang Z, Xiang Q, Tan X, Zhang YD, Zhu HQ, Pu J, et al. Functionalized cortical bone-inspired composites adapt to the mechanical and biological properties of the edentulous area to resist fretting Wear. *Adv Sci*. (2023) 10:e2207255. doi: 10.1002/advs.202207255

20. Wu D, Bhalekar RM, Marsh JS, Langton DJ, Stewart AJ. Periarticular metal hypersensitivity complications of hip bearings containing cobalt-chromium. *EFORT Open Rev*. (2022) 7:758–71. doi: 10.1530/EOR-22-0036

21. Huber M, Reinisch G, Trettenhahn G, Zweymuller K, Lintner F. Presence of corrosion products and hypersensitivity-associated reactions in periprosthetic tissue after aseptic loosening of total hip replacements with metal bearing surfaces. *Acta Biomater*. (2009) 5:172–80. doi: 10.1016/j.actbio.2008.07.032

22. He J, Li J, Wu S, Wang J, Tang Q. Accumulation of blood chromium and cobalt in the participants with metal objects: findings from the 2015 to 2018 National Health and nutrition examination survey (NHANES). *BMC Geriatr*. (2023) 23:72. doi: 10.1186/s12877-022-03710-3

23. Liu X, Liu X, Wang Y, Zeng B, Zhu B, Dai F. Association between depression and oxidative balance score: National Health and nutrition examination survey (NHANES) 2005-2018. *J Affect Disord*. (2023) 337:57–65. doi: 10.1016/j.jad.2023.05.071

24. Qu H. The association between oxidative balance score and periodontitis in adults: a population-based study. *Front Nutr*. (2023) 10:1138488. doi: 10.3389/fnut.2023.1138488

25. Wang X, Hu J, Liu L, Zhang Y, Dang K, Cheng L, et al. Association of Dietary Inflammatory Index and Dietary Oxidative Balance Score with all-cause and disease-specific mortality: findings of 2003-2014 National Health and nutrition examination survey. *Nutrients*. (2023) 15:3148. doi: 10.3390/nu15143148

26. Shahriarpour Z, Nasrabadi B, Hejri-Zarifi S, Shariati-Bafghi SE, Yousefian-Sanny M, Karamati M, et al. Oxidative balance score and risk of osteoporosis among postmenopausal Iranian women. *Arch Osteoporos*. (2021) 16:43. doi: 10.1007/s11657-021-00886-w

27. Sohouli MH, Baniasadi M, Hernández-Ruiz Á, Melekoglu E, Zendehdel M, José Soto-Méndez M, et al. Adherence to oxidative balance scores is associated with a reduced risk of breast cancer; a case-control study. *Nutr Cancer*. (2023) 75:164–73. doi: 10.1080/01635581.2022.2102658

28. Demirer B, Yardımcı H, Erem BS. Inflammation level in type 2 diabetes is associated with dietary advanced glycation end products, Mediterranean diet adherence and oxidative balance score: a pathway analysis. *J Diabetes Complicat*. (2023) 37:108354. doi: 10.1016/j.jdiacomp.2022.108354

29. Lee J-H, Joo YB, Han M, Kwon SR, Park W, Park KS, et al. Relationship between oxidative balance score and quality of life in patients with osteoarthritis: data from the Korea National Health and nutrition examination survey (2014-2015). *Medicine*. (2019) 98:e16355. doi: 10.1097/MD.0000000000016355

30. Chen Z, Chen J, Song C, Sun J, Liu W. Association between serum Iron status and muscle mass in adults: results from NHANES 2015-2018. *Front Nutr*. (2022) 9:941093. doi: 10.3389/fnut.2022.941093

31. Lei X, Xu Z, Chen W. Association of oxidative balance score with sleep quality: NHANES 2007-2014. *J Affect Disord*. (2023) 339:435–42. doi: 10.1016/j.jad.2023.07.040

32. Chen K, Yin Q, Guan J, Yang J, Ma Y, Hu Y, et al. Association between the oxidative balance score and low muscle mass in middle-aged US adults. *Front Nutr*. (2024) 11:1358231. doi: 10.3389/fnut.2024.1358231

33. Sampson B, Hart A. Clinical usefulness of blood metal measurements to assess the failure of metal-on-metal hip implants. *Ann Clin Biochem*. (2012) 49:118–31. doi: 10.1258/acb.2011.011141

34. Sun X, Deng Y, Fang L, Ni M, Wang X, Zhang T, et al. Association of Exposure to heavy metal mixtures with systemic immune-inflammation index among US adults in NHANES 2011-2016. *Biol Trace Elem Res*. (2024) 202:3005–17. doi: 10.1007/s12011-023-03901-y

35. Liu B, Sun Y, Xu G, Snetselaar LG, Ludewig G, Wallace RB, et al. Association between body Iron status and leukocyte telomere length, a biomarker of biological aging, in a nationally representative sample of US adults. *J Acad Nutr Diet*. (2019) 119:617–25. doi: 10.1016/j.jand.2018.09.007

36. Nugroho P, Susanto TH, Bonar M, Rizka A, Lydia A, Koesno S, et al. The correlation of MicroRNA-21 with the Nephrin, Podocin, and urinary albumin-creatinine ratio in patients with type 2 diabetes and albuminuria: a cross-sectional study. *Can J Kidney Health Dis*. (2024) 11:20543581241260948. doi: 10.1177/20543581241260948

37. Amouzegar A, Mirzaasgari Z, Mehrabi A, Malek M, Alaei-Shahmiri F, Najafi L, et al. Association of monocyte/high-density lipoprotein cholesterol ratio and the carotid intima-media thickness in diabetic patients. *BMC Endocr Disord*. (2022) 22:323. doi: 10.1186/s12902-022-01246-6

38. Zhang Y, Meng Y, Chen M, Baral K, Fu Y, Yang Y, et al. Correlation between the systemic immune-inflammation indicator (SII) and serum ferritin in US adults: a cross-sectional study based on NHANES 2015-2018. *Ann Med*. (2023) 55:2275148. doi: 10.1080/07853890.2023.2275148

39. Yu Y, Zhong Z, Yang W, Yu J, Li J, Guo X, et al. Neutrophil percentage-to-albumin ratio and risk of mortality in patients on peritoneal Dialysis. *J Inflamm Res*. (2023) 16:6271–81. doi: 10.2147/JIR.S437256

40. Shao R, Chen R, Zheng Q, Yao M, Li K, Cao Y, et al. Oxidative stress disrupts vascular microenvironmental homeostasis affecting the development of atherosclerosis. *Cell Biol Int*. (2024) 48:1781–801. doi: 10.1002/cbin.12239

41. Bej E, Cesare P, Volpe AR, d'Angelo M, Castelli V. Oxidative stress and neurodegeneration: insights and therapeutic strategies for Parkinson's disease. *Neurol Int*. (2024) 16:502–17. doi: 10.3390/neurolint16030037

42. Xu JW, Zhang Y, Huang YJ, Chang L, Chen T, Ren T, et al. Dynamic response of chain mail fabrics with variable stiffness. *Int J Mech Sci*. (2024) 264:108840. doi: 10.1016/j.ijmecsci.2023.108840

43. Xu JW, Chang LJ, Chen TW, Ren T, Zhang Y, Cai Z. Study of the bending properties of variable stiffness chain mail fabrics. *Compos Struct*. (2023) 322:117369. doi: 10.1016/j.compstruct.2023.117369

44. Xu J, Yang J, Nyga A, Ehteramyan M, Moraga A, Wu Y, et al. Cobalt (II) ions and nanoparticles induce macrophage retention by ROS-mediated down-regulation of RhoA expression. *Acta Biomater*. (2018) 72:434–46. doi: 10.1016/j.actbio.2018.03.054

45. Sabbioni E, Fortaner S, Farina M, del Torchio R, Olivato I, Petrarca C, et al. Cytotoxicity and morphological transforming potential of cobalt nanoparticles, microparticles and ions in Balb/3T3 mouse fibroblasts: an in vitro model. *Nanotoxicology*. (2014) 8:455–64. doi: 10.3109/17435390.2013.796538

46. Speer RM, The T, Xie H, Liou L, Adam RM, Wise JP Sr. The cytotoxicity and genotoxicity of particulate and soluble cobalt in human urothelial cells. *Biol Trace Elem Res*. (2017) 180:48–55. doi: 10.1007/s12011-017-0989-z

47. Kim E-C, Kim M-K, Leesungbok R, Lee SW, Ahn SJ. Co-Cr dental alloys induces cytotoxicity and inflammatory responses via activation of Nrf2/antioxidant signaling pathways in human gingival fibroblasts and osteoblasts. *Dent Mater*. (2016) 32:1394–405. doi: 10.1016/j.dental.2016.09.017

48. Brodner W, Bitzan P, Meisinger V, Kaider A, Gottsauner-Wolf F, Kotz R. Serum cobalt levels after metal-on-metal total hip arthroplasty. *J Bone Joint Surg Am*. (2003) 85:2168–73. doi: 10.2106/00004623-200311000-00017

49. Heuer C, Streit A-C, Sprengel K, Hasler RM, Ziegenhain F, Zahorecz M, et al. Cobalt intoxication: mitochondrial features and condition. *J Neurol*. (2022) 269:6655–7. doi: 10.1007/s00415-022-11243-3

50. Signorello LB, Ye W, Fryzek JP, Lipworth L, Fraumeni JF, Blot WJ, et al. Nationwide study of cancer risk among hip replacement patients in Sweden. *J Natl Cancer Inst*. (2001) 93:1405–10. doi: 10.1093/jnci/93.18.1405

51. Fleury C, Petit A, Mwale F, Antoniou J, Zukor DJ, Tabrizian M, et al. Effect of cobalt and chromium ions on human MG-63 osteoblasts in vitro: morphology, cytotoxicity, and oxidative stress. *Biomaterials*. (2006) 27:3351–60. doi: 10.1016/j.biomaterials.2006.01.035

52. Skjöldebrand C, Tipper JL, Hatto P, Bryant M, Hall RM, Persson C. Current status and future potential of wear-resistant coatings and articulating surfaces for hip and knee implants. *Mater Today Bio*. (2022) 15:100270. doi: 10.1016/j.mtbio.2022.100270

53. Basnet TB, Khatri B. Oxidative stress-related genetic variation and antioxidant vitamin intake in intact and ruptured abdominal aortic aneurysm: does sex matter? *Eur J Prev Cardiol*. (2024) 31:59–60. doi: 10.1093/eurjpc/zwad342

54. Fernández-Espejo E, Rodríguez de Fonseca F, Gavito AL, Córdoba-Fernández A, Chacón J, Martín de Pablos Á. Myeloperoxidase and advanced oxidation protein products in the cerebrospinal fluid in women and men with Parkinson's disease. *Antioxidants*. (2022) 11:1088. doi: 10.3390/antiox11061088

55. Cao Y, Zhou Y, Zhong Y, Liao X, Chen X, Pi Y. Association between oxidative balance score in adults with and without chronic kidney disease: 2011-2028 NHANES. *Front Nutr*. (2024) 11:1374719. doi: 10.3389/fnut.2024.1374719

56. Wang JQ, Li ZJ, Gao H, Sheng J, Liang CM, Hu YB, et al. Gender associations between phthalate exposure and biomarkers of oxidative stress: a prospective cohort study. *Toxicol Ind Health*. (2024) 40:312–22. doi: 10.1177/07482337241245453

57. di Florio DN, Sin J, Coronado MJ, Atwal PS, Fairweather DL. Sex differences in inflammation, redox biology, mitochondria and autoimmunity. *Redox Biol*. (2020) 31:101482. doi: 10.1016/j.redox.2020.101482

58. Chen Y, Liu Y, Dorn GW. Mitochondrial fusion is essential for organelle function and cardiac homeostasis. *Circ Res*. (2011) 109:1327–31. doi: 10.1161/CIRCRESAHA.111.258723

59. Wang T, McDonald C, Petrenko NB, Leblanc M, Wang T, Giguere V, et al. Estrogen-related receptor α (ERRα) and ERRγ are essential coordinators of cardiac metabolism and function. *Mol Cell Biol*. (2015) 35:1281–98. doi: 10.1128/MCB.01156-14

60. Itagaki T, Shimizu I, Cheng X, Yuan Y, Oshio A, Tamaki K, et al. Opposing effects of oestradiol and progesterone on intracellular pathways and activation processes in the oxidative stress induced activation of cultured rat hepatic stellate cells. *Gut*. (2005) 54:1782–9. doi: 10.1136/gut.2004.053728

61. Sun Z, Qu J, Xia X, Pan Y, Liu X, Liang H, et al. 17β-estradiol promotes LC3B-associated phagocytosis in trained immunity of female mice against sepsis. *Int J Biol Sci*. (2021) 17:460–74. doi: 10.7150/ijbs.53050

62. Xiao H, Jedrychowski MP, Schweppe DK, Huttlin EL, Yu Q, Heppner DE, et al. A quantitative tissue-specific landscape of protein redox regulation during aging. *Cell*. (2020) 180:968–983.e24. doi: 10.1016/j.cell.2020.02.012

63. Joshi CS, Salazar AM, Wang C, Ligon MM, Chappidi RR, Fashemi BE, et al. D-mannose reduces cellular senescence and NLRP3/GasderminD/IL-1β-driven pyroptotic uroepithelial cell shedding in the murine bladder. *Dev Cell*. (2024) 59:33–47.e5. doi: 10.1016/j.devcel.2023.11.017

64. Nemeckova I, Eissazadeh S, Rathouska JU, Silhavy J, Malinska H, Pravenec M, et al. Transgenic human C-reactive protein affects oxidative stress but not inflammation biomarkers in the aorta of spontaneously hypertensive rats. *BMC Cardiovasc Disord*. (2024) 24:211. doi: 10.1186/s12872-024-03870-7

65. Huang X, Zhang J, Liu J, Sun L, Zhao H, Lu Y, et al. C-reactive protein promotes adhesion of monocytes to endothelial cells via NADPH oxidase-mediated oxidative stress. *J Cell Biochem*. (2012) 113:857–67. doi: 10.1002/jcb.23415

frontiers | Frontiers in Nutrition

TYPE Original Research
PUBLISHED 13 December 2024
DOI 10.3389/fnut.2024.1469952

OPEN ACCESS

EDITED BY
Jagannath Misra,
Purdue University Indianapolis, United States

REVIEWED BY
Georgia Damoraki,
National and Kapodistrian University of Athens, Greece
Gang Wei,
Capital Medical University, China

*CORRESPONDENCE
Johnny Amer
✉ johnnyamer@hotmail.com

†These authors have contributed equally to this work

RECEIVED 24 July 2024
ACCEPTED 11 November 2024
PUBLISHED 13 December 2024

CITATION
Amer J, Amleh A, Salhab A, Kolodny Y, Yochelis S, Saffouri B, Paltiel Y and Safadi R (2024) High-fat diet mouse model receiving L-glucose supplementations propagates liver injury.
Front. Nutr. 11:1469952.
doi: 10.3389/fnut.2024.1469952

High-fat diet mouse model receiving L-glucose supplementations propagates liver injury

Johnny Amer[1]*†, Athar Amleh[1†], Ahmad Salhab[1], Yuval Kolodny[2], Shira Yochelis[2], Baker Saffouri[1], Yossi Paltiel[2] and Rifaat Safadi[1]

[1]Liver Institute, Hadassah-Hebrew University Hospital, Jerusalem, Israel, [2]Applied Physics Department, Center for Nanoscience and Nanotechnology, Hebrew University Givaat Ram, Jerusalem, Israel

Background and aims: Limited data link manufactured sweeteners impact on metabolic dysfunction-associated steatotic liver disease (MASLD). We aimed to evaluate the effects of manufactured sugars (L-glucose) compared to natural sugars (D-glucose) on phenotype, molecular and metabolic changes in mice models fed with either regular diet (RD) or high fat diet (HFD).

Methods: C57BL/6 mice fed 16-weeks with either RD; 70% carbohydrate or HFD; 60% fat, with or without additional glucose (Glu, at 18% w/v) to drinking tap water at weeks 8–16; of either natural (D-Glu) or manufactured (L-Glu) sugars. Liver inflammation (ALT and AST serum levels, liver H&E histologic stains and cell viability profile by p-AKT), liver fibrosis [quantitated α smooth-muscle-actin (αSMA) by western blot and RT-PCR, Masson Trichrome staining (MTC) of liver tissue], liver lipid [steatosis stain by H&E, Adipose Differentiation-Related Protein (ADRP) lipid accumulation, serum and lipid peroxidation Malondialdehyde (MDA) markers by ELISA], glucose hemostasis (serum Glucose and C-peptide with HOMA-IR score calculation) and liver aspects [hepatic glucose transporter 2 (GLUT2), insulin receptor (IR) expressions and GYS2/PYGL ratio] evaluated.

Results: D- and L-Glu supplementations propagate hepatocytes ballooning and steatosis in HFD-fed mice and were associated with αSMA down-expressions by 1.5-fold compared to the untreated group while showed an acceleration in liver fibrosis in the RD-fed mice. Lipid profile (Steatosis, ADRP and MDA) significantly increased in HFD-fed mice, both Glu supplementations (mainly the L-Glu) increased serum MDA while decreased ADRP. HOMA-IR score and IR significantly increased in HFD-fed mice, with further elevation in HOMA-IR score following Glu supplementations (mainly L-Glu). The increase in HOMA-IR negatively correlated with IR and Glut2 expressions. D- and L-Glu supplementations showed significant decrease of Glycogenesis (low GYS2/PYGL ratio) and unchanged p-AKT pattern compared to their RD counterparts.

Conclusion: Our data indicate an increase in rate of de-novo lipogenesis (DNL) in RD-fed mice (High carbohydrate diet) and liver fibrosis following additional sugar supplementations. In contrast, HFD-fed mice (with pre-existing high lipid profile) supplemented with sugar showed less liver fibrosis, because of reduced de-novo fatty acids synthesis and subsequently, the lipid oxidation pathways become dominated and induce the net results of lipid clearance.

KEYWORDS

D-glucose, GLUT-2, HFD-fed mice, l-glucose, MASLD

Introduction

Metabolic dysfunction–associated steatotic liver disease (MASLD) has become a prevalent health concern in the modern world, affecting up to 35–50% of the adult population and up to 20% of children (1). This condition, characterized by the accumulation of fat in the liver cells, occurs without significant alcohol consumption and is often linked to unhealthy lifestyle choices, including poor diet and lack of exercise (2).

Given the association between unhealthy lifestyle choices and the development of MASLD (3), it is crucial to examine how specific dietary components, such as different forms of glucose, might influence the disease's progression (4). D-glucose (D-Glu), the naturally occurring form, is a fundamental carbohydrate in human metabolism, participating in essential processes such as glycolysis and the citric acid cycle (5). High levels of D-Glu, particularly in the form of high-fructose corn syrup and other sweeteners, can lead to increased expression of glucose transporters GLUT2, further promoting glucose and contributing to MASLD progression (6). Conversely, L-glucose (L-Glu); a Non-Nutritive Sugars (NNS), is a synthetic stereoisomer of glucose, and not metabolized by the body in the same manner as D-Glu (7). Due to its unique structure, L-Glu is poorly absorbed in the intestines and does not contribute significantly to caloric intake or blood glucose levels (7, 8). This raises intriguing questions about NNS potential impact on liver metabolism and MASLD as a dietary supplement.

A high-carbohydrate diet can prime the hepatic de-novo lipogenesis (DNL) pathway (9). DNL has been suggested to be abnormally increased in and contribute to the pathogenesis of MASLD (10), a highly prevalent metabolic disease that is linked to the development of type 2 diabetes mellitus (T2DM) (11).

One area of interest in MASLD research is dietary sugars' role in the disease's development and progression. While much attention has been given to the impact of natural sugars such as D-Glu, the effects of synthetic sugars like L-Glu still need to be explored. Our study aims to investigate the metabolic and phenotypic consequences of L-Glu supplementation compared to D-Glu in a high-fat diet (HFD) mouse model.

Methods

High fat diet animal model

The *in vivo* experiment was performed according to the regulations and guidelines of the National Institutes of Health (NIH) and the Hebrew University of Jerusalem under a protocol approved by the animal facility at the Hebrew University of Jerusalem with ethic number MD-18-154943. Six-week-old C57BL/6 J male mice ($n = 60$) were purchased from Harlan Laboratory, Jerusalem. Mice were placed on either a regular diet (RD) of isocaloric low-fat control diet (10% kcal energy from fat, 20% protein, and 70% carbohydrates) (Cat. # D12450B) or high-fat diet (HFD) (60% kcal energy from fat, 20% protein, and 20% carbohydrates) (Cat. # D12492) for 16 weeks. From week 8 to week 16, mice were watered with either tap water or 18% (w/v) D-Glu or 18% (w/v) L-glucose in RD and HFD mice groups. Mice's initial maternal body weight and weekly weights and total food intake were recorded each week during the experiment. By week 16, mice were sacrificed, liver and body weights were recorded, and liver and serum samples were stored at −80°C until use.

Western blot analysis

Whole liver protein extracts were prepared with RIPA buffer (Sigma, Cat# R0278) containing protease and phosphatase inhibitors (Roche, 1183617011). Protein concentrations and quantification were determined by following the manufacturer's instructions for the BCA protein assay kit (Thermo Fisher Scientific, Cat# 23225). Band visualization and quantification were performed on SDS-PVDF membranes of 10% Acrylamide gels. Protein of 40 µg was loaded on each well. The following are the detected antibodies. Rabbit anti-Human/Mouse GYS2 (Proteintech, 22371-1-AP), Rabbit anti-Human/Mouse Glycogen synthase [p Ser641] (Novus bio, NBP2-67315), rabbit anti-human/mouse PYGL antibody (Proteintech, 15851-1-AP), rabbit anti-human/mouse Glut2 polyclonal antibody (Proteintech, 20436-1-AP), rabbit anti-human/mouse ADRP/Perilipin 2 Polyclonal antibody (Proteintech, 15294-1-AP), rabbit anti-human/mouse Alpha Smooth Muscle antibody (Novus, NBP1-30894), mice anti-human/mouse AKT antibody (R&D, MAB 2055), mice anti-human/mouse phospho-AKT antibody (R&D, MAB 887), rabbit anti-human/mouse Insulin Receptor-beta antibody (Proteintech, 20433-1-AP), and rabbit anti-human/mouse beta Actin polyclonal antibody (Proteintech, 20536-1-AP).

RNA isolation and cDNA preparation

Total RNA was extracted from 50 to 100 mg of liver samples using Trizol (TRI) reagent (Bio-Lab, Cat# 009010233100) in which liver sample was homogenized in 1 mL of TRI reagent for 5 min at room temperature using Tissuelyser LT (QIAGEN), followed by the addition of 0.2 mL chloroform (Bio-Lab, Cat#03080521), tightly covered, shacked vigorously for 15 s and allowed to stand for 2–15 min at room temperature. The mixture was centrifuged at 12,000 × *g* for 15 min at 2–8°C. The colorless upper aqueous phase (containing RNA) was transferred to a fresh tube, and 0.5 mL of 2-propanol (Bio Lab, Cat# 16260521) was added, mixed, and allowed to stand for 5–10 min at room temperature, then centrifuged at 12,000 × *g* for 10 min at 2–8°C. The supernatant was removed, and

Abbreviations: ADRP, Adipose differentiation-related protein; ALT, Alanine aminotransferase; AST, Aspartate aminotransferase; D-Glu, D-Glucose; Glu, Glucose; GLUT2, Glucose Transporter 2; HFD, High fat diet; HOMA-IR, Homeostasis model assessment of insulin resistance; MDA, Malondialdehyde; MTC, Masson trichrome staining; p-AKT, Phosphorylated AKT; RD, Regular diet; αSMA, Alpha-smooth muscle actin; L-Glu, L-glucose; PYGL, Glycogen phosphorylase L; GYS2, Glycogen synthase 2.

the RNA pellet was washed by adding a minimum of 1 mL of 75% ethanol; the sample was vortexed and then centrifuged at 7,500 × *g* for 5 min at 2–8°C. The RNA pellet was briefly dried for about 5–10 min by air-drying, and then the pellet was re-suspended in RNase-DNase-free water. RNA was quantified using a Nanodrop machine at the central research lab, the Hebrew University of Jerusalem. Samples were stored at −80°C until needed. Complementary DNA (cDNA) was synthesized from 2 μg of total RNA using a High-Capacity cDNA Reverse Transcription Kit with RNase Inhibitor (Applied Biosystems, Cat # 4374966) following the manufacturer's instructions. Samples were stored at −20°C until needed. RT-PCR was performed for the quantification of the expression of the genes that encoded *alpha-smooth muscle actin* (*αSMA*) (Applied Biosystems, Mm0072512_S1 Acta2, Lot # 1812381) and *Glucose transporter 2* (*Glut2*) (Applied Biosystems, Mm00446229_m1 SLC2a2, Lot # 1790842) compared to *GAPDH* as a housekeeping gene (Applied Biosystems, Mm99999915_g1, Lot # 1703322) by using a TaqMan™ Fast Advanced Master Mix (Applied Biosystems, Cat # 4444964) following the manufacturer's instructions.

Serum biochemistry

Mice cardiac blood samples were collected on the day of sacrifice and centrifuged at 5,000 rpm for 15 min at 4°C. Serum ALT (Abcam; ab285263, sensitivity: 4 pg/mL), AST (Abcam; ab263882, sensitivity: 39 pg/mL), and TRG (Abcam; ab65336, sensitivity: > 2 μM) were measured using Enzyme-Linked Immunosorbent Assay (ELISA) kits. All reagents and samples were brought to room temperature (18–25°C) before use. A volume of 100 μL of each standard and sample was added to the appropriate wells and incubated for 2.5 h at room temperature with gentle shaking. The solution was discarded, and the wells were washed four times with 1X wash solution; washing was performed by filling each well with wash buffer (300 μL) using a multichannel pipette or auto-washer. After washing, the liquid was completely removed at each step. A 100 μL of 1× prepared detection antibody was added to each well and incubated for 1 h at room temperature with gentle shaking. One hundred microliters of a prepared streptavidin solution were added to each well and incubated for 45 min at room temperature with gentle shaking. A 100 μL of TMB One-Step Substrate Reagent (Item H) was added to each well and incubated for 30 min at room temperature in the dark with gentle shaking. Finally, 50 μL of Stop Solution (Item I) was added to each well. The absorbance at 450 nm was immediately read using an ELISA reader (Tecan M100 plate reader).

Serum C-peptide levels

The serum C-peptide 2 level was determined by ELISA using Rat/Mouse C-peptide 2 kit (Merck Millipore, Cat# EZRMCP2-21 K, sensitivity: 15 pM).

Serum malondialdehyde assay

The serum MDA level was determined by ELISA using MDA assay kit (Abcam, Cat#ab238537).

Homeostasis model assessment

Homeostasis model assessment (HOMA-IR) is a model of the relationship between glucose and insulin that predicts fasting steady-state glucose (mmol/l) and fasting serum C-peptide (nmol/l). The product of fasting glucose and fasting C-peptide is an index of hepatic insulin resistance. Here, we used a computerized model with a higher accuracy, the HOMA 2 calculator,[1] to calculate the HOMA-IR score. The formula involves the introduction of data regarding glycemia (mmol/l or mg/dl), insulinemia (pmol/l or μU/mL), or C-peptide (nmol/l or ng/mL), automatically calculating %B, %S, and IR.

Histological assessments of liver injury

One-third of the posterior liver was fixed with 4% formalin for 24 h at room temperature and then embedded in paraffin in an automated tissue processor (HIS-TSQ; MRC). Microtome Sectioning Tutorial (7 μm; HIS-2268; MRC) was deparaffinized by immersion in xylene. The sections were then rehydrated by passing them through a graded alcohol series, starting with absolute alcohol and ending with distilled water. H&E staining was used to evaluate steatosis, necro-inflammatory regions, and apoptotic bodies as mentioned in Table 1. Masson's trichrome (MTC, ab150686, Abcam) was used to visualize the connective tissue. A veterinary pathologist assessed all histopathological findings and reported assessment grades. To quantify the fibrotic area, stained slides were scanned using a Zeiss microscope equipped with image analysis software (ImageJ), which was used to outline the fibrotic areas within the tissue section.

Statistical analysis

Statistical differences will be analyzed either with the two-tailed unpaired Student's *t*-test (For comparison between two groups) with one-way or two-way ANOVA with Newman–Keuls' post-tests among multiple groups using Graph pad Prism 5.0 (GraphPad Software, La Jolla, CA).

Results

Total body weights were reduced in RD-fed following D- and L-Glu supplemented and were unchanged in HFD-fed mice

D- and L-Glu were supplemented to drinking water starting from week 8 of the experiment, as mentioned in the section "Materials and methods." At week 16 (sacrifice date), HFD-fed mice exhibited a ~ 32.7% increase in body weight (Figure 1A) compared to RD-fed mice. Additional water supplementation of D-Glu to the RD mice groups caused a decrease of 13.55% in their total body weight, while the L-Glu had reduced body weight by about 20% ($p < 0.002$). HFD-fed mice receiving D- and L-Glu supplementations had

1 https://www.dtu.ox.ac.uk/homacalculator/download.php

10.3389/fnut.2024.1469952

TABLE 1 H&E assessment parameters.

Item	Definition	Score/Grade
Steatosis grade	Lower to medium evaluation of parenchymal involvement by steatosis	
	<5%	0
	5–33%	1
	>33–66%	2
	>66%	3
Location	Predominant distribution pattern	
	Zone3	0
	Zone1	1
	Azonal	2
	Panacinar	3
Fibrosis stage	None	0
	Persinusoidal or periportal	1
	Mild, Zone3, persinusoidal	1A
	Moderate, Zone3, persinusoidal	1B
	Portal/ periportal	1C
	Persinusoidal and Portal/ periportal	2
	Bridging fibrosis	3
	Cirrhosis	4
Inflammation		
Lobular inflammation	Overall assessment of all inflammatory foci	
	No foci	0
	<2 foci per 200X field	1
	2–4 foci per 200X field	2
	>4 foci per 200X field	3
Microgranulomas	Small aggregates of macrophages	
	Absent	0
	Present	1
Large lipogranulomas	Usually in portal areas or adjacent to central veins	
	Absent	0
	Present	1
Portal inflammation	Assessed from low magnification	
	None to minimal	0
	Greater than minimal	1
Liver cell injury		
Ballooning	None	0
	Few balloons' cells	1
	Many cells/prominent ballooning	2
Acidophil bodies	None to rare	0
	Many	1
Pigmented macrophages	None to rare	0
	Many	1
Megamitochondria	None to rare	0
	Many	1

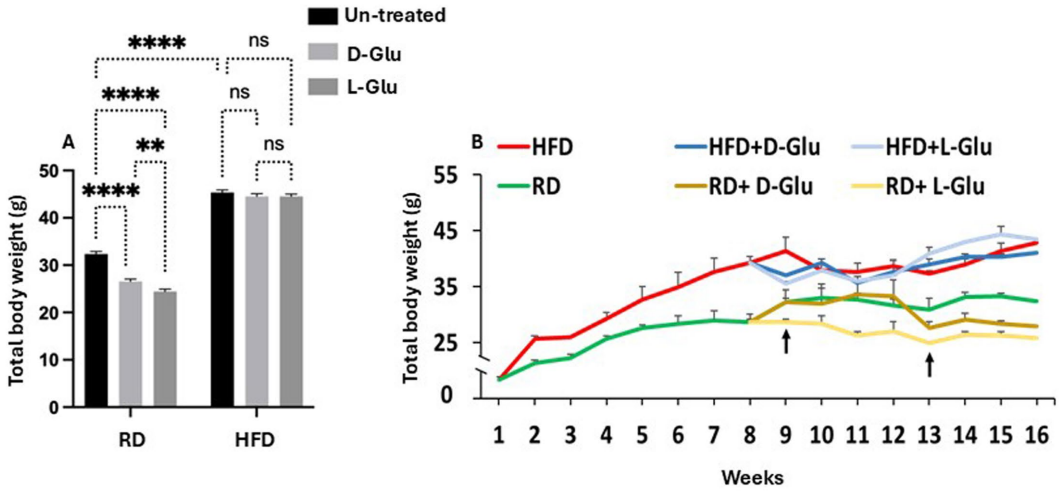

FIGURE 1
Changes in body weight following glucose supplementation. **(A)** Body weight measurements in grams (g) following D- and L-Glu supplementations in RD and HFD-fed mice groups at week 16. **(B)** Changes in body weight kinetics through 1-week interval readings for 16 weeks. Paired and unpaired Student's *t*-test and ANOVA were used for statistically significant differences. *p* value was compared between RD and HFD control groups or within RD or HFD groups. *$p < 0.05$; **$p < 0.01$; ***$p < 0.001$.

comparable body weight to the untreated counterparts (P = ns). Figure 1B shows kinetic changes in body weight from week 1 to week 16. In the RD-fed mice group, a reduction in body weight was noticed at week nine following supplementations of L-Glu; this was considered an early effect. However, a reduction in body weight was observed at week 13 in the RD-fed mice following supplementations of D-Glu (late effect) (Figure 1B).

TABLE 2 Daily consumed water in ml/week.

Daily drink volume (mL/week)	NT	D-Glu	L-Glu
RD	5	5	5
HFD	9	10	11

L-Glu caused increased water consumption and total calories in HFD-fed mice

To address changes in body weight observed in the RD-fed mice, we calculated total food consumption and diet calories obtained from consumed food and glucose supplementation in drinking water. The total amount of consumed diet and water intake was measured weekly. In addition, total food consumption was calculated before and following supplementations with glucose. Figure 2A summarizes averages of total food consumed calculated by grams before glucose supplementation (week 0 to week 8). Results show no differences in total food consumption between RD and HFD-fed mice groups. In parallel, HFD-fed mice display more calorie intake (1.6-fold; $p < 0.001$) as compared to RD-fed mice (Figure 2B). We also assessed total food consumption and calculated diet calorie intake following glucose supplementation from week 8 to week 16. Figure 2C shows similar food consumption patterns between mice fed with RD compared to HFD (P = ns). Both mice groups receiving the D- and L-Glu supplementations caused a reduction in total food intake to 1.03-fold in all mice groups ($p < 0.001$). These reductions were accompanied by reduced diet calorie intake in RD and HFD-fed mice (Figure 2D). Although RD and HFD-fed mice with no glucose supplementations had comparable food intake, the HFD-fed mice showed high (1.56-fold) total calorie intake. The results also demonstrate that the HFD-fed mice might not need to increase their eating habit because of the high-calorie intake. Consumed water glucose supplementations were also included to better calculate total diet calories. Table 2 shows the amounts of drinking water consumed and glucose supplementations in mice groups in ml volume/week. Figure 2E shows the total calorie intake obtained from water. Results showed an increase in calculated calories from water consumption in mice fed with HFD compared to the RD ones, while RD-fed mice showed similar water intake and water calories. These data were comparable to the expected increase in water consumption observed in Table 3 and showed significant effects in favor of L-Glu in the HFD-fed mice. Figure 2F represents a summary of total calories calculated following food and water consumption in all mice groups. Data indicate reduced total calories in mice fed with RD receiving the D- and L-Glu supplementations in consistent with their reduced total food consumptions (Figure 2B) and same water intake (Table 3), which might explain the reductions in their body weight summarized in Figure 1B and may suggest fluctuations in their diet behavior resulted in loss of appetite. Moreover, the same calorie intake between mice groups HFD-fed mice with or without the Glu supplementations may explain their sustained body weight, as seen in Figure 1B.

Our results indicated a reduction in food intake in the HFD-fed mice received Glu supplementations, however, high-calorie intake was apparent in mice with the L-Glu supplementation, which drank more water and substituted the reduced calories obtained from food, indicating the significant effects of sweeteners in contributing to total calorie gain.

10.3389/fnut.2024.1469952

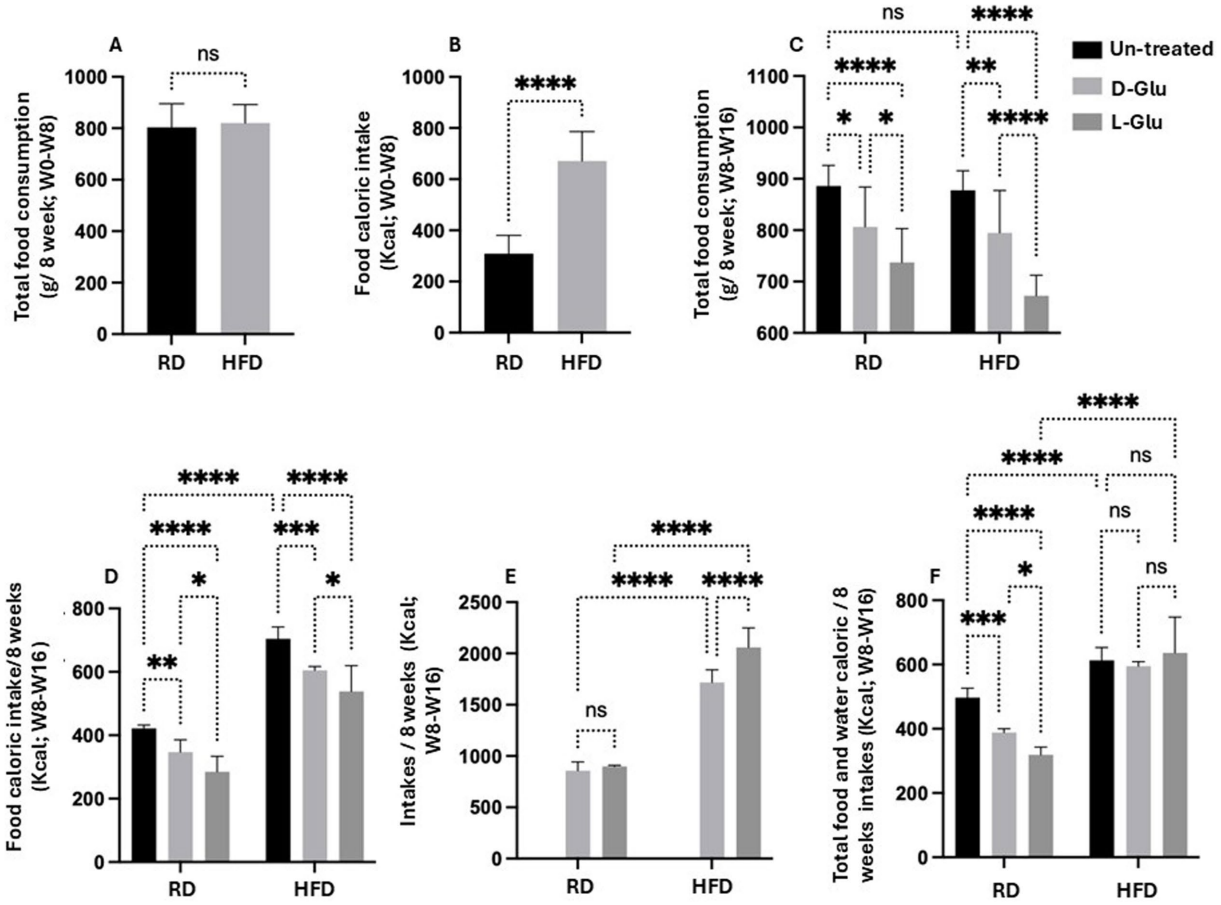

FIGURE 2
Calculated calories from consumed food and glucose supplementation in drinking water. **(A)** Total food consumption in g/8 weeks from week 0 to week 8 **(B)** Food caloric intakes in Kcal from week 0 to week 8 **(C)** Total food consumption in g/8 weeks from week 8 to week 16. **(D)** Food caloric intakes/8 weeks in Kcal from week 8 to week 16. **(E)** Total water caloric intakes in Kcal from week 8 to week 16. **(F)** Total-food and water-caloric intakes/8 weeks in Kcal from week 8 to week 16. Paired and unpaired Student's *t*-test and ANOVA were used for statistically significant differences. *p* value was compared between RD and HFD control groups or within RD or HFD groups. **p* < 0.05; ***p* < 0.01; ****p* < 0.001; *****p* < 0.0001.

TABLE 3 NAS activity score.

	RD	RD + D-Glu	RD + L-Glu	HFD	HFD + D-Glu	HFD + L-Glu
Hepatic ballooning	0	0	0	2	1	0
Lobular inflammation (LI)	0	0	0	1	0	0
Steatosis (S)	0	0	0	3 (63%)	3 (74%)	3 (85%)
NAS scoring	0	0	0	6	4	3

HFD-fed mice developed larger livers while significantly reduced following D- and L-Glu supplementations

To further characterize our HFD-fed mice model, livers were obtained from all mice groups and weighed. HFD-fed mice with no D- and L-Glu supplementations developed larger livers (Figure 3A) and were significantly heavier than the RD-fed mice by 2.17-fold increase. Liver weights in RD-fed mice showed no changes following the D- and L-Glu supplementations, while fewer liver weights were significantly noticed in the HFD-fed mice group of about 18.2 and 18.1% following the D- and L-Glu supplementations, respectively. The same pattern of data was obtained concerning liver to body weight ratio (Figure 3B). Our data indicate that both D- and L-Glu supplementations had comparable results in achieving lower liver weights in HFD-fed mice.

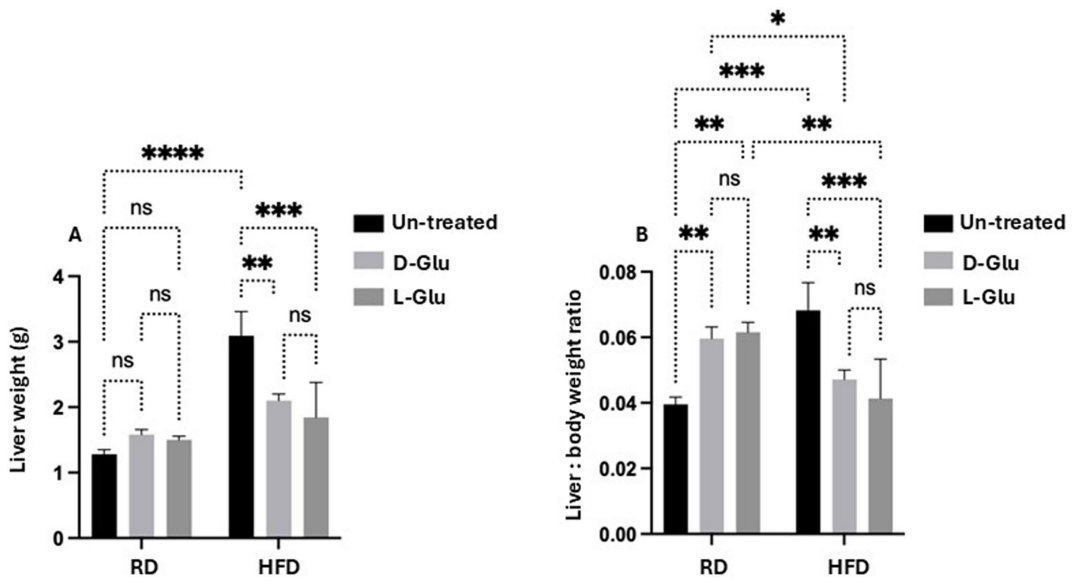

FIGURE 3
Changes in liver weight. **(A)** The whole mouse's liver was weighed in week 16, and **(B)** liver to body weight ratio was calculated. Our data indicate that both D- and L-Glu supplementations had; data are presented in grams (g). Paired and unpaired Student's *t*-test and ANOVA were used for statistically significant differences. The *p* value was compared between the RD and HFD control groups or within the RD or HFD groups. *$p < 0.05$; **$p < 0.01$; ***$p < 0.001$; ****$p < 0.0001$.

Characterization of inflammatory profile in mice fed with RD and HFD following sugar supplementations

To better understand alterations in histopathological findings, livers were assessed for inflammation and steatosis by H&E and for histological visualization of collagenous connective tissue fibers by Masson's trichrome (MTC) staining. In Figure 4A, no histopathological finding was observed on liver tissues obtained from the RD-fed mice. In contrast, microscopic examination of H&E tissue slides revealed higher hepatocyte lipid droplet accumulation in the livers of HFD-fed mice of steatosis grade of 3 with panacinar location and micro-vesicular steatosis (Figure 4D). In addition, livers showed portal inflammation greater than minimal, prominent ballooning, many acidophil bodies, and many mega-mitochondria. D- and L-Glu supplementations did not affect histopathology on livers obtained from mice fed with RD (Figures 4B, C). In parallel, D- and L-Glu supplementations showed increased hepatocyte ballooning (Figure 4E) and steatosis (Figure 4F). Table 3 summarizes the differences in MASLD activity score (NAS) between and among the experimental groups. Data indicate steatosis sub-grading scores in the liver of HFD-fed mice receiving the D-Glu of 74% and L-Glu of 85% compared to 63% in untreated mice. The increase in steatosis grading is well noticed following the L-Glu supplementation in Figure 4F. Biochemical marker outcomes of ALT and AST serum levels were evaluated. Figure 4G shows ALT, and Figure 4H shows AST serum levels with no significant changes in their levels in the mice groups fed with RD following the D- and L-Glu supplementations; results were consistent with the H&E staining. In parallel, both D- and L-Glu supplementations caused a significant reduction in ALT and AST serum levels comparable with the H&E assessments. These data suggest that propagation in liver injury following the L-Glu supplementation in HFD-fed mice resulted in more steatosis and reduced hepatocyte ballooning, which might, in part, indicate accelerated de-novo lipogenesis and, therefore, accumulated lipids in the liver. In addition, reduced ALT/AST serum levels could indicate a chronic liver injury and highlight the issue of the fast uptake rhythm of L-Glu inside the cells, which needs further and future study to confirm this phenomenon.

Characterization of liver fibrosis profile in RD and HFD-fed mice following sugar supplementations

Discrepancies in inflammatory profile severities in HFD-fed mice drinking Glu could highlight a more advanced state of liver fibrosis because of Glu supplementation's continuous (prolonged) insults in drinking water. For this purpose, we aimed to stain liver fibrosis using MTC staining for histological visualization of collagenous connective tissue fibers in liver sections. In Figure 5A, no liver fibrosis was observed in RD-fed mice; in contrast, the HFD-fed mice group (Figure 5D) showed high intensities of MTC staining. D- and L-Glu supplementations in RD-fed mice caused more stained tissues with MTC (Figures 5B,C) in favor of the L-Glu group. Data indicate accelerated fibrogenesis in the mice fed with RD mice following D- and L-Glu supplementations. No difference in liver fibrosis visualization was noticed in the HFD-fed mice group following the D- and L-Glu supplementations (Figures 5E,F); however, accumulation of lipid droplets could be observed as presented in Figures 5E,F. We next quantitate liver αSMA (fibrosis marker) using the western blot analysis [Figure 5G, Supplementary Figure 1 (original gels)] and by the RT-PCR (Supplementary Figure 2). Figure 5G shows significant elevations

10.3389/fnut.2024.1469952

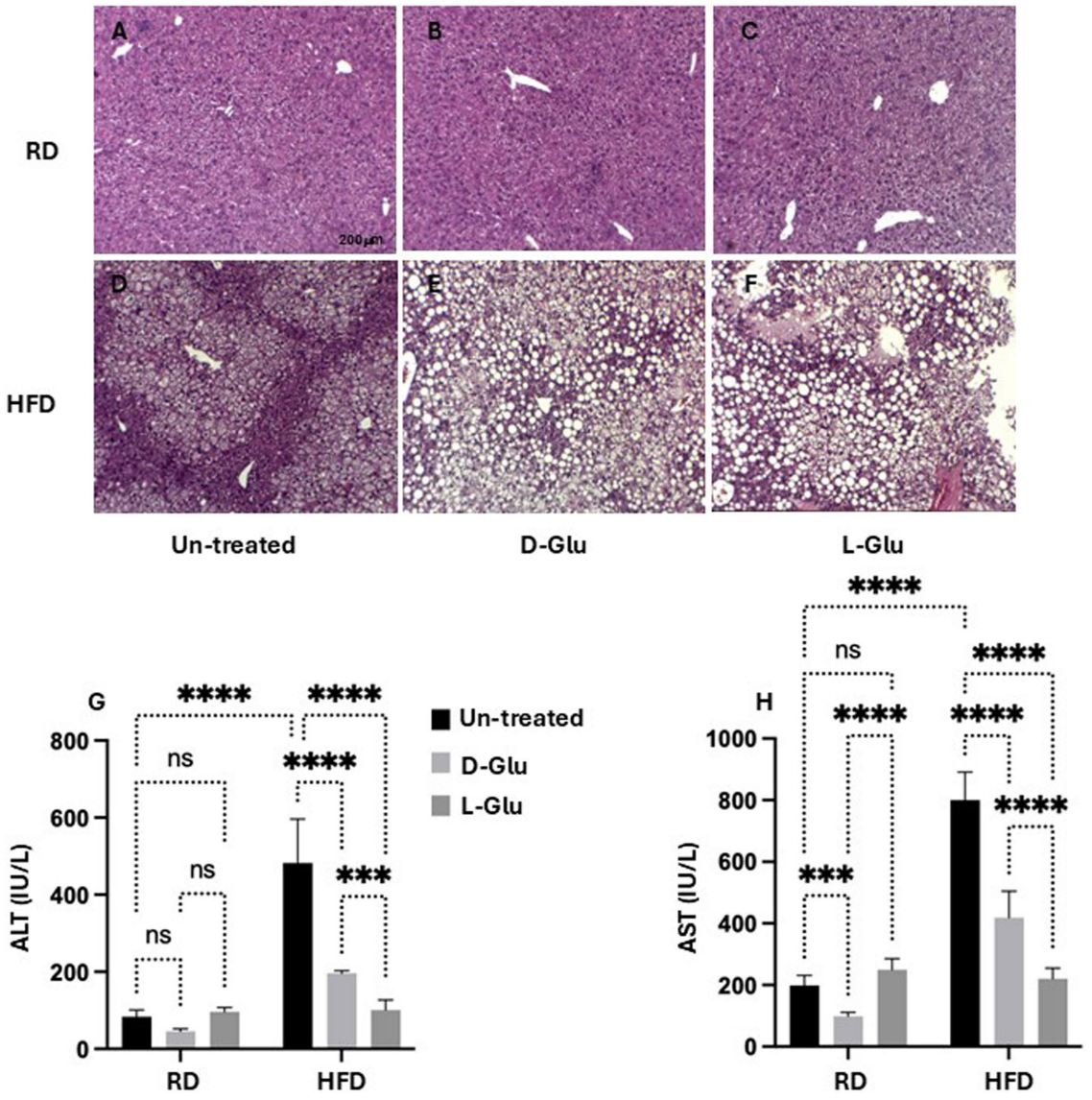

FIGURE 4
Inflammatory profile assessment: Representative sections of immunohistochemically liver staining with H&E (original magnification 10×) are shown **(A–F)**, scale 200 µM. Liver injury markers of **(G)** serum ALT and **(H)** serum AST were assessed. Paired and unpaired Student's *t*-test and ANOVA were used for statistically significant differences. *p* value was compared between RD and HFD control groups or within RD or HFD groups. $^{**}p < 0.01$; $^{***}p < 0.001$; $^{****}p < 0.0001$.

in *αSMA* in the HFD-fed mice (16.4-fold increase; $p = 0.00005$) compared to RD-fed mice. Both D- and L-Glu supplementations significantly induced 2.5-fold and 6.5-fold elevations in αSMA, respectively. In the HFD-fed mice group, both D- and L-Glu supplementations repress αSMA to nearly 1.5-fold compared to the untreated group ($p = 0.002$). These results were also confirmed using the RT-PCR with the same achieved patterns (Supplementary Figure 2). The data obtained from the HFD-fed mice could suggest (1) amelioration in liver fibrosis or (2) severe disruption in liver histology leading to clearance of fibrosis in liver sections. Therefore, several experiments were conducted to clarify the effects of glucose on regulating liver injury profiles.

Reduce hepatic ADPR expression in the HFD-fed mice receiving the D-and L-Glu supplementations, indicating less hepatic lipid uptake

The overall data indicates several clinical outcomes from glucose supplementations in the RD and HFD-fed mice groups. While D- and L-Glu supplementations showed a pro-fibrotic effect in the RD-fed mice model, both supplementations caused a reduction in inflammatory as well as fibrotic markers in their HFD-fed counterparts. These data were accompanied by reduced liver weights in the HFD-fed mice model. Therefore, we next asked

10.3389/fnut.2024.1469952

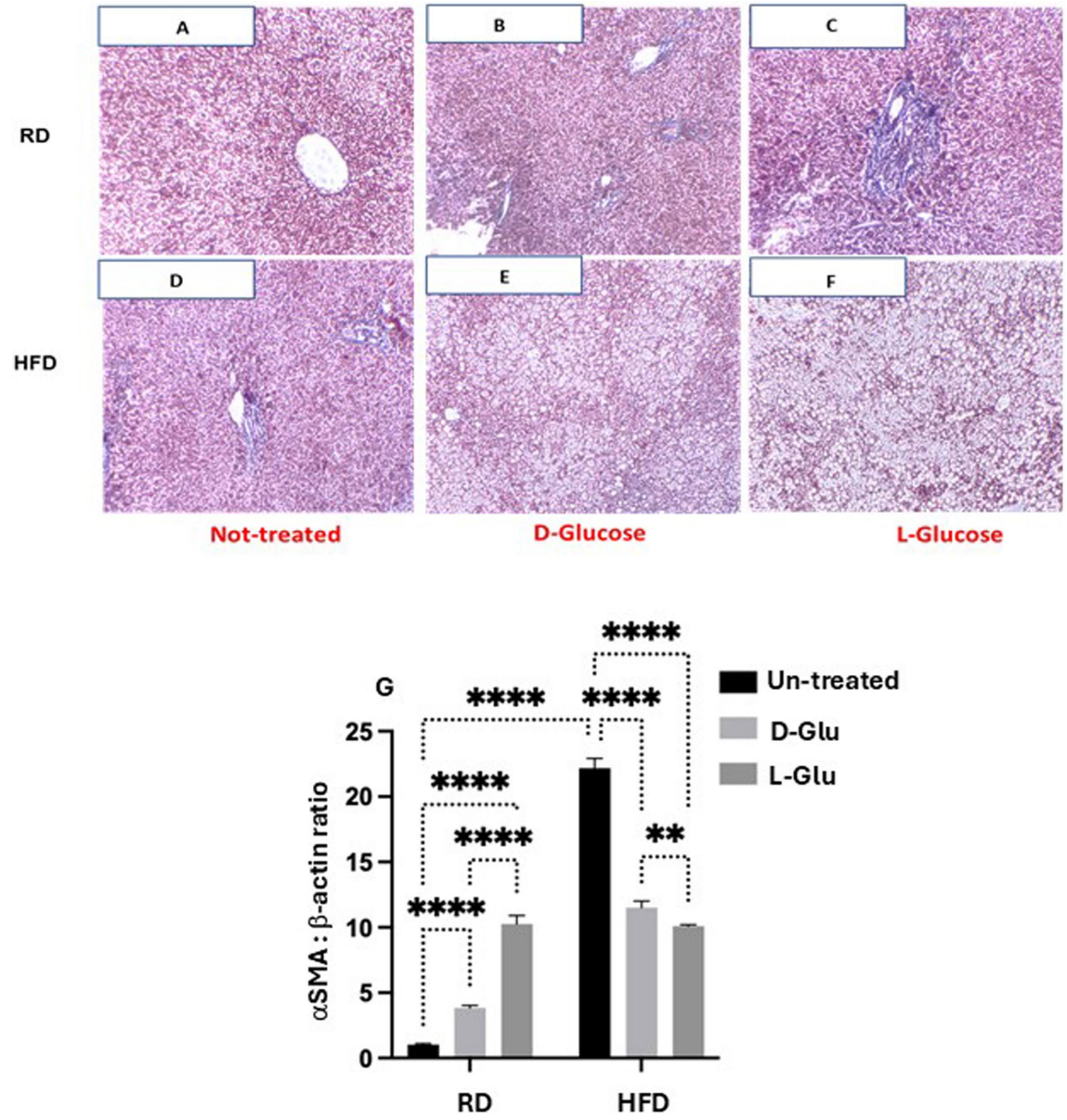

FIGURE 5
Fibrotic profile assessment: Representative sections of immunohistochemically liver staining with trichrome stain (original magnification 100×) are shown **(A–F)**. Liver fibrosis markers of hepatic αSMA expressions were assessed by **(G)** western blot analysis. For western blot analysis, results are presented as the ratio of αSMA to the housekeeping protein (β-actin). Paired and unpaired Student's *t*-test and ANOVA were used for statistically significant differences. *p* value was compared between RD and HFD control groups or within RD or HFD groups. $^{**}p < 0.01$; $^{***}p < 0.001$; $^{****}p < 0.0001$.

whether the decrease in liver weight observed in the HFD-fed mice following glucose supplementation could result from less accumulation in fat deposits. For this purpose, we evaluated expressions of adipose differentiation-related protein (ADRP), which facilitates the uptake of long-chain fatty acids and the formation of lipid droplets in lipid-accumulating cells in hepatocytes (12). It has been shown that decreased expression of ADRP decreases the fatty liver while increasing its expression is associated with several metabolic diseases like type 2 diabetes, insulin resistance, and heart diseases. Figure 6A (Supplementary Figure 1, original gels) shows elevated ADRP expressions in HFD-fed mice (6.8-fold, $p = 0.003$). Supplementation of D- and L-Glu to the RD-fed mice caused elevated expressions of ADRP, which may indicate higher fat uptake and an active lipogenesis process. In contrast, D- and L-Glu supplementations to the HFD-fed mice caused a significant reduction in ADRP expressions to 1.3 and 2.8-fold, respectively. While these results could suggest less lipid uptake in the HFD-fed mice, we hypothesized that lipids could accumulate outside the livers. For this reason, serum triglycerides were evaluated. Figure 6B shows serum TG elevated in the HFD-fed mice at 1.2 mmol/L compared to 1.06 mmol/L in the RD-fed mice ($p < 0.05$). These results indicate more lipid uptake and accumulation in the HFD-fed mice. Following the Glu supplementations, the same high lipid uptake and accumulation patterns were obtained in the RD-fed mice (1.15 mmol/L in the D-Glu and 1.34 mmol/L in the L-Glu).

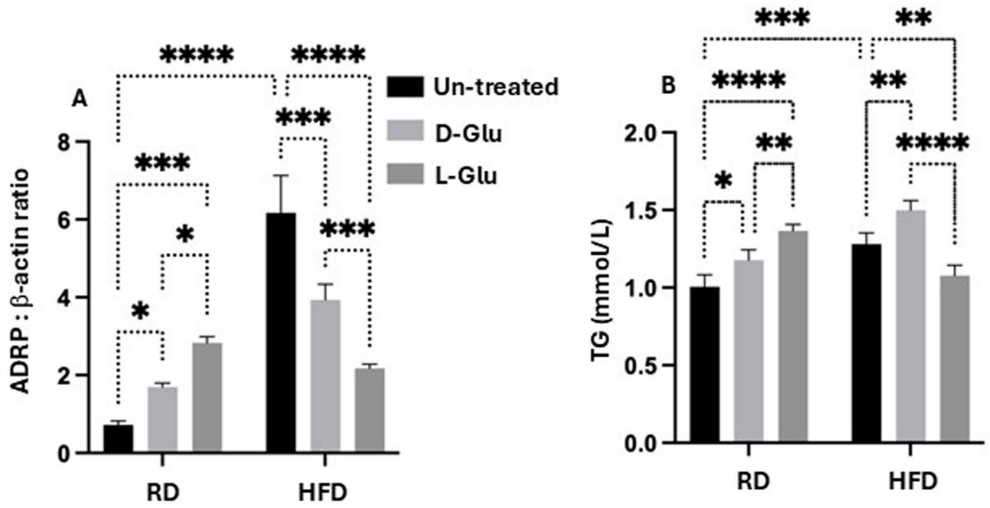

FIGURE 6
Lipid profile assessment: **(A)** Adipose differentiation related-protein (ADRP) was assessed by western blot analysis, and data were represented by the ratio of ADRP to the housekeeping protein (β-actin). **(B)** Serum triglyceride (TG mmol/L) levels were assessed. Paired and unpaired Student's *t*-test and ANOVA were used for statistically significant differences. The *p* value was compared between the RD and HFD control groups or within the RD or HFD groups. *$p < 0.05$; **$p < 0.01$; ***$p < 0.001$; ****$p < 0.0001$.

In the HFD-fed mice, further elevations in serum TG were observed only following the D-Glu (1.6 mmol/L; $p = 0.0003$), however were reduced following the L-Glu supplementations to 1.2 mmol/L; $p = 0.0003$. The results obtained so far could indicate the following: 1-In the RD-fed mice group, serum levels of TG following glucose supplementations were elevated, together with an increase in their hepatic uptake, indicating normal hemostasis of lipid trafficking (efflux) and the liver's ability to deal with additional sugar intake (later converted to fat; known as de-novo lipogenesis (DNL)). 2-Reduced hepatic ADPR expressions were noticed in the HFD-fed mice group receiving the D-Glu, which was in line with its accumulation in the blood, indicating less hepatic lipid uptake. 3- Although hepatic ADRP expressions were also reduced in the HFD-fed mice group receiving the L-Glu, a significant decrease in serum TG levels was noticed, suggesting less accumulation of lipids in the blood and raising the issue of lipid accumulation in other organs or/and increase in clearance of lipid through lipid peroxidation as a result diffusion of lipids. The above data speculates that reduced fat storage in HFD-fed mice could partly explain the reduced liver weight observed in the HFD-fed mice following the glucose supplementations.

Glucose induces lipid peroxidation in both RD and the HFD-fed mice

To explain the less lipid uptake and less serum TG in the HFD-fed mice receiving the L-Glu, we assessed lipid peroxidation, hepatic glucose transporter expression, and insulin serum levels. We have checked for malondialdehyde (MDA), a product of oxidative degradation of lipids. Several studies showed oxidative stress to be implicated in the pathogenesis of type 2 diabetes and its complications. Metabolic disturbances contribute to oxidative stress and compromise the antioxidant defense system in type 2 diabetes patients (13). Figure 7 shows high serum MDA levels in HFD-fed mice compared to the RD-fed mice (1.7-fold, $p < 0.0001$). In the RD-fed mice, D- and L-Glu caused significant elevation in serum MDA to 1.14 and 1.21 –folds, respectively ($p < 0.0001$). The same patterns were obtained in the HFD-fed mice, showing further elevated serum MDA levels following the glucose supplementations ($p < 0.0001$). These data suggested the direct effects of glucose on accelerating lipid peroxidation in both RD and HFD-fed mice, which was in favor of the latter. The high extent of lipid peroxidation in HFD-fed mice could result from inhibited expressions of ARDP. In the RD-fed mice, it could be suggested due to the increase in de-novo lipogenesis (RD contains a high-carbohydrate diet).

Decreased in Glut2 transporter in HFD-fed mice

To further assess the metabolic assessments of glucose on lipid peroxidation, we evaluate fasting blood sugar (FBS) in our mice model. In hepatocytes, glucose can be stored as glycogen, degraded through the glycolytic pathway, or converted to fatty acids by the lipogenic pathway. The release of glucose in circulation follows the degradation of glycogen or gluconeogenesis. Glucose also modifies cellular metabolism by allosteric and transcriptional regulation. HFD-fed mice showed high FBS levels (19.2 mmol/L) compared to the RD-fed mice (13.1 mmol/L; $p = 0.001$, Figure 8A). While D-Glu had no significant effects on FBS in the RD-fed mice, L-Glu significantly elevated FBS to 1.1–fold ($p = 0.02$). D- and L-Glu supplementations increased FBS in the HFD-fed groups to 1.2-fold in both groups ($p = 0.01$). These results indicate that glucose supplementation and high FBS insults could contribute to lipid peroxidation, as shown in Figure 7. Hyperglycemia obtained in our HFD-fed mice following glucose supplementations could indicate less hepatic glucose uptake and point to modulation in hepatic glucose transporter in these mice. GLUT2 is the major glucose transporter of hepatocytes in rodents and humans (44) The generally accepted role of this transporter is to take up glucose during the absorptive phase

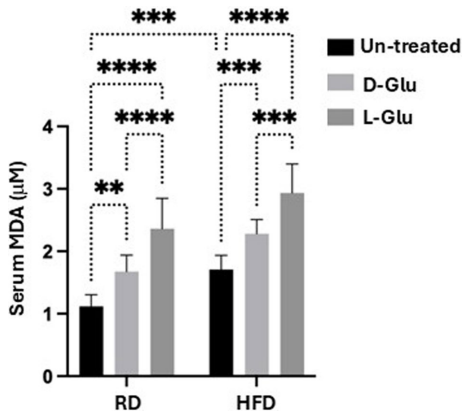

FIGURE 7
Serum lipid peroxidation: Malondialdehyde (MDA) was used as a marker of lipid peroxidation. Results show serum MDA levels as evaluated by ELISA. Paired and unpaired Student's *t*-test and ANOVA were used for statistically significant differences. *p* value was compared between RD and HFD control groups or within RD or HFD groups. $^{**}p < 0.01$; $^{***}p < 0.001$; $^{****}p < 0.0001$.

and to release it in the blood during fasting (14). We evaluated hepatic *GLUT2* expressions by the western blot and RT-PCR methods. Figure 8B (Supplementary Figure 1, original gels) indicates high expressions of GLUT2 in the HFD-fed mice compared to the RD-fed mice (1.2-fold, $p = 0.001$). D- and L-Glu supplementations, while inducing elevated expressions of *GLUT2* in the RD-fed mice, significantly inhibited *GLUT2* expressions in the HFD-fed mice groups ($p < 0.01$). The RT-PCR analysis achieved the same pattern of results (Figure 8C). Our results indicate that adding sugar to the existing high-carbohydrate diet (70% Kcal) in the RD-fed mice stimulates GLUT2 expression. HFD-fed mice [weaning on a high-carbohydrate diet (20% Kcal)], while having elevated GLUT2 expressions, most probably to uptake more glucose, were unexpectedly shown to be inhibited when the HFD-fed mice were combined with additional sugar supplementations.

Hyperinsulinemia in HFD-fed mice is correlated with elevated serum glucose

Although the carbohydrate content in the HFD-fed mice, even with the addition of sugar supplementations, did not reach the RD content with no expected elevation in the GLUT2, this could point to an inhibitory pathway that led to GLUT2 downregulation. In this aspect, we sought to evaluate whether insulin could induce reductions in GLUT2. Hepatic GLUT2 is not pathologically involved in states of glucose intolerance. Therefore, serum insulin C-peptide levels were evaluated as a marker of insulin production rate and hepatic insulin receptors (15). Figure 8D shows a significantly higher serum insulin C-peptide level in the HFD-fed mice compared to the RD-fed mice 1.6-fold ($p < 0.001$). In the RD-fed mice, D- and L-Glu supplementations induce a reduction in serum insulin C-peptide, reflecting a state of hypo-insulinemia. These results were associated with elevations in the hepatic insulin receptor [Figure 8E, Supplementary Figure 1 (original gels)] to 1.67-fold and 1.2-fold in the D- and L-Glu supplemented groups, respectively ($p < 0.05$). This data, together with the elevation in the GLUT2 observed in Figures 8B,C, suggests normal glucose hemostasis due to the normal response of the liver to elevated concentrations of sugar and are in less need of insulin interference. In contrast, in the HFD-fed mice, further increases in the serum insulin C-peptide levels (Hyperinsulinemia) were observed following glucose supplementation accompanied by a reduction in the expression of hepatic insulin receptor (Figure 8E) and inhibited GLUT2 seen in Figures 8B,C suggested a state of insulin resistance. Figure 8F summarizes HOMA–IR score as summarized in the section "Materials and methods." HFD-fed groups receiving the D- and L-Glu supplementations showed high HOMA-IR to 1.3-fold and 3.4-fold, respectively ($p < 0.001$).

Glucose flux balance in HFD-fed mice with Glu supplementation

To evaluate whether changes observed in the metabolic profile alter glucose flux and, as a consequence, may affect hepatocytes viability, we assessed the enzymes necessary for glucose storage (GYS2; a Glycogen synthase is a key enzyme in glycogenesis, the conversion of glucose into glycogen) as well as for glycogen degradation (PYGL; a liver glycogen phosphorylase, catalyzes the phosphorolysis of an α-1, 4-glycosidic bond in glycogen to yield glucose 1-phosphate; glycogen degradation) (16). Moreover, cell survival and metabolism (p-Akt) pathways were evaluated. Figure 9A (Supplementary Figure 1, original gels) shows the ratio of p-GYS2/PYGL assessed by the western blot analysis. Figure 9A indicates that RD-fed mice receiving the D-Glu had a similar ratio to the untreated mice, suggesting the balance of glucose storage and glucose degradation and demonstrate normal glucose hemostasis. In contrast, RD-fed mice receiving the L-Glu had reduced glycogen degradation in favor of glucose storage, indicating high glucose flux [high L-Glu uptake (increase in GLUT R)]. In parallel, both D-and L-Glu supplementations caused an increased glycogen degradation in the HFD-fed mice group (represented as a low p-GYS2/PYGL ratio); results may indicate the demand of the cells to maintain normal levels of the intracellular glucose and suggest less glucose uptake into the cell. These results also align with the high HOMA scores in these two groups. We next evaluated p-Akt as it is being suggested as a mediator for insulin activity (17). p-Akt disturbance, on the other hand, may cause insulin resistance (17). Therefore, we quantitated p-Akt expression in livers obtained from our mice model. Figure 9B (Supplementary Figure 1, original gels) shows elevated expressions of hepatic p-Akt following the D- and L-Glu supplementations in the RD-fed mice. D- and L-Glu supplementations in the HFD-fed mice caused no changes in the liver p-Akt expressions, indicating less responsiveness of the cells to the metabolic stimulation needed for cell survival and viability. The above results may conclude that the livers of HFD-fed mice receiving an extra diet of sugars may affect cell phenotype viability through inhibited p-Akt expressions. Indeed, insulin has been suggested to activate GYS2 through p-Akt (17) and in insulin resistance state, this process could be diminished.

Discussion

Overconsumption of diet rich in fat and sugar-sweetened beverages are risk factors for developing obesity, insulin resistance and

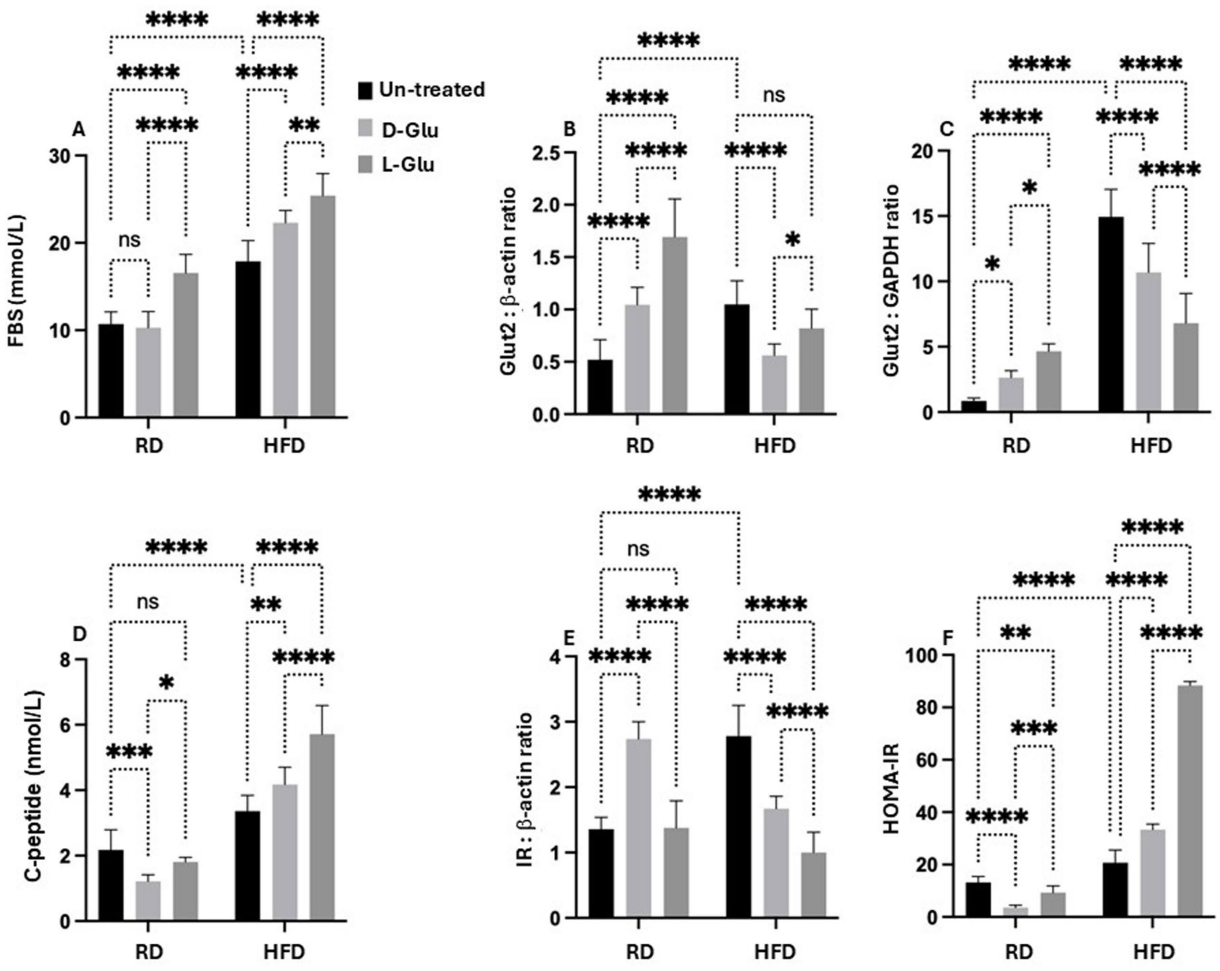

FIGURE 8
Metabolic profile assessment: **(A)** Fasting blood sugar (FBS) was assessed as indicated in materials and methods. *GLUT2* expressions were quantitated by **(B)** western blot and **(C)** RT-PCR methods. **(D)** Serum insulin C-peptide measured by ELISA. **(E)** Hepatic expression of inulin receptor (IR) was evaluated from liver sections by western blot **(F)** HOMA2 calculator calculated HOMA-IR. Paired and unpaired Student's *t*-test and ANOVA were used for statistically significant differences. *p* value was compared between RD and HFD control groups or within RD or HFD groups. *$p < 0.05$; **$p < 0.01$; ***$p < 0.001$; ****$p < 0.0001$.

fatty liver disease (18). Some epidemiological studies have shown that artificial sweeteners are beneficial for weight loss and for those who suffer from glucose intolerance and type 2 diabetes mellitus (19). However, accumulating evidence in recent years suggests that artificial sweetener consumption could perturb human metabolism, especially glucose regulation (20, 21). Artificial sweeteners have been found to cause glucose intolerance and induce metabolic syndrome and are associated with higher body weight gain (21). These findings suggest that artificial sweeteners may increase the risk of obesity. However, the specific mechanism through which artificial sweeteners dysregulate the host metabolism remains elusive.

Artificial sweeteners are marketed as a healthy alternative to sugar and as a tool for weight loss, however, the evidence that they are helpful over a longer period is limited (20). By dissociating sweetness from calories, NNS could interfere with physiological responses that control homeostasis (20). Second, by changing the intestinal environment, NNS could affect microbiota and in turn trigger inflammatory processes that are associated with metabolic disorders (20). Third, by interacting with novel sweet-taste receptors discovered in the gut, NNS could affect glucose absorptive capacity and glucose homeostasis (20). Up to date, five NNS (acesulfame potassium, aspartame, neotame, saccharin, and sucralose) are approved by the US food and drug administration (FDA) (20). For instance, Acesulfame potassium (Ace-K), an artificial sweetener, is found to be 200 times sweeter than sucrose (common sugar), present in used soft drinks, drink mixes, frozen desserts, baked goods, candy, gum, and tabletop sweeteners, and in athlete's protein shake. Although it is considered safe by the FDA, still there are debates about their long-term use and doses (22). Indeed, data suggests that the intended effects of artificial sweeteners do not correlate with what is seen in clinical practice (22).

From this concept, we aimed to study effects of L-Glu (artificial synthesized sugar) intake on animal model of HFD-fed mice. This hypothesis is derived from the idea that obese patients could use artificial sweeteners in an attempt to control their weight and maintain a diet with low calorie. No previous studies were conducted to assess differences in D- and L-Glu intake in patients with obesity and/or with

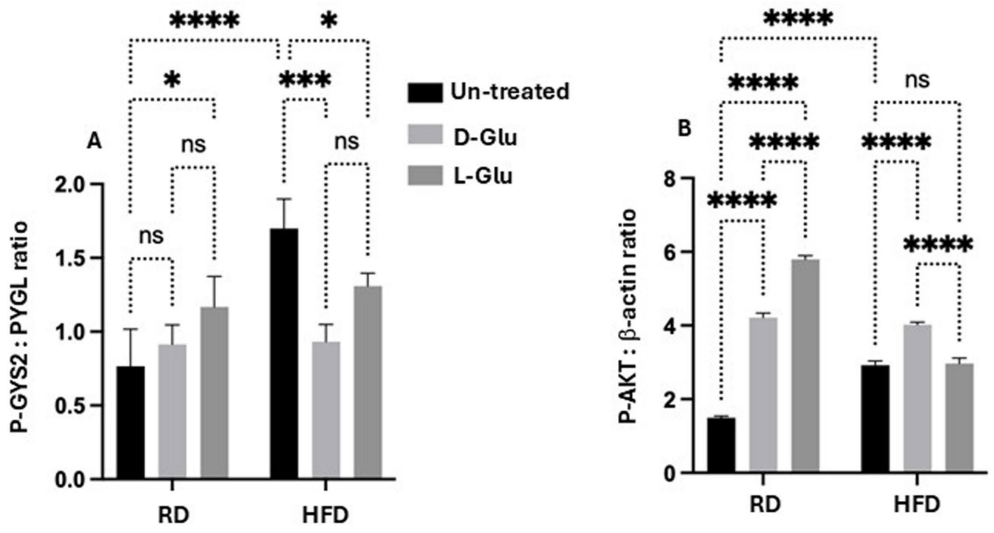

FIGURE 9
Glucose flux balance regulation and hepatic survival: **(A)** phosphor-glycogen synthase (p-GYS2) to Glycogen degradation (PYGL) ratio was assessed by western blot. A decrease in the ratio indicates a decrease in glycogen degradation. **(B)** Hepatic phosphorylated Akt was quantitated through western blot analysis. Paired and unpaired Student's *t*-test and ANOVA were used for statistically significant differences. The *p* value was compared between the RD and HFD control groups or within the RD or HFD groups. *$p < 0.05$; ***$p < 0.001$; ****$p < 0.0001$.

MASLD. For this reason, we adapted the mice model of HFD-fed mice to study effects of D- and L-Glu supplementations on glucose and lipid homeostasis. Moreover, liver profile was also assessed following glucose supplementations.

Our research has concluded some evidence on how glucose supplementations could alter health and disease outcome status. Pre-existing insulin resistance in HFD-fed mice with additional sugar intake caused them to develop a more severe HOMA-IR score (hyperglycemia and hyperinsulinemia), consistent with elevated serum triglyceride levels. Surprisingly, L-Glu induced a more severe HOMA-IR score than D-Glu. Moreover, the hepatic expression of ADRP was suppressed in the mice group receiving the L-Glu, indicating less formation of lipid droplets in lipid-accumulating cells in hepatocytes. This data indicates that the lipid content in the cells regulates ADRP, and its inhibitions are attributed to a preexisting increase in lipid accumulation in the liver. These results were compatible with increased lipid peroxidation following L-Glu intake. Studies showed that fructose-sweetened beverages consumed by human subjects for several weeks resulted in increased hepatic lipogenesis, accumulation of intra-abdominal fat, production of atherogenic lipids, and a marked reduction in insulin sensitivity compared with an isocaloric consumption of glucose (9). The overload of fatty acids and lipid accumulation in MASLD may mechanistically inhibit the synthesis of de-novo fatty acids. Subsequently, the lipid oxidation pathways dominate and induce the net results of lipid clearance (23). An increase in lipid peroxidation following L-Glu supplementation could partly explain reduced liver weights obtained in HFD-fed mice (Figure 3).

Glucose induces oxidative stress and contributes to the inflammatory pathways associated with diabetes and atherosclerosis pathophysiology (24). Specifically, oxidative stress contributes to insulin resistance through an "oxidative-inflammatory cascade (OIC)." Glucose, obesity, and oxidative stress reduce intracellular antioxidant defense mechanisms while activating inflammatory responses from transcription factors and kinases, such as c-Jun N-terminal kinase (JNK), protein kinase C (PKC), and inhibitor of kappa B kinase-β (IKKβ) (25). Moreover, some inflammatory pathways, such as activation of IKKβ, have a causative role in the harmful effects of high glucose on endothelial cell function (26).

Non-Nutritive Sugars has been shown to play a role in the pathways regulating glucose absorption from the intestinal lumen into enterocytes in the gut (27). Data obtained in rodents suggest that intestinal sweet taste receptors control both active glucose absorption by modulating expression of sodium-dependent glucose transporter isoform 1 (SGLT) and passive glucose absorption by modulating apical GLUT2 insertion to the intestine (27). No available data on NNS effects on hepatic GLUT2 expressions were studied previously. GLUT2 is the major glucose transporter of hepatocytes in rodents and humans. The generally accepted role of this transporter is to take up glucose during the absorptive phase and release it in the blood during fasting. Hepatic expression on the role of GLUT2 in HFD-fed mice and its modulatory signaling pathway is not well understood. Our data showed elevated hepatic expressions of GLUT2 in HFD-fed mice compared to the RD-fed mice. While D- and L-Glu supplementations induced elevated expressions of GLUT2 in the RD mice, they significantly inhibited GLUT2 expressions in the HFD-fed mice. Our results indicate that additional sugar supplementations to the existing high carbohydrate diet (70% Kcal) in the RD mice stimulate GLUT2 expression. HFD-fed mice weaned on a high carbohydrate diet (20% Kcal) while having elevated GLUT2 expressions, most probably in an attempt to uptake more glucose, have shown to be unexpectedly inhibited when the HFD-fed was combined with additional sugar supplements. Although total sugar content in the HFD-fed mice was less than their RD-fed counterparts, even though they were supplemented with sugar, this did not induce the expected elevation in the GLUT2 and pointed to inhibitory pathways leading to GLUT2 downregulation (elevated

insulin). Activation of Akt is the integral result of multiple inputs to regulate hepatic glucose and lipid metabolism. Indeed, studies have shown that insulin regulates GLUT2 expression through phosphorylation of Akt (28). A survey by Rathinam et al. (29); concludes a possible link between Akt activation and GLUT2 synthesis and translocation. In obesity, insulin resistance increases GLUT2 levels, which may further exacerbate metabolic dysfunction in MASLD. However, excess glucose led to internalized GLUT-2 and the insulin receptor together into endosomes in response to insulin (30).

Our data showed a lack of hepatic insulin receptors and GLUT2 in the glucose-supplemented HFD-fed mice, associated with HOMA-IR scores and low p-Akt signaling pathways. A significant association was demonstrated between NNS consumption and obesity in a meta-analysis conducted by Ruanpeng et al. (8). According to a review study by Pearlman et al. (31) in both animal models and humans, NNS may change the host microbiome, leading to decreased satiety, alteration in glucose homeostasis, increased calorie intake, weight gain, and metabolic syndrome. There is no clear evidence of the direct link between NNS and liver injury. Most studies focused on NNS's potential role in microbiota alteration and dysbiosis and consequently contribute to the progression of MASLD. Dietary factors and increased plasma fatty acid levels may be due to increased triglyceride synthesis, lipolysis, and DNL in the liver, which induce liver injury and fibrosis (32). It has been shown that hepatic steatosis is correlated with the progression of fibrosis (33). Although the mechanism is not fully understood, lipotoxicity induced by severe macrovesicular steatosis may result in chronic inflammation and oxidative stress, leading to the activation of hepatic stellate cells (34). A high-carbohydrate diet can prime the DNL pathway with a large substrate load and increase rates of DNL importantly this leads to an accumulation of DNL products, fatty acyl chains linked to coenzyme A, which can be incorporated into a plethora of lipid species (9). These lipids may then have further metabolic functions, which may be deleterious in cases of elevated DNL.

Our data indicate the development of liver fibrosis in mice fed with RD (High carbohydrate diet) with additional sugar supplementations, underlining a state of increased rate of DNL, which could partly explain liver fibrosis. In contrast, HFD-fed mice (already with a pre-existing high lipid profile) supplemented with additional sugar intake showed less progression of hepatic fibrosis, most probable because of reduced de-novo fatty acids synthesis. Subsequently, the lipid oxidation pathways become dominant and induce the net results of lipid clearance.

Conclusion

Individuals widely use non-nutritive sweeteners (NNS) in attempts to lower their overall daily caloric intake, lose weight, and sustain a healthy diet. In our current study, we showed evidence in linking NNS and their implications on the development of metabolic syndrome. The study has suggested that NNS may contribute to the development or worsening of metabolic diseases, including metabolic syndrome, obesity associated with elevated oxidative stress and development of insulin resistance in particularly in mice receiving the HFD with pre-existing high calorie intake and high food consumption.

Data availability statement

The datasets presented in this study can be found in online repositories. The names of the repository/repositories and accession number(s) can be found in the article/Supplementary material.

Ethics statement

The animal study was approved by Animal Facility at the Hebrew University of Jerusalem. The study was conducted in accordance with the local legislation and institutional requirements.

Author contributions

JA: Conceptualization, Investigation, Project administration, Writing – original draft, Writing – review & editing. AA: Formal analysis, Methodology, Software, Writing – original draft. AS: Data curation, Formal analysis, Methodology, Validation, Visualization, Writing – review & editing. YK: Validation, Resources, Software, Writing – review & editing. SY: Validation, Resources, Software, Writing – review & editing. BS: Validation, Resources, Software, Writing – review & editing. YP: Validation, Resources, Software, Writing – review & editing. RS: Funding acquisition, Project administration, Resources, Supervision, Visualization, Writing – original draft.

Funding

The author(s) declare that no financial support was received for the research, authorship, and/or publication of this article.

Conflict of interest

The authors declare that the research was conducted in the absence of any commercial or financial relationships that could be construed as a potential conflict of interest.

Publisher's note

Supplementary material

The Supplementary material for this article can be found online at: https://www.frontiersin.org/articles/10.3389/fnut.2024.1469952/full#supplementary-material

References

1. Teng ML, Ng CH, Huang DQ, Chan KE, Tan DJ, Lim WH, et al. Global incidence and prevalence of nonalcoholic fatty liver disease. *Clin Mol Hepatol*. (2023) 29:S32–42. doi: 10.3350/cmh.2022.0365

2. Vancells Lujan P, Viñas Esmel E, Sacanella ME. Overview of non-alcoholic fatty liver disease (NAFLD) and the role of sugary food consumption and other dietary components in its development. *Nutrients*. (2021) 13:1442. doi: 10.3390/nu13051442

3. Ling Z, Zhang C, He J, Ouyang F, Qiu D, Li L, et al. Association of Healthy Lifestyles with non-alcoholic fatty liver disease: a prospective cohort study in Chinese government employees. *Nutrients*. (2023) 15:604. doi: 10.3390/nu15030604

4. Basaranoglu M, Basaranoglu G, Bugianesi E. Carbohydrate intake and nonalcoholic fatty liver disease: fructose as a weapon of mass destruction. *Hepatob Surg Nutr*. (2015) 4:109–16. doi: 10.3978/j.issn.2304-3881.2014.11.05

5. Gurung P, Zubair M, Jialal I. Plasma glucose In: StatPearls. Treasure Island, FL: StatPearls Publishing. (2024). Available at: https://www.ncbi.nlm.nih.gov/books/NBK541081/

6. Pereira RM, Botezelli JD, da Cruz Rodrigues KC, Mekary R, Cintra D, Pauli J, et al. Fructose consumption in the development of obesity and the effects of different physical exercise on the hepatic metabolism. *Nutrients*. (2017) 9:405. doi: 10.3390/nu9040405

7. Anastasiou IA, Eleftheriadou I, Tentolouris A, Mourouzis I, Pantos C, Tentolouris N. The use of L-glucose in Cancer diagnosis: results from in vitro and in vivo studies. *Curr Med Chem*. (2021) 28:6110–22. doi: 10.2174/0929867328666210311112240

8. Ruanpeng D, Thongprayoon C, Cheungpasitporn W, Harindhanavudhi T. Sugar and artificially sweetened beverages linked to obesity: a systematic review and meta-analysis. *QJM*. (2017) 110:513–20. doi: 10.1093/qjmed/hcx068

9. Sanders FW, Griffin JL. De novo lipogenesis in the liver in health and disease: more than just a shunting yard for glucose. *Biol Rev Camb Philos Soc*. (2016) 91:452–68. doi: 10.1111/brv.12178

10. Ipsen DH, Lykkesfeldt J, Tveden-Nyborg P. Molecular mechanisms of hepatic lipid accumulation in non-alcoholic fatty liver disease. *Cell Mol Life Sci*. (2018) 75:3313–27. doi: 10.1007/s00018-018-2860-6

11. Dharmalingam M, Yamasandhi PG. Nonalcoholic fatty liver disease and type 2 diabetes mellitus. *Ind J Endocrinol Metab*. (2018) 22:421–8. doi: 10.4103/ijem.IJEM_585_17

12. Fukushima M, Enjoji M, Kohjima M, Sugimoto R, Ohta S, Kotoh K, et al. Adipose differentiation related protein induces lipid accumulation and lipid droplet formation in hepatic stellate cells. *In vitro Cell Dev Biol Anim*. (2005) 41:321–4. doi: 10.1007/s11626-005-0002-6

13. Aouacheri O, Saka S, Krim M, Messaadia A, Maidi I. The investigation of the oxidative stress-related parameters in type 2 diabetes mellitus. *Can J Diabetes*. (2015) 39:44–9. doi: 10.1016/j.jcjd.2014.03.002

14. Thorens B. GLUT2, glucose sensing and glucose homeostasis. *Diabetologia*. (2015) 58:221–32. doi: 10.1007/s00125-014-3451-1

15. Leighton E, Sainsbury CA, Jones GC. A practical review of C-peptide testing in diabetes. *Diabetes Ther*. (2017) 8:475–87. doi: 10.1007/s13300-017-0265-4

16. Berg JM, Tymoczko JL, Stryer L. Biochemistry. Section 21.1, Glycogen Breakdown Requires the Interplay of Several Enzymes. *5th* ed. New York: W H Freeman (2002).

17. Samuel VT, Shulman GI. The pathogenesis of insulin resistance: integrating signaling pathways and substrate flux. *J Clin Invest*. (2016) 126:12–22. doi: 10.1172/JCI77812

18. Arsenault BJ, Lamarche B, Després JP. Targeting overconsumption of sugar-sweetened beverages vs. overall poor diet quality for cardiometabolic diseases risk prevention: place your bets! *Nutrients*. (2017) 9:600–12. doi: 10.3390/nu9060600

19. Gardner C, Wylie-Rosett J, Gidding SS, Steffen LM, Johnson RK, Reader D, et al. Nonnutritive sweeteners: current use and health perspectives: a scientific statement from the American Heart Association and the American Diabetes Association. *Diabetes Care*. (2012) 35:1798–808. doi: 10.2337/dc12-9002

20. Pepino MY, Bourne C. Non-nutritive sweeteners, energy balance, and glucose homeostasis. *Curr Opin Clin Nutr Metab Care*. (2011) 14:391–5. doi: 10.1097/MCO.0b013e3283468e7e

21. Suez J, Korem T, Zeevi D, Zilberman-Schapira G, Thaiss CA, Maza O, et al. Artificial sweeteners induce glucose intolerance by altering the gut microbiota. *Nature*. (2014) 514:181–6. doi: 10.1038/nature13793

22. Cong WN, Wang R, Cai H, Daimon CM, Scheibye-Knudsen M, Bohr VA, et al. Long-term artificial sweetener acesulfame potassium treatment alters neurometabolic functions in C57BL/6J mice. *PLoS One*. (2013) 8:e70257. doi: 10.1371/journal.pone.0070257

23. De Stefanis D, Mastrocola R, Nigro D, Costelli P, Aragno M. Effects of chronic sugar consumption on lipid accumulation and autophagy in the skeletal muscle. *Eur J Nutr*. (2017) 56:363–73. doi: 10.1007/s00394-015-1086-8

24. Oguntibeju OO. Type 2 diabetes mellitus, oxidative stress and inflammation: examining the links. *Int J Physiol Pathophysiol Pharmacol*. (2019) 11:45–63.

25. Lamb RE, Goldstein BJ. Modulating an oxidative-inflammatory cascade: potential new treatment strategy for improving glucose metabolism, insulin resistance, and vascular function. *Int J Clin Pract*. (2008) 62:1087–95. doi: 10.1111/j.1742-1241.2008.01789.x

26. Yung JHM, Giacca A. Role of c-Jun N-terminal kinase (JNK) in obesity and type 2 diabetes. *Cells*. (2020) 9:706. doi: 10.3390/cells9030706

27. Margolskee RF, Dyer J, Kokrashvili Z, Salmon KSH, Ilegems E, Daly K, et al. T1R3 and gustducin in gut sense sugars to regulate expression of Na+−glucose cotransporter 1. *Proc Natl Acad Sci USA*. (2007) 104:15075–80. doi: 10.1073/pnas.0706678104

28. Czech MP. Insulin action and resistance in obesity and type 2 diabetes. *Nat Med*. (2017) 23:804–14. doi: 10.1038/nm.4350

29. Rathinam A, Pari L. Myrtenal ameliorates hyperglycemia by enhancing GLUT2 through Akt in the skeletal muscle and liver of diabetic rats. *Chem Biol Interact*. (2016) 256:161–6. doi: 10.1016/j.cbi.2016.07.009

30. Leturque A, Brot-Laroche E, Le Gall M. GLUT2 mutations, translocation, and receptor function in diet sugar managing. *Am J Physiol Endocrinol Metab*. (2009) 296:E985–92. doi: 10.1152/ajpendo.00004.2009

31. Pearlman M, Obert J, Casey L. The association between artificial sweeteners and obesity. *Curr Gastroenterol Rep*. (2017) 19:64. doi: 10.1007/s11894-017-0602-9

32. Knebel B, Fahlbusch P, Dille M, Wahlers N, Hartwig S, Jacob S, et al. Fatty liver due to increased de novo lipogenesis: alterations in the hepatic peroxisomal proteome. *Front Cell Dev Biol*. (2019) 7:248. doi: 10.3389/fcell.2019.00248

33. McPherson S, Hardy T, Henderson E, Burt AD, Day CP, Anstee QM. Evidence of NAFLD progression from steatosis to fibrosing-steatohepatitis using paired biopsies: implications for prognosis and clinical management. *J Hepatol*. (2015) 62:1148–55. doi: 10.1016/j.jhep.2014.11.034

34. Brenner DA. Molecular pathogenesis of liver fibrosis. *Trans Am Clin Climatol Assoc*. (2009) 120:361–8.

Frontiers in Nutrition

Explores what and how we eat in the context of health, sustainability and 21st century food science

A multidisciplinary journal that integrates research on dietary behavior, agronomy and 21st century food science with a focus on human health.

Discover the latest Research Topics

See more →

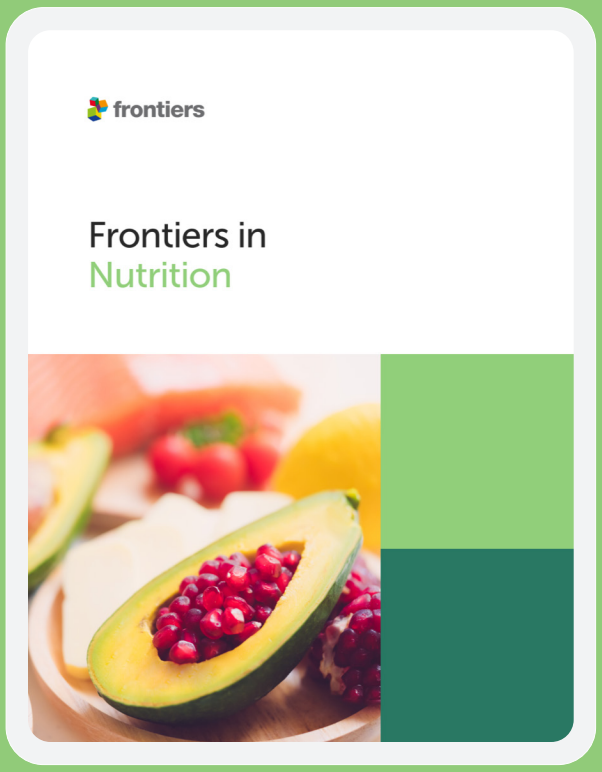

Frontiers

Avenue du Tribunal-Fédéral 34
1005 Lausanne, Switzerland
frontiersin.org

Contact us

+41 (0)21 510 17 00
frontiersin.org/about/contact